

MSC-03824

# SPACE SHUTTLE SYSTEM PROGRAM DEFINITION

(NASA-CR-134333) SPACE SHUTTLE SYSTEM  
PROGRAM DEFINITION. VOLUME 2:  
TECHNICAL REPORT Final Report (Grumman  
Aerospace Corp.) 248 p HC \$15.50

N74-30309

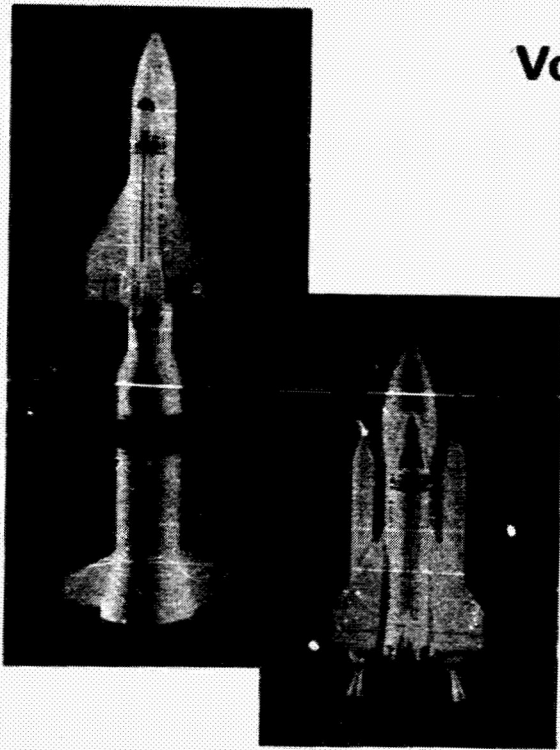
Includes

OSDL 225 33/31 54518

## PHASE B EXTENSION FINAL REPORT

## TECHNICAL REPORT

### Volume II



*DRA*

CONTRACT: NAS 9-11160  
MODIFICATION NO. 11S  
B34-43 RP-33  
15 March 1972

GRUMMAN  
BOEING



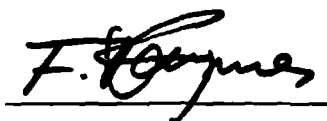
**SPACE SHUTTLE SYSTEM  
PROGRAM DEFINITION**

**PHASE B EXTENSION  
FINAL REPORT**

**TECHNICAL REPORT**

**Volume II**

**GRUMMAN APPROVAL**



F. Raymes  
Assistant Director,  
Space Shuttle Program  
Contract Study Manager

CONTRACT: NAS 9-11160, MOD 11S  
DRL: T-752, LINE ITEM: 6  
DRD: SE-420T, DATA TYPE 2  
B35-43 RP-33

15 March 1972





## CONTENTS

Section		Page
1	INTRODUCTION . . . . .	1-1
	1.1 Report Organization . . . . .	1-4
2	SERIES BRB AND PARALLEL SRM. . . . .	2-1
	2.1 Trending and Point Desig., Selection . . . . .	2-1
	2.2 Stack Configurations . . . . .	2-3
	2.3 HO Tank Comparison . . . . .	2-7
	2.3.1 Structural arrangement, HO Tank, Series Burn . . . . .	2-8
	2.3.2 HO Tank Structural Design criteria . . . . .	2-10
	2.3.3 Tank TPS . . . . .	2-13
	2.4 Abort . . . . .	2-13
	2.4.1 Introduction . . . . .	2-15
	2.4.2 Abort Modes . . . . .	2-16
	2.4.3 Configuration Options . . . . .	2-16
	2.5 Induced Environment . . . . .	2-23
	2.5.1 Introduction . . . . .	2-23
	2.5.2 Acoustics . . . . .	2-23
	2.5.3 Vibration . . . . .	2-25
	2.5.4 Heating . . . . .	2-28
	2.6 Control Considerations . . . . .	2-31
	2.6.1 Introduction . . . . .	2-31
	2.6.2 Configuration Characteristics . . . . .	2-32
	2.6.3 Orbiter/Booster Roll-Yaw Coupling (No Booster TVC) . . . . .	2-32
	2.6.4 Aerodynamic Disturbance Due to Winds . . . . .	2-33
	2.6.5 Aerosurface Control Capability. . . . .	2-34
	2.6.6 SRM TVC Control Capability. . . . .	2-37
	2.6.7 Reduction of Roll-Yaw Control Requirements . . . . .	2-38
	2.6.8 Control Studies Summary . . . . .	2-40
	2.7 Flight Performance Reserves . . . . .	2-40
	2.7.1 Introduction . . . . .	2-40
	2.7.2 Sensitivity Analysis . . . . .	2-41
	2.7.3 Orbiter Propellant Utilization System Comparisons . . . . .	2-44





CONTENTS (Cont.)

Section		Page
	2.7.4	Booster Propellant Utilization System Comparisons . . . 2-45
	2.7.5	Summary of FPR Results . . . . . 2-48
	2.8	Costs . . . . . 2-49
	2.9	Summary . . . . . 2-49
	2.9.1	Introduction . . . . . 2-49
	2.9.2	Configuration Characteristics . . . . . 2-50
	2.9.3	HO Tank Mass Fraction . . . . . 2-50
	2.9.4	Abort . . . . . 2-51
	2.9.5	Induced Environment . . . . . 2-51
	2.9.6	Control . . . . . 2-52
3		ORBITER DESIGN STATUS . . . . . 3-1
	3.1	15 x 60 Orbiter . . . . . 3-1
	3.1.1	Impact of Changes on Orbiter . . . . . 3-2
	3.1.2	Aerodynamic Development of the 15 x 60 Orbiter . . . . . 3-6
	3.2	14 x 45 Payload Bay Orbiter . . . . . 3-13
	3.2.1	14 x 45 Orbiter Aero Options . . . . . 3-13
	3.3	Summary . . . . . 3-16
4		14 x 45 PAYLOAD BAY ORBITER . . . . . 4-1
	4.1	Stacked Configurations . . . . . 4-1
	4.2	Costs . . . . . 4-4
	4.3	Effect of Payload Weight and Payload Bay Size Reduction . 4-6
	4.4	Summary . . . . . 4-8
5		BOOSTER DESIGN AND ANALYSIS . . . . . 5-1
	5.1	SRM Boosters . . . . . 5-1
	5.1.1	Parallel Burn . . . . . 5-3
	5.1.2	Series Burn . . . . . 5-27
	5.1.3	Preferred SRM Booster . . . . . 5-28
	5.1.4	SRM Booster Reuseability . . . . . 5-30
	5.1.5	SRM Booster Conclusions . . . . . 5-33
	5.2	Liquid Propellant Boosters . . . . . 5-34
	5.2.1	Pressure-fed Series Burn Booster . . . . . 5-35
	5.2.2	Pump-fed Series Burn Booster . . . . . 5-64

CONTENTS (Cont.)

Section		Page
	5.2.3 Parallel Burn Pressure-fed BRB . . . . .	5-86
	5.2.4 Series Burn vs Parallel Burn Pressure-fed Boosters . . .	5-88
	5.2.5 Pressure-fed vs Pump-fed Liquid Boosters . . . . .	5-88
	5.3 Summary and Conclusions . . . . .	5-90
	5.3.1 Weight Comparison . . . . .	5-90
	5.3.2 Cost Comparison . . . . .	5-92
6	PAD ABORT . . . . .	6-1
	6.1 Introduction . . . . .	6-1
	6.2 Failure Modes and Criteria . . . . .	6-1
	6.3 Vehicle Design Constraints . . . . .	6-3
	6.4 Flight Requirements . . . . .	6-3
	6.5 Configurations Considered . . . . .	6-5
	6.5.1 SSME Configuration . . . . .	6-5
	6.5.2 Swing Engine Configuration . . . . .	6-7
	6.6 Results . . . . .	6-12
	6.6.1 Warning Time . . . . .	6-12
	6.6.2 Fall-Back Zone . . . . .	6-13
	6.6.3 Gantry Clearance . . . . .	6-14
	6.6.4 Performance and Cost . . . . .	6-14
	6.7 Conclusion . . . . .	6-14
7	ENVIRONMENTAL IMPACT . . . . .	7-1
	7.1 Introduction . . . . .	7-1
	7.2 Air Quality and Pollution Control . . . . .	7-2
	7.3 Solid Wastes . . . . .	7-5
	7.4 Orbiter Reentry Noise . . . . .	7-6
	7.5 Summary . . . . .	7-7
8	TEST, OPERATIONS, AND FACILITIES . . . . .	8-1
	8.1 Test . . . . .	8-1
	8.1.1 Summary . . . . .	8-1
	8.1.2 Ground Development Testing . . . . .	8-2
	8.1.3 Horizontal Flight Test . . . . .	8-4
	8.1.4 Vertical Flight Test . . . . .	8-5



CONTENTS (Cont.)

Section		Page
8	8.1.5 Tradeoff Studies . . . . .	8-6
	8.2 Operational Flow . . . . .	8-10
	8.2.1 Overall Flow . . . . .	8-10
	8.2.2 Safing Area . . . . .	8-10
	8.2.3 RSI Spray Shop . . . . .	8-11
	8.2.4 Orbiter Maintenance and Checkout . . . . .	8-11
	8.2.5 Tank Processing . . . . .	8-12
	8.2.6 Orbiter/HO Tank Mate . . . . .	8-13
	8.2.7 Booster/Orbiter Mate . . . . .	8-13
	8.2.8 Mated Processing VAB . . . . .	8-13
	8.2.9 Rollout and Pad Processing . . . . .	8-14
	8.2.10 Pad and LUT Refurbish . . . . .	8-15
	8.2.11 Booster Processing . . . . .	8-15
	8.2.12 SRM/HO/Orbiter Operational Concepts . . . . .	8-18
	8.2.13 Booster/Orbiter Mate . . . . .	8-18
	8.2.14 Mated Processing VAB . . . . .	8-18
	8.2.15 Rollout and Pad Processing . . . . .	8-19
	8.2.16 Conclusions . . . . .	8-19
	8.3 Facilities . . . . .	8-20
9	SUMMARY AND CONCLUSIONS . . . . .	9-1
	9.1 Series/BRB vs Parallel/SRM . . . . .	9-1
	9.1.1 What are the Physical Configuration Characteristics? . .	9-1
	9.1.2 What Is the Difference Between Series and Parallel HO Tanks? . . . . .	9-2
	9.1.3 What is the SSME EPL for No Abort Gap? . . . . .	9-4
	9.1.4 Do Launch Acoustics and Interference Heating Penalize Parallel SRM? . . . . .	9-5
	9.1.5 Can TVC and Thrust Termination be Eliminated on Parallel SRM? . . . . .	9-5
	9.1.6 How Do these Configurations Compare on Costs? . . . . .	9-7
	9.2 Orbiter Status . . . . .	9-8
	9.2.1 How Has the 15 x 60 Bay Orbiter Changed Since December 1971? . . . . .	9-8
	9.2.2 Is the 14 x 45 Payload Bay Orbiter feasible? . . . . .	9-9

CONTENTS (Cont.)

Section		Page
9.3	15 x 60/Series/BRB, 14 x 45/Parallel/SRM . . . . .	9-10
9.3.1	What are the Physical Characteristics of a 14 x 45/Parallel/SRM Configuration? . . . . .	9-10
9.3.2	How Do Payload and Bay Size Weight Reductions Affect Cost? . . . . .	9-11
9.4	Booster Design . . . . .	9-11
9.4.1	Solid Propellant Boosters . . . . .	9-11
9.4.2	Liquid Propellant Boosters . . . . .	9-14
9.5	Pad Abort . . . . .	9-17
9.5.1	What Requirements are We Trying to Meet? . . . . .	9-17
9.5.2	Configuration Approaches . . . . .	9-18
9.5.3	What Is the Impact of Providing Pad Abort Capability? . . . . .	9-19
9.6	Systems Evaluation and Conclusions . . . . .	9-19



## ILLUSTRATIONS

No.		Page
1-1	Program Options . . . . .	1-2
1-2	Study Key Issues . . . . .	1-3
1-3	System Characteristics . . . . .	1-3
1-4	Design Groundrules . . . . .	1-3
2-1	S. Polar From WTR Series BRB Trending - 15x60 Orbiter . . . . .	2-1
2-2	S. Polar From WTR, 2 156" SRM's Parallel/SRM Trending - 15x60 Orbiter . . . . .	2-1
2-3	Series/Pump Fed Trending - 15x60 Orbiter . . . . .	2-2
2-3a	Cost of Payload . . . . .	2-2
2-4	Mission Profile - Series BRB (Pressure-Fed). . . . .	2-4
2-5	Mission Profile - Series BRB (Pump-Fed). . . . .	2-5
2-6	Mission Profile - Parallel SRM - 156" . . . . .	2-5
2-7	Mission Profile - Parallel SRM - 120" . . . . .	2-5
2-8	Series BRB Launch Configuration . . . . .	2-5
2-9	Pump Fed Launch Configuration . . . . .	2-6
2-10	Parallel 1207 Launch Configuration . . . . .	2-6
2-11	Parallel 156" SRM Launch Configuration . . . . .	2-6
2-12	Total Inert Launch Configurations Characteristic Comparison . . . . .	2-6
2-13	BRB, 15x60 Orbiter Structural Arrangement, HO Tank, Series Burn . . . . .	2-8
2-14	SRM, 15x60 Orbiter Structural Arrangement, Parallel Burn HO Tank . . . . .	2-9
2-15	Series LO <sub>2</sub> Tank Wall Thickness Variation . . . . .	2-12
2-16	Parallel LO <sub>2</sub> Tank Wall Thickness Variation . . . . .	2-12
2-17	Series LH <sub>2</sub> Tank Wall Thickness Variation . . . . .	2-12
2-18	Parallel LH <sub>2</sub> Tank Wall Thickness Variation . . . . .	2-12
2-19	HO Tank Design Limit Loads Envelope . . . . .	2-12
2-20	HO Tank Structural Design Criteria . . . . .	2-15
2-21	HO Tank Mass Fractions . . . . .	2-16
2-22	Series BRB Abort Modes . . . . .	2-18
2-23	Parallel SRM (156") Abort Modes . . . . .	2-18
2-24	Mode II Abort From 32K Ft . . . . .	2-19
2-25	Mode III Effects of Tank Staging Conditions on Orbiter Abort Entry . . . . .	2-19
2-26	Mode III Abort Return to Launch Site . . . . .	2-20
2-27	Mode IV Entry Corridor . . . . .	2-20

ILLUSTRATIONS (Con't)

No.		Page
2-28	Mode IV Engine Out Abort Insertion Conditions . . . . .	2-21
2-29	Abort Gap . . . . .	2-22
2-30	Due East Mission MPS Reserve Requirement for No Abort Gap . . . . .	2-22
2-31	Typical Acoustic Spectra Used to Determine Sonic Fatigue Weight Penalty . . . . .	2-24
2-32	Orbiter - Acoustic Weight Penalty of Parallel Burn . . . . .	2-24
2-33	Aft End Vibration Environment Comparison. . . . .	2-26
2-34	Cabin Vibration Environment With Computer Qual Levels . . . . .	2-27
2-35	Cabin Vibration Environment with IMU Qual Levels . . . . .	2-27
2-36	Areas of Concern . . . . .	2-28
2-37	Parallel Burn Ascent. . . . .	2-28
2-38	HO Tank Heating Due to Shock Interference . . . . .	2-29
2-39	Plume Induced Recirculation . . . . .	2-29
2-40	Plume Boundaries . . . . .	2-30
2-41	HO Tank Baseline Thermal Protection System. . . . .	2-30
2-42	Tank Base Heating Penalty From Plume Radiation. . . . .	2-31
2-43	Ascent Control Study - Configuration Characteristics . . . . .	2-31
2-44	Orbiter/Booster Roll Yaw Coupling . . . . .	2-32
2-45	Aerodynamic Disturbance vs Altitude . . . . .	2-35
2-46	Aero Disturbance - Control Requirements - 1207's . . . . .	2-35
2-47	Aero Disturbance - Control Requirements - 156's . . . . .	2-35
2-48	Aero Disturbance - Aero Surface Control - 1207's. . . . .	2-36
2-49	Aero Disturbance - Aero Surface Control - 156's . . . . .	2-36
2-50	Asymmetric Elevon Deflection Requirement Parallel Burn SRM . . . . .	2-37
2-51	Ascent Control - Aero Disturbance Data . . . . .	2-38
2-52	Aero Disutrbance - SRM TVC Control 4-1207 SRM . . . . .	2-38
2-53	Aero Disturbance - Effect of Fins . . . . .	2-39
2-54	15x60 Orbiter Series BRB vs Parallel SRM, Cost Data. . . . .	2-49
3-1	15x60 PLB Orbiter General Arrangement. . . . .	3-2
3-2	Changing Requirements and Ground Rules Orbiter Status . . . . .	3-2
3-3	15x60 Orbiter Landed Weight History . . . . .	3-3





ILLUSTRATIONS (Con't)

No.		Page
3-4	Orbiter Evolution . . . . .	3-3
3-5	15x60 Orbiter, 3 x 472K - Main Engine Instl . . . . .	3-4
3-6	15x60 Orbiter . . . . .	3-5
3-7	Comparison of Soft and Hard Chine Fuselage Sections . . . . .	3-7
3-8	Effect of Subsonic Static Margin . . . . .	3-9
3-9	Effect of Hypersonic Trim Margin . . . . .	3-9
3-10	Trailing Edge Angle Effects . . . . .	3-9
3-11	Effects of Wing Chamber . . . . .	3-11
3-12	Effect of Extending Basic Fuselage Length . . . . .	3-11
3-13	Design Velocity Effect on Wing Trending . . . . .	3-11
3-14	Effect of Landed Weight Change . . . . .	3-12
3-15	15x60 Configuration Hard Chine . . . . .	3-12
3-16	15x60 Configuration Sort Chine . . . . .	3-12
3-17	15x60 Optimum Configuration 3 x 472K SSME . . . . .	3-13
3-18	14x45 Orbiter Aero Options . . . . .	3-13
3-19	14x45 Configuration Soft Chine. . . . .	3-14
3-20	14x45 Configuration Hard Chine . . . . .	3-15
3-21	14x45 Optimum Configuration 3 x 380K SSME . . . . .	3-15
3-22	General Arrangement 14x45 Orbiter 3 x 380K SSME . . . . .	3-15
3-23	14x50 Orbiter 3 x 472K SSME . . . . .	3-16
3-24	Orbiter Comparison . . . . .	3-17
4-1	Parallel/SRM Trending (3 x 380K SSME) . . . . .	4-2
4-2	Parallel/SRM Trending (3 x 472K SSME) . . . . .	4-2
4-3	Launch Configuration Performance . . . . .	4-2
4-4	Parallel/1205 SRM 3 x 472K SSME Launch Configuration . . . . .	4-3
4-5	Parallel/156" SRM 3 x 472K SSME Launch Configuration . . . . .	4-3
4-6	Parallel/1207 SRM 3 x 380K SSME Launch Configuration . . . . .	4-3
4-7	Parallel/156" SRM 3 x 380K SSME Launch Configuration . . . . .	4-4
4-8	Series BRB 15x60 vs Parallel SRM 14x45 . . . . .	4-5
4-9	Bay Geometry & Payload Weight Effects on Orbiter . . . . .	4-7

**ILLUSTRATIONS (Con't)**

<b>No.</b>		<b>Page</b>
5-1	<b>Booster Options . . . . .</b>	<b>5-2</b>
5-2	<b>SRM Booster Configurations Candidates . . . . .</b>	<b>5-2</b>
5-3	<b>Parallel Burn SRM General Arrangement Model 976-164. . . . .</b>	<b>5-5</b>
5-4	<b>SRM Stage Build-up . . . . .</b>	<b>5-5</b>
5-5	<b>156" SRM Parallel-Burn Booster Trajectory-Model 979-164 . . . . .</b>	<b>5-7</b>
5-6	<b>SRM Booster Trades. . . . .</b>	<b>5-9</b>
5-7	<b>Structural Design Details. . . . .</b>	<b>5-10</b>
5-8	<b>Structural Sizing Conditions . . . . .</b>	<b>5-12</b>
5-9	<b>Results, Parallel Burn Dynamic Analysis . . . . .</b>	<b>5-14</b>
5-10	<b>156" Diameter SRM - Design . . . . .</b>	<b>5-15</b>
5-11	<b>Parallel Burn - Ascent Control . . . . .</b>	<b>5-15</b>
5-12	<b>TVC Subsystem - Solid Rocket Motor (typical) . . . . .</b>	<b>5-17</b>
5-13	<b>Separation Approach. . . . .</b>	<b>5-18</b>
5-14	<b>Separation Motor Sizing . . . . .</b>	<b>5-19</b>
5-15	<b>Booster Avionics Functional &amp; Interface Diagram. . . . .</b>	<b>5-21</b>
5-16	<b>SRM Booster - Reliability and Safety . . . . .</b>	<b>5-22</b>
5-17	<b>Operational Concept Parallel Burn SRM . . . . .</b>	<b>5-23</b>
5-18	<b>Parallel SRM Boosters (979-164) . . . . .</b>	<b>5-26</b>
5-19	<b>Series Burn SRM Boosters . . . . .</b>	<b>5-29</b>
5-20	<b>Selection SRM Booster . . . . .</b>	<b>5-29</b>
5-21	<b>LOX/RP-1 Series Burn, Pressure-fed BRB - Model 979-176B . . . . .</b>	<b>5-37</b>
5-22	<b>Pressure-fed Booster Trajectory - Model 979-176B. . . . .</b>	<b>5-38</b>
5-23	<b>Pressure-fed Recoverable Booster Structural Arrangement and Major Structural Design Conditions . . . . .</b>	<b>5-40</b>
5-24	<b>Water Impact Pressures, Pressure-fed Series Burn, BRB . . . . .</b>	<b>5-41</b>
5-25	<b>Water Impact Loads, Pressure-fed Series Burn, BRB . . . . .</b>	<b>5-42</b>
5-26	<b>Water Impact Structural Weight Penalty . . . . .</b>	<b>5-42</b>
5-27	<b>Tanks are a Major Weight Driver Because of Pressure . . . . .</b>	<b>5-44</b>
5-28	<b>Engine/Vehicle Integration is a Key Booster Issue . . . . .</b>	<b>5-47</b>
5-29	<b>Pressurization Subsystem (Model 979-176B) Single Thread Schematic. . . . .</b>	<b>5-49</b>



ILLUSTRATION (Con't)

No.		Page
5-30	Development Testing Series & Parallel-Burn, Pressure-fed BRB's - Models 979-176, -171 . . . . .	5-50
5-31	Ascent Stability - Pressure-fed . . . . .	5-51
5-32	Roll Stability - Pressure-fed . . . . .	5-51
5-33	Reentry Ballistic Coefficients. . . . .	5-52
5-34	Zero Lift Drag Buildup - Pressure Fed . . . . .	5-52
5-35	Static Stability - Pressure Fed . . . . .	5-52
5-36	Pressure-fed Ascent and Recovery Characteristics . . . . .	5-54
5-37	Series Burn Pressure-fed BRB (-176) Nominal Separation . . . . .	5-54
5-38	Series Burn Pressure-fed BRB Separation Characteristics . . . . .	5-55
5-39	Recovery System Selection . . . . .	5-55
5-40	Recovery Sequence - Booster Model 979-176 . . . . .	5-57
5-41	Drag Brake Concept . . . . .	5-60
5-42	E/E Equipment Location . . . . .	5-61
5-43	Operations and Refurbishment Cycle Complete in 60 Shifts (30 Days) . . . . .	5-63
5-44	Test Program - Pressure-fed BRB . . . . .	5-64
5-45	Pump-fed LOX/RP-1 Series Burn BRB-Model 979-073A . . . . .	5-65
5-46	Pump-fed Booster Trajectory - Model 979-066B . . . . .	5-68
5-47	F-1 Pump-fed Booster Permits Heavier Orbits . . . . .	5-69
5-48	Pump-fed Recoverable Booster General Arrangement . . . . .	5-70
5-49	Bending Moments Pump-fed, Series Burn Booster Model 979-066-073 . . . . .	5-71
5-50	Water Impact Loads, Pump-fed BRB 979-066, -073 . . . . .	5-71
5-51	Water Impact Lateral Acceleration, Pump-fed BRB 979-066, -073 . . . . .	5-72
5-52	Pump-fed BRB . . . . .	5-74
5-53	Development Testing, Pump-fed BRB - Model 979-073A Propulsion System Test Requirements . . . . .	5-77
5-54	Ascent Stability - Pump-fed . . . . .	5-78
5-55	Ascent Roll Stability - Pump-fed . . . . .	5-78
5-56	Reentry Ballistic Coefficients . . . . .	5-78
5-57	Zero Lift Drag - Pump-fed . . . . .	5-79

ILLUSTRATION (Con't)

No.		Page
5-58	Static Stability - Pump-fed . . . . .	5-80
5-59	Pump-fed Ascent and Recovery Characteristics. . . . .	5-80
5-60	Recovery Sequence - Pump-fed Booster . . . . .	5-82
5-61	Engine Protection Model 979-066 . . . . .	5-85
5-62	Test Program - Pump-fed BRB . . . . .	5-87
5-63	General Arrangement - LOX/RP-1 Parallel Burn Pressure- fed BRB Model 979-171A . . . . .	5-87
5-64	Series Burn vs Parallel Burn Liquid Boosters . . . . .	5-88
5-65	Pressure-fed vs Pump-fed Issue . . . . .	5-89
5-66	Booster Weight Comparison . . . . .	5-91
5-67	Shuttle Booster Comparison (\$ Millions) . . . . .	5-93
5-68	Alternative Booster Costs, March 2, 1972 . . . . .	5-94
5-69	The Issues . . . . .	5-94
6-1	Abort Regimes . . . . .	6-2
6-2	Failure Criticalities . . . . .	6-2
6-3	Blast Wave Characteristics . . . . .	6-2
6-4	Pad Abort Design Constraints. . . . .	6-4
6-5	KSC Landing Strip Location . . . . .	6-4
6-6	Pad Abort Flight Profile . . . . .	6-4
6-7	Burnout Conditions As A Function of Energy Level . . . . .	6-4
6-8A	Configurations Considered for Pad Aborts . . . . .	6-6
6-8B	Additional Configuration Approaches Considered . . . . .	6-6
6-9	Configurations Selected for Study . . . . .	6-8
6-10	Abort SRM Characteristics. . . . .	6-8
6-11	Abort SRM Characteristics - Swing Engine Configuration . . . . .	6-8
6-12	Swing Engine Installation . . . . .	6-8
6-13	Launch Configuration . . . . .	6-10
6-14	Swing Engine Orbiter Design . . . . .	6-10



ILLUSTRATION (Con't)

No.		Page
6-15	Structural Arrangement Swing Engine Design HO Tank. . . . .	6-10
6-16	Effect of Swing Mechanism Failure . . . . .	6-13
6-17	Warning Time Requirements . . . . .	6-13
6-18	Pad Abort - Minimum Safe Altitude . . . . .	6-15
6-19	Pad Abort Tower Clearance . . . . .	6-15
6-20	Weight GLOW/Inert For Pad Abort . . . . .	6-16
6-21	Pad Abort Cost Comparisons . . . . .	6-16
7-1	EIS Considerations . . . . .	7-2
7-2	Potential Shuttle Impact Items . . . . .	7-2
7-3	Total Contaminant Products . . . . .	7-3
7-4	Representative Exposure to Peak HCL Concentrations . . . . .	7-4
7-5	Solid Wastes . . . . .	7-5
7-6	Orbiter Re-Entry Noise . . . . .	7-7
8-1	HO Orbiter Development Test Program . . . . .	8-4
8-2	Orbiter Horizontal Flight Test . . . . .	8-5
8-3	ABPS/MPS Envelope Expansion Profile . . . . .	8-8
8-4	HO-Orbiter Suborbital Launch Study . . . . .	8-9
8-5	BRB/HO/Orbiter Operational Flow . . . . .	8-10
8-6	BRB/HO Orbiter Operational Flow . . . . .	8-12
8-7	BRB-HO/Orbiter Operational Flow . . . . .	8-16
8-8	BRB/HO/Orbiter Operational Flow . . . . .	8-16
8-9	BRB-HO/Orbiter Operational Flow . . . . .	8-17
8-10	BRB/HO/Orbiter Flow . . . . .	8-17
9-1	Launch Configuration Performance . . . . .	9-1
9-2	Launch Configurations Characteristic Comparison . . . . .	9-2
9-3	Series BRB Vs Parallel SRM . . . . .	9-7
9-4	15 X 60 Orbiter Landed Weight History . . . . .	9-8
9-5	Orbiter Comparison . . . . .	9-10
9-6	Launch Configuration Characteristics Comparison . . . . .	9-10

ILLUSTRATION (Con't)

No.		Page
9-7	Series BRB 15 X 60 Parallel SRM 14 x 45 . . . . .	9-11
9-8	SRM Booster Configurations Candidates . . . . .	9-12
9-9	Stage Cost (Parallel Burn - 156 In SRM Booster) . . . . .	9-15
9-10	Liquid Booster Configuration . . . . .	9-15
9-11	Blast Wave Characteristics . . . . .	9-17
9-12	Configurations Considered For Pad Aborts . . . . .	9-18
9-13	Configuration Comparison Summary . . . . .	9-20





## TABLES

No.		Page
2-1	Characteristics Summary . . . . .	2-4
2-2	Parallel - Series Comparison . . . . .	2-14
2-3	HO Tank Structural Design Criteria . . . . .	2-14
2-4	Tank Weight Comparison . . . . .	2-16
2-5	Post Staging Mode III Abort Capability . . . . .	2-20
2-6	Effect of Acoustic Environment on Structural Weight - Parallel Burn vs Series Burn . . . . .	2-26
2-7	Series Burn BRB - 15x60 P/L Bay - Due East Launch From ETR . . . . .	2-42
2-8	Parallel Burn SRM (4 UTC 1207) - 15x60 P/L Bay - Due East Launch From ETR . . . . .	2-43
2-9	Reference Design Points Characteristics Due East Launch From ETR . . . . .	2-44
2-10	Sensitivity Coefficients Series Burn BRB . . . . .	2-45
2-11	Sensitivity Coefficients Parallel Burn SRM (4 UTC 1207) . . . . .	2-45
2-12	FPR Requirements - Series Burn BRB . . . . .	2-46
2-13	FPR Requirements - Parallel Burn SRM (4 UTC 1207) . . . . .	2-47
2-14	Orbiter Propellant Utilization System Comparisons . . . . .	2-47
2-15	Orbiter Active vs Passive PU Comparison . . . . .	2-48
2-16	Booster Propellant Utilization Study Weight Comparison Series Burn BRB . . . . .	2-48
2-17	Booster Active PU System Cost, Series BRB . . . . .	2-48
3-1	Small Payload Bay Orbiter Detailed Weight Statement . . . . .	3-17
4-1	Orbiter Comparison . . . . .	4-1
4-2	Vehicle Characteristics Summary Due East From ETR . . . . .	4-5
5-1	Weight Statement - Model 979-164 . . . . .	5-7
5-2	SRM Diameter Selection . . . . .	5-14
5-3	Stage Cost - Parallel Burn - 156" SRM Booster . . . . .	5-27
5-4	Weights and Other Parameter Implications of Recovery . . . . .	5-32
5-5	Booster Cost Impact of SRM Recovery . . . . .	5-32
5-6	Weight Statement - Pressure-Fed Booster . . . . .	5-36
5-7	Weight Statement - Model 979-073A . . . . .	5-67
5-8	Pump-Fed Booster 979-073 Materials, Heat Sink Requirements, Design Conditions. . . . .	5-73
6-1	Propellant Required . . . . .	6-6
6-2	Orbiter Weight Changes . . . . .	6-11

**TABLES (Con't)**

<b>No.</b>		<b>Page</b>
6-3	Tank Weight Comparison - No Pad Abort . . . . .	6-12
7-1	Propellant Manufacture . . . . .	7-5
8-1	Booster Development Tests . . . . .	8-2
8-2	Flight Hour Summary . . . . .	8-4
8-3	Test Point Identification - Envelope Expansion MPS . . . . .	8-8
8-4	15x60 Orbiter /BRB - Facilities . . . . .	8-20
8-5	15x60 Orbiter/SRM - Facilities . . . . .	8-20



REPRODUCIBILITY OF THE ORIGINAL PAGE IS POOR.

## Section 1

### INTRODUCTION

In January 1972 the second half of the Phase B Extension of the Space Shuttle System Program Definition study was redirected to apply primary effort to consideration of space shuttle systems utilizing either recoverable pressure fed liquids or expendable solid rocket motor boosters. Two orbiter configurations were to be considered, one with a 15x60 foot payload bay and a 65,000 lb, due East, up-payload capability and the other with a 14x45 payload bay with 45,000 lb of due East, up-payload. Both were to use three SSME engines with 472,000 lb of vacuum thrust each. Parallel and series burn ascent modes were to be considered for the launch configurations of primary interest.

A recoverable pump-fed booster is included in the study in a series burn configuration with the 15x60 orbiter.

To explore the potential of the swing engine orbiter configuration in the pad abort case, it is included in the study matrix in two launch configurations, a series burn pressure fed BRB and a parallel burn 120" SRM.

The resulting matrix of configuration options is shown in Figure 1-1.

The principle objectives of this study are to evaluate the cost and technical differences between the liquid and solid propellant booster systems and to assess the development and operational cost savings available with a smaller orbiter. Other key issues address the impact of providing pad abort capability, the implications of the National Environmental Policy Act on the shuttle configuration and the status of the baseline orbiter and booster development. Figure 1-2 summarizes these key study issues.

In Figure 1-3, the system requirements for this study extension are presented and compared with the requirements in effect prior to the Mid-Term Briefing in December 1971. The most significant changes are the elimination of the phased development approach, the increase in initial payload capability, the decrease in the minimum staging velocity, the elimination of the ablative TPS, and the revision of the intact abort requirements to include all mission phases.

The list of Design Groundrules shown in Figure 1-4 were selected to provide a consistent requirements base for the sizing and design of all booster configurations.

# PROGRAM OPTIONS

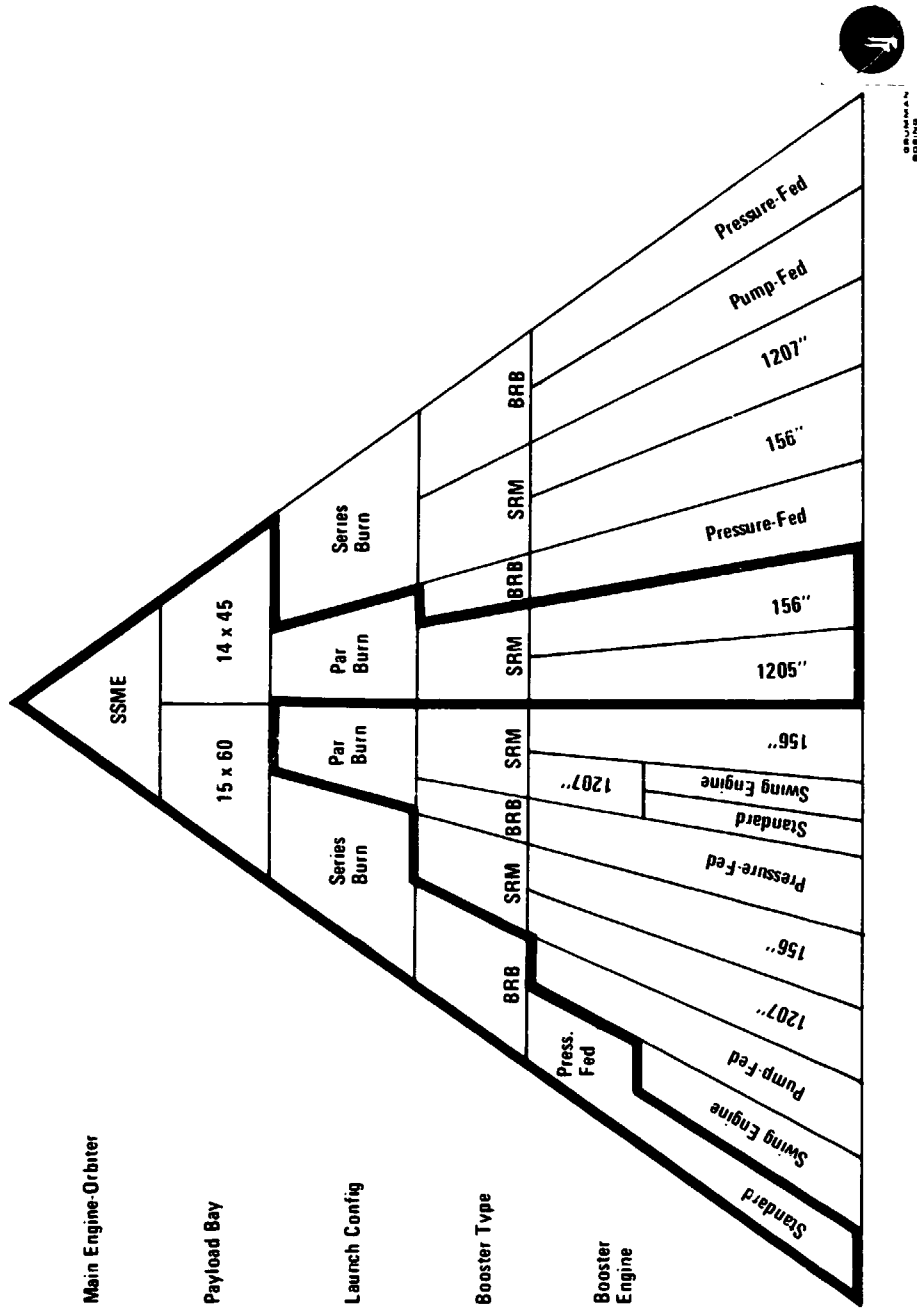


Figure 1-1 Program Options

- What Are Technical & Cost Differences Between Series/BRB & Parallel SRM?
- How Much Weight & Cost Reduction for Smaller Payload-Bay Size Orbiter?
  - What Is Booster Design & Cost Status?
    - What Is Orbiter Design Status?
      - How Can We Achieve Pad Abort Capability?
        - What Are Implications of National Environmental Policy Act On Shuttle?

Figure 1-2 Study Key Issues

	WAS		IS NOW	
	Mk I	Mk II		
Orbiter Payload	15 x 60	15 x 60	15 x 60	14 x 45
Payload Up-East/Polar/55°	?/25/?	65/40/?	65K/40K/25K	45K/?/25K
Payload Down	25K	40K	40K	25K
V <sub>Stage</sub> , fps	6000 + 1000	6000 + 1000	>4000	>4000
Main Engine Type/T <sub>vac</sub>	J-2S/265K	SSME/TBD	SSME/472K	SSME/472K
TPS	Ablative	RSI	RSI	RSI
Avionics	Low Cost	Upgraded	Low Cost/ Evolutionary	Low Cost/ Evolutionary
OMS/RCS	Storable	Storable	Storable	Storable
OMS ΔV, fps	650/1000	650/1000	650/1000/ 1400	650/1000/ 1400
Cross Range, N Mi	1100	1100	1100	1100
Abort	Intact (Not Pad)	Intact (Not Pad)	Intact All Phases	Intact All Phases

Figure 1-3 System Characteristics

- All SRMs Have Thrust Termination Capability
- 1207s & 1205s to Be Used with Existing TVC, Thrust Termination, & Thrust Tailoring (Except if Max G & Max Q Constraints are Violated)
- All Booster Separation for Parallel Burn Configuration to Use Separation Rockets
- All Boosters Are Single-Stage
- All Booster λ' Curves to Be Used for Sizing to Assume TVC
- 15 x 60 PLB Sized for Polar, 14 x 45K Sized for Due East Missions – All Payload Requirements Met
- T/W<sub>L0</sub> to Be 1.25, Max Q to Be at or Below 650 psf for All Configurations
- All SRM Nozzles to Be Canted to Allow Thrust Through CG at Burn-out, Including Thrust-Vectoring Capability

Figure 1-4 Design Groundrules





## 1.1 REPORT ORGANIZATION

The organization of this Technical Volume of the Final Report parallels the listing of Study Key Issues shown in Figure 1-2. Each section presents the technical and cost data relevant to the issues and trades involved in resolving the key issue. A brief description of the contents of Sections 2 through 9 follows.

- Section 2 provides a comparison of parallel burn and series burn launch configurations. The procedure for sizing and trending is explained and the rationale given for the selection of the point design. Data is presented in support of the HO tank mass fractions used in sizing. The abort regimes (except pad abort) are investigated and the relationship between "abort gap" and the emergency power level of the orbiter engine established. The acoustic, vibration and thermal induced environments associated with the series and parallel burn launch configurations are compared and an assessment of the penalties made. The ascent control capability available from the orbiter aero surfaces and orbiter and booster thrust vectoring systems, separately and in combination, is compared to the control authority required and a determination of the need for booster thrust vector control is made. Finally the configurations are compared and their characteristics summarized.
- Section 3 concerns itself with the status of the 15x60 payload bay orbiter design. The evolution of the 15x60 design resulting from requirements changes is traced and the impact of these changes on the orbiter weight shown. The feasibility of a 14x45 payload bay orbiter with three 472,000 lb thrust engines which meets the current aerodynamic performance requirements is investigated. Two alternate configurations are defined.
- Section 4 discusses the effect on the orbiter configuration and DDT&E costs of the smaller payload bay size and the reduction in payload weight. The portion of the total reduction in dry weight and DDT&E costs attributable to each of these changes is determined. Two 14x45 payload bay orbiters are configured, one using three 380,000 lb thrust SSME's and one using three standard 472,000 lb SSME's. Parallel/SRM launch configurations using these two orbiters are trended and point designs selected. The performance and cost characteristics of these designs are compared.
- Section 5 summarizes the status of the solid and liquid propellant booster designs. The issues of ascent control and separation associated with the parallel burn SRM

approach and the safety and cost implications of operating with SRM's are discussed. A series burn configuration using strap-on SRM's with the orbiter is also presented.

Pump-fed and pressure-fed liquid ballistic recoverable boosters are compared with regard to recovery systems, development requirements and costs. Both series and parallel burn configurations are presented.

- Section 6 examines the pad abort requirements and presents the configuration options available to provide the capability. The swing engine orbiter design has attractive advantages for pad abort and a discussion of that configuration is included here. Cost and performance penalties for pad abort capability are summarized for the candidate configurations.
- Section 7 investigates the impact on the environment as a configuration selection parameter.
- Section 8 considers the test, operations and facility costs and requirements associated with the candidate configurations.
- Section 9 provides a summary comparison of the performance, costs and operational aspects of the candidate configurations and presents the conclusions relative to the key issues.



SERIES BRB &  
PARALLEL SRM

REPRODUCIBILITY OF THE ORIGINAL PAGE IS POOR.

## SECTION 2

### SERIES BRB AND PARALLEL SRM

This section discusses the trending and point design selection rationale for the primary configurations, defines the launch configuration of each selected design, discusses the key issues associated with the configurations being studied, and summarizes the major characteristics for all the configurations considered.

#### 2.1 TRENDING AND POINT DESIGN SELECTION

Trend data is obtained for all the launch configurations of interest except those using 120" SRM's as boosters. By varying orbiter  $\Delta V$ , and constraining the max q to 650 psf, characteristics are obtained of various configurations meeting the system requirements and ground rules specified in Section 1.

The updated vehicle sizing program from which the trending data was derived is based on the use of fixed orbiter weights, inert vs. propellant weight data for both HO tank and booster(s), estimated and wind tunnel based launch configuration drag vs. mach no. data and actual trajectory runs to size each point considered.

The resulting trending data for the primary 15x60 orbiter configurations is shown in Figures 2-1, 2-2, and 2-3. No trending is required for the 1207 SRM design as the propellant quantity of each SRM was assumed to be the same as the existing 1207's with only the thrust profile being tailored to meet the 650 psf,  $q_{max}$  requirement. Thus, the orbiter must supply a specific  $\Delta V$  to deliver the required payload to orbit, and the HO tank is sized for that requirement.

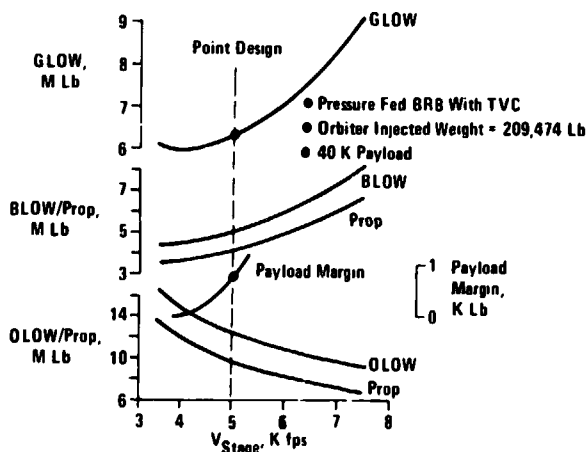


Figure 2-1 S. Polar From WTR Series BRB Trending - 15 x 60 Orbiter

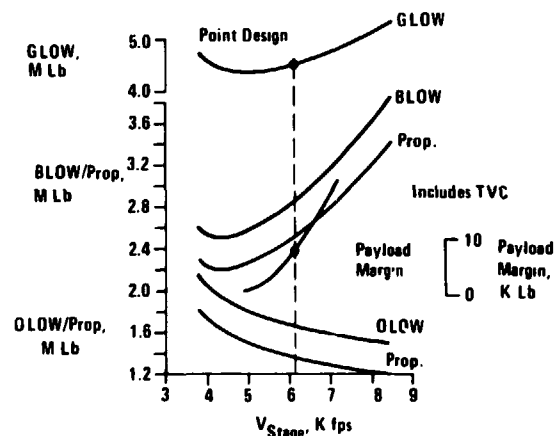


Figure 2-2 S. Polar From WTR, 2 156" SRM'S Parallel/SRM Trending - 16 x 60 Orbiter



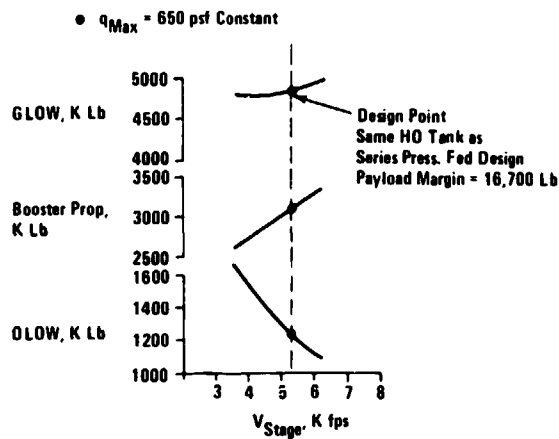


Figure 2-3 Series/Pump Fed BRB Trending – 15 x 60 Orbiter

All the trending data includes 10% growth allowance on the orbiter and booster dry weights, exclusive of main propulsion engines, and 2% growth allowance on the HO tank dry weight.

Point designs are selected which will permit a 5% growth in orbiter inert weight or payload to be accommodated by an increase in HO tank propellant, only.

The total program cost is typically minimum at a slightly higher staging velocity than that corresponding to minimum GLOW. Thus, selecting the point design at a slightly higher staging velocity than that for minimum GLOW provides the 5% growth potential for a very small addition to the total program cost (only \$20M out of a total program cost of ~ \$10.0B (See Figure 2-3a)).

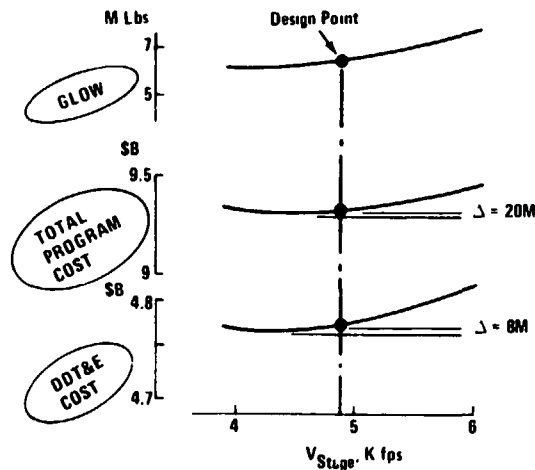


Figure 2-3a Cost of Payload Margin – Series BRB

## 2.2 STACK CONFIGURATIONS

Table 2-1 summarizes the launch configuration characteristics for the configurations derived from the trending data by the application of the 5% payload margin criterion. The shaded columns represent the configurations of primary interest. Figures 2-4, 2-5, 2-6 and 2-7 portray the mission profile for these primary configurations.

As expected, the parallel burn/SRM configurations have higher staging velocities and lower total inert weights than the series pressure fed BRB configuration due primarily to the higher propellant fraction ( $\lambda'$ ) of the SRM's. The propellant fraction,  $\lambda'$ , is the ratio of the nominal propellant to the total weight of the loaded tank. The series pump fed BRB also has a higher  $\lambda'$  and lower total inert weight but its staging velocity is higher than the parallel burn SRM vehicles. This results from the use of the existing F-1 engines in the pump-fed BRB, the established thrust of which requires a more highly lofted trajectory and a higher staging flight path angle to hold  $q_{\max}$  to 650 psf.

Note that only the series/pressure fed BRB and the parallel 156" SRM have payload margins of 5% orbiter inert weight. The parallel/120" SRM and series pump fed BRB payload margins are fallouts related to the sizing constraints identified earlier. The series pump fed BRB payload margin is a direct fallout of the sizing constraint. In the case of the parallel/120" SRM configuration with the booster thrust profile tailored to meet the trajectory constraints, the fallout payload margin is actually only 1400 lb. The noted payload margin (10,700 lb) is achievable by using the existing 1207 thrust profile and propellant quantity and increasing the HO tank propellant capacity from 1.459 M lb to 1.618 M lb. This would result in a GLOW of 4.833 M lb, a staging velocity of 4120 fps, a liftoff  $T/W = 1.41$  and a  $q_{\max}$  of 650 psf.

The other stated payload margins are attainable by increasing the HO tank capacity, with no change to the booster.

The principal dimensional and weight characteristics of the primary configurations are shown in Figures 2-8, 2-9, 2-10 and 2-11 and compared in Figure 2-12. For both the parallel burn and the series burn stack configurations, the orbiter-tank interface is essentially the same. The HO tank, typically, is mounted along the centerline of the lower surface of the orbiter, with the  $LO_2$  tank located forward to hold orbiter engine gimbal angles for cg tracking and control within acceptable limits. Drag loads are transmitted thru the aft orbiter-tank interface only. Both vertical and side loads are transmitted thru both forward and aft interfaces.





Table 2-1 Characteristics Summary

15 x 60							
Launch Configuration	Series				Parallel		
Booster Type	156" SRM	1207 SRM	PR. F. BRB	PMP. F. BRB	1207 LITVC SRM	156" SRM	PR. F. BRB
GLOW, M Lb	4,989	5,363	6,396	4,998	4,580	4,553	5,969
V <sub>Stage</sub> , fps	5367	5615	4879	5298	5067	5095	5373
t <sub>Stage</sub> , Sec	143	143	139	142	137	148	143
Q <sub>Stage</sub> , psf	77	77	70	11	78	55	45
T/W <sub>Stage</sub>	1.184	1.219	1.108	1.100	1.036	1.142	1.071
Alt <sub>Stage</sub> , K Ft	141	143	138	190	138	154	154
Q <sub>Max</sub> , psf	617	653	631	650	647	635	665
W <sub>Stage</sub> , K Lb	1195	1161	1277	1282	1366	1248	1321
Orbiter							
Inject Weight, K Lb	243.8	243.8	243.8	247.8	245.7	245.7	245.7
Inert Weight, K Lb	150.5	150.5	150.5	150.5	152.1	152.1	152.1
Landed Weight, K Lb	184.2	184.2	184.2	184.2	185.8	185.8	185.8
Dry Weight, K Lb	139.4	139.4	139.4	139.4	141.0	141.0	141.0
HO Tank							
Total Weight, K Lb	951	917	1034	1034	1546	1453	1518
V Prop. Weight, K Lb	892	859.7	969	969	1459	1372	1432
Inert Weight, K Lb	59.3	57.4	64.9	64.9	86.7	81.7	86.3
Dry Weight, K Lb	49.7	47.9	54.0	54.0	70.6	68.4	72.5
Booster							
Number	3	6	1	1	4	2	2
Total Weight Ea, K Lb	1265	700.5	5119	3616	697	1427	2102
ΔV Prop. Weight Ea, K Lb	1111	607	4176	3180	607	1280	1701
Inert Weight-Ea, K Lb	153	93.5	943	516	90	167	401
N	878	870	815	857	870	883	809
No. Engines-Ea	1	1	7	4	1	1	4
FSL per Eng, K Lb	2065	1110	1138	1522	1155	2312	790
Payloads							
S. Polar WTR, K Lb	42.7	42.7	42	40	48.5	40.6	39.3
55° ETR, K Lb	41.3	41.3	39.8	43.8	48.3	40	40.7
Due East ETR, K Lb	65	65	65	68.9	65	65	65
Total Inert Weight, K Lb	669	769	1158	736	588	568	1039
Payload Margin, Lb	7500	11,800	7508	16,708	10,708	7500	7500

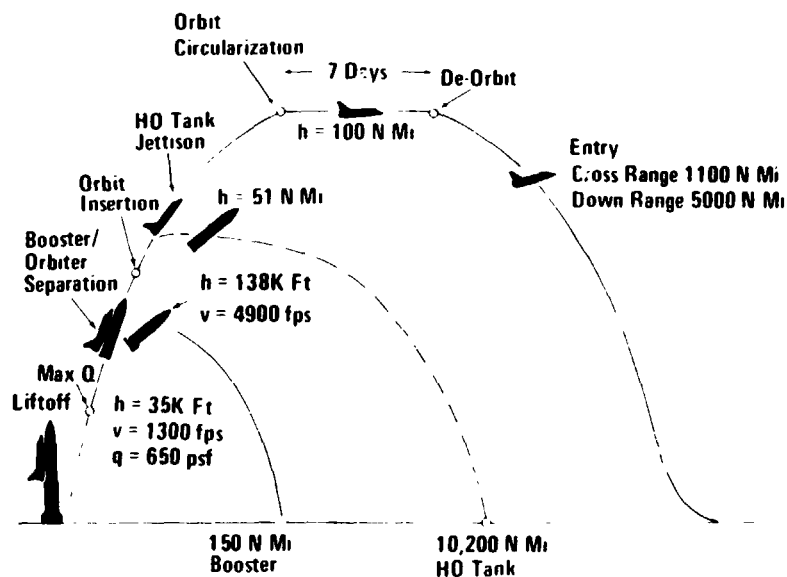


Figure 2-4 Mission Profile - Series BRB (Press-Fed)

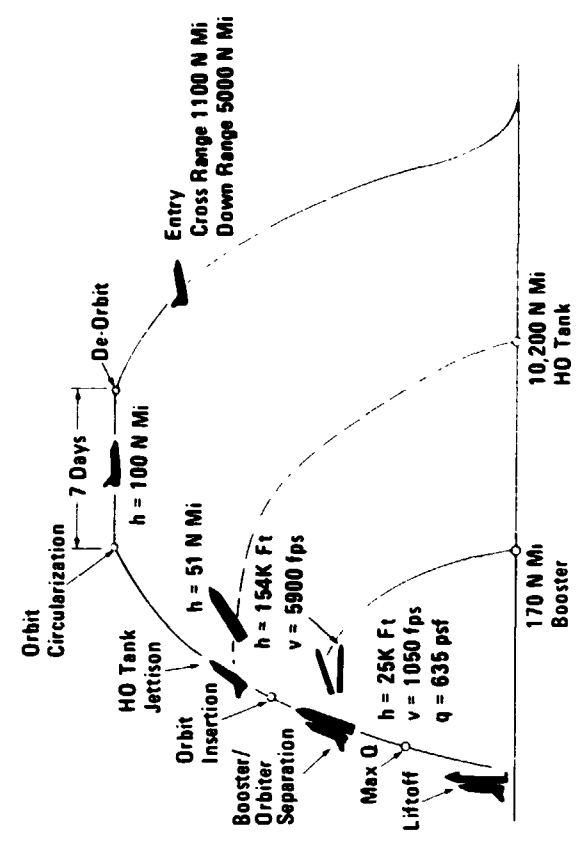


Figure 2-6 Mission Profile - Parallel SRM - 156

PAYLOAD BAY SIZE 15 x 60	
GLOW, M Lb	6 396
BLOW, M Lb	5 118
HO Tank Liftoff Weight, M Lb	1 034
Orbiter Injected Weight, K Lb	244
Total Inert Weight, M Lb	1 158
V <sub>Stage</sub> , fps	4879

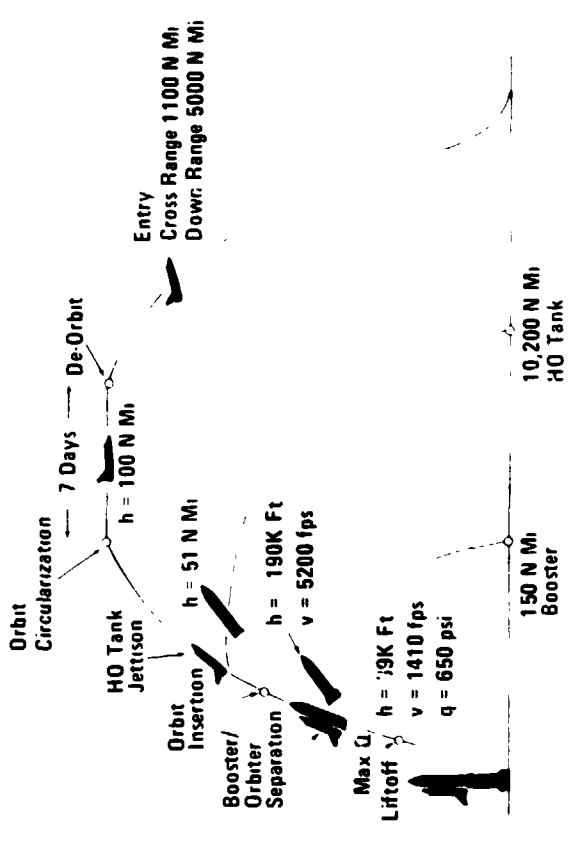
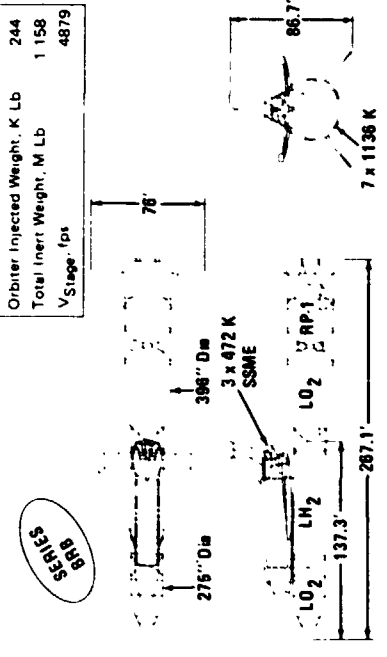


Figure 2-5 Mission Profile - Series BRB (Pump-Fed)

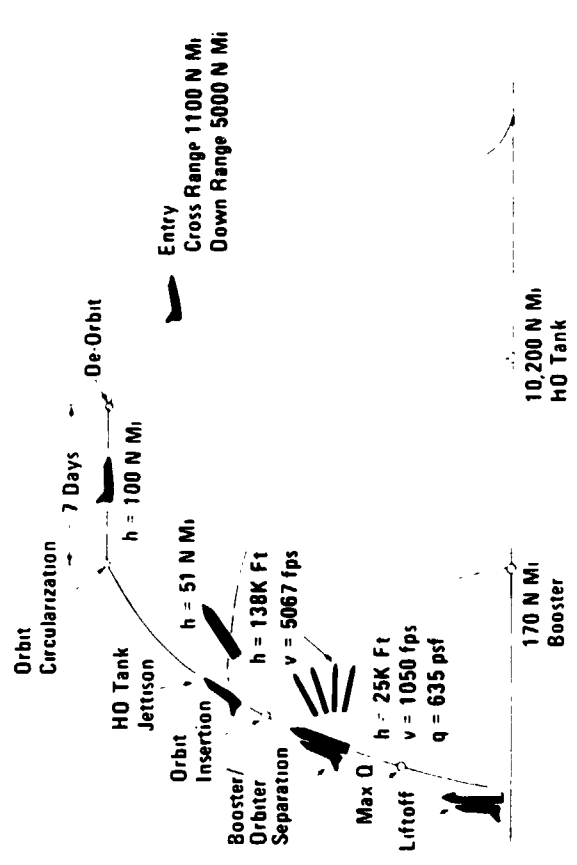


Figure 2-7 Mission Profile - Parallel SRM - 120



Figure 2-8 Series BRB Launch Configuration

PAYLOAD BAY SIZE 15 x 60	
GLOW, M Lb	4,898
BLOW, M Lb	3,616
HO Tank Liftoff Weight, M Lb	1,034
Orbiter Injected Weight, K Lb	246
Total Inert Weight, K Lb	736
V Stage, fps	5208

PUMP  
FEED

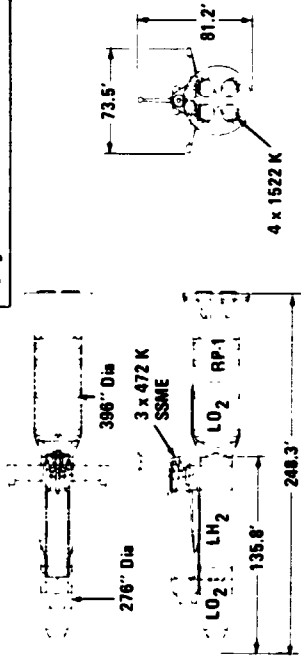


Figure 2-9 Pump Fed Launch Configuration

LAUNCH CONFIGURATION

PAYLOAD BAY SIZE 15 x 60	
GLOW, M Lb	4,553
BLOW, M Lb	2,854
HO Tank Liftoff Weight, M Lb	1,453
Orbiter Injected Weight, K Lb	246
Total Inert Weight, K Lb	568
V Stage, fps	5895

PARALLEL  
SRM

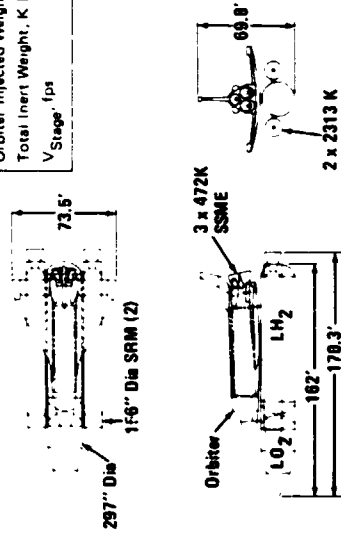


Figure 2-11 Parallel 156 inch SRM Launch Configuration

PAYLOAD BAY SIZE 15 x 60	
GLOW, M Lb	4,560
BLOW, M Lb	2,788
HO Tank Liftoff Weight, M Lb	1,546
Orbiter Injected Weight, K Lb	246
Total Inert Weight, K Lb	598
V Stage, fps	5067

PARALLEL  
SRM

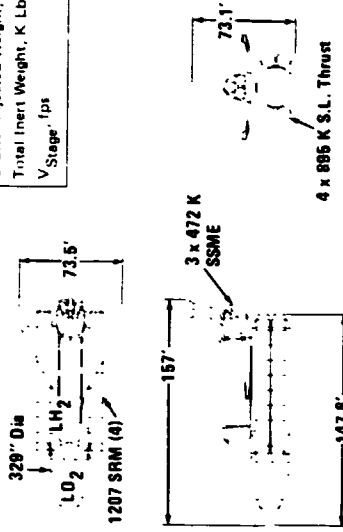


Figure 2-10 Parallel 1207 Launch Configuration

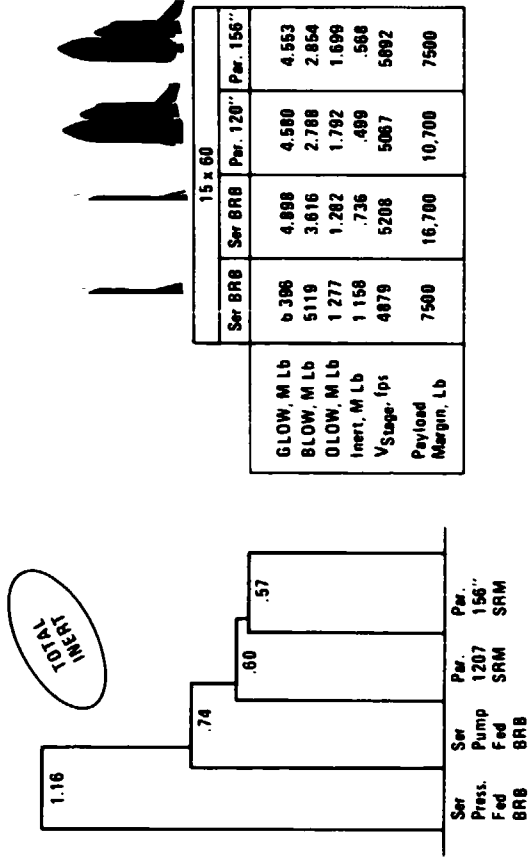


Figure 2-12 Total Inert Launch Configuration Characteristic Comparison

The booster-tank interface, however differs significantly between the series burn and parallel burn configurations. In the series burn arrangement the tank and the booster are mated in tandem by means of an interstage skirt which also distributes the boost loads to the LH<sub>2</sub> tank wall. Consequently, the LH<sub>2</sub> tank walls must sustain the compression loads resulting from the large mass of the liquid oxygen located at the forward end of the tank assembly. To limit the first bending mode frequency of the stack to an acceptable value imposes a more severe requirement on the long slender series stack, and results in a structural weight increase on the HO tank relative to a parallel configuration.

The parallel stack, on the other hand, provides a tank-booster interface that introduces the boost loads at the intertank skirt just below the LO<sub>2</sub> tank. This relieves the LH<sub>2</sub> tank of the large compression loads associated with the LO<sub>2</sub> mass during maximum longitudinal acceleration. Because the boosters and the tank are mated in parallel, the stack height is greatly reduced and the first bending mode frequency limitation imposes no penalty on the parallel burn tank.

This results in a more efficient tank for the parallel burn configuration, that is, less structural weight per pound of propellant carried. This coupled with the improved boost performance of the parallel burn configuration resulting from the simultaneous burn of the orbiter and booster engines (higher average specific impulse) provides a highly efficient launch configuration with lower GLOW's and significantly smaller total inert weight.

However, several technical issues are inherent in the parallel burn configurations that require assessment relative to the series burn configurations:

- HO Tank Mass Fractions and Weights
- Abort Considerations
- Induced Environments
- Control Considerations
- Costs

### 2.3 HO TANK COMPARISON

The assessment of the HO tank mass fractions and weights for the parallel burn configuration relative to the series includes discussions of the structural arrangements and the structural design criteria, each of which contribute to the improved mass fractions for the parallel burn configuration.



### 2.3.1 Structural Arrangement - HO Tank, Series Burn

The series burn HO tank structure shown (Figure 2-13) is designed to minimize structural weight. It is composed of six major subassemblies, the nose cone, retro-motor thrust structure, LO<sub>2</sub> tank, intertank skirt, LH<sub>2</sub> tank and interstage skirt. The nose cone provides the required forebody shape, supports the protective ablator to maintain the thermal environment of the retro-motor and the LO<sub>2</sub> tank forward end. It is constructed of frame-and-stringer-stabilized (semi-monocoque) aluminum alloy sheet. The thrust structure, constructed of stiffened aluminum alloy sheet, with stringers outside and frames inside the web, supports the retro-motor.

The LO<sub>2</sub> tank is a welded aluminum-alloy shell, stabilized in flight by the pressurant gas required for system operation. No stabilizing stiffeners are required; a circumferential flange is provided to support a slosh baffle assembly.

The intertank skirt provides separation between the LO<sub>2</sub> and LH<sub>2</sub> tank end domes, supports the LO<sub>2</sub> tank and incorporates the orbiter forward attachment structure. Retro-

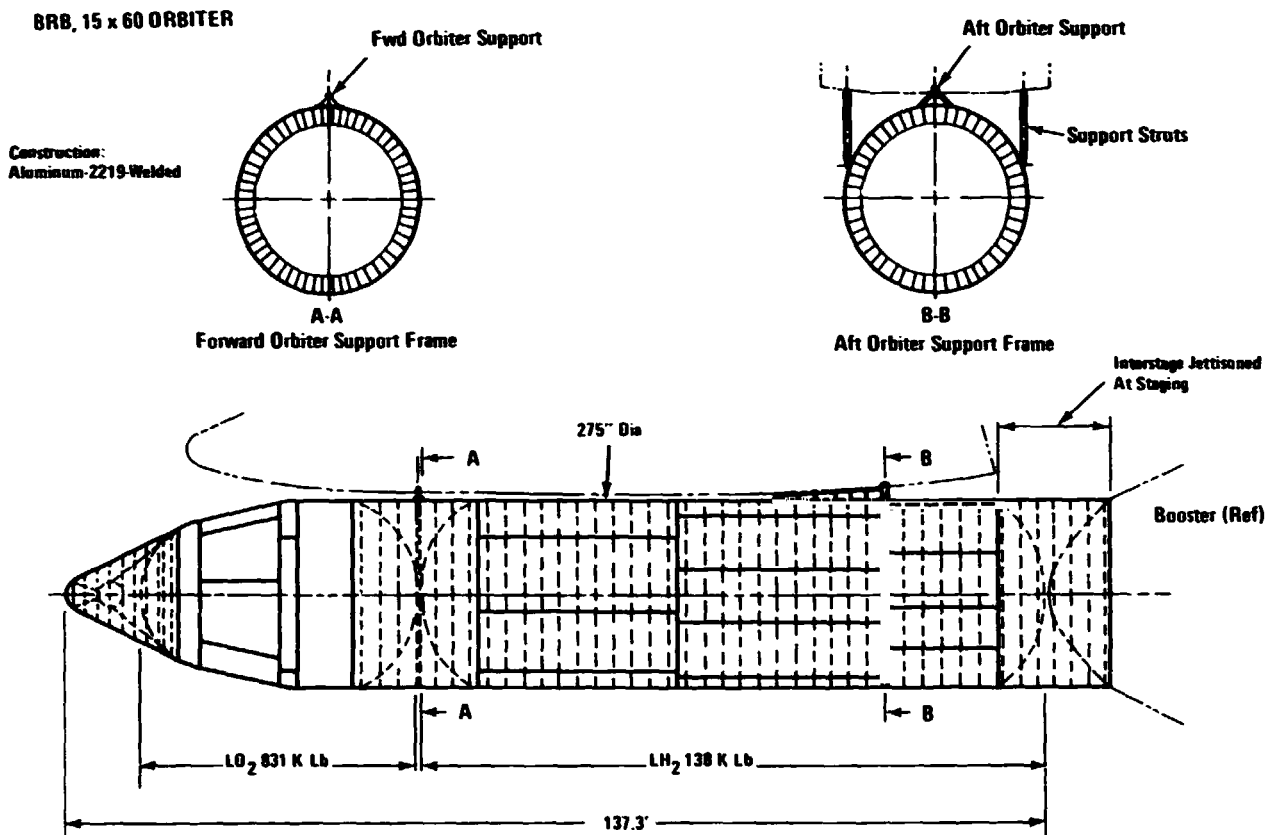


Figure 2-13 BRB, 15 x 60 Orbiter Structural Arrangement, HO Tank, Series Burn

motor ignition and attitude monitoring equipment are supported in this subassembly. Construction is of stiffened aluminum alloy sheet with stringers and frames inside.

The LH<sub>2</sub> tank incorporates the orbiter aft attachment fitting and lateral support strut fittings. Construction is of light-weight grid - stiffened aluminum alloy plates welded into a shell, plus mechanically attached frames for shell stability and shear redistribution. The orbiter aft attachment frame is butt-welded into the pressure vessel.

The interstage skirt provides the interface between the series burn booster and the LH<sub>2</sub> tank. The booster-interstage interface separates at booster burn-out on ignition of a pyrotechnic shaped-charge assembly. The interstage tank interface separates a few seconds later on ignition of a second pyrotechnic shaped-charge assembly.

### 2.3.1.1 Structural Arrangement - HO Tank, Parallel Burn

The structural arrangement of the parallel burn HO tank (Figure 2-14) is similar in construction detail to the series burn arrangement.

The intertank skirt incorporates the forward booster support fittings. The booster thrust is introduced to the skirt structure at these fittings and distributed to the LO<sub>2</sub> tank

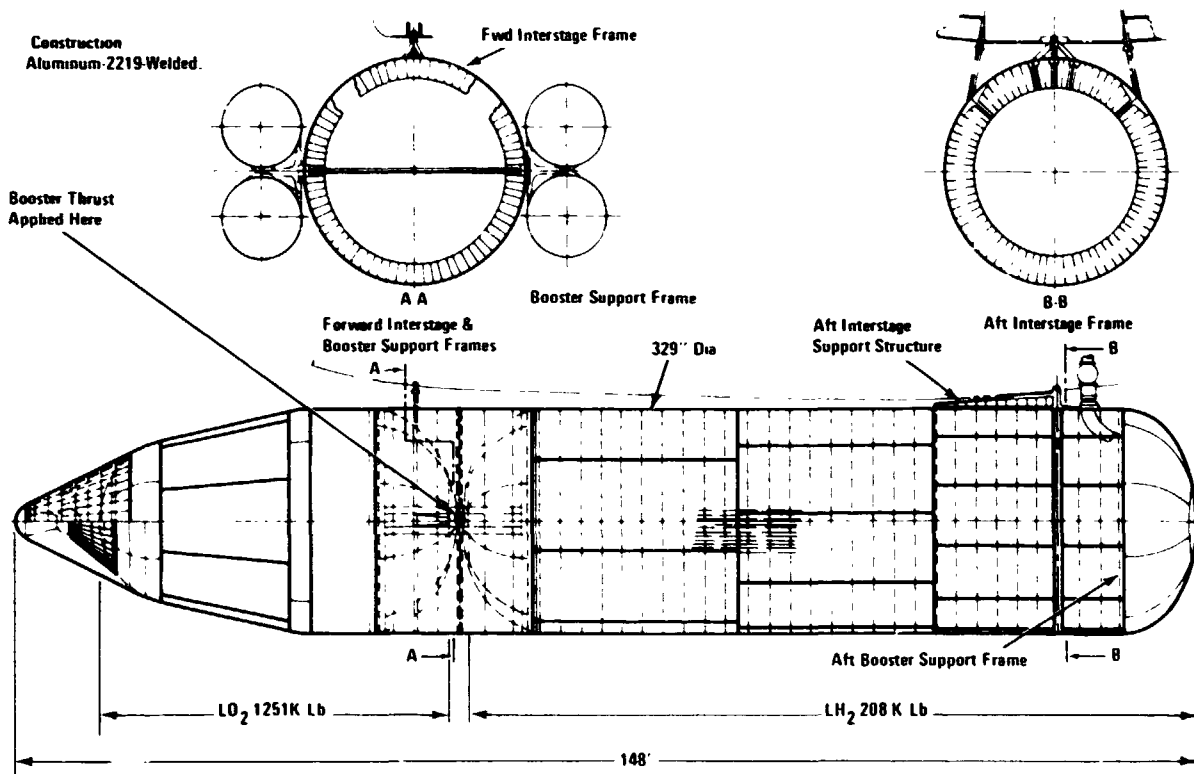


Figure 2-14 SRM, 15 x 60 Orbiter Structural Arrangement, Parallel Burn HO Tank



walls by the skirt. The LH<sub>2</sub> tank aft end incorporates the booster lateral load support fittings in the aft ring, which becomes a major frame. The orbiter aft interstage support structure is located near the LH<sub>2</sub> tank aft ring.

No aft interstage skirt is required.

Both the series and parallel burn HO tanks are of the same basic structural configurations. Welded aluminum construction is used in the pressurized areas, the LO<sub>2</sub> tanks are located and define most of the forward nose cone, and separate tank bulkheads close the LO<sub>2</sub> and the LH<sub>2</sub> tanks. As a result of the parallel burn feature, the HO tank carries from 45% to 70% more propellant than its series burn counterpart.

Although, in general, heavier, the parallel tank is structurally more efficient for the following reasons:

- 1) Booster thrust loads are introduced directly into the intertank area just aft of the LO<sub>2</sub> tank thereby minimizing compression loads in the LH<sub>2</sub> tank.
- 2) At maximum longitudinal acceleration, approximately 30% of the propellants are depleted, thus reducing static pressure head loads.
- 3) No interstage skirt is required at the aft end of the tank.

### 2.3.2 HO Tank Structural Design Criteria

The basic design criteria utilized in sizing the series and parallel burn HO tank structures are the same. Safety factors are 1.40 on ultimate and 1.10 on yield. For both LO<sub>2</sub> tanks, limit system pressure is 38 psia decreasing to 24 psia and the pressurant gases are introduced at 500<sup>0</sup>F. For the LH<sub>2</sub> tanks, limit system pressure is 36 psi and pressurant gases are introduced at 200<sup>0</sup>F. Wall thickness requirements are presented for series and parallel burn HO tanks of equal propellant capacity.

The design conditions for the two tanks are not the same, however, and therein lies one of the advantages of a parallel configuration - namely, a better HO tank. For example, in parallel burn, HO tank propellants are depleted during booster firing such that at booster burnout the propellant tanks are only 70% full. This reduces the design loads which determine tank wall thickness.

#### 2.3.2.1 LO<sub>2</sub> Tank

In both series and parallel burn vehicles, the LO<sub>2</sub> tank is a monocoque design. Combined system and hydrostatic head pressures are the primary design factors and are used to relieve the compression forces due to external loads. The system pressure used in

both cases was 38 psia which decreases with time to 24 psia. Cryogenic allowables were used for the 2219-T87 aluminum walls.

The series tank has two basic design conditions, tank empty and maximum g level. Though the system pressure during the tank empty condition is only 24 psia, the high temperatures due to the 500<sup>o</sup>F autogenous gases make this condition critical for the forward end of the tank. The maximum g level condition designs the aft end of the tank. See Figure 2-15.

The parallel tank, is not full at maximum g level, and thus is partially designed by the lift-off condition. In this tank, the high temperature effects of the 500<sup>o</sup>F autogenous gases again design the forward end, but here a middle portion is designed by the lift-off condition. This is due to the shorter hydrostatic head of the LO<sub>2</sub> during the maximum g level. See Figure 2-16.

#### 2.3.2.2 Mid Skirt

The mid skirt for both the parallel burn and the series burn are designed by axial load at maximum g condition and external bending loads. The structure is integrally stiffened sheet with supporting frames at equal intervals.

The bending loads are small compared to the axial loads. The intertank skirt for the parallel burn configuration is designed to redistribute booster loads to achieve a uniform load distribution at the LO<sub>2</sub> tank joint.

#### 2.3.2.3 LH<sub>2</sub> Tank

In series burn and parallel burn vehicles the LH<sub>2</sub> tank is an integrally stiffened structure with equally spaced frames. The structural sizing of the tank can be examined in two parts; the tank wall analysis and the stiffener analysis.

2.3.2.3.1 Wall Analysis - The series tank wall is designed by the empty tank condition and maximum g level condition. Because hydrostatic head effects on LH<sub>2</sub> are so low, the combination of system pressure (36 psia) and autogenous gas temperatures (200<sup>o</sup>F) design most of the tank wall from the forward end aft. The maximum g condition designs the aft most part of the tank wall. See Figure 2-17.

The parallel LH<sub>2</sub> tank, is again partially designed by the lift-off condition. The autogenous gas temperatures (200<sup>o</sup>F) in the tank cause the forward end to be designed by a hot tank empty condition. The middle section of the tank is designed by the higher pressures of the liftoff condition, and the maximum g condition takes over in the aft end. See Figure 2-18.





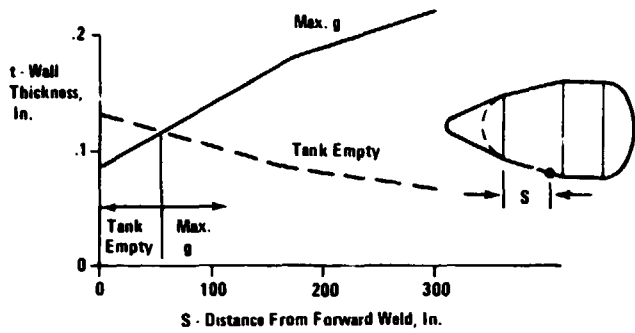


Figure 2-15 Series LO<sub>2</sub> Tank Wall Thickness Variation

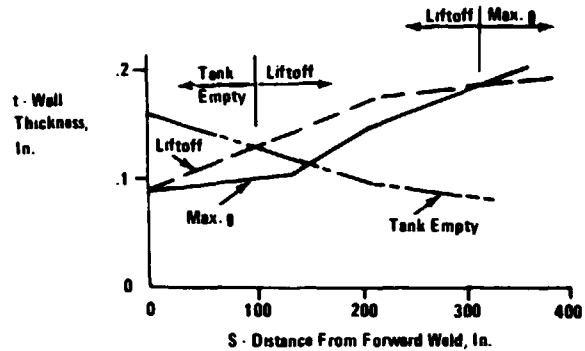


Figure 2-16 Parallel LO<sub>2</sub> Tank Wall Thickness Variation

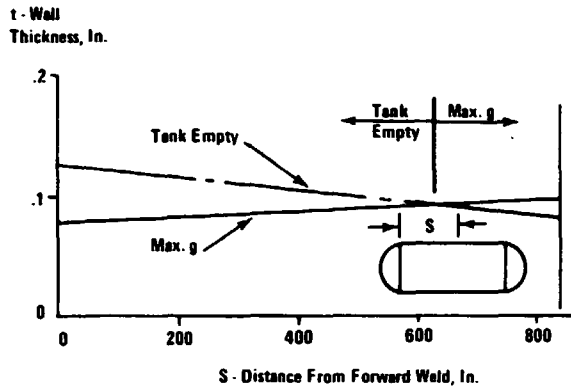


Figure 2-17 Series LH<sub>2</sub> Tank Wall Thickness Variation

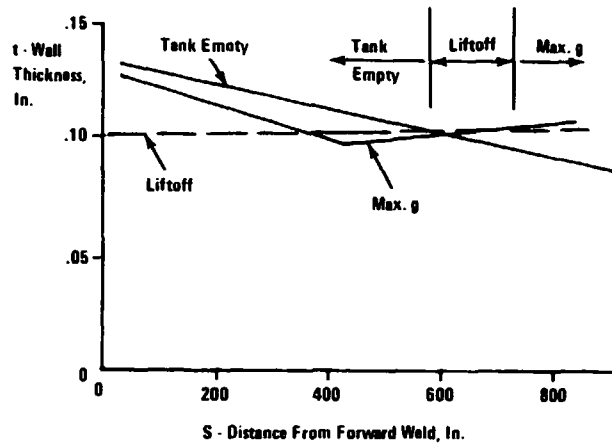


Figure 2-18 Parallel LH<sub>2</sub> Tank Wall Thickness Variation

2.3.2.3.2 Stiffener Design - The stiffeners on the LH<sub>2</sub> tank are sized using the loads calculated from bending and axial design loads at maximum longitudinal acceleration. See Figure 2-19. The ultimate loads are relieved by the limit pressure loads.

The series tank stiffeners are designed by the maximum g condition, and by the bending moment resulting from the off-set orbiter and from the vertical load factor (N<sub>z</sub>) on the LO<sub>2</sub> mass. A longeron, runs along the top of the tank from the drag fitting forward to carry the drag load after separation and from the drag fitting aft for drag loads at maximum g.

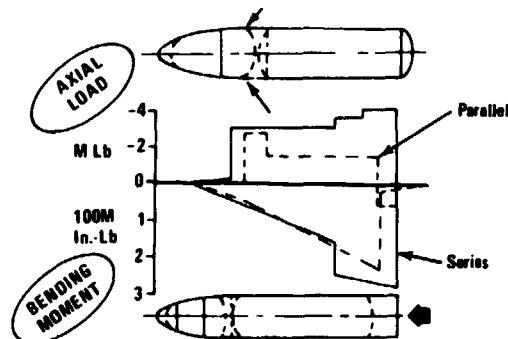


Figure 2-19 HO Tank Design Limit Loads Envelope

The stiffeners on the parallel burn LH<sub>2</sub> tank are designed by two conditions. These are the maximum g condition and the post separation condition. The maximum g condition gives maximum axial load, where the post separation condition gives maximum bending.

The forward section of the tank is designed by the axial load and bending moment of the maximum g condition, and is relieved by the system pressure. The aft end, aft of the drag fitting, has no external loads on it, and therefore is pressure designed.

The top longeron carries the drag load from the orbiter and runs forward of the drag fitting. The two side longerons carry the drag load from the boosters and run aft of this drag fitting. The longerons are needed to shear the drag loads into the HO tank. The center section of the LH<sub>2</sub> tank is designed for this shear lag effect, which is a combination of the effects of the drag loads alone plus the body loads alone, with proper effectiveness factors for the drag only cases. The maximum g conditions and the post separation conditions design this section of the tank.

#### 2.3.2.4 Aft Skirt

The series burn tank requires a small skirt at the aft end to locate the booster-tank separation plane outside the tank structure.

The skirt is designed by the maximum g condition, and is constructed of integrally stiffened sheet. The skirt provides a transition structure between booster and tank which uniformly distributes the loads from skirt to tank.

#### 2.3.3 Tank TPS

The series and parallel burn propellant tankage thermal protection and insulation protects the primary structure from ascent heating from liftoff until tank jettison. The dry nose cone is protected with high density (35lb/ft<sup>3</sup>) ablator (AVCO 5026). The frustum portion of the oxidizer tank is minimum gage SLA561 ablator. The liquid hydrogen tankage is covered with 0.75 in. of polyurethane foam coated to prevent water absorption during ground operations. Ablator protects the interference heat regions between the external tank and the orbiter. Orbiter/external tank supports are protected due to high heat in this area. Feed line and equipment insulation is included in the TPS weight. The parallel burn tank differs from the series burn tank due to the base heating protection required on the exterior of the lower dome of the liquid hydrogen tank. This base heating results from rocket engine plume radiation. The series burn tank does not experience this heating.

#### 2.3.4 Parallel Burn-Series Burn Comparison

A preliminary investigation of parallel tanks compared to series tanks indicates that



each like component is designed by similar types of loads. The LO<sub>2</sub> tanks on both are monocoque and designed by system pressure plus hydrostatic head. The walls of the LH<sub>2</sub> tanks are designed by system pressure plus hydrostatic head. Both require stiffeners for axial and bending loads.

If two tanks of equal propellant capacity were designed for series burn and parallel burn application, we could expect the results shown in Table 2-2 which presents the comparative tank component weights based on the design criteria shown in Table 2-3.

The skirt areas on both are axial and bending load designed. The similarities are apparent, but the conditions which cause these loads and design these areas are different. See Figure 2-20.

Table 2-2 Parallel - Series Comparison

	Series	Parallel	Δfrom Series
LO <sub>2</sub> Tank	9274	7336	-1938
Mid Skirt	4807	3641	-1166
LH <sub>2</sub> Tank	22,320	20,718	-1602
Miscellaneous	620	820	+200
Aft Skirt (Series)	1218		-1218
Booster Attach (Par)		314	+314
Nose Cone	732	732	-
TPS/Insulation	3997	4937	+940
Systems	7200	6645	-555
Dry Weight	50,168	45,143	-5025
Dry Weight Loaded Propellant	.05351	.04842	

Table 2-3 HO Tank Structural Design Criteria

Tank Component	Designed By	Design Condition	
		Series	Parallel
LO <sub>2</sub> Tank	Sys Press. + Head	500°F at 24 psi 3.25g Axial Load, Full Tank	500°F at 24 psi 1.25g at Liftoff 3.2g at 70% Full Tank
Mid Skirt	Axial Load, Primarily	3.25g Axial Load	3.2g + Axial Load
LH <sub>2</sub> Tank Wall Fwd Sect Wall Mid Sect Wall Aft Sect	Sys Press. + Head	200°F at 36 psi 3.25g at Bstr 80 3.25g at Bstr 80	200°F at 36 psi 1.25g at Liftoff 3.0g + at Bstr 80
LH <sub>2</sub> Tank Stiffeners	Bending & Axial Loads	Full Length Cantilever, Bstr 80: N <sub>z</sub> = 0.05 ± 0.1 N <sub>y</sub> = ± 0.1 N <sub>x</sub> = 3.25	Two-Point Support: N <sub>z</sub> = -0.14   Max N <sub>x</sub> = 3.0+   Accel N <sub>z</sub> = -0.27   After Sep

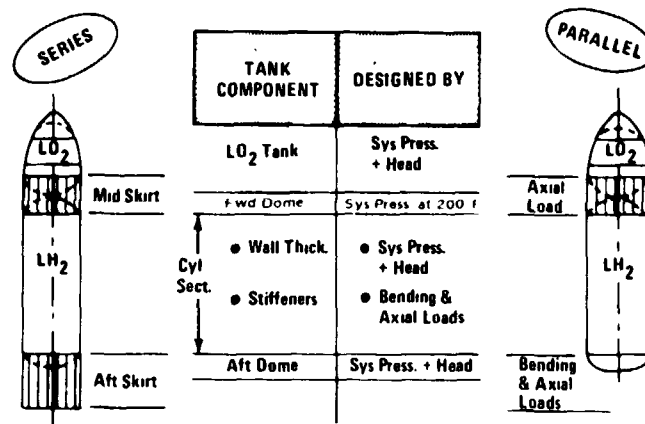


Figure 2-20 HO Tank Structural Design Criteria

Both the series burn and parallel burn tanks are designed by tank empty conditions and maximum g conditions, but since the parallel burn is only 70% full at maximum g, a portion of the tank becomes liftoff critical.

The bending on a series stack is due to the offset of the combined cg from the center-line of the stack plus dynamic effects. The parallel design has the orbiter engines thrusting through this combined cg, but at a very sharp angle. This causes large vertical (Nz) load factors.

Table 2-4 presents a tank weight comparison between the series BRB and the parallel/120" SRM point designs.

The parallel burn tank, though heavier, shows the results of the more efficient structure in the higher propellant fraction and lower structural fraction.

Mass fraction data for HO tanks are presented as two different ratios for both parallel and series tandem configurations. The booster thrust is reacted in the tanks as shown on the diagram.

The mass fraction data was calculated by weight analysis using the previous criteria and design data. See Figure 2-21.

## 2.4 ABORT

### 2.4.1 Introduction

Intact abort is a basic requirement of the Space Shuttle program. This means that at any point in any mission, the vehicle (orbiter and payload) must be capable of returning to a safe landing. The question to be answered by the abort study, then, is not "does the vehicle

Table 2-4 Tank Weight Comparison

Item	Series/BRB 15 x 60	Parallel/SRM 15 x 60
Propellant Weight	968,794	1,458,896
LH <sub>2</sub> Tank	23,628	29,457
Miscellaneous	630	886
Integral/Tank Support	4185	5,591
LO <sub>2</sub> Tank	10,134	12,134
Aft Skirt	885	-
TFS/Insulation	4067	7574
Nose Cone	722	1384
Separation/De-Orbit	3800	4916
Propulsion	2189	2228
Electronics	350	483
Contingency	1012	1291
Thrust Structure	-	-
Total Dry Weight	51,593	65,844
Propellant Fraction	.9372	.9439
$\frac{\text{Dry Weight}}{\text{Loaded Propellant}}$	.0525	.0445

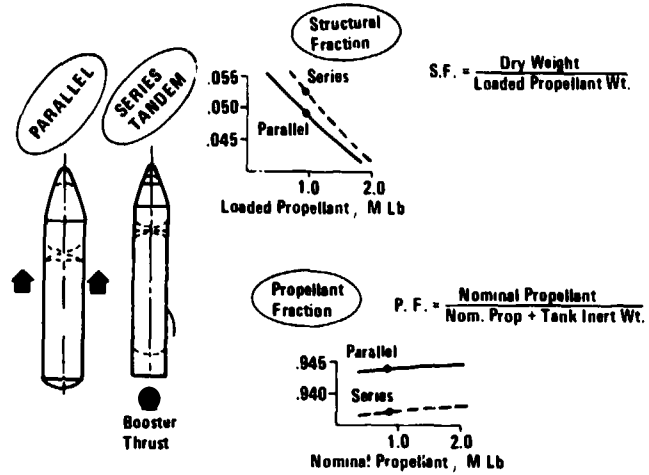


Figure 2-21 HO Tank Mass Fractions

satisfy the intact abort requirements?" but rather "how does the vehicle satisfy the intact abort requirement and how does it impact the design?"

#### 2.4.2 Abort Modes

The first step in any abort study is the determination of the operational modes to meet the intact abort requirement. For this study the following abort modes were established:

- Mode I - Pad Aborts/Fallback Zone
- Mode II - Orbiter Glide Returns
- Mode III - Orbiter Powered Returns
- Mode IV - Abort to Once Around
- Mode V - Abort to Safe Orbit

These abort modes were developed based on the type of critical failures and the time of occurrence. Mode I aborts are designed to eliminate the fall-back zone and to provide escape from an imminent booster explosion. (See Section 6). Mode II and III aborts (pre-staging) are considered sufficient to guarantee intact abort in the event of a booster malfunction. Modes III, IV and V (post-staging) are developed for the case of an orbiter engine failure.

#### 2.4.3 Configuration Options

Once the operational modes have been established, it is then necessary to determine the most feasible design option which permits performance of the abort modes.

The abort mode regions for the two basic configurations, series BRB and parallel SRM (156"), are shown respectively in Figures 2-22 and 2-23 for both the south polar and due east mission.

#### 2.4.3.1 Mode II Aborts

In the region of maximum dynamic pressure during nominal ascent the abort mode is a glide return to the launch site. In this mode the orbiter separates from the booster and the HO tank (the booster and tank remain mated) and flies with only aerodynamic control (no power). The orbiter's initial maneuver is an inverted flight at high normal loads, not exceeding the structural limits to bring the velocity vector to near horizontal. Once this is achieved, the vehicle performs a banked turn at a bank angle of approximately 45 degrees until the velocity vector is directed at the launch site. The orbiter then continues to glide to a landing at the launch site. The abort mode is possible for either the parallel or series configuration during the region of the ascent between approximately 10,000 and 80,000 ft altitude. Figure 2-24 shows a representative abort from an altitude of 32,000 ft.

This abort mode is satisfactory for recovery since the orbiter is positioned such that a glide return to the launch site is possible and a certain amount of excess energy is available for maneuvering. None of the profiles in this abort mode violate any of the vehicle design limits. After the initial maneuver to achieve horizontal velocity vector, the descent profile is similar to the terminal landing phase for the nominal re-entry.

#### 2.4.3.2 Mode III Aborts Pre-and Post-Staging

For abort conditions at higher altitudes (above 8000 ft) the abort mode involves separation from the booster at the booster/tank interface, continued thrusting of the orbiter main engines to depletion of the HO tank propellant, separation of orbiter and tank and a glide return to the landing site. In this mode, Mode III, the problem of the separation of the tank from the orbiter in a sensible atmosphere at orbiter burn-out conditions permitting a safe entry must be considered. Figure 2-25 shows the relationship of tank staging and orbiter entry conditions. To avoid exceeding the entry acceleration defined by the orbiter structural limit, tank staging must occur at dynamic pressures of 5 to 10 psf. This is within the design capability of the present tank separation mechanism.

The Mode III abort technique developed for return of the orbiter vehicle to the launch site consists of orbiter separation with the main engines at full thrust and then, shortly after separation, throttled down to climb to an altitude above 200,000 ft with a minimum use of propellant. The OMS is ignited at an altitude of approximately 150,000 ft to assist the ascent and to ensure that its propellants are depleted prior to landing. At altitudes above

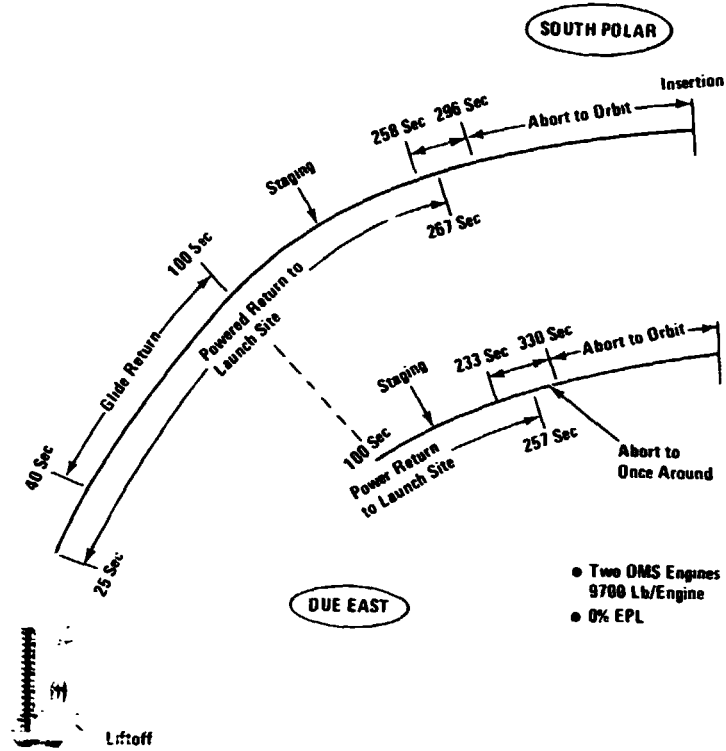


Figure 2-22 Series BRB Abort Modes

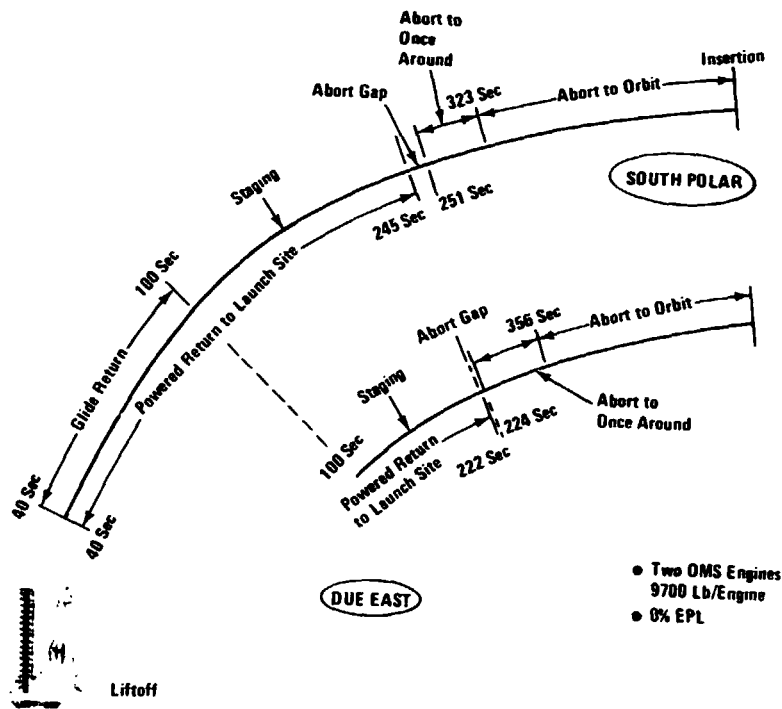


Figure 2-23 Parallel SRM (156'') Abort Modes

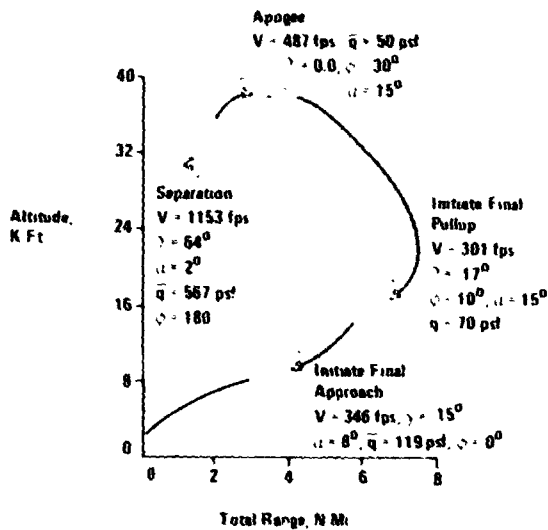


Figure 2-24 Mode II Abort From 32K Ft

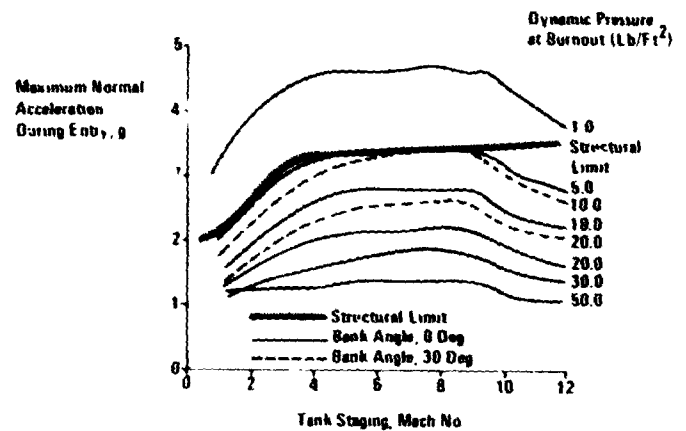


Figure 2-25 Mode III Effects of Tank Staging Conditions on Orbiter Abort Entry

200,000 ft, and dynamic pressures of less than one psf, the orbiter is reoriented and the thrust increased to maximum to reduce the forward downrange velocity to zero and then to gain velocity in the direction of the launch site. Throughout this portion of the flight, the explicit guidance is targeted to achieve a zero flight path, and a velocity and attitude which are compatible with tank staging requirements. Control of the downrange location of the burnout point relative to the landing site is performed by the appropriate selection of the guidance parameters used to achieve the proper burnout altitude and velocity. During the early period of thrusting orbiter angles of attack up to 180 degrees are required. Preliminary studies performed have indicated that these conditions are acceptable from an aerodynamic stability and orbiter heating standpoint since the dynamic pressures are less than 1 - 2 psf.

Figure 2-26 presents a Mode III abort flight profile. The procedure outlined is typical of Mode III aborts from pad abort through nominal staging and into the orbiter burn. Table 2-5 presents the limit for Mode III aborts after staging for both the series BRB and parallel SRM (156") configurations for the polar and due east missions.

#### 2.4.3.3 Mode IV Abort To Once Around

Prior to orbiter burnout there exists a region in which insertion into the nominal 51x100 n mi orbit is no longer feasible nor is a return to the launch site possible with one orbiter engine inoperative. In this region, abort to a once-around (16x176 n mi) orbit and subsequent return to the launch site can be accomplished. The procedure in this region necessitates the retargeting of orbiter guidance to alternate burnout conditions whose resulting orbit provides a high degree of flexibility in achieving entry interface conditions.





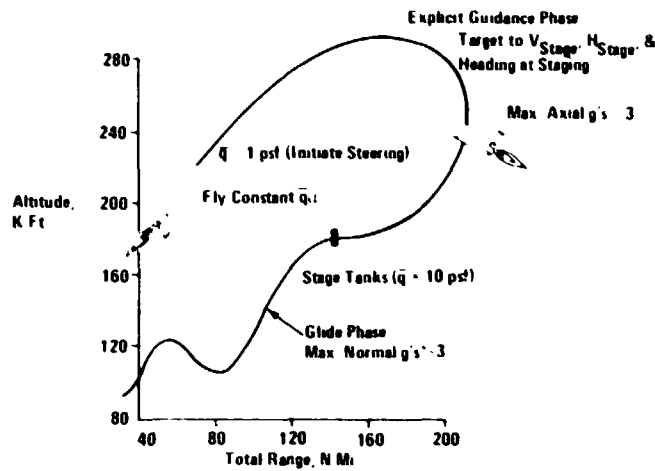


Table 2.5 Post Staging Mode III Abort Capability

Mission	Mode III Abort Limit, Seconds After Staging	
	Series BRB/SSME	Parallel SRM (156")/SSME
Due East	118	74
South Polar	127	96

Figure 2-26 Mode III Abort Return to Launch Site

Aborts to once around are predicated upon the use of the OMS firing in parallel to allow capability from the limiting time for Mode III aborts.

The orbital parameters of the once around orbit satisfy the following considerations:

- Inertial velocity and flight path angle at entry interface falls within the entry corridor (Figure 2-27), and the flight path angle is at least 0.1 degrees below the skip out boundary to safely compensate for navigational uncertainties.
- Orbiter downrange requirement from entry interface to the launch site is less than the orbiter's maximum downrange capability.
- The required once-around insertion velocity for the orbiter at 300,000 ft is attainable with one engine out at design EPL on the remaining engines.

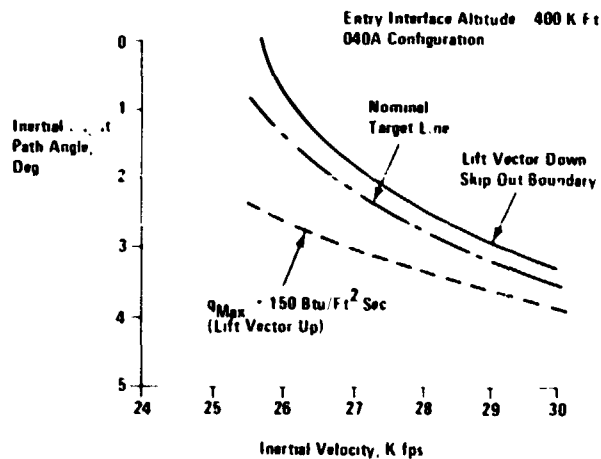


Figure 2-27 Mode IV Entry Corridor

Figure 2-28 presents the Mode IV one-engine-out insertion conditions compatible with the above constraints.

The use of a once around orbit provides an effective means of providing abort capability in the region bounded by Mode III and by abort to the nominal orbit.

#### 2.4.3.4 Mode V Abort To Orbit

As the orbiter nears nominal insertion, the orbiter can abort to the nominal 51 x 100 n mi orbit. If sufficient OMS propellant is retained (approximately 6,900 lb) to allow for circularization and deorbit, degraded missions can be performed for non-time critical aborts. The minimum OMS requirement is 3,200 lb to allow for a targeted de-orbit maneuver whose entry interface conditions satisfy the requirements for Mode IV aborts.

#### 2.4.3.5 Abort Gap

In the vehicle ascent there is a point in time beyond which it is no longer possible to perform a one-engine-out powered return to the launch site. At this point there is just sufficient energy remaining to turn the vehicle around, using the main propulsion system, and glide to the launch site. There is also another point in the ascent prior to which an abort to once-around, with one engine out, cannot be accomplished. At the threshold point there is just sufficient OMS propellant to compensate for the additional  $\Delta V$  required for the one-engine-out conditions. When the abort to once-around threshold occurs later in the ascent than the powered return to the launch site limit, then there exists what is known as an "abort gap". If a failure requiring abort occurs within this region, no abort mode would return the vehicle to the launch site. An alternate landing site would be required to satisfy the intact abort requirement.

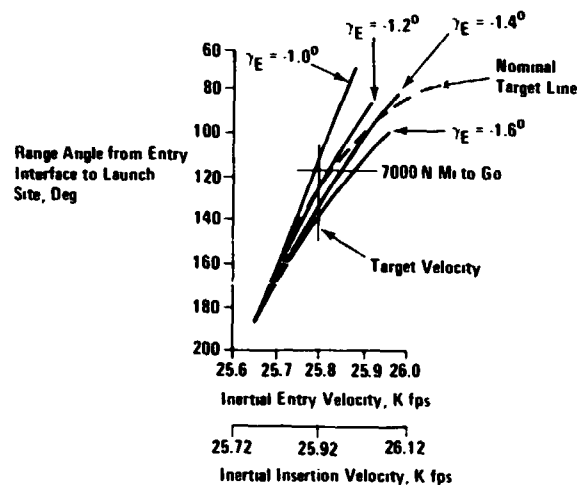


Figure 2-28 Mode IV Engine Out Abort Insertion Conditions



Rather than require the development of alternate landing sites, it is desirable to eliminate the gap through vehicle design modifications. To close the abort gap, we can increase the main engine emergency power level (EPL), increase the OMS thrust level or increase the main propulsion system (MPS) propellant reserves.

Combinations of these three methods were considered, the first being increased OMS thrust and increased main engine EPL. Figure 2-29 shows the relationship of OMS thrust and main engine EPL to the abort gap abort mode overlap. The figure shows that at an OMS thrust level of 7,000 lb per engine (with two OMS engines) a sizeable abort gap exists for both the parallel and series configurations unless a large main engine EPL is used (9% for the series and greater than 15% for the parallel). Increasing the OMS thrust level to 9,700 lb completely eliminates the abort gap in the series configuration and requires less than a 3% main engine EPL (less than the design EPL) to close the gap for the parallel configuration. Increasing the OMS thrust level to 9,700 lb, a level which appears to be a minimum requirement from the standpoint of orbital maneuvers as well, is a simple and economic method of eliminating the abort gap.

Another approach considered to close the abort gap was a combination of increasing the MPS propellant reserves and increasing the main engine EPL. Figure 2-30 shows, for both the series and parallel configurations, the MPS propellant reserves required as a function of the main engine EPL to eliminate the abort gap. The data is for the due east mission only at an OMS thrust level of 7,000 lb which represents the worst case mission. The figure shows that at 0% EPL the additional MPS propellant reserves required for the series and parallel configurations are 2,700 lb and 5,600 lb respectively. If this additional MPS propellant reserves is included in the flight performance reserves (FPR) then the in-

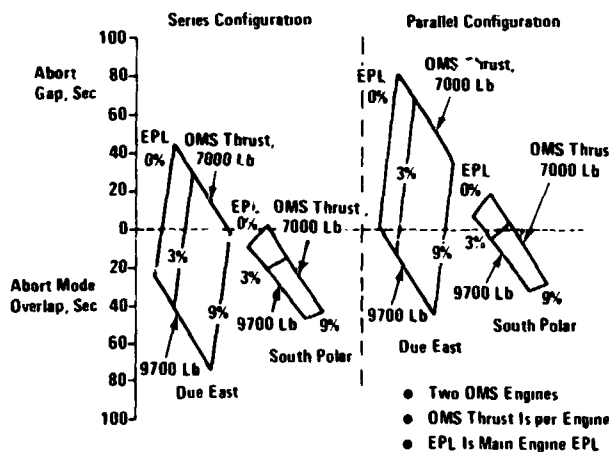


Figure 2-29 Abort Gap

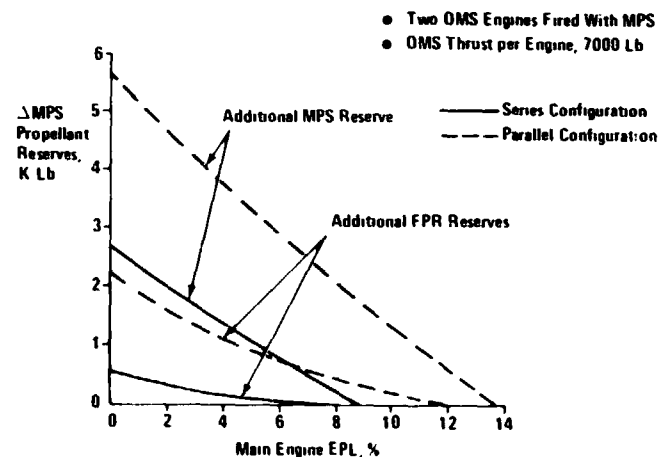


Figure 2-30 Due Mission MPS Reserve Requirement for No Abort Gap

creases in the FPR are 600 lb and 2,200 lb, respectively, for the series and parallel configurations. At higher levels of EPL the MPS propellant reserves are significantly reduced but not in comparison to the reduction achieved by increasing the OMS thrust level. At an OMS thrust level of 9,700 lb the abort gap is closed with no additional MPS propellant reserves at 0% EPL for the series configuration and at 3% EPL for the parallel configuration.

Therefore the intact abort requirement can be readily satisfied without the necessity for considering alternate landing sites.

## 2.5 INDUCED ENVIRONMENT

### 2.5.1 Introduction

The nature of the parallel burn launch arrangement and the relationship between orbiter and booster engines, produces an acoustics, vibration and interference heating environment which imposes penalties on the orbiter and the HO tank structure not present in the series burn configuration.

### 2.5.2 Acoustics

An assessment of typical acoustic spectra was made for both series burn and parallel burn configurations in order to perform an acoustic fatigue analysis on various parts of the orbiter/tank structure.

Some typical spectra used in the sonic fatigue analysis are shown in Figure 2-31. The other spectra used in the analysis were similar in spectral shape but slightly different in overall sound pressure level. All, except one applicable to the fin area, were derived from the rocket engine firing during lift-off, using the Wilhold, Jones, Guest method presented in CPIA Publication 194 (October 1971). The fin spectrum for the series burn was derived from transonic flow conditions as measured during recent wind tunnel tests at AMES and fitted to a spectrum which was essentially constant below 100 Hz and rolled off at 6 db per decade above 100 Hz. This was dictated by previous experience in transonic phenomena. More recently, actual spectra for three locations have been received from AMES and these show excellent agreement with the fitted data in the frequency range below 400 Hz.

The overall sound pressure levels that occur during liftoff for both the parallel and series burn configuration are shown in Figure 2-32. These levels were derived using the G. Wilhold, S. Guest, and J. Jones method which takes into account such engine characteristics as nozzle diameter, weight flow rate, exit velocity and thrust.



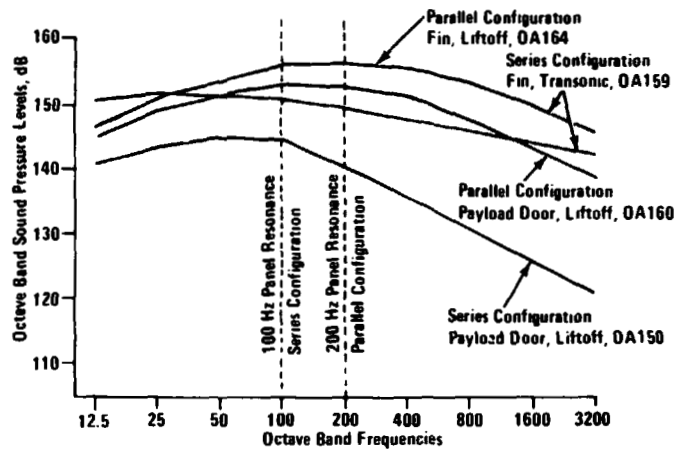


Figure 2-31 Typical Acoustic Spectra To Determine Sonic Fatigue Weight Penalty

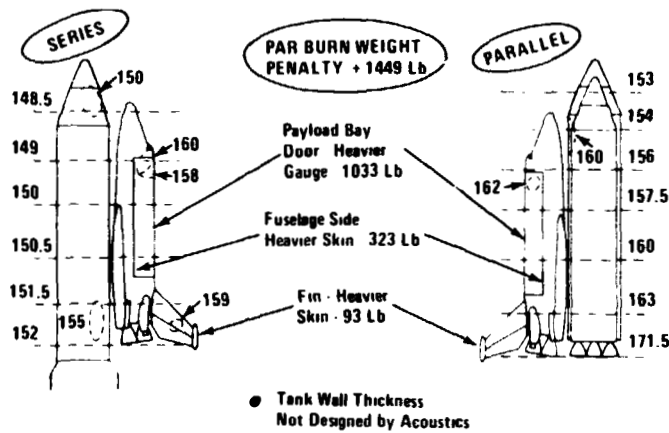


Figure 2-32 Orbiter - Acoustic Weight Penalty of Parallel Burn

In addition to the liftoff environment, areas are shown where it is expected that transonic boundary layer pressure fluctuations will cause the dominant panel response. These areas were located using measured data from a 1/25th scale model test conducted in the 11 ft x 11 ft transonic wind tunnel at the Ames Research Center. The fluctuating pressure levels were then adjusted to account for the inefficiency of the boundary layer pressures to excite the fundamental panel resonance. Information presented by Barnoski, et al., NASA CR-1302, indicates that at the fundamental resonance, the panel response to boundary layer pressure fluctuations will be 6 db less than the response to a reverberant noise field. The transonic wind tunnel test data therefore was reduced by 6 db and inserted in those areas where it exceeded the liftoff environment.

Acoustic fatigue analyses incorporating both the transonic and liftoff environment were conducted for the payload doors, side fuselage area, and fin. The payload doors and

side fuselage consist of corrugated aluminum structure with insulating material attached to the external skin. Procedures presented in "Structural Design for Acoustic Fatigue", ASD-TDR-63-820, were used to check the design of this structure. For the series burn configuration it was assumed that the fundamental resonance occurred at 100 Hz. The spectrum level and the number of cycles to failure were based on this frequency. A scatter factor of four in time was incorporated into the fatigue life calculation. For the parallel burn configuration, stiffer structure is required to withstand the higher sound pressure levels. Here the fundamental resonance was taken as 200 Hz along with the appropriate spectrum level at this frequency. The analysis of the two configurations indicates that the more severe parallel burn environment requires an increase in structural weight of the cargo doors and side fuselage as shown in Figure 2-32.

The fin structure, which is aluminum skin-stringer construction, was analyzed using procedures presented in AFFDL-TR-67-156 "Refinement of Sonic Fatigue Structural Design Criteria", to determine the structural weight penalty for the parallel burn acoustic environment. The transonic flight acoustic environment designs the fin for the series burn configuration while the more severe liftoff acoustic environment is the design condition for the parallel burn. The analysis is based on an assumed resonance at frequencies of 100 and 200 Hz and the sound levels defined for the two configurations (Figure 2-32). The sonic fatigue analysis is conducted using a damping ratio of .02, based on the assumption that no increase results from the insulating material attached to the external skin. The resulting weight penalty is shown in Figure 2-32.

Because of the short life of the expendable HO tank, fatigue is not a critical consideration thus the tank structure, as designed by boost loads, internal pressure and the launch thermal environment meets the requirements of the acoustic environment without penalty.

Table 2-6 details the weight penalty for the particular orbiter structural element and states the assumptions made.

### 2.5.3 Vibration

The vibration environments experienced by the fin-mounted RCS Regulator for series and parallel burn configurations are shown in Figure 2-33. The RCS Regulator is an off-the-shelf equipment used in the Apollo program in the LM and the CSM. It was qualified to the levels shown. The vibration environment, derived from the acoustic excitation resulting from the rocket engine firing, is 20 db higher for the parallel burn than for the series burn configuration. In order to derive vibration environments a scaling technique was used taking into account a data bank of vibro-acoustic information collected for struc-



Table 2-6 Effect of Acoustic Environment on Structural Weight – Parallel Burn Versus Series Burn

Structure	Required Structure Series Burn	Required Structure Parallel Burn	Design SPL Series Burn	Design SPL Parallel Burn	Weight Penalty, Lb
Payload Doors	Sta 700 to 1314 Corrugated Sheet 0.016" Face Sheet 0.016" Corrugation	Sta 700 to 985 Corrugated Sheet 0.031" Face Sheet 0.024" Corrugation Sta 985 to 1314 0.052" Face Sheet 0.041" Corrugation	Liftoff Noise 144 db in 100 Hz Octave, Sta 700 to 985 Liftoff Noise 146.5 db in 100 Hz Octave, Sta 985 to 1314	Liftoff Noise 151 db in 200 Hz Octave, Sta 700 to 985 Liftoff Noise 156.5 db in 200 Hz Octave, Sta 985 to 1314	1033
Fuselage Side Area	Same as for Payload Doors Over About 20% of Area	Same as for Payload Doors Over About 20% of Area	Same as for Payload Doors Over About 20% of Area	Same as for Payload Doors Over About 20% of Area	323
Fin	0.040" Sheet (Skin & Zee Stringer Construction)	0.054" Sheet (Skin & Zee Stringer Construction)	Transonic Aero. Noise 159 db O.A.	Liftoff Noise 164 db O.A.	93
				Total	1449

ASSUMPTIONS

- For the series configuration the 0.016" corrugated structure has a fundamental resonance in the 100 Hz octave band
- For the parallel configuration, the corrugated structure will be heavier resulting in a higher fundamental resonance (in the 200 Hz octave band)
- Aerodynamic boundary layer noise is less efficient at exciting the fundamental resonance than lift off noise. The same level of aerodynamic noise will induce 50% of the response that lift off noise would induce or a 6 db difference (see p. 66 of NASA CR 1302)
- The design methods used were
  - For skin stringer designs use 2% damping ratio  
Reference: "Refinement of Sonic Fatigue Structural Design Criteria", AFFDL TR 67 156, Ballentine, J.R., et al
  - For corrugated structure damping is not explicitly called for  
Reference: "Structural Design for Acoustic Fatigue", ASD-TDR 63 820

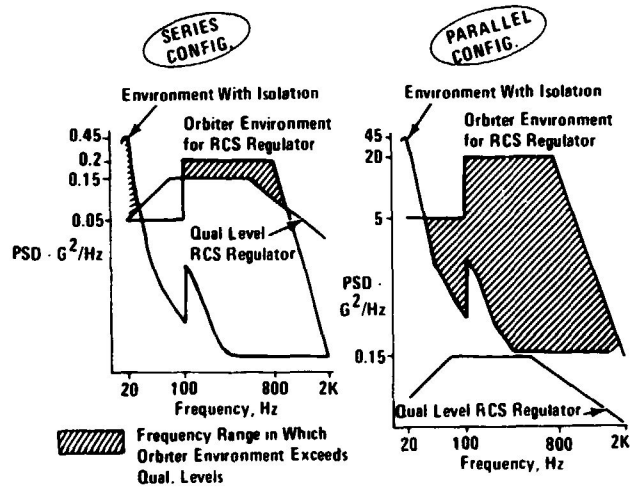


Figure 2-33 Aft End Vibration Environment Comparison

ture similar to that of the orbiter. This data bank is presented in Boeing Report D5-17129 of August 31, 1971 - "Development of Vibro-Acoustics Structural Data Banks." The curves in the left hand portion of Figure 2-33 portray the relative severity of the series configuration fin environment, the RCS Regulator qualification levels and the environment as modified by an isolator system for the regulator. The hatched area represents the region in which the environment exceeds the qualification levels of the equipment. For the isolated equipment only the low frequencies are involved. By using sinusoidal qualification data (not shown) the integrity of the equipment can be demonstrated in this frequency range. In the right hand set of curves, representing the parallel burn vibration environment it makes little difference whether isolation is employed or not. The vibration environment is so much higher than the qualification levels that isolation is incapable of reducing the environment sufficiently to gain confidence in the equipments ability to withstand the vibration without additional tests or equipment modification.

In the cabin equipment bay, the difference between parallel and series burn levels is only 6 db. Still there is off-the-shelf equipment which has not been qualified to the parallel burn levels in some frequency regions. Figures 2-34 and 2-35 show three such items; the Air Data Computer and the Primary Computer, plotted on Figure 2-34 and the Inertial Measuring Unit plotted on Figure 2-35. The qualification levels are exceeded by the parallel burn environment in the frequency range above 200 Hz for the IMU and over the entire frequency range for both computers. The design of an isolator system for each piece of equipment, however, reduces the vibration levels experienced by each equipment to within the qualification levels.

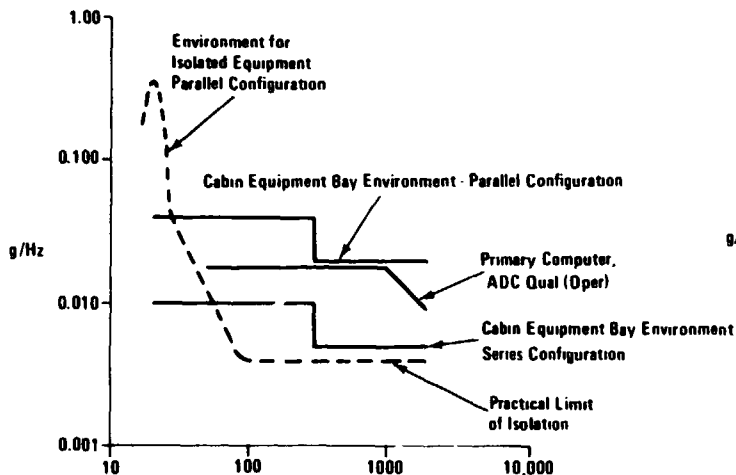


Figure 2-34 Cabin Vibration Environment With Computer Qual Levels

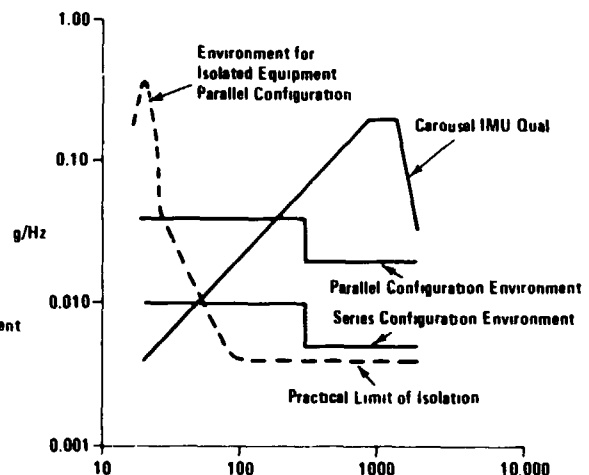


Figure 2-35 Cabin Vibration Environment with IMU Qual Levels





#### 2.5.4 Heating

The heating environment for the HO tank during ascent is more complex and more severe for a parallel burn/SRM configuration than for a series burn/BRB configuration. The shocks generated by the SRM noses amplify the heating on the HO tank while the SRM plumes heat the base of the HO tank and cause plume induced recirculation heating as shown in Figure 2-36. However, since the SRM's are carried for a relatively short duration through the low-altitude, low-velocity portion of the ascent trajectory, the magnitude of flow dependent heating effects tend to be small as shown in Figure 2-37.

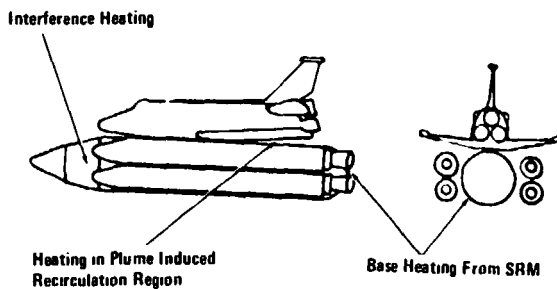


Figure 2-36 Areas of Concern

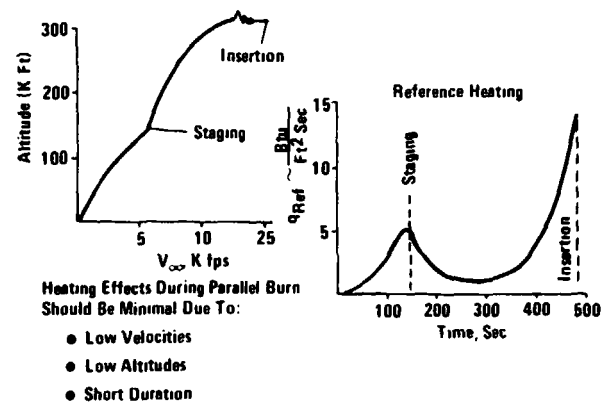


Figure 2-37 Parallel Burn Ascent

The shocks generated by the SRM noses impact the HO tank on the intertank structure. Except for a small region protected by ablators for Orbiter/HO tank interference heating, the baseline series burn/BRB HO tank intertank region is bare aluminum. The amplification of heating due to shock interference is a strong function of Mach number and the state of the boundary layer. It increases with increasing Mach number and is greater for a laminar than for a turbulent boundary layer. Since the SRM is separated from the HO tank at a low Mach number, Mach 6, and since the boundary layer is turbulent during most of the parallel burn duration, amplifications are small. The bare aluminum intertank region, designed for structural purposes, can easily accommodate the small increase in heating, never seeing a temperature higher than 280°F. See Figure 2-38.

The plume induced recirculation phenomena is sufficiently complex so that reliance must be placed on existing flight data rather than analytical methods. The S-IC data base is summarized in Figure 2-39. From this data it can be seen that the extent of recirculation region and the increase in heating it causes are minimal up to an altitude of 120,000 ft.

The parallel burn configuration stages at 140 K ft. To fully account for differences between S-IC and SSME characteristics and geometries, plume boundaries were established

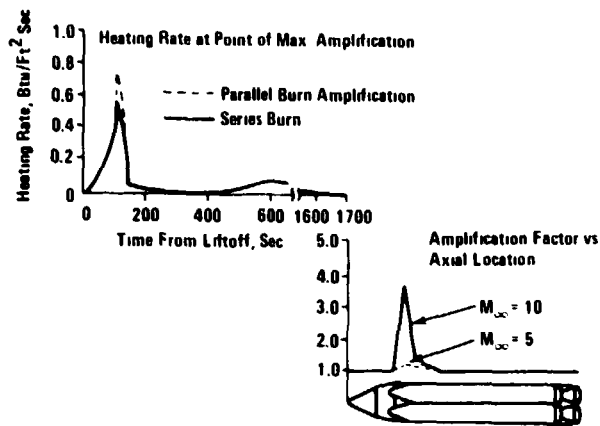


Figure 2-38 HO Tank Heating Due to Shock Interference

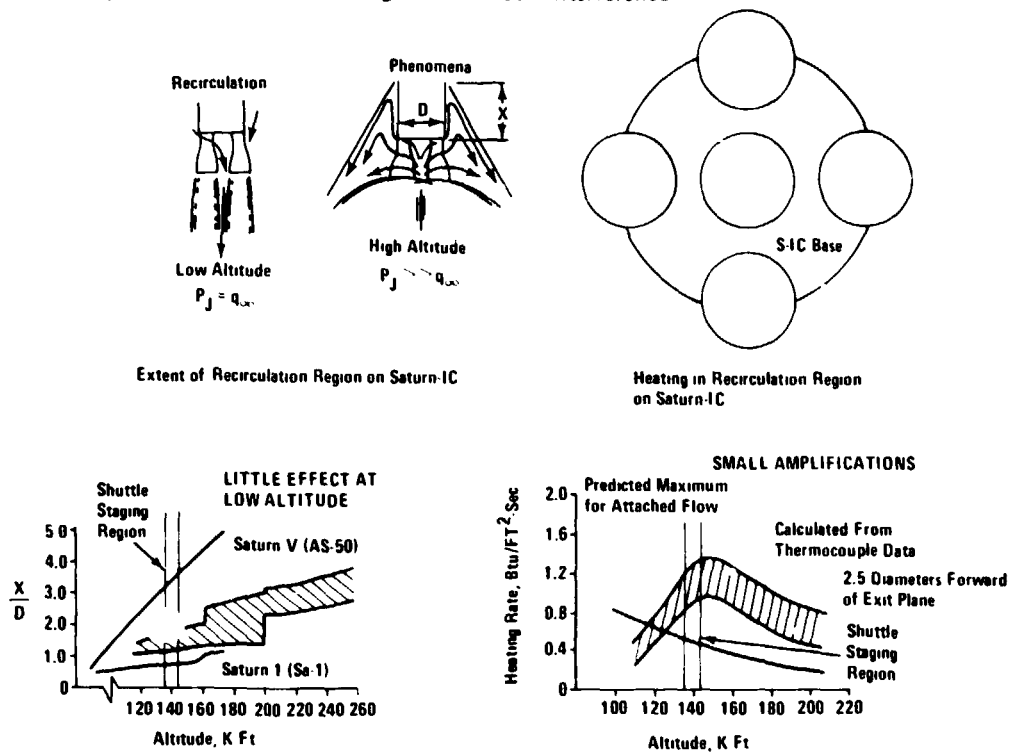


Figure 2-39 Plume Induced Recirculation

for the parallel burn 120" SRM/3 SSME orbiter configuration which are shown on Figure 2-40. These boundaries show that, while recirculation due to the interaction of the paired SRM occurs rather early in the trajectory, significant recirculation due to interaction of SRM's and SSME plumes does not occur until staging. The recirculation from the paired SRM's will effect the side of the HO tank. The material in the region of influence is NOPCO foam. This foam, designed primarily to minimize hydrogen residuals, has been found in numerous Arc Jet Tests to have an outstanding overtemperature capability. Even using the most pessimistic assumptions on the heating from the paired SRM's, the impact on the NOPCO foam is found to be negligible. See Figure 2-41.



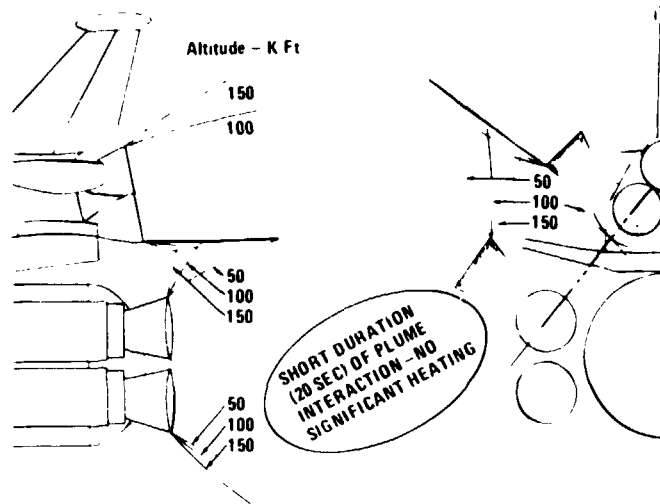


Figure 2-40 Plume Boundaries

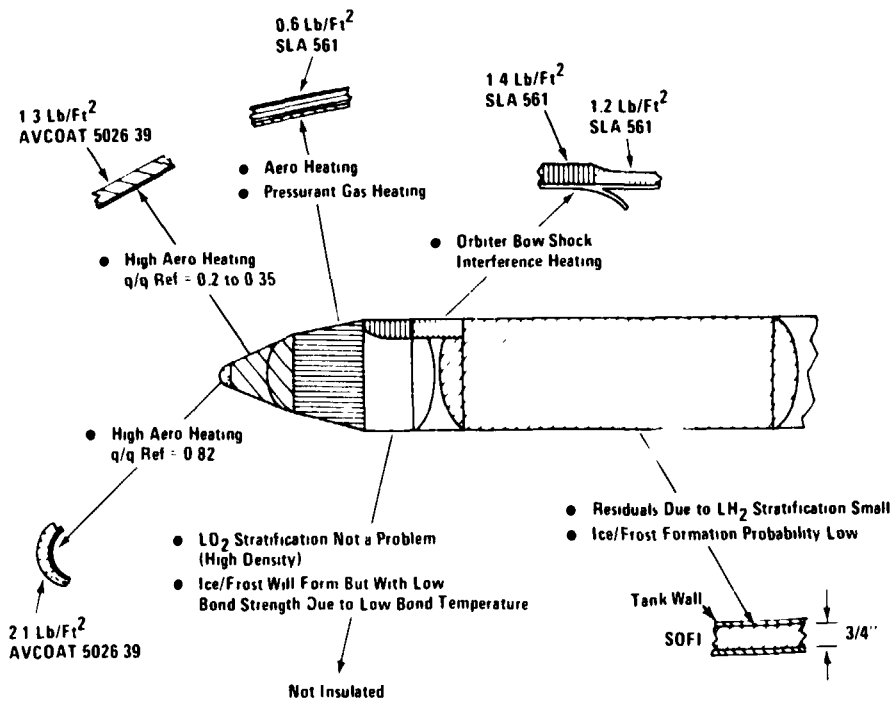


Figure 2-41 HO Tank Basel Thermal Protection System

Hot gas radiation from the SRM plumes onto the base region of the HO tank however is significant. A reasonable data base exists from the Titan III to give a high degree of confidence in the prediction. The series burn HO tank is protected completely up until staging by the interstage skirt and is protected thereafter by 3/4-in. of NOPCO foam. The high heating rates from the SRM's necessitate an ablative heat shield over the foam. A representative cork ablative system would weight 940 lb. See Figure 2-42.

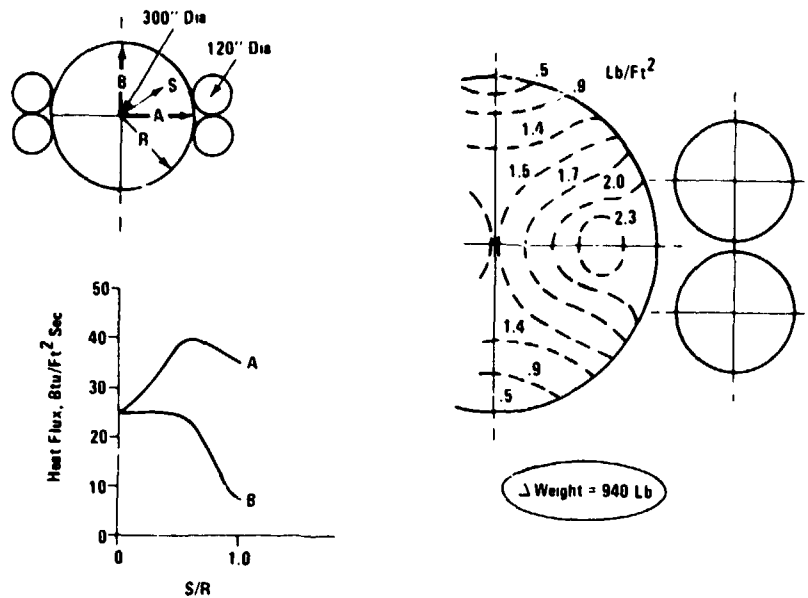


Figure 2-42 Tank Base Heating Penalty From Plume Radiation

## 2.6 CONTROL CONSIDERATIONS

### 2.6.1 Introduction

Ascent control studies were performed for two parallel burn configurations. Both configurations utilized a three engine orbiter with SRM boosters, one configuration having two 156" diameter motors, the other having four 120" (1207) motors. Control issues studied include the following:

- Orbiter/Booster roll-yaw coupling due to
  - Booster thrust misalignment
  - Booster thrust magnitude differential
  - Booster tail-off characteristics
- Aero disturbances due to winds
- Aerosurface control capability
- SRM TVC control capability

It was assumed that control must be provided with one orbiter engine, or its TVC actuators, inoperative. In addition, when aerosurface control is used, the required control torque must be available with one aerosurface actuator or hydraulic system failure.

## 2.6.2 Configuration Characteristics

The two SRM parallel burn configurations studied are very similar in terms of trajectory characteristics, mass properties and aerodynamic data. Gross liftoff weight is 4.4 M lb for the two 156" configuration and 4.8 M lb for the four 120" configuration. The most significant differences are that the longitudinal cg location is further forward and the rolling moment due to sideslip slightly lower for the two 156" configuration. These differences are illustrated in Figure 2-43. In the figure, the dimensions have been normalized to the HO tank length and diameter for the four 120" configuration. The configuration similarity has enabled many conclusions drawn for one configuration to be applicable to the other and in some cases to the pressure-fed parallel burn configuration, as well. The data presented herein for the four 120" and the two 156" configurations were generated by Grumman and Boeing through six-degree-of-freedom digital simulation.

## 2.6.3 Orbiter/Booster Roll-Yaw Coupling (No Booster TVC)

If attitude control is to be provided without booster thrust vector control, the effect of the orbiter thrust line offset from the booster thrust line must be considered. Figure 2-44 is an illustration of the problem. If a yaw moment is induced by booster thrust misalignment or by differing thrust magnitudes on each side, and orbiter engines are gimballed to null this moment, a roll torque is created. This torque must be balanced by gimbaling the orbiter engines about their center of thrust, as shown. Since the roll control moment arm of the orbiter engines is much smaller than their effective distance to the SRM thrust axis, the roll torque requirement uses about three times as much gimbal travel as the associated yaw.

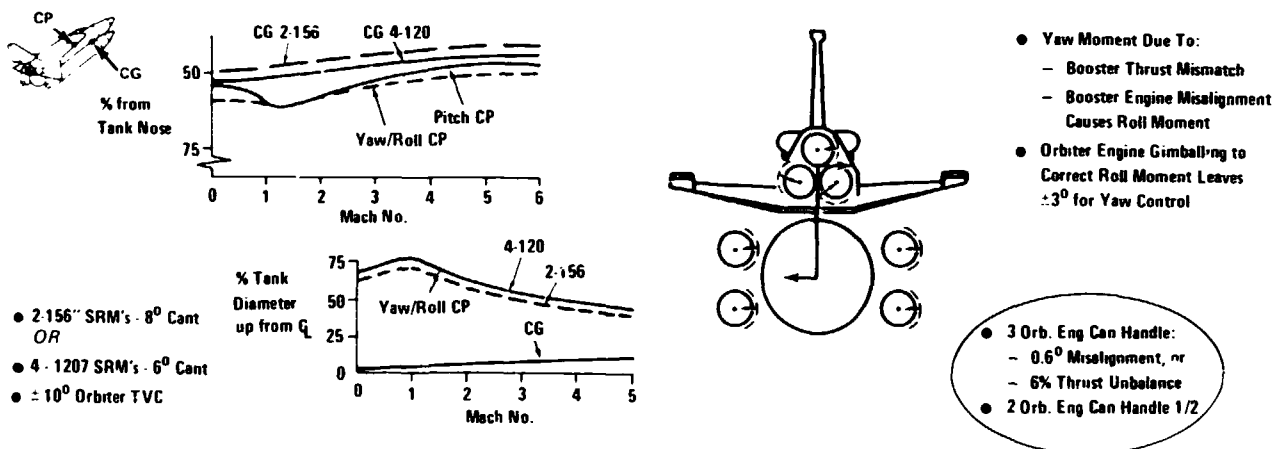


Figure 2-43 Ascent Control Study - Configuration Characteristics

Figure 2-44 Orbiter/Booster Roll Yaw Coupling

The result is that with three orbiter engines operating, for either SRM configuration approximately  $0.6^\circ$  of thrust misalignment in yaw or an unbalance of 6% of the total thrust (with a  $6^\circ$  design value of nozzle cant) would use the full gimbal travel at lift-off. At SRM burnout, due to decreased SRM thrust and a further forward cg location, a 19% thrust unbalance can be handled. For the case of one orbiter engine failed, about one-half of these values would saturate the gimbaling capability. The largest thrust unbalance condition occurs at SRM burnout during tail-off. It is estimated that this thrust unbalance will be equivalent to 50% of the thrust of one SRM per pair. The Martin Company specification for 120" motors on the Titan III allows a 400,000 lb thrust difference. For two SRM's the thrust unbalance is then 25% of the total thrust; for four SRM's the RSS equivalent is 17% of the total thrust. The orbiter TVC capability with one engine failed can not accommodate these magnitudes of thrust unbalance. At liftoff the expected maximum thrust unbalance is 3% of the total thrust per pair of SRM's. If this occurs in the yaw axis with one engine out, it requires the maximum gimbaling capability of the orbiter TVC to balance it. Thus, it is clear that a nozzle cant angle of more than the  $6^\circ$  we used for the initial design is required to bring the net moment unbalance within controllable limits.

If the nozzles are canted through the burnout cg, the tail-off thrust unbalance problem is minimized. The required cant angles are  $13^\circ$  for the four 120" configuration and  $16^\circ$  for the two 156" configuration. For these cant angles the lift-off thrust unbalance condition requires about  $3^\circ$  of orbiter gimbal travel for the engine-out condition on the four 120" configuration and  $1\frac{1}{2}^\circ$  of gimbal travel for the two 156" configuration. There is, of course, a thrust loss associated with these large cant angles, the effect of which has not yet been evaluated.

The maximum thrust vector misalignment is assumed to be  $1/4^\circ$  per SRM which corresponds to the Titan III specification value. This gives an RSS total thrust misalignment of  $1/8^\circ$  for four SRM's and  $0.18^\circ$  for two SRM's. For these conditions  $3^\circ$  of orbiter engine gimbaling are required with one engine-out for the four 120" configuration and  $5^\circ$  for the two 156". If the total SRM thrust misalignment is  $0.36^\circ$  in the yaw axis on the two 156" configuration, maximum orbiter gimbal travel would be required to hold vehicle attitude. Therefore, it is apparent that the parallel burn stack alignment is critical

#### 2.6.4 Aerodynamic Disturbance Due to Winds

Six-degree-of-freedom ascent simulation data has been obtained using two different control techniques for the parallel burn configuration. One approach uses orbiter engine gimbaling combined with rudder and elevon aerodynamic control; the other approach uses



orbiter engines and SRM thrust vector control. Both techniques utilize a minimum drift acceleration feedback control system for the pitch and yaw channels. Trajectory shaping is used in the pitch plane to decrease the headwind aerodynamic loading ( $q \alpha$ ). The method of shaping the trajectory involves deviating slightly from a gravity turn during the high dynamic pressure portion of ascent. This decreases the no wind angle-of-attack which results in decreased headwind  $q \alpha$  and increased tailwind  $q \alpha$ . Figure 2-15 presents the envelope of the maximum values of  $q \alpha$  and  $q \beta$  as a function of wind gust altitude for the aerosurface control technique. The simulated winds are based on the 95% scalar wind speed, 99% shear plus gust model for all launch locations from NASA TMX-64589. The SRM TVC control technique gives approximately the same results. Typical maximum attitude errors for these data are up to  $10^\circ$  in roll and  $3^\circ$  to  $5^\circ$  in pitch or yaw. The maximum roll rate does not exceed  $2^\circ/\text{sec}$ .

The most critical aerodynamic control problem with the parallel burn configuration is the large rolling moment induced by sideslip. This situation is illustrated in Figures 2-46 and 2-47. The torque requirements quoted are for the maximum headwind  $q \alpha$  condition and maximum crosswind  $q \beta$  condition. The estimated orbiter gimballed angle requirement for non-aerodynamic control requirements - primarily body bending, propellant slosh damping, and booster misalignment - is  $2^\circ$  in pitch and  $2\ 1/2^\circ$  in yaw. Booster misalignment contributes significantly to the gimballed angle requirement for roll control. It should be noted that the maximum yaw and roll torque requirements always occur simultaneously, but the maximum pitch torque requirement cannot occur simultaneously with maximum yaw and roll requirements since a worst case headwind and crosswind cannot occur together.

#### 2.6.5 Aerosurface Control Capability

The Aerosurface control technique utilizes the orbiter elevons and rudder to provide control in all three axes which augments the orbiter SSME engine TVC capability. Control system studies indicate that an aerosurface deflection rate of  $25^\circ/\text{sec}$  is the minimum acceptable to provide stable attitude control unless a fin is used on the underside of the HO tank. The presently specified design rate capability for the aerosurfaces is  $25^\circ/\text{sec}$ , but the maximum design dynamic pressure in the aircraft mode is approximately one-half that incurred during boost. The elevon actuation system capability would have to be increased to provide the hinge moments required for ascent control. An estimate of the orbiter weight increase to provide this deflection rate during boost is 1000 - 1200 lb. Figures 2-48 and 2-49 show the effect of the addition of aerosurface control authority for the four 120" SRM and the two 156" SRM configuration respectively. The elevon and rudder deflection limits required for yaw and roll control are  $\pm 20^\circ$ . The torque available for pitch is based on limits of  $\pm 10^\circ$  as this is more than adequate.

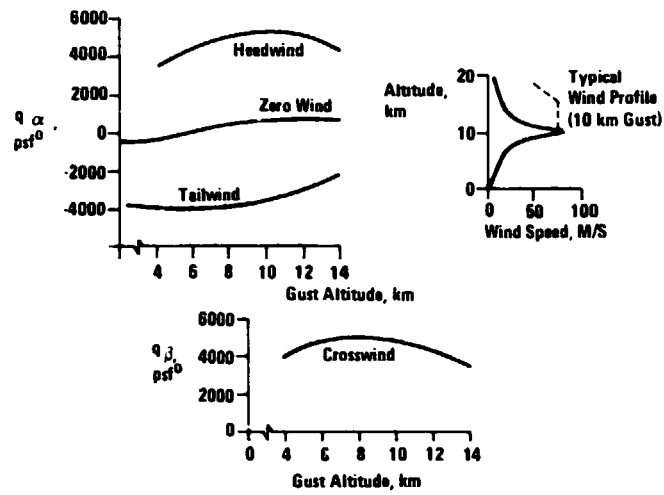


Figure 2-45 Aerodynamic Disturbance  $q_\alpha, q_\beta$  vs Altitude

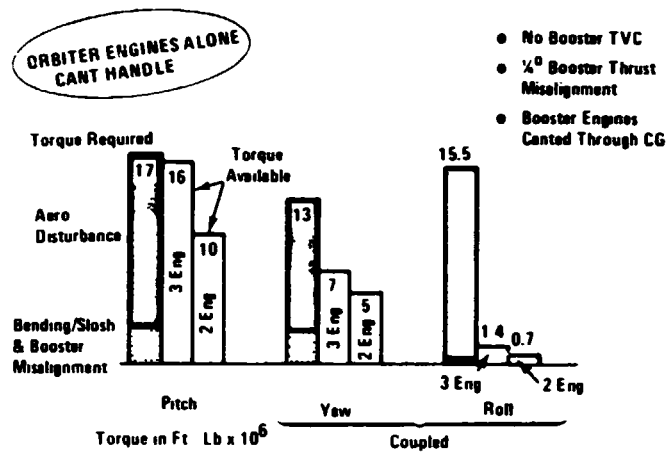


Figure 2-46 Aero Disturbance - Control Requirements - 1207's

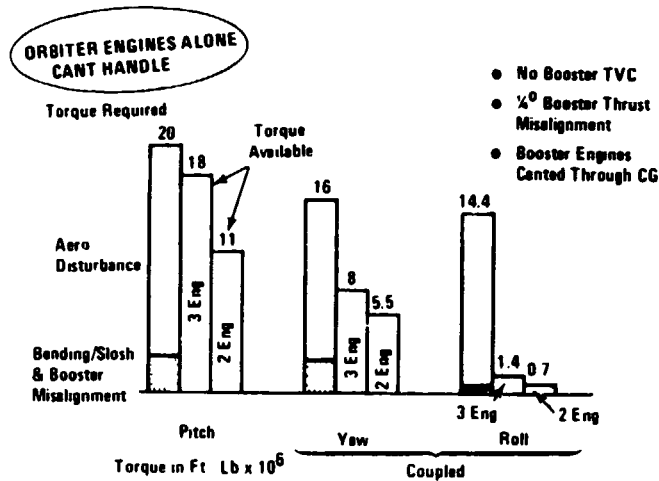


Figure 2-47 Aero Disturbance - Control Requirements - 156'S





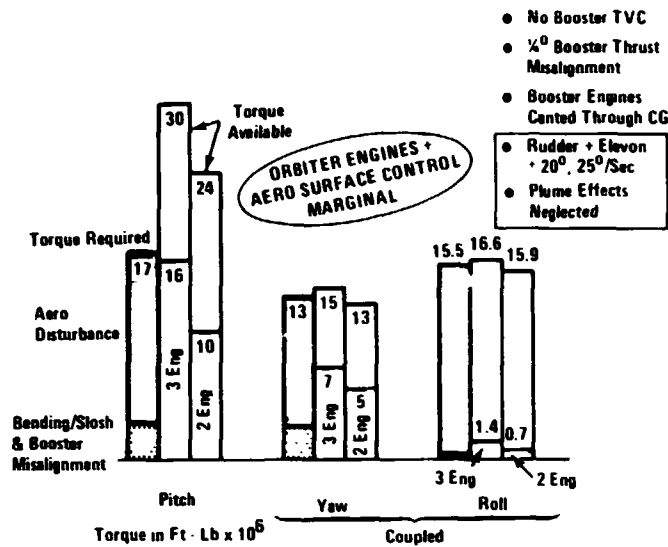


Figure 2-48 Aero Disturbance – Aero Surface Control – 1207'S

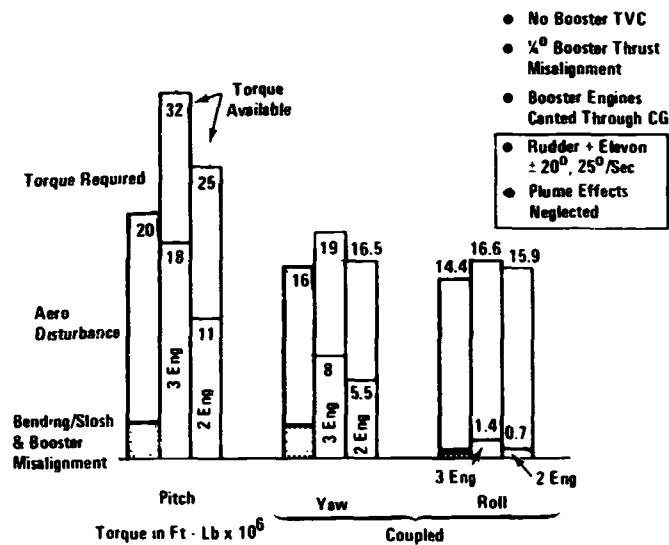


Figure 2-49 Aero Disturbance – Aero Surface Control – 156'S

As noted in the figures, the effect of the rocket engine exhaust plumes on the aerosurface control capability is not included. Wind tunnel tests have indicated that as much as 20% degradation may occur in the elevon effectiveness coefficient at Mach 1.5 due to the plume interaction with airflow past the wings. (This data was obtained by simulating the plumes as solid bodies which should give conservative results). Figure 2-50 presents the elevon deflection requirement for roll control as a function of wind gust altitude and the associated Mach number. Data is presented with and without the estimated plume degradation of control effectiveness. Two conclusions may be drawn from the figure:

- The plume effect causes the elevon deflection to go beyond the  $\pm 20^\circ$  limit.
- The deflection requirement, even without plume effect, is greatest at altitudes higher than that for the maximum  $q \beta$  condition. (Note from Figure 2-45 that maximum  $q \beta$  occurs at 8 KM but maximum elevon deflection occurs at 12-13 KM as shown in Figure 2-50).

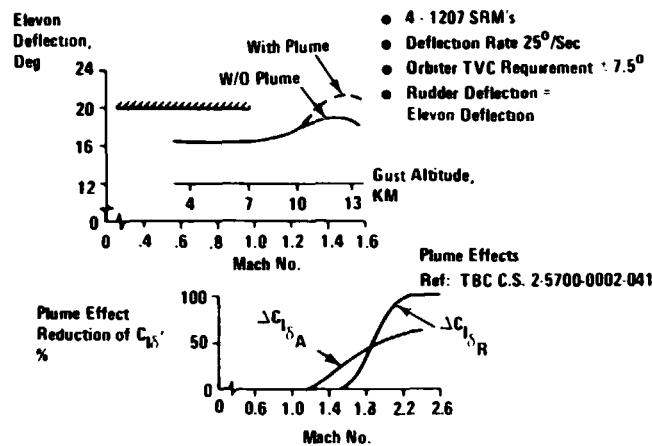


Figure 2-50 Asymmetric Elevon Deflection Requirement Parallel Burn SRM

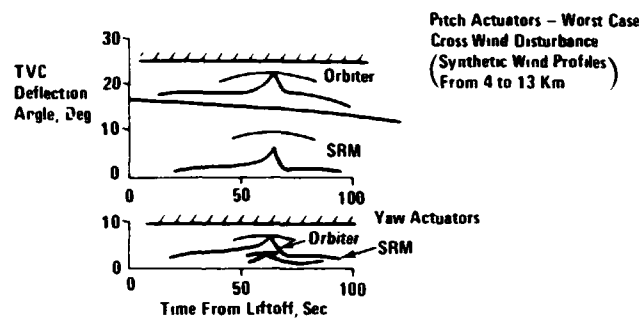
The variation in elevon deflection requirement versus altitude without the plume effects is due to the nominal variation of elevon control effectiveness with Mach number. For altitudes above about 8 KM  $q \beta$  decreases but control effectiveness decreases also, with the result that the maximum elevon deflection requirement occurs at approximately 12 KM. This is the most critical control condition even without accounting for the plume effects. Note that there is only  $1^\circ$  of elevon travel left at the 12 KM gust altitude with a  $\pm 2^\circ$  limit. With one orbiter engine failed, the deflection requirement is  $20^\circ$ . Thus without some means of alleviating the roll control torque requirement, the control authority of the aerosurfaces plus orbiter TVC is too marginal to provide an acceptable control scheme.

#### 2.6.6 SRM TVC Control Capability

The SRM TVC control data are presented in Figures 2-51 and 2-52. Figure 2-51 gives both the orbiter and booster TVC gimbal angles as a function of time for wind gust altitudes from 4 to 13 KM. For the orbiter the worst gimbal angle condition is for the left engine pitch actuator and upper engine yaw actuator (with a right crosswind). Maximum deflections requirements are  $7.5^\circ$  for the orbiter and  $10.5^\circ$  for the 120" SRM's. Since the roll control law utilizes only pitch motion of the SRM nozzles, the 120" SRM nozzle deflection could be decreased  $1-2^\circ$  by using yaw motion for roll control. The two 156" configuration requires about  $9^\circ$  of nozzle deflection.



Figure 2-52 summarizes the 120" SRM TVC requirements. A  $\pm 12^\circ$  gimbaling capability for the SRM nozzles is shown to provide a control margin of about 6% when all control requirements are considered. Since additional roll control capability can be obtained by vectoring the four nozzles differentially in yaw an additional margin of about 15% is available.  $10.5^\circ$  of nozzle deflection will provide a 10% margin for the two 156" SRM's. Since the control torque capability of a TVC system is more predictable than that of an aerosurface, a 10% margin seems reasonable.



- Booster TVC Required for Roll Control (if No Aero Surface Control)
- $10.5^\circ$  of Booster TVC Required

Figure 2-51 Ascent Control - Aero Disturbance Data

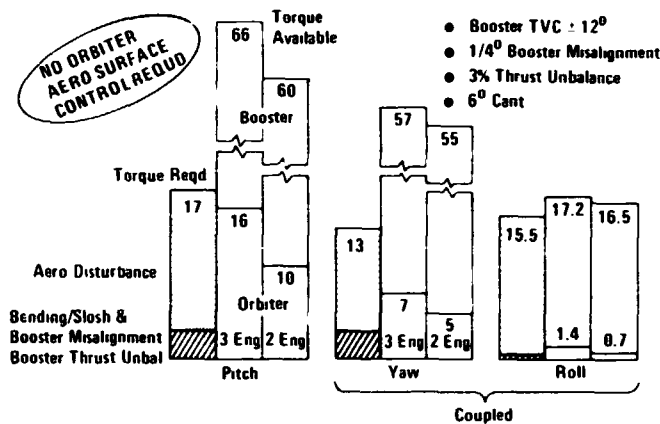


Figure 2-52 Aero Disturbance - SRM TVC Control 4-1207 SRM

### 2.6.7 Reduction of Roll-Yaw Control Requirements

Two methods of reducing the roll and yaw torque requirements were considered. Fins on the underside of the HO tank can reduce the aerodynamic yaw and roll torque caused by a given  $q \beta$  condition. Allowing the vehicle to roll through large angles during the maximum wind condition will reduce the torque required for a given  $q \beta$  condition and will reduce

$q \beta$  as well. These methods were studied for the aerosurface plus orbiter TVC control system.

Two fin sizing conditions were considered. A  $410 \text{ ft}^2$  fin can provide a 20% control capability margin or a  $470 \text{ ft}^2$  fin can alleviate the need for increasing the elevon actuator system capability. Figure 2-53 shows the effect of adding a  $410 \text{ ft}^2$  fin on the underside of the HO tank interstage structure for the four 120" SRM configuration. The required roll torque is reduced from 15.5 million ft-lb to 12 million at the maximum  $q$  condition. The effect on yaw torque is similar if the fin is located forward of the vehicle cg. This fin provides a 20% control margin at the 12 KM gust altitude with one orbiter engine out. It has been estimated that this fin would weigh 2,600 lb including penalties to HO tank structure weight and fin jettison hardware.

The other approach to reducing roll-yaw control requirements is to permit large roll angle errors which can be accomplished by decreasing the roll attitude gain. This method of allowing vehicle roll will maintain rate damping by preventing saturation of the control torque capability. A roll control gain study was performed to examine the effects of allowing roll angle errors of greater than  $10^\circ$ . The roll gain was reduced as a function of estimated (no wind) dynamic pressure. It was found that through this technique a similar 20% margin for aerosurface control could be achieved as was obtained with the  $410 \text{ ft}^2$  fin but at no weight penalty. The associated roll angle error was  $50^\circ$  with a maximum roll rate of  $5^\circ/\text{sec}$ .

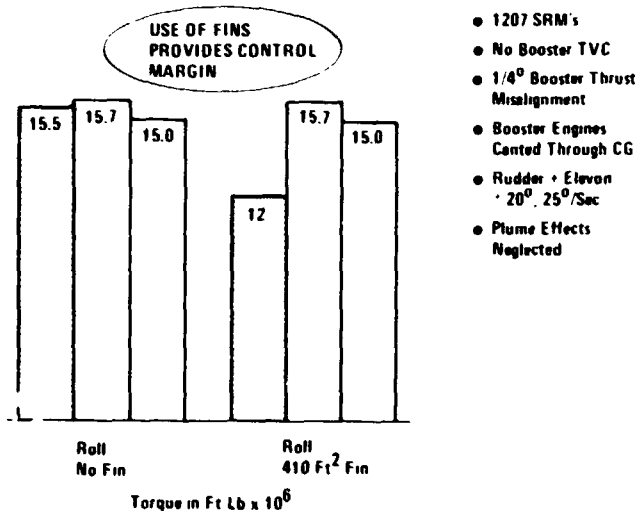


Figure 2-53 Aero Disturbance -- Effect of Fins



### 2.6.8 Control Studies Summary

We performed extensive six-degree-of-freedom ascent control studies to determine the capability of various combinations of control actuators to provide the required control authority with sufficient margin to be confident that the analytical results will hold up in practice.

We found that orbiter engine TVC was clearly inadequate to handle the worst case aerodynamic disturbance torques that could be experienced. When we added orbiter aerosurface control capability we found that, even increasing our rudder and elevon deflection and hinge moment capability to the maximum possible extent, we were still marginal in our ability to counteract the maximum applied disturbance torques. Combined with a possible degradation in aerosurface control capability due to orbiter plume interaction, this result led us to conclude that, unless some roll-yaw control alleviation was provided, orbiter-only control of the combined configuration was not feasible.

We looked at two techniques to reduce the roll-yaw control requirements. Adding a large fin on the underside of the tank near the nose can lower the CP to provide a 20% margin for orbiter-only control with about 410 ft<sup>2</sup> of fin area, at a tank weight penalty of about 2600 lb. Permitting up to 50° roll rotation has the same effect at no attendant weight penalty. A 20% margin appears adequate to allow for discrepancies between analysis and actual flight performance and for possible degradation in aerosurface control capability. Thus, booster TVC can be dispensed with by adopting one of the above approaches. The penalty of designing the aerosurfaces for greater moment and deflection capability than is required for re-entry, and sub-sonic flight can be eliminated by increasing the fin area by about 400 ft<sup>2</sup> at a weight increment of about 4000 lb. or by using a 470 ft<sup>2</sup> fin and allowing 50° of roll.

If booster TVC is utilized, however, approximately 10° to 11° booster engine gimballing in conjunction with the orbiter engine thrust vectoring capability is sufficient to provide the required control authority without the use of orbiter aerosurfaces.

## 2.7 FLIGHT PERFORMANCE RESERVES

### 2.7.1 Introduction

A prerequisite to the evaluation of propellant requirements for a launch vehicle are the Flight Performance Reserves (FPR) allowances for off-nominal operations. The primary contributors to the need for flight performance reserves are propellant utilization efficiency, propellant loading accuracy, propulsion system variations, and inert weight variations.

We performed the analyses aimed at establishing the extent of flight performance reserves required on the series/BRB and parallel/120" SRM configurations. We were aided in these studies by the Martin Marietta Co. (Denver Division) whose experience with the Titan system also proved helpful in developing the analytical approach.

### 2.7.2 Sensitivity Analysis

Accurate evaluation of flight performance reserve requirements for a given launch system is dependent on the  $3\sigma$  dispersions of the various subsystems performance, and the degree of sophistication used in determining its effects on the overall system. For preliminary design purposes, the procedure used in estimating the effects of subsystem performance variations is to determine sensitivity coefficients, assuming independence and linearity of each subsystem and determine the effects on the overall system by averaging (root-sum-square) the individual errors for various levels of variation in subsystem performance. From these results, tradeoffs can be made between cost and subsystem performance requirements.

This procedure of estimating the impact of subsystem performance variation will result in a conservative estimate. A more sophisticated procedure is to perform a Monte Carlo analysis and statistically vary all subsystem performance levels and establish the "n-sigma" dispersion envelope.

Sensitivity coefficients were determined employing a moment balance simulation of each reference ascent trajectory (see Tables 2-7, 2-8 and 2-9) using a series of constant rates from liftoff to staging and then explicit steering (linear tangent) to orbit insertion. The linear tangent steering algorithm simulates the response of a near optimum (minimum  $\Delta V$ ) closed loop guidance law which simultaneously compensates for performance dispersion while allowing the vehicle to meet the targeted orbit insertion.

The performance parameters included in this analysis were restricted to thrust, specific impulse, mixture ratio, propellant loading, inert weight, and aerodynamic drag. Dispersions from other aerodynamic coefficients, winds and GN&C sources are generally small and were not considered in this analysis.

In establishing the sensitivities of FPR to individual performance parameters two dispersion magnitudes were simulated for each parameter. One value was chosen near the estimated  $3\sigma$  variation and a second of approximately twice the first. This approach determines the linear region of each parameter and broadens the applicability of each sensitivity for future FPR requirements. In cases where the two dispersion values produced slightly different sensitivities, but still considered in the acceptable range of linearity, the two sensitivities were averaged.



TIME	VEL	GM	ALT	T/H	WFCUT	Q BAR	Q DOT S	ALP	HEMG	BST	HEMG	ORB	RNG	HEAD	LNT	LOYC
C.C	5.0	90.00	0.	1.281	45.9741.	0.	0.0	0.0	0.0	0	0	0	0.	89.92	28.475	-80.365
A.0	41.6	90.00	266.	1.292	4402279.	5.	0.00	0.0	0.0	4	4	3	0.	89.92	28.475	-80.365
25.9	275.1	90.00	3208.	1.439	4006461.	79.	0.02	0.0	0.0	4	4	3	0.	89.92	28.475	-80.365
25.8	275.1	87.25	3208.	1.439	4006461.	79.	0.02	0.0	0.0	4	4	3	0.	89.92	28.475	-80.365
31.9	394.2	84.08	5974.	1.523	3824497.	153.	0.04	0.0	0.0	4	4	3	0.	89.92	28.475	-80.365
81.8	548.3	79.65	9593.	1.620	3652037.	257.	0.11	0.0	0.0	4	4	3	0.	89.92	28.475	-80.365
82.8	777.5	74.85	18491.	1.730	3474577.	383.	0.23	0.0	0.0	4	4	3	0.	89.92	28.475	-80.365
57.9	919.3	68.81	26045.	1.854	3297117.	517.	0.44	0.0	0.0	4	4	3	1.	89.92	28.475	-80.365
68.0	1293.1	64.32	26940.	1.959	3170057.	637.	0.67	0.0	0.0	4	4	3	1.	89.92	28.475	-80.365
72.0	1531.6	58.43	34730.	1.886	3016883.	637.	0.96	0.0	0.0	4	4	3	2.	89.92	28.475	-80.365
80.0	1539.7	52.55	48022.	2.016	2843110.	633.	1.35	0.0	0.0	4	4	3	3.	89.92	28.475	-80.365
98.0	1439.7	46.95	58285.	2.153	2684935.	559.	1.82	0.0	0.0	4	4	3	8.	89.92	28.475	-80.365
99.0	2201.1	41.77	65528.	2.301	2526561.	481.	2.31	0.0	0.0	4	4	3	6.	89.92	28.475	-80.365
108.0	2675.4	37.11	77735.	2.462	2368188.	335.	2.86	0.0	0.0	4	4	3	9.	89.92	28.475	-80.365
112.0	3117.5	32.94	93465.	2.688	2209413.	288.	3.47	0.0	0.0	4	4	3	12.	89.92	28.475	-80.365
120.0	3574.0	29.35	104867.	2.851	2051481.	177.	4.09	0.0	0.0	4	4	3	16.	89.92	28.475	-80.365
137.2	5069.0	23.03	137638.	3.000	1726154.	78.	5.17	0.0	0.0	4	4	3	27.	89.92	28.475	-80.365
STA:18F																
137.2	5069.0	23.03	137638.	3.000	1726154.	78.	5.17	0.0	0.0	4	4	3	27.	89.92	28.475	-80.365
142.2	5395.1	19.17	165776.	1.072	1320069.	29.	3.57	8.7	8.7	0	0	3	33.	89.92	28.475	-80.365
168.2	5737.1	15.62	192816.	1.118	1270526.	13.	2.72	11.9	11.9	0	0	3	51.	89.92	28.475	-80.365
250.2	6731.7	10.08	236096.	1.209	1171480.	3.	1.77	16.3	16.3	0	0	3	84.	89.92	28.475	-80.365
232.2	7437.9	6.23	264352.	1.320	1072354.	1.	1.31	18.6	18.6	0	0	3	125.	89.92	28.475	-80.365
268.2	9095.6	3.55	290784.	1.455	973268.	0.	1.10	19.2	19.2	0	0	3	165.	89.92	28.475	-80.365
295.2	10543.5	1.92	305240.	1.620	874182.	0.	1.13	18.6	18.6	0	0	3	216.	89.92	28.475	-80.365
322.2	12270.6	0.73	312752.	1.827	775396.	0.	1.41	16.8	16.8	0	0	3	275.	89.92	28.475	-80.365
367.2	14339.2	0.11	315552.	2.095	676319.	0.	2.02	12.7	12.7	0	0	3	383.	89.92	28.475	-80.365
376.2	15229.2	-0.56	315616.	2.260	624467.	0.	2.52	12.7	12.7	0	0	3	382.	89.92	28.475	-80.365
392.2	16415.9	-0.17	315772.	2.454	576924.	0.	3.21	10.9	10.9	0	0	3	423.	89.92	28.475	-80.365
418.2	17718.5	-0.22	314128.	2.685	527381.	0.	4.14	9.0	9.0	0	0	3	467.	89.92	28.475	-80.365
418.2	18419.4	-0.23	313552.	2.817	502610.	0.	4.73	8.0	8.0	0	0	3	490.	89.92	28.475	-80.365
428.2	19157.8	-0.21	312962.	2.963	477438.	0.	5.41	7.1	7.1	0	0	3	515.	89.92	28.475	-80.365
432.2	19923.7	-0.21	312394.	3.000	453456.	0.	6.18	6.3	6.3	0	0	3	540.	89.92	28.475	-80.365
448.2	20692.5	-0.19	311809.	3.000	430271.	1.	7.04	5.6	5.6	0	0	3	566.	89.92	28.475	-80.365
458.2	21462.2	-0.16	311296.	3.000	408272.	1.	7.97	4.8	4.8	0	0	3	598.	89.92	28.475	-80.365
456.2	22212.5	-0.13	310888.	3.000	387197.	1.	8.97	4.0	4.0	0	0	3	622.	89.92	28.475	-80.365
468.2	23033.5	-0.09	310512.	3.000	367589.	1.	10.03	3.1	3.1	0	0	3	651.	89.92	28.475	-80.365
472.2	23774.9	-0.04	310288.	3.000	348793.	1.	11.15	2.3	2.3	0	0	3	682.	89.92	28.475	-80.365
479.5	24675.6	0.00	310240.	3.000	332558.	1.	12.18	0.6	0.6	0	0	3	710.	89.92	28.475	-80.365
INSERTION																

Table 1-8 - Parallel Burn SRM (4 UTC 1207) - 15 x 60 P/L Bay - Due East Launch From ETR

TIME	VEL	GMI	ALT	T/W	WEIGHT	Q BAR	Q OCT S	ALF	MFNG RST	MFNG ORR	RNG	HEAD	LAT	LONG
2.0	0.0	0.0	0	1.244	6306390.	0.	0.0	0.0	7	0	0.	89.92	28.475	-80.535
8.0	70.7	0.0	272	1.307	6102738.	6.	0.00	0.0	7	0	0.	89.92	28.475	-80.535
25.5	288.0	0.0	3277	1.500	5460300.	87.	0.02	0.0	7	0	0.	89.92	28.475	-80.535
33.5	426.7	85.81	3277	1.500	5460298.	87.	0.02	0.0	7	0	0.	89.92	28.475	-80.535
41.5	507.4	83.37	6110	1.620	5166646.	175.	0.05	0.0	7	0	0.	89.92	28.475	-80.535
50.5	610.3	78.98	10132	1.767	4872995.	304.	0.14	0.0	7	0	0.	89.92	28.475	-80.535
59.5	710.1	74.11	15573	1.941	4579343.	473.	0.32	0.0	7	0	0.	89.92	28.475	-80.535
67.5	803.7	71.01	19805	2.064	4395887.	500.	0.52	0.0	7	0	0.	89.92	28.475	-80.535
70.5	893.7	65.78	27454	1.506	4186136.	586.	0.66	0.0	5	0	1.	89.92	28.475	-80.615
78.5	1051.3	60.03	35777	1.722	3976385.	574.	0.85	0.0	5	0	2.	89.92	28.475	-80.533
85.5	1216.0	54.20	44833	1.854	3766635.	547.	1.13	0.0	5	0	3.	89.92	28.475	-80.533
94.5	1437.3	42.08	54689	1.990	3550884.	477.	1.46	0.0	5	0	4.	89.92	28.475	-80.533
102.5	1621.0	38.00	65391	2.133	3347133.	381.	1.84	0.0	5	0	6.	89.92	28.475	-80.533
110.5	1822.6	33.54	76902	2.288	3137383.	297.	2.29	0.0	5	0	8.	89.92	28.475	-80.533
118.5	2033.6	29.61	89211	2.459	2927632.	227.	2.82	0.0	5	0	11.	89.92	28.475	-80.533
126.5	2269.3	26.16	102245	2.654	2717882.	170.	3.39	0.0	5	0	14.	89.92	28.475	-80.533
134.5	2531.3	21.49	115938	2.879	2508131.	124.	3.99	0.0	5	0	19.	89.92	28.475	-80.533
142.5	2821.5	15.49	138706	3.133	2219805.	70.	4.51	0.0	4	0	27.	89.92	28.475	-80.533
150.5	3137.0	17.82	158704	3.408	1777536.	70.	4.51	8.4	0	3	27.	89.92	28.475	-80.533
158.5	3479.4	14.49	164160	3.693	1231090.	20.	3.39	11.5	0	3	39.	90.09	28.475	-79.902
166.5	3848.7	10.38	182416	4.088	1181547.	14.	2.79	14.0	0	3	53.	90.29	28.474	-79.642
174.5	4245.9	7.85	228672	4.593	1082461.	4.	2.00	17.2	0	3	84.	90.72	28.469	-79.043
182.5	4670.8	5.85	259072	5.218	983375.	1.	1.77	18.4	0	3	122.	91.20	28.459	-78.322
190.5	5123.8	4.47	280976	5.963	884289.	1.	1.58	18.1	0	3	167.	91.74	28.440	-77.452
198.5	5605.9	3.91	295744	6.828	785203.	0.	1.08	16.7	0	3	219.	92.35	28.408	-76.488
206.5	6117.3	3.58	304752	7.813	686117.	0.	0.68	14.3	0	3	281.	93.04	28.360	-75.322
214.5	6652.8	3.36	307504	8.918	636574.	0.	0.42	12.8	0	3	316.	93.41	28.322	-74.667
222.5	7220.8	3.26	309344	10.143	587031.	0.	0.22	11.7	0	3	353.	93.82	28.282	-73.957
230.5	7820.0	3.26	310400	11.498	537498.	0.	0.62	9.4	0	3	394.	94.25	28.241	-73.199
238.5	8450.0	3.26	310400	12.983	487045.	0.	1.57	7.5	0	3	438.	94.71	28.183	-72.357
246.5	9120.7	3.26	310404	14.598	437251.	0.	3.18	6.7	0	3	486.	94.95	28.150	-71.914
254.5	9830.7	3.26	310864	16.353	395566.	0.	5.85	6.0	0	3	512.	95.20	28.114	-71.653
262.5	10580.5	3.26	310736	18.258	3575531.	1.	6.59	5.3	0	3	538.	95.46	28.075	-70.974
270.5	11370.7	3.26	310592	20.313	3166330.	1.	7.40	4.6	0	3	566.	95.72	28.032	-70.476
278.5	12190.6	3.26	310408	22.528	2755310.	1.	8.29	3.8	0	3	594.	96.00	27.985	-69.960
286.5	13040.6	3.26	310370	24.903	2346111.	1.	9.27	2.9	0	3	624.	96.28	27.934	-69.426
294.5	13910.7	3.26	310256	27.438	1931111.	1.	10.27	2.2	0	3	654.	96.57	27.879	-68.873
302.5	14810.1	3.26	310240	30.143	1516111.	1.	11.35	-0.3	0	3	684.	96.87	27.820	-68.303
310.5	15730.1	3.26	310240	33.000	1101111.	1.	12.18	0.0	0	3	714.	97.09	27.774	-67.876

Table 2-7 - Series Burn BRB - 15 x 60 P/L Bay - Due East Launch From ETR

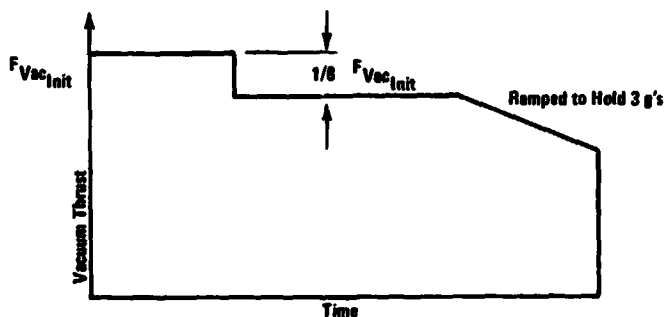




**Table 2-9 Reference Design Points Characteristics  
Due East Launch From ETR**

Parameters	Parallel Burn SRM	Series Burn BRB
GLOW, K Lb	4580	6398
BLOW, K Lb	2788	5119
OLOW, K Lb	1767	1277
Booster Propellant, K Lb	2429	4177
Orbiter Propellant, K Lb	1459	989
HO-Tank Inert Weight, K Lb	8.4	66.3
Number/Type of Booster Engines	4/1207	7/Press. Fed
Booster Vacuum $I_{sp}$ , Sec	287.3*	276.7
Booster S.L. $I_{sp}$ , Sec	241.8*	216.7
Number/Type of Orbiter Engines	3/SSME	3/SSME
Orbiter Vacuum $I_{sp}$ , Sec	467.3	467.3
Orbiter S.L. $I_{sp}$ , Sec	352.4	362.4
Booster Shut-down Sequence	12.5% @ 64 Sec	2-1-4
Orbiter Shut-down Sequence	Throttle	Throttle
Booster Vacuum Thrust/Engine, K Lb	1278	1448
Orbiter Vacuum Thrust/Engine, K Lb	472	472

\*SRM Nozzle Canted 6 Deg



Tables 2-10 and 2-11 are the sensitivities of FPR (pounds of propellant and equivalent delta velocity) to individual performance parameters for the series burn and parallel burn SRM configurations, respectively. Caution must be exercised when applying these sensitivities to parameter variations greater than investigated by this analysis.

Tables 2-12 and 2-13 present the FPR and  $\Delta V$  requirements for the series burn BRB and parallel burn SRM, respectively. Included in these tables are the magnitude of the  $3\sigma$  performance variations for both configurations.

### 2.7.3 Orbiter Propellant Utilization System Comparisons

The orbiter active PU system is baselined as consisting of a segmented capacitance probe in each propellant tank, plus associated electronics in the orbiter fuselage. The weight and cost of this hardware is shown in Table 2-14.

**Table 2-10 Sensitivity Coefficients Series Burn BRB**

Booster	$\frac{\partial P.M.}{\partial Par}$ (Lb/%)	$\frac{\partial \Delta V}{\partial Par}$ (fps/%)
Thrust ( $\pm 2\%$ )	1371.5	66.7
( $\pm 4\%$ )	1634.5	73.5
Specific Impulse ( $\pm 0.7\%$ )	1952	93.5
Propellant Load ( $\pm 1\%$ )	818	39.2
Inert Weight ( $\pm 0.6\%$ )	-680	-32.6
Outage ( $\pm 1.3\%$ )	-3733.8	178.8
Axial Force Coefficient ( $\pm 20\%$ )	-86.9	-4.2
<b>Orbiter</b>		
Thrust ( $\pm 2\%$ )	521	24.9
Specific Impulse ( $\pm 0.6\%$ )	4238	202.7
Propellant Load ( $\pm 0.9\%$ )	1565	74.9
Inert Weight ( $\pm 2\%$ )	1272	-60.9
Outage	-8888	-464

**Table 2-11 Sensitivity Coefficients Parallel Burn SRM (4 UTC 1207)**

Booster	$\frac{\partial P.M.}{\partial Par}$ (Lb/%)	$\frac{\partial \Delta V}{\partial Par}$ (FPS/%)
Thrust ( $\pm 1\%$ )	1036	48.6
Specific Impulse ( $\pm 0.6\%$ )	1459	69.9
Propellant Load ( $\pm 0.6\%$ )	410	18.6
Inert Weight ( $\pm 0.5\%$ )	-388	-18.6
Axial Force Coefficient ( $\pm 20\%$ )	-104.9	-5.0
<b>Orbiter</b>		
Thrust ( $\pm 2\%$ )	698	33.4
Specific Impulse ( $\pm 0.6\%$ )	5327	265.2
Propellant Load ( $\pm 1\%$ )	1488	71.3
Inert Weight ( $\pm 2\%$ )	-1316	-63.0
Outage	-14589	-698.8

With an active PU this fuel bias will be 704 lb (series BRB) and 1060 lb (parallel SRM). With a passive PU the values will be 1200 lb (series BRB) and 1800 lb (parallel SRM). These propellant quantities as well as flight performance reserves may be assigned transportation costs of \$11,000/lb. Table 2-15 lists the hardware and development costs (from Table 2-14) plus bias and FPR differences (from Tables 2-12 and 2-13), and indicates the total DDT&E and operations costs for either a passive and active PU system.

As may be seen the active PU system carries a cost penalty of from \$0.2 to \$9.6 M. With a series BRB configuration the PU system DDT&E would have to be reduced to zero for the trade to break even. For the parallel SRM vehicle the program costs associated with an active and passive PU are about the same. However, consideration of the difficulties encountered with past PU systems leads to a recommendation of passive PU for either the series or parallel configuration.

#### 2.7.4 Booster Propellant Utilization System Comparisons

Table 2-16 compares the weight penalties associated with passive and active PU methods for the series burn BRB.

Table 2-12 shows that with no PU in the orbiter and 0.5% load and 2% MR tolerance, a 1754 lb reduction in FPR is possible with an active PU system in the booster. Table 2-17 shows a cost trade of the booster PU system with the difference in FPR costed at \$11,000/lb program cost.



Table 2-12 FPR Requirements – Series Burn BRB

Parameter	Booster		
	3 $\sigma$ Dispersion, %	Required FPR	
		Prop. Lb	Vel. fps
Thrust	-1.01	-2082	-119
$i_{sp}$	-0.622	-1015	-49
Outage (No P.U.)	+1.23	-4583	-220
Outage (w/P.U.)	+0.489	-1063	-89
Propellant Load	-0.39	-319	-15
Inert Weight	+0.3	-204	-10
$C_A$	+10	-859	-42
	R.S.S. (w/PU)	3480	163
	R.S.S. (w/o PU)	5482	259

Orbiter

Parameter	No. PU System				Active PU	
	Load $\pm$ 1%		Load $\pm$ 0.5%		Load $\pm$ 1%	Load $\pm$ 0.5%
	M.R. $\pm$ 2%	M.R. $\pm$ 1%	M.R. $\pm$ 2%	M.R. $\pm$ 1%		
Thrust, %	0.734	0.734	0.734	0.734	0.734	0.734
$\Delta$ P.M./ $\Delta$ V, Lb/fps	382/18	382/18	382/18	382/18	382/18	382/18
$i_{sp}$ Disp. %	0.2925	0.2900	0.2925	0.2900	0.2915	0.2915
$\Delta$ P.M./ $\Delta$ V, Lb/fps	1237/59	1238/59	1237/59	1238/59	1233/59	1233/59
Outage, %	0.256	0.215	0.181	0.130	0.1	0.1
$\Delta$ P.M./ $\Delta$ V, Lb/fps	2488/119	2883/100	1858/89	1259/69	969/46	969/46
Prop. Load, %	0.869	0.869	0.435	0.435	0.869	0.435
$\Delta$ P.M./ $\Delta$ V, Lb/fps	1388/65	1388/65	683/33	683/33	1388/65	683/33
Inert, %	0.2	0.2	0.2	0.2	0.2	0.2
$\Delta$ P.M./ $\Delta$ V, Lb/fps	254/12	254/12	254/12	254/12	254/12	254/12
R.S.S. Lb/fps	3121/149	2813/135	2373/114	1943/83	2126/101	1771/85

Combination

Flight Performance Reserve

Booster	Orbiter	Lb	fps	%V* (38325)
w/P.U.	w/P.U., 1% Load	4010	192	.64
w/P.U.	w/P.U., 0.5% Load	3834	184	.61
w/P.U.	w/o P.U., 1% Load, 2% MR	4615	221	.73
w/P.U.	w/o P.U., 1% Load, 1% MR	4413	212	.70
w/P.U.	w/o P.U., 0.5% Load, 2% MR	4146	198	.66
w/P.U.	w/o P.U., 0.5% Load, 1% MR	3916	188	.62
w/o P.U.	w/P.U., 1% Load	5085	278	.92
w/o P.U.	w/P.U., 0.5% Load	5685	273	.98
w/o P.U.	w/o P.U., 1% Load, 2% MR	6239	299	.99
w/o P.U.	w/o P.U., 1% Load, 1% MR	6091	292	.96
w/o P.U.	w/o P.U., 0.5% Load, 2% MR	5880	283	.93
w/o P.U.	w/o P.U., 0.5% Load, 1% MR	5741	275	.91

Passive propellant utilization by use of a fuel bias was selected for the series burn BRB Space Shuttle booster. This selection is consistent with experience acquired with both methods in the Saturn/Apollo, Centaur, Titan and Atlas programs. Generally, active PU systems are unnecessary in large, multi-engine boosters.

Table 2-13 FPR Requirements – Parallel Burn SRM (4 UTC 1207)

BOOSTER			
Parameter	3 $\sigma$ Dispersion, %	Required FPR	
		Prop., Lb	Vel, fps
Thrust	1.12	-1160	-57
$I_{sp}$	-0.35	- 510	-25
Prop. Weight	-0.15	- 62	- 3
Inert Weight	+0.60	- 194	- 9
$C_A$	+10	-1050	52
	R.S.S.	1658	81

ORBITER						
Parameter	No P.U. System					
	Load - 1%		Load - 0.5%		Active P.U.	
	Engine M.R.		Engine M.R.		Load	Load
	- 2%	- 1%	- 2%	- 1%	- 1%	- 0.5%
Thrust, %	0.734	0.734	0.734	0.734	0.734	0.734
$\Delta PM/\Delta V$ , Lb/fps	500/24	500/24	500/24	500/24	500/24	500/24
$I_{sp}$ , %	0.2925	0.2908	0.2925	0.2908	0.2915	0.2915
$\Delta PM/\Delta V$ , Lb/fps	1580/76	1580/76	1580/76	1580/76	1584/76	1584/76
Outage, %	0.256	0.215	0.191	0.130	0.1	0.1
$\Delta PM/\Delta V$ , Lb/fps	3735/179	3136/150	2786/134	1896/91	1459/70	1459/70
Wt Prop., %	0.869	0.869	0.435	0.435	0.869	0.435
$\Delta PM/\Delta V$ , Lb/fps	1293/62	1293/62	647/31	647/31	1293/61.9	647/31
Inert, %	0.2	0.2	0.2	0.2	0.2	0.2
$\Delta PM/\Delta V$ , Lb/fps	264/12	264/12	264/12	264/12	264/12	264/12
RSS (ORB) Lb/fps	4288/206	3785/182	3321/160	2613/126	2575/124	2319/111
RSS (VEH) Lb/fps	4607/221	4132/200	3712/180	3095/150	3063/150	2851/140
% of V* (30057)	0.75	0.68	0.62	0.52	0.52	0.49

Table 2-14 Orbiter Propellant Utilization System Comparisons

	Weight, Lb	DDT&E SM	Operations, SM
Tank Hardware	216	-	3.1
Transportation Cost	-	2.2	-
Vehicle Hardware	140	10.9	-
Transportation Cost	-	2.2	-
<b>Total</b>	<b>356</b>	<b>14.4</b>	<b>3.1</b>

The selected PU method involves no overall weight penalty to the booster nor does it involve additional equipment beyond that required for propellant loading. Total program cost is reduced by \$11.3M. This selection simplifies interface requirements, maintainability, operability, checkout, logistics, and GSE considerations.



**Table 2-15 Orbiter Active vs Passive PU Comparison**

Configuration	Booster P.U.	Orbiter P.U.	Hardware			Fluids			Total Prog Cost \$M
			Weight Lb	DDT&E \$M	Ops \$M	Bias Lb	FPR Lb	Transportation Cost \$M	
Series BRB	Active	Active	356	14.4	3.1	704	3034	48.8	67.3
Series BRB	Active	Passive	0	0	0	1200	4148	58.8	58.8
Series BRB	Passive	Active	356	14.4	3.1	704	5885	78.2	87.7
Series BRB	Passive	Passive	0	0	0	1200	5900	78.1	78.1
Parallel SRM	-	Active	356	14.4	3.1	1860	2851	43.0	68.5
Parallel SRM	-	Passive	0	0	0	1800	3712	68.7	68.7

**Table 2-16 Booster Propellant Utilization Study Weight Comparison Series Burn BRB**

Item	Booster Inert Weight, Lb	
	Passive Fuel Bias	Active Capacitance
Propellant Utilization System Hardware:	(0)	(2500)
Sensor Installation	0	1078
Temperature Reference	0	78
Control Valve Delta Weight	0	1310
Electronics	0	150
Control Valve Delta P Penalty	(0)	(10,600)
Propellant Utilization Residuals - (Moon)	21,700	(8,768)
Total Inert Weight Penalty	21,700 Lb	21,968 Lb

**Table 2-17 Booster Active P.U. System Cost Series/BRB**

Item	Program Cost Increase, \$M
Reduction in Orbiter FPR	-18.3
PU System DDT&E	18.8
PU System Hardware Cost	7.3
Engine DDT&E Increase	3.5
Engine Recurring Cost Increase	9.8
Net Cost Increase	11.3

**2.7.5 Summary**

Review of the FPR results presented in Tables 2-12 and 2-13 reveals that for both configurations an FPR based on 1% of ideal velocity ( $V^*$ ) is adequate, and in most cases conservative. The propellant utilization (PU) system is more effective on the booster in reducing total FPR. However, when comparing the effectiveness of PU on the booster and orbiter separately, significant FPR savings can be seen in both stages. The effects of propellant loading errors and engine-to-engine mixture ratio are somewhat smaller on total FPR.

Cost trades have shown that although the reserves are smaller with an active PU system in either the orbiter or booster the savings are not sufficient to offset the high development and operational cost of the active system and therefore such a system is not recommended.

## 2.8 COSTS

To complete the comparison of the 15x60 launch configurations studied in this section, a brief cost summary is included. A more detailed presentation of the cost data, how it was derived, and what conclusions can be drawn, is given in the Cost and Schedule Volume of this report.

The summary cost data applicable to this section is presented in Figure 2-54. Total program costs and costs-per-flight are based on the 445 flight traffic schedule and thus emphasize the cost impact of the greater quantity of expendable elements associated with the parallel/SRM configurations. Typically, the lower DDT&E costs for the parallel/SRM's reflect the lower total inert weight and the maturity of the development of the solid motors as compared to either the pump fed or pressure fed liquid engines.

This comparison favors the series/BRB configurations on a program cost basis, but it should be noted that the parallel/SRM regains its competitive position in costs at a lower traffic schedule (approximately 200 flights).

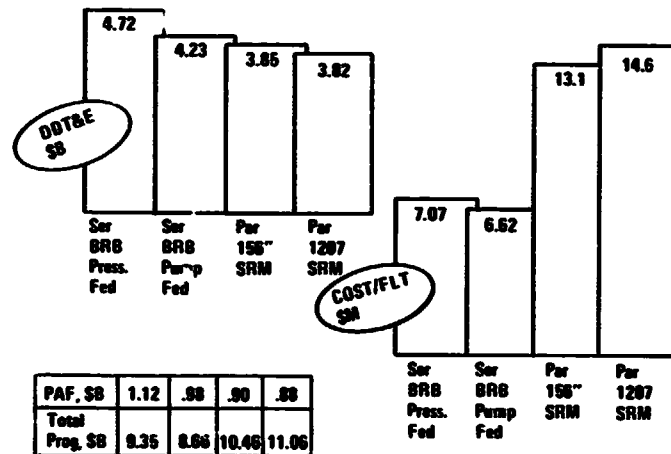


Figure 2-54 Series BRB vs Parallel SRM 15 x 60 Orbiter

## 2.9 SUMMARY

### 2.9.1 Introduction

Several parallel and series launch configurations, designed to meet the system requirements noted in Figure 1-3 for the 15x60 orbiter, have been presented in this section. In addition, the technical issues involved in a comparison of series and parallel burn stacks



have been identified and examined. The following summarizes the results of this investigation of the technical and cost differences between the series/BRB and the parallel/SRM.

### 2.9.2 Configuration Characteristics

A summary of the physical characteristics of all the 15x60 stack configurations is shown in Table 2-1. The configurations germane to this comparison are indicated by the shaded columns. The remaining columns summarize the characteristics of the series/SRM and parallel/BRB stacks included in the original configuration matrix and are presented for information only.

To provide a common base for the comparison of these data, the characteristics representative of the due east mission are used. As expected, the parallel burn/SRM stacks show significantly lower total inert weights, the two 156" stack showing the least. This is solely attributable to the lower inert weights associated with solids and the lower BLOW resulting from the increased boost efficiency of the parallel burn concept. However, more of this inert is expended in the SRM booster configurations.

### 2.9.3 HO Tank Mass Fraction

A weight comparison of a parallel burn and a series burn HO tank designed for the same propellant mass discloses the parallel burn tank to be more efficient, that is, more propellant is carried per pound of tank weight. Two ratios are used to measure this efficiency, the propellant fraction, which is the ratio of the weight of the nominal propellant to the total loaded tank weight, and the structural fraction which is the ratio of the dry weight of the tank to the loaded propellant weight (nominal plus reserves and residuals). These fractions are plotted in Figure 2-21.

Several effects contribute to the higher efficiency of the parallel tank:

- The booster thrust is introduced at the base of the large  $\text{LO}_2$  mass rather than the  $\text{LH}_2$  tank base. This relieves the  $\text{LH}_2$  tank walls and stiffeners of a large part of the compression load resulting from the  $\text{LO}_2$  inertia.
- The maximum longitudinal acceleration occurs in the parallel burn ascent after approximately 30% of the propellant has been turned, thus reducing the structural weight of the portion of the tank walls designed by system pressure and fluid head.
- The booster interface is simpler and no interstage skirt is required. This skirt weight is included in the structural weight of the series tank.

#### 2.9.4 Abort

An examination of the abort modes defined for the various phases of the ascent trajectory (excluding pad abort) identifies the existence of an "abort gap" for all missions with the current orbiter configuration and main propulsion system emergency power levels (EPL).

Three approaches are examined which separately or in combination would eliminate the gap:

- Increase the EPL of the SSME
- Increase the OMS thrust level, or
- Provide additional flight performance reserves for the main propulsion system.

Figure 2-29 plots the interrelationship of OMS engine thrust and EPL and "abort gap", and Figure 2-30 shows the effect of increasing the flight performance reserves and the EPL. The most feasible method to close the abort gap is to increase the OMS thrust level to 9700 lb for each of the two engines. This provides zero abort gap at zero percent EPL for all configurations and missions except the south polar missions for the parallel burn configuration. This mission requires approximately  $1\frac{1}{2}$  to 2% EPL to close the gap.

Abort Mode III requires separating the tank and orbiter in the sensible atmosphere. The burnout conditions of the orbiter must be such that entry can be achieved within the structural limitations of the orbiter, and the dynamic pressure permits jettisoning the tank with a minimum penalty to the nominal separation mechanism. Figure 2-25 shows the relationship at burnout, of the entry acceleration and the dynamic pressure and mach number, indicating that tank staging should occur at a dynamic pressure of 10 to 20 psf which is within the capability of the current system.

#### 2.9.5 Induced Environment

The parallel burn configuration experiences an induced environment during ascent that imposes structural, thermal and cost penalties not present in the series burn. The location of the orbiter in relation to the booster engines and the simultaneous firing of booster and orbiter engines produces acoustic sound pressure levels more severe than the series burn which result in a structural weight increase of 1450 lb. Heating due to hot gas radiation, plume impingement, and plume induced recirculation add 940 lb of insulation to the HO tank. In addition, vibration levels at the cabin level and other equipment locations are high enough to exceed the qualification levels of some of the off-the-shelf items intended for Shuttle use.





Although isolation will reduce the vibration environment to acceptable levels in some cases, there still exists an incremental cost associated with the retest and/or redesign of many items.

#### 2.9.6 Control

The ascent control studies conducted here indicate that control with the orbiter thrust-vector control system alone is inadequate to handle the attitude disturbance torques predicted for the ascent phase. Coupled with the orbiter aerosurface control provides only marginal capability without considering the potential degradation of effectiveness due to the orbiter engine plume interaction.

A 20% control margin using orbiter control only is available with the addition of a 410 ft<sup>2</sup> fin to the bottom centerline of the HO tank at a structural weight penalty of 2600 lb. Allowing up to 50° of roll rotations during ascent would provide the same margin for no weight penalty.

About 10 to 11° of booster engine gimbaling in conjunction with the orbiter TVC is sufficient to provide the required control authority with no augmentation from the aerosurfaces.

Clearly, without providing roll alleviation or permitting vehicle roll during ascent, the parallel burn launch configuration will require booster TVC.

REPRODUCIBILITY OF THE ORIGINAL PAGE IS POOR.

## Section 3

### ORBITER DESIGN STATUS

As a result of NASA direction and design evolution, the HO 15x60 orbiter last reported on in December 1971, has undergone several changes. In addition, NASA requested a study of a 14x45 payload bay orbiter with lower payload requirements in parallel with the 15x60 orbiter study. Both orbiters were to be combined with the same family of boosters for the purpose of comparison.

This section discusses the changes made to the 15x60 orbiter, and its aerodynamic evolution, discusses the feasibility of the 14x45 orbiter, and compares the weights and dimensional characteristics of the resulting designs.

#### 3.1 15x60 ORBITER (SEE FIGURE 3-1)

The changes incorporated into the 15x60 orbiter are as follows:

- NASA-Directed
  - Engines from four J-2S to three 372K SSME
  - Landed payload from 25K to 40K
  - V Design from 156 kts to 150 kts.
- GAC-Initiated
  - Increased directional stability
  - Structurally integral cabin
  - Monopropellant ACS
  - Forward docking
  - RSI TPS
  - Docking ring weight added to orbiter.

These changes resulted in alterations to aerodynamic surfaces, movement of center of gravity positions, and inevitably a heavier orbiter. Specifically the landed weight increased from 161,000 lb to 190,000 lb, the zero payload cg (most aft) moved from 67% of body length to 68.1%, wing leading edge sweep changed from 60° to 49°, and wing cross-section changed from an 8% symmetrical to a 9% cambered section. Figures 3-2, 3-3, and 3-4 summarize these changes and their effects.



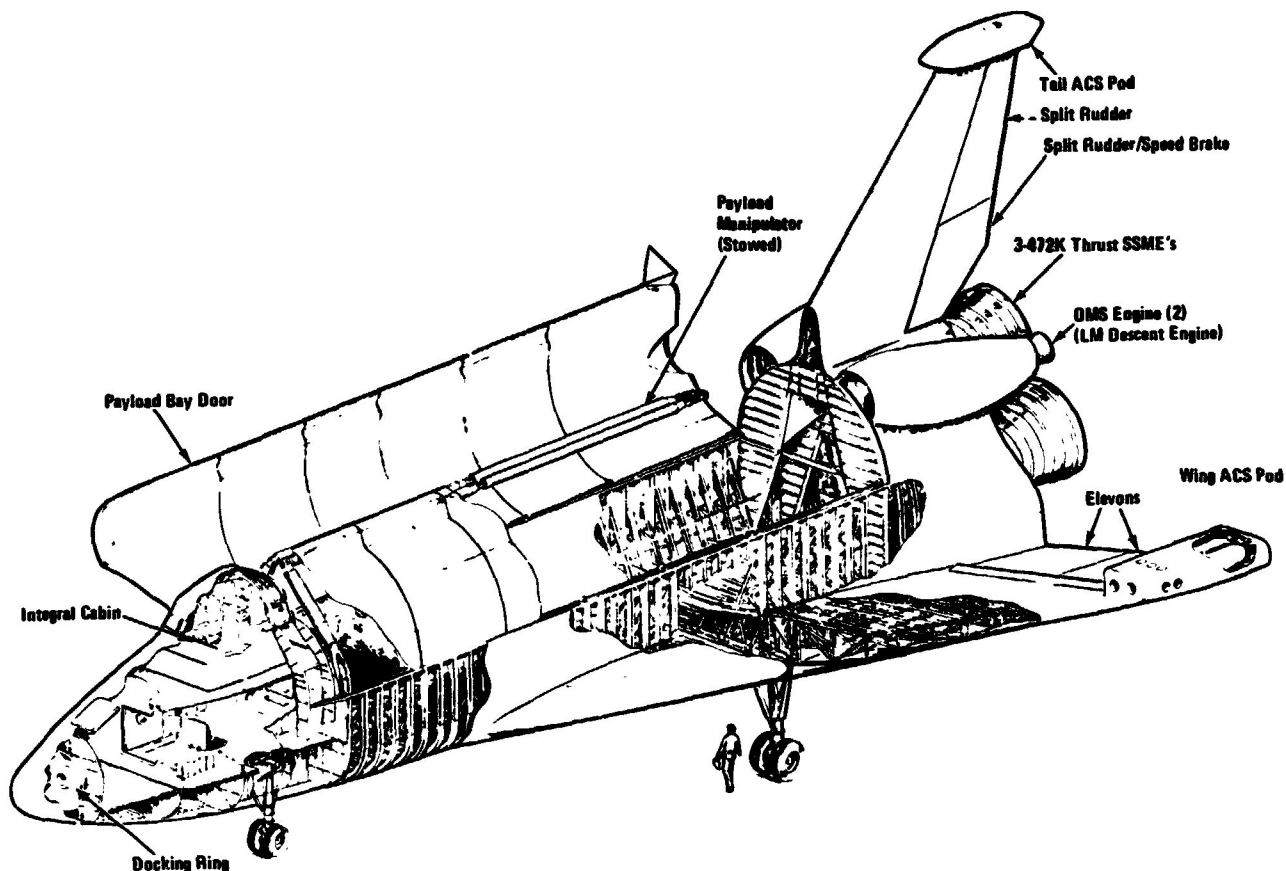


Figure 3-1 15 x 60 PLB Orbiter General Arrangement

	Sept 71 - Dec 71 - 040A -	Feb 72 - 15 x 60 Orb
	Mk I	Mk II
Main Engines	4 x J-2S	4 x 265K
Payload Up - Polar	< 25K	40K
Payload Down	25K	40K
V <sub>Design</sub>	156 Kts	150 Kt
Subsonic Long. Stability	← 2% →	← 2% →
C.G. Range	← 2% →	← 2% →
Hypersonic α Range	← 20° - 35° →	← 20° - 35° →
External Shape	Communal 040A	Bigger Wing Less Sweep
Directional Stability	$C_{n\beta} = .0007$	.0015
TPS	Ablative	RSI & Carbon/Carbon
ACS Propellant	Bi-Prop.	Mono-Prop.
Docking Location	Hood	Nose
Cabin	Floating	Integral

Figure 3-2 Changing Requirements and Ground Rules Orbiter Status

### 3.1.1 Impact of Changes on Configuration

The current 15x60 orbiter is shown in Figure 3-5. The impact of the aforementioned changes are discussed in the following paragraphs.

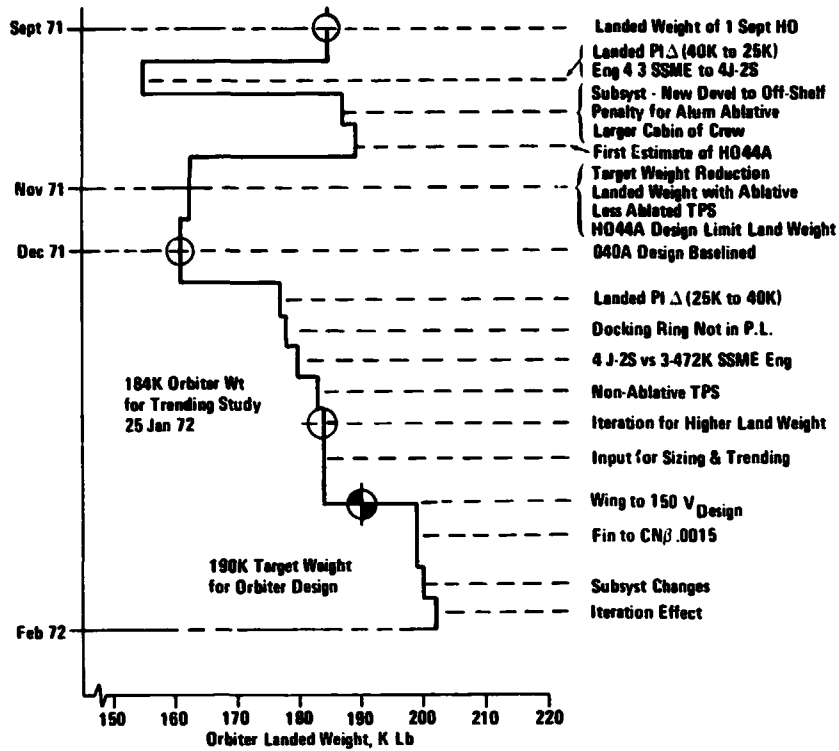


Figure 3-3 15 x 60 Orbiter Landed Weight History

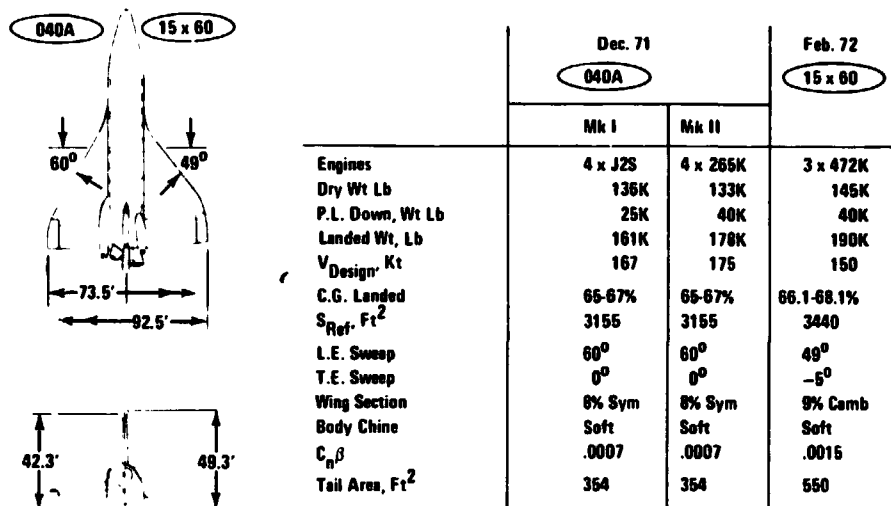
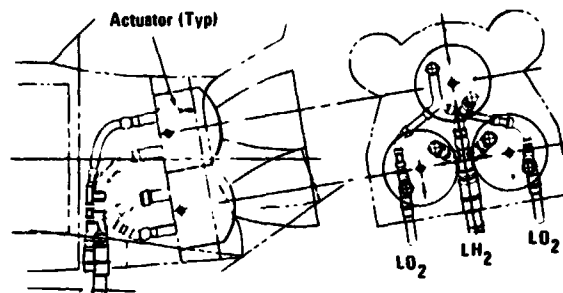


Figure 3-4 Orbiter Evolution





- Fits Inside 040A Fuselage With Minimal Adjustment
- Dual LO<sub>2</sub> Lines Provide Natural Recirculation for Propellant Conditioning
- Tank Disconnects/GSE All in Aft Section of Orbiter
- Single LH<sub>2</sub> Line Provides Compact System

*Figure 3-5 3 x 472K – Main Engine Instl*

### 3.1.1.1 Main Engines

The change from four J-2S engines to three 472K thrust SSME's caused the orbiter cg to shift aft. The effect of this shift was to increase the size of the vertical tail and increase the ACPS rocket size and propellant quantity. As a further result of the center of gravity movement, the payload in/out cg shift increased.

The contour of the aft end of the orbiter changed as a result of the change in engine arrangement from two-over-two, to one-over-two. This arrangement allows the OMS pods to be positioned on both sides of the upper engine, and be structurally connected to its thrust structure. The body transition to the triangular engine pattern reduces the size of the OMS pod protrusion at the aft contour.

With the larger gimbale angle capability of the SSME, greater control authority can be achieved during ascent. In addition greater flexibility in HO tank location and/or geometry is available.

With the one-over-two engine arrangement, the mean center of thrust is closer to the combined orbiter/tank cg. This reduces gimbale angle requirements for cg tracking.

Having one less engine reduces the number of propellant lines, and simplifies the feed system.

Figure 3-6 shows the installation of three 472K SSME engines within the 040A body.

### 3.1.1.2 Change in Down Payload

The increase in down payload from 25K to 40K has various effects on the configuration. As a result of the increased payload weight differential the orbiter landed cg increases its

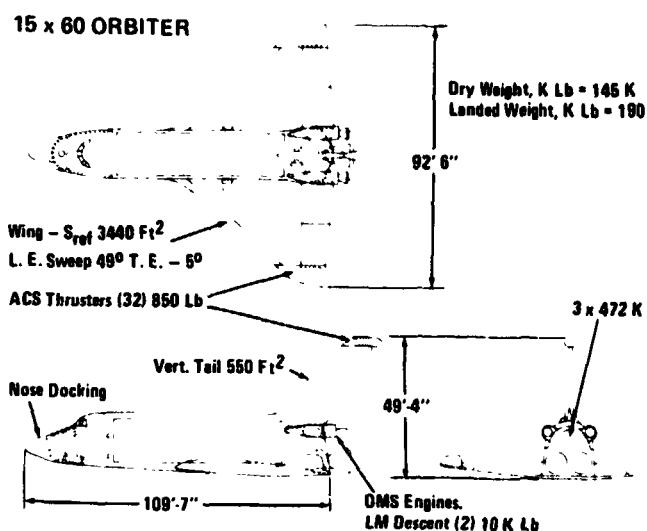


Figure 3-6 15 x 60 Orbiter

fore and aft shift for the case of zero and maximum payload. This forces a decrease in the fuselage nose chine radius to maintain adequate hypersonic trim capability. A weight increase of 4500 lb is incurred due to an increase in wing area to accommodate the higher landed weight. There is also an increase in landing gear weight due to the higher taxi weight of the orbiter. No additional weight was added for increased landing loads since the orbiter is not critical for this condition. There are also weight increases of OMS and ACS propellants which result in increased injected weight.

### 3.1.1.3 Design Velocity Change

The new design velocity requirement of 150 kt, rather than 156 kt for which the December 1971 vehicle wing was sized, required increased wing area for the same landing weight and cg position. This resulted in a 4.2% increase in wing reference area with a consequent increase in wing and vehicle weight.

### 3.1.1.4 Increased Directional Stability

In order to satisfactorily meet minimum flying quality requirements with the backup flight control system, the directional stability ( $C_{n\beta}$ ) level had to increase from 0.0007 to 0.0015 at Mach 0.2, zero angle of attack. This increased the fin area from 354 ft<sup>2</sup> to 550 ft<sup>2</sup>.

The upper and lower rudder segments, each of which is split vertically to open into a wedge shaped section, provide adequate directional stability throughout the supersonic/transonic flight regime.



### 3.1.1.5 Secondary Changes

Changes in subsystems had a secondary effect on the weight and center of gravity position. In brief, the most significant of these changes were:

- Introduction of a structurally integral cabin which provides an increase of 40% in the pressurized volume of the cabin and a 1% reduction in weight
- Reallocation of the weight of the docking ring from payload to the orbiter, resulting in an orbiter weight increase of 1159 lb
- A cost saving, which led to the change in ACS fuel from bi-propellant to mono-propellant, carries a weight penalty to the vehicle of approximately 3500 lb

### 3.1.1.6 Impact of Changes on Configuration

- The net weight change to the vehicle in going from hood to nose docking is 26 lb. However, the new position allows for better cabin and air lock arrangement, more direct docking loads paths, and docking visibility is improved.
- The change in baseline TPS from ablative to RSI offers no change in weight up to entry, since the two systems weigh the same. However, since an ablative TPS loses weight during entry, the December 1971 version of the orbiter showed a 3400 lb lower landed weight relative to the current vehicle.

Figure 3-5 show the resulting orbiter configuration.

## 3.1.2 Aerodynamic Development of the 15 x 60 Orbiter

The 15x60 payload bay orbiter described in the previous sections was developed from an extensive series of wing-body trade studies. These studies were based on analysis of two distinct fuselage designs. Fuselage Design 1 is the MSC 040A nose lines and planform. Design 2 represents a hard-chined configuration with increased forebody planform area. Figure 3-7, represents the two fuselages under discussion and shows graphically the differences in section shape, planform area and nose camber.

The wing-planforms studied were restricted so that the elevon chord was never greater than 60% of the local chord and the elevon area was equal to 12.2% of the total planform area. An additional constraint requiring the elevon hinge line to be perpendicular to the streamwise air flow was imposed to minimize adverse yaw due to elevon deflection. This attention to elevon size and planform allowed the selection of a finite number of realistic planforms. The following table lists the planforms used for these studies:



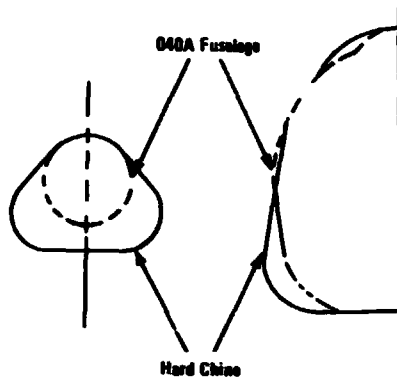


Figure 3-7 Comparison of Soft and Hard Chine Fuselage Sections

L. E.	AR	Taper Ratio for a Trailing Edge Angle				
		-9°	-5°	0°	+5°	+9°
45	2.6	.141	.165	.200	.255	.293
50	2.3	.126	.150	.180	.223	.255
55	2.0	.115	.135	.160	.197	.223
60	1.85	.067	.100	.110	.136	.158

These planforms selected have a maximum aspect ratio while satisfying the elevon requirements. Thus the wings selected provide the best aerodynamic performance (landing speed and stability) for minimum wing weight.

The basic design criteria are a blend of landing performance, flying qualities and hypersonic trim/stability requirements. The landing performance requirement is a design velocity of 150 kt with a 40K payload at the most forward center of gravity. The flying qualities criteria translates to minimum subsonic static margin of 2% of body length at the most aft cg. The hypersonic trim criteria is a  $C_p$  position of 3% aft of the center of gravity at  $\alpha = 60^\circ$ . This provides a trimmed angle of attack range to  $35^\circ$  with full elevon deflection at the most forward cg.

To perform the trades necessary to evolve a viable design, a computer program was developed to size any vehicle. This sizing program blends the subsonic and hypersonic characteristics of the vehicle by means of wing area and planform. The vehicles generated by the program meet the flying qualities and hypersonic trim requirements. These vehicles are analyzed to obtain the design which meets all stated requirements about the 'actual' most aft center of gravity location.

The trade studies performed have not only evolved a vehicle which meets all design requirements but have also identified the alternate designs which result from relaxing these



requirements. In performing these studies several constraints were placed on the design. One, the basic length of both fuselages studied was held at 109.58 ft. Secondly, the trailing edge of the exposed wing was constrained at the aft end of the fuselage. Also, for all studies the landed weight was assumed to be 100,000 lb. Under these ground rules the following major studies will be discussed: 1) static margin variation, 2) hypersonic trim margin variation, 3) trailing edge sweep variation, 4) wing twist and camber effects, 5) extension of fuselage length, 6) variation of design velocity, and 7) effect of landed weight variation.

#### 3.1.2.1 Static Margin Variation

To obtain adequate 'bare airframe' flying qualities a study has shown that a minimum of 2% static margin is necessary. Figure 3-8 presents the results of a study comparing the wing area, sweep angle and required center of gravity for vehicles with the required 2% and a 1.5% static margin.

The important conclusion from this study is that upon reducing the subsonic static margin the required wing area 'increases'. This increase in wing area is due mainly to the constraint holding the wing trailing edge to the aft end of the fuselage. Thus, in order to reduce the static margin, wing area is added in front of the leading edge. Along with increased wing area comes an increase in leading edge sweep angle. This increase in sweep is due to the increase in area being added largely to the inboard section of the wing.

#### 3.1.2.2 Hypersonic Trim Margin Variation

The study of the effects of varying the hypersonic trim margin shows a relatively small sensitivity of wing area for a given center of gravity location. Thus the hypersonic trimmed alpha range can be varied by judicious modeling of the nose camber and planform lines without changing the landing performance or the subsonic static stability. The only side effect of this variation is a change in the leading edge sweep angle, Figure 3-9.

#### 3.1.2.3 Trailing Edge Sweep Angle Variation

The effects of varying the trailing edge sweep angle is graphically presented in Figure 3-10. The results show a marked increase in wing area with increased sweep angle. A practical maximum forward sweep angle must be established in the selection of an optimum planform. In selecting the optimum trailing edge sweep angle, notice was taken of the rate of change of the leading edge sweep angle. At angles less than  $-5^{\circ}$  the leading edge sweep angle starts to decrease rapidly and the wing area required begins to reach an optimum level. Thus at angles less than  $-5^{\circ}$  the minimum wing area is reached and  $-5^{\circ}$  was selected as the trailing edge sweep.

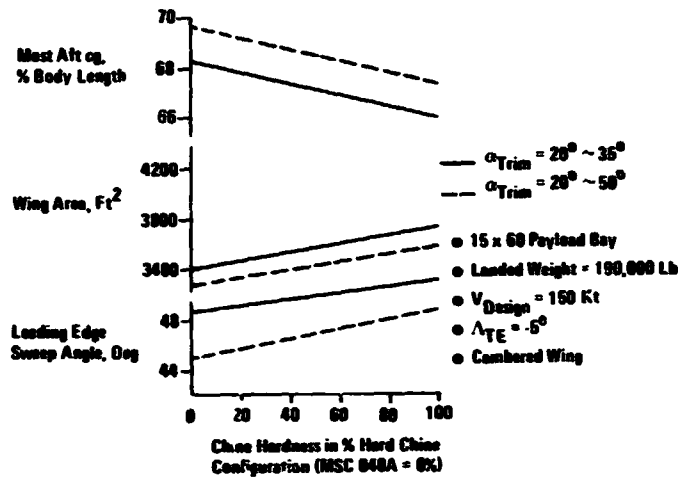


Figure 3-8 Effect of Subsonic Static Margin

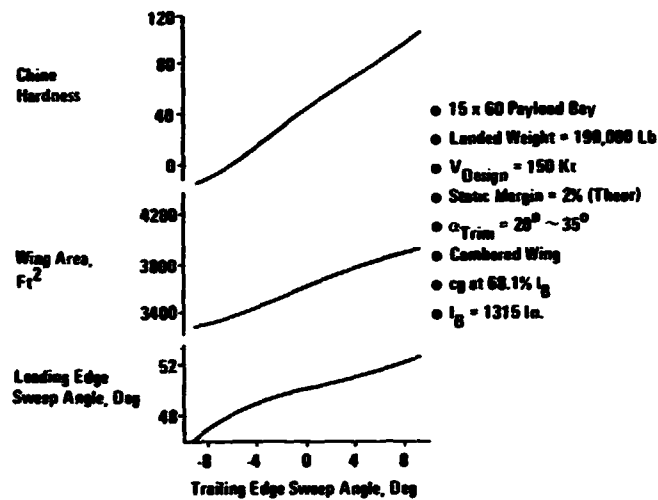


Figure 3-9 Effect of Hypersonic Trim Margin

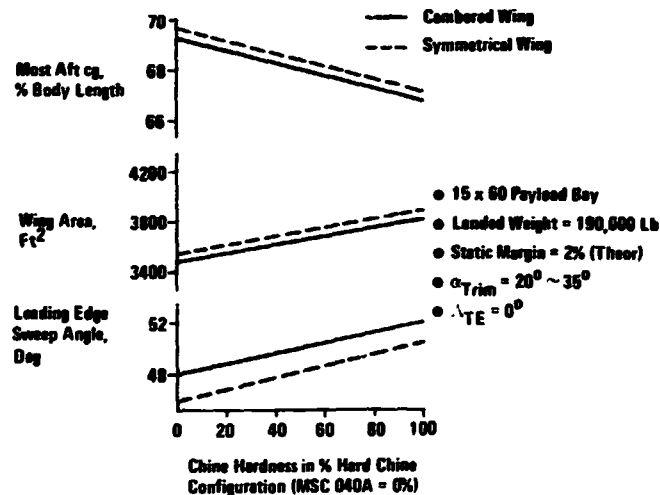


Figure 3-10 Trailing Edge Angle Effects



#### **3.1.2.4 Wing Twist and Camber Effects**

The introduction of a cambered wing airfoil section allows a decrease in wing area and an increase in leading edge sweep angle. This effect is due to the increase in the maximum useable lift resulting from optimizing the wing airfoil section. Figure 3-11, graphically presents these results and shows approximately 130 ft<sup>2</sup> of wing area reduction and an increase in leading edge sweep of one degree for a camber wing.

#### **3.1.2.5 Extension of Fuselage Length**

Extension of the fuselage length results in an increase in wing area. (See Figure 3-12) One advantage of this alternative is an increase in leading edge sweep angle and a reduction in wing loading. The increase in weight due to the increased fuselage length and the increased wing area show this alternative to be a costly fix to achieve adequate tail arms for satisfactory control.

#### **3.1.2.6 Variation of Design Velocity**

Figure 3-13 presents the effects of changing the design velocity. This shows that allowing an increase in design velocity allows an increased leading edge sweep angle and a reduction in wing area.

#### **3.1.2.7 Effect of Landed Weight Variation**

The effect of an increase in landed weight is presented in Figure 3-14. The necessary increase in wing area necessary to hold the design velocity is minimized by the increased efficiency of the wing planform.

#### **3.1.2.8 15x60 Payload Bay Orbiter Configuration**

The 15x60 payload bay design evolved out of a blending of the MSC 040A fuselage and a fuselage with hard chine nose lines. For both fuselages a wing was selected (see Figures 3-15 and 3-16) for a targeted landed weight of 190,000 lb and a design velocity of 150 kt. Both point designs meet the subsonic stability and the hypersonic trim requirements. These point designs were balanced and the most aft center of gravity was established for the payload out condition. Figure 3-17 presents a series of optimum vehicle designs and the center gravity locations where these designs balance in both subsonic and hypersonic modes. The final design was then selected as the design point at which the actual and the balance point center of gravities coincide. The resulting design is presented in Figure 3-5.

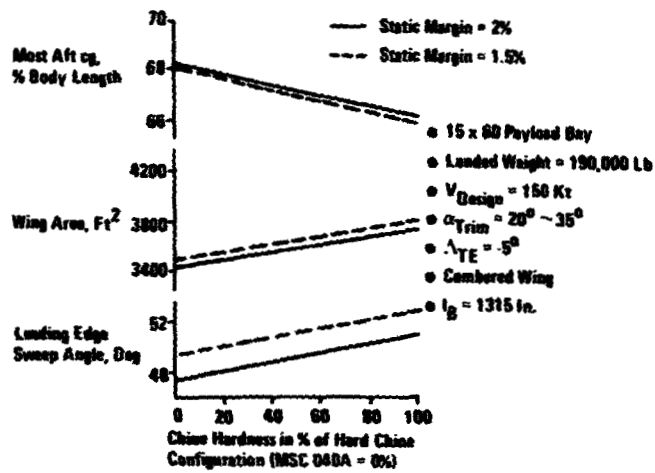


Figure 3-11 Effects of Wing Chamber

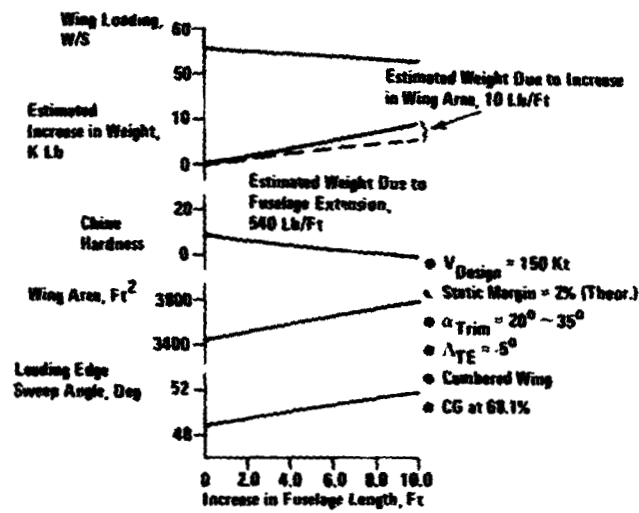


Figure 3-12 Effect of Extending Basic Fuselage Length

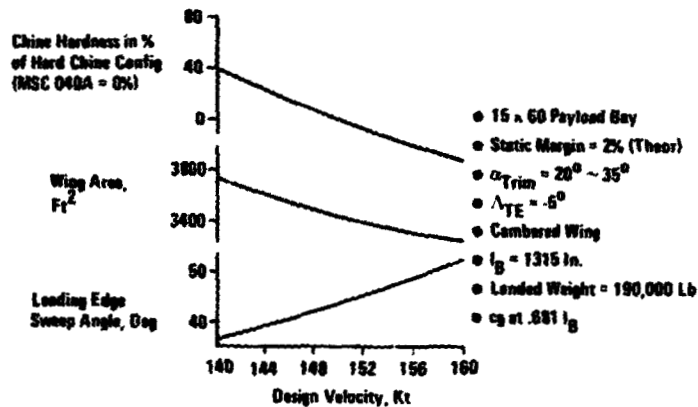


Figure 3-13 Design Velocity Effect on Wing Trending



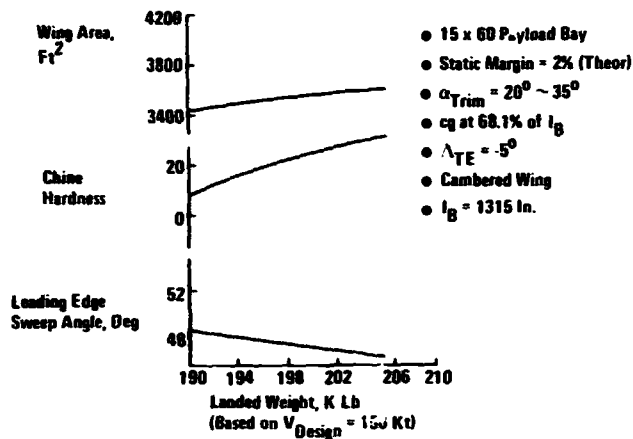


Figure 3-14 Effect of Landed Weight Change

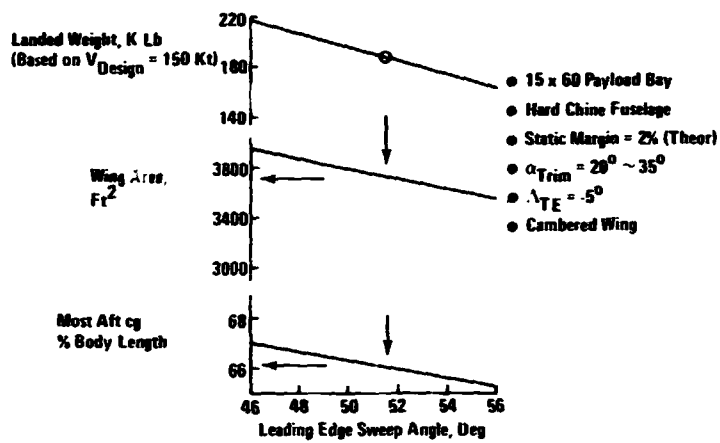


Figure 3-15 15 x 60 Configuration Hard Chine

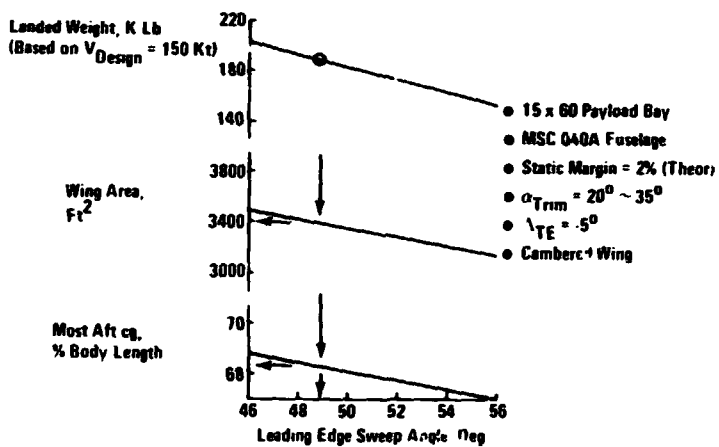


Figure 3-16 15 x 60 Configuration Soft Chine

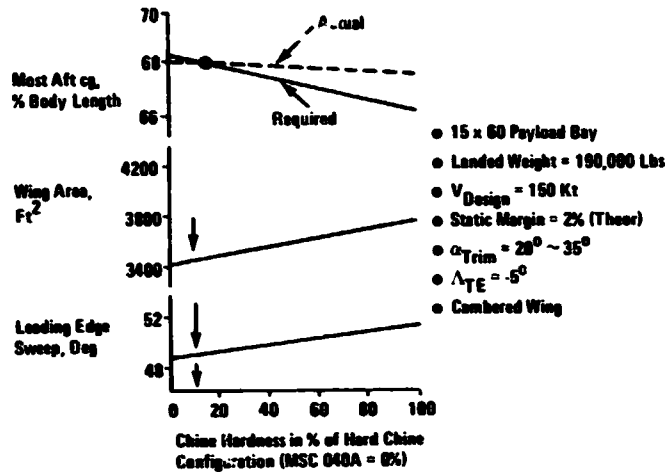


Figure 3-17 15 x 60 Optimum Configuration 3 x 472K SSME

### 3.2 14x45 PAYLOAD BAY ORBITER

By NASA direction, we included a study of an orbiter with a 14x45 payload compartment, a reduced payload weight and three 472K thrust main engines. Our first design, which was virtually the 15x60 orbiter with 15 ft removed from the payload bay, had a center of gravity, landed without payload, at 69% of body length. The most aft cg for which a practicable wing could be provided to achieve aerodynamic balance was 66.2% body length.

#### 3.2.1 14x45 Orbiter Aero Options

Three alternate solutions to the problem of achieving an acceptable aero configuration of an orbiter with a small payload bay were investigated: (see Figure 3-18)

- Reduce the main engine thrust level to 380K each, change the ACS to wing/wing/nose and move the APU's forward

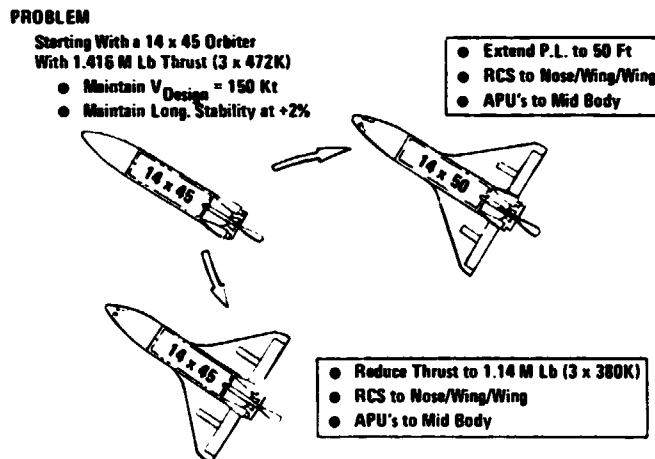


Figure 3-18 14 x 45 Orbiter Aero Options



- Change the ACS locations to wing/wing/nose, move the APU's forward and increase the body length
- Add 2300 lb of ballast in the nose of the vehicle to position the center of gravity at 66.2% of body length with a landed weight of 166,380 lb. This solution was not pursued since the use of ballast, in this instance, carries a weight penalty with no benefits as compared to the alternate solutions.

### 3.2.1.1 Reduce Engine Thrust

The reduced thrust option of the 14x45 payload bay orbiter was configured aerodynamically in the same manner as the 15x60 design (refer paragraph 3.1.2). Figures 3-19 and 3-20 were generated from empirical and analytical data for each of two fuselage nose configurations and represent a family of orbiters aerodynamically configured to meet the requirements of  $V_{Design}$ , static margin and hypersonic trim. From these data, Figure 3-21 is derived for orbiters with a landed weight of 158,400 lb. The most aft cg in the landing configuration occurs with zero payload and for this orbiter configuration, lies at 66.2% of the body length. Engineering Figure 3-21 at this value defines the orbiter wing area, leading edge sweep and fuselage chine shape. The resulting configuration is shown in Figure 3-22.

### 3.2.1.2 Lengthen Fuselage

To retain the 472,000-lb thrust SSME, configuration changes must be made to the 14x45 payload bay orbiter to shift the most aft cg location to approximately 67% of the body length.

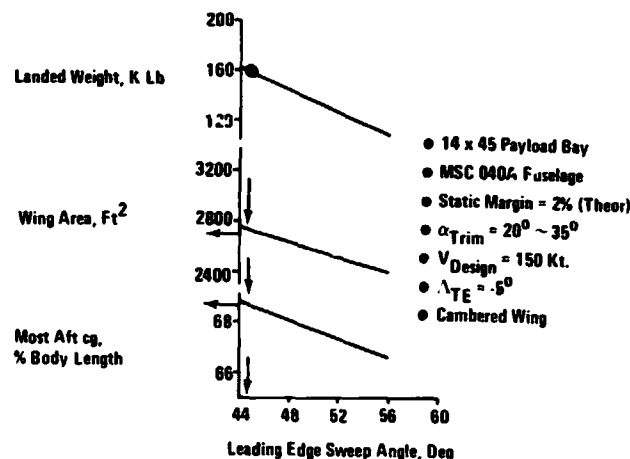


Figure 3-19 14 x 45 Configuration Soft Chine



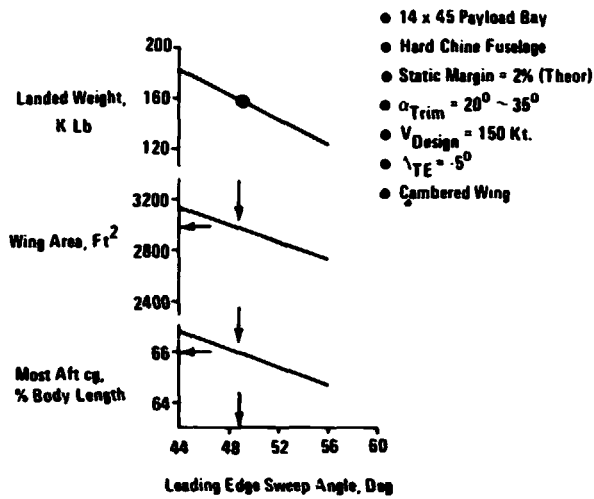


Figure 3-20 14 x 45 Configuration Hard Chine

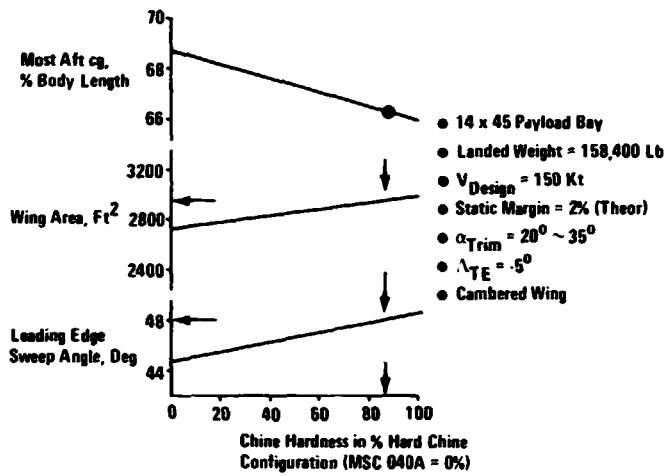


Figure 3-21 14 x 45 Optimum Configuration 3 x 380K SSME

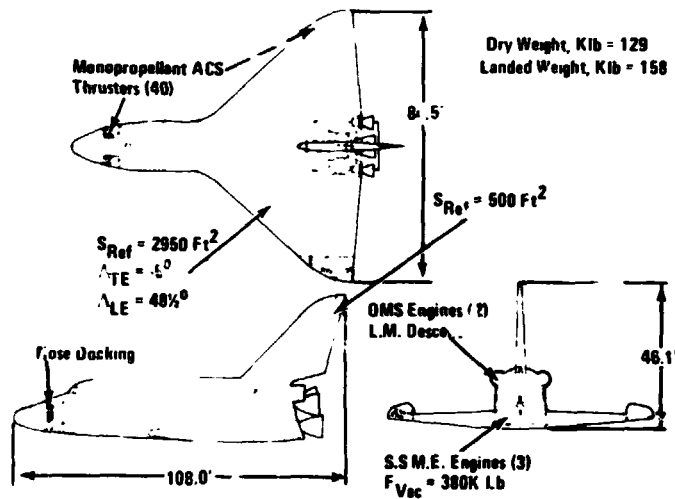


Figure 3-22 General Arrangement 14 x 45 Orbiter 3 x 380K SSME



This is accomplished by moving the APU's forward, relocating the ACS tail pod to the fuselage nose and adding 5 ft to the fuselage length. The most effective way to utilize the fuselage length increase is to consider it part of the payload bay. The resulting configuration meets the aerodynamic requirements and has a landed weight with payload of 167,000 lb. The configuration is shown in Figure 3-23.

### 3.3 SUMMARY

Recent requirement changes and the continuing evolution of the 15x60 orbiter design have resulted in the configuration shown in Figure 3-5. The most significant differences between this orbiter and its predecessor are: the increase in landed weight from 161,000 to 190,000 lb, primarily the result of the reduced V Design and the increase in installed engine weight; the increase in the vertical tail area due to the reduction in tail arm and the required increase in the directional stability; the revised wing planform and the increase in wing area which results from the combined effects of the lower V Design and the rearward shift of the most aft cg position.

The design of an orbiter which meets the same aerodynamic requirements specified for the 15x60 orbiter and has a smaller payload bay depends primarily on the ability to locate the most aft cg sufficiently far forward to provide the necessary aero balance with a practical wing. By reducing the main engine thrust (lighter weight engines), or lengthening the fuselage, two acceptable configurations were developed (Figures 3-22 and 3-23). Utilizing the additional fuselage length to increase the length of the payload bay results in the more practical configuration, in that it retains the higher thrust main engines for improved ascent and abort performance and sacrifices less payload capability.

A physical comparison of the three orbiters presented here is shown in Figure 3-24 and a detailed weight breakdown of each tabulated in Table 3-1.

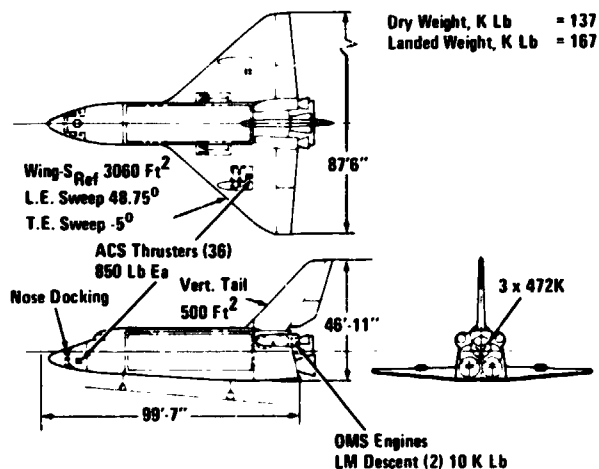


Figure 3-23 14 x 50 Orbiter 3 x 472K SSME

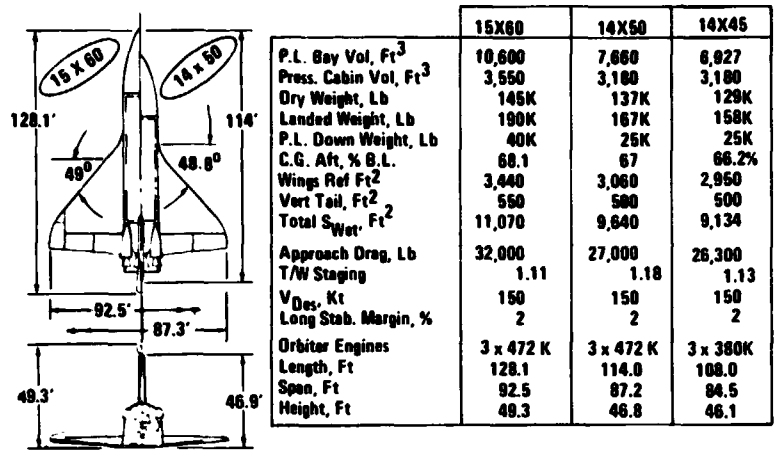


Figure 3-24 Orbiter Comparison

Table 3-1 Small Payload Bay Orbiter Detailed Weight Statement

Subsystem	14 x 50 Orbiter Weight, Lb 3 x 472K SSME's	15 x 60 Orbiter Weight, Lb 3 x 472K SSME's	14 x 45 Orbiter 3 x 380K SSME's
Wing Group	12,867	14,702	12,365
Tail Group	2,801	3,029	2,718
Body Group	31,263	33,173	29,551
TPS	23,599	24,907	22,355
Land Recovery Dock			
Docking	8,443	9,181	8,056
Propulsion - Main	21,883	21,743	17,172
Propulsion - Secondary	6,990	8,580	7,729
Pri. to Power	3,363	3,315	1,666
Elect. Conv & Distr	2,732	2,693	2,653
Hydraulics & Surface Control	3,450	3,402	3,351
Avionics	5,314	5,239	5,162
Environ. Control & Pers. Prov.	3,784	3,371	3,676
Growth/Uncertainty	10,975	11,896	10,500
Dry Weight	137,464	145,391	128,552
Pers./Res./Resid.	4,536	4,609	4,448
Landed Weight W/O Payload	142,000	150,000	133,000
Cargo	25,000	40,000	25,000
Landed Weight W/Payload	167,000	190,000	158,000



14 x 45 PAYLOAD  
BAY ORBITER

REPRODUCIBILITY OF THE ORIGINAL PAGE IS POOR.

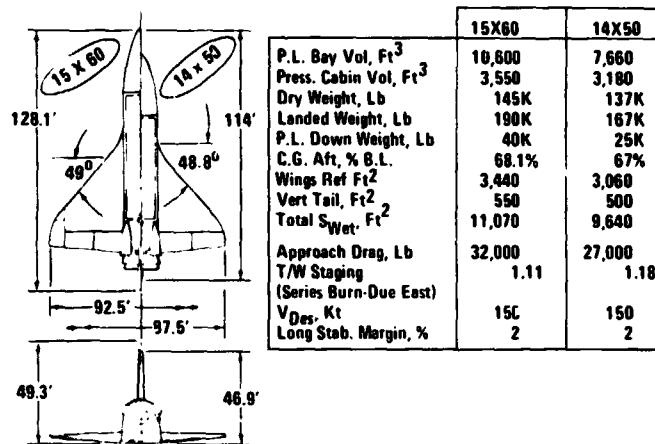
## Section 4

### 14x45 PAYLOAD BAY ORBITER

An investigation was conducted to determine whether significant development and operational cost savings are achievable in the parallel burn/SRM configurations by reducing the orbiter payload bay size and payload weight.

Two orbiters were configured with a small payload bay, one with three 472K lb thrust SSME's and the other with three 380K lb thrust engines. The evolution of these configurations is described in Section 3 of this volume. The significant characteristics of these orbiters are compared with the baseline 15x60 orbiter in Table 4-1.

*Table 4-1 Orbiter Comparison*



#### 4.1 STACKED CONFIGURATIONS

Using the trending program described in Section 2, characteristics were obtained for various stacked configurations of the two small payload bay orbiters. These stacks satisfy the systems requirements and groundrules specified in Section 1. For the reasons cited for the 15x60 orbiter trending, only the 156" SRM configurations are trended (refer to Sub-section 2.1).

From these data, point designs are selected which will permit a 5% growth in orbiter inert weight to be accommodated by an increase in the HO tank capacity only - no booster re-sizing is necessary. Figures 4-1 and 4-2 show the trending data and the point designs



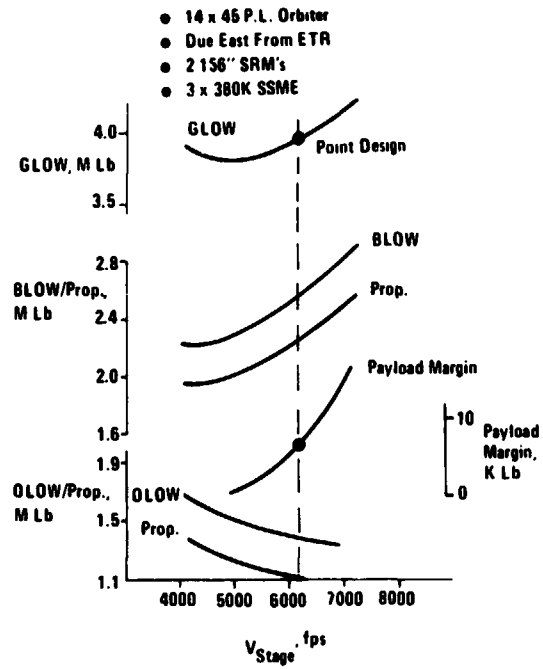


Figure 4-1 Parallel/SRM Trending

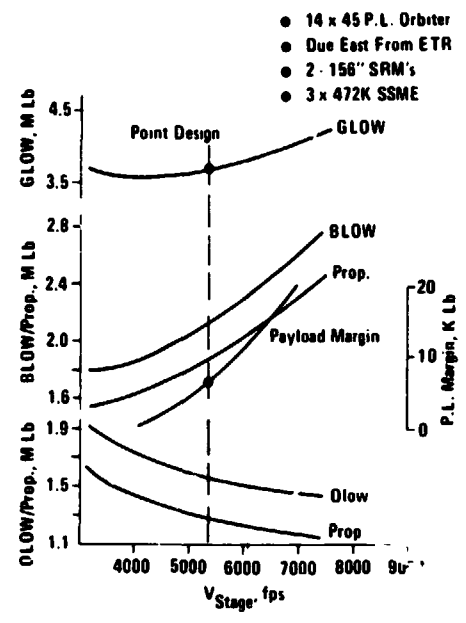


Figure 4-2 Parallel/SRM Trending

selected for the two small payload bay orbiters, and Figure 4-3 compares these data with that resulting from the trending of the 15x60 orbiter baseline configuration.

The stack characteristics of the 120'' SRM launch configurations are determined in the same manner as for the 15x60 orbiter sizing (refer to subsection 2.1). The resulting stacks are shown in Figures 4-4, 4-5, 4-6 and 4-7.

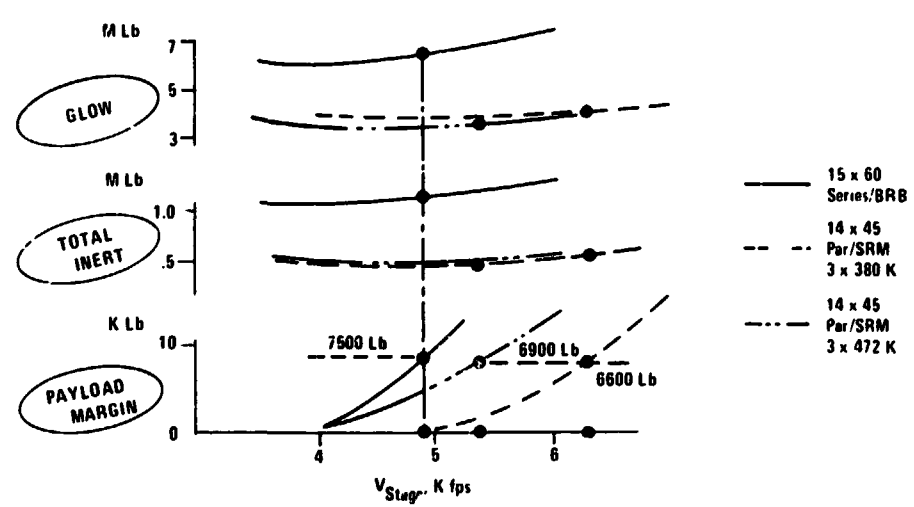


Figure 4-3 Launch Configuration Performance

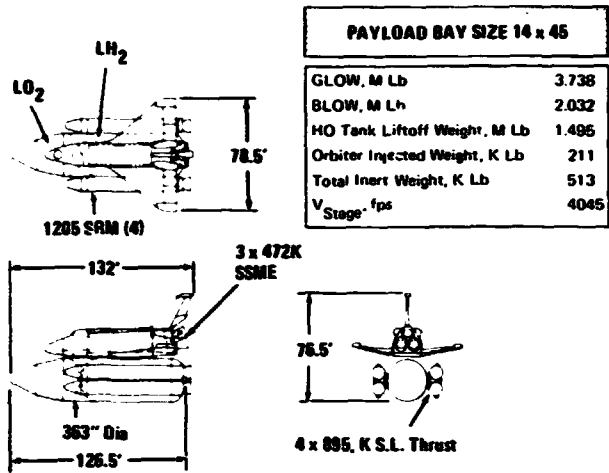


Figure 4-4 Parallel/120S SRM 3 x 472K SSME Launch Configuration

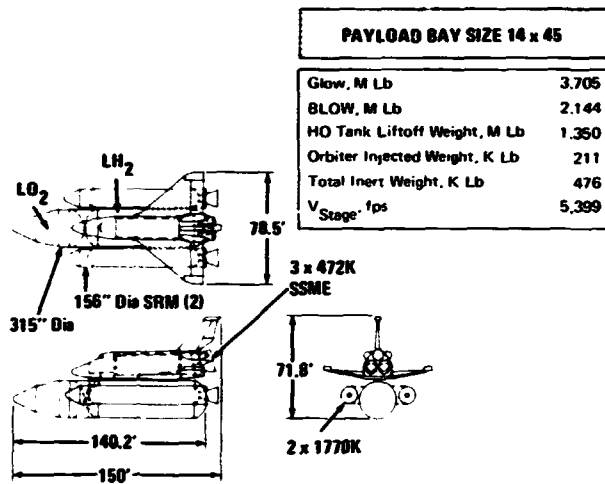


Figure 4-5 Parallel/156\"/>

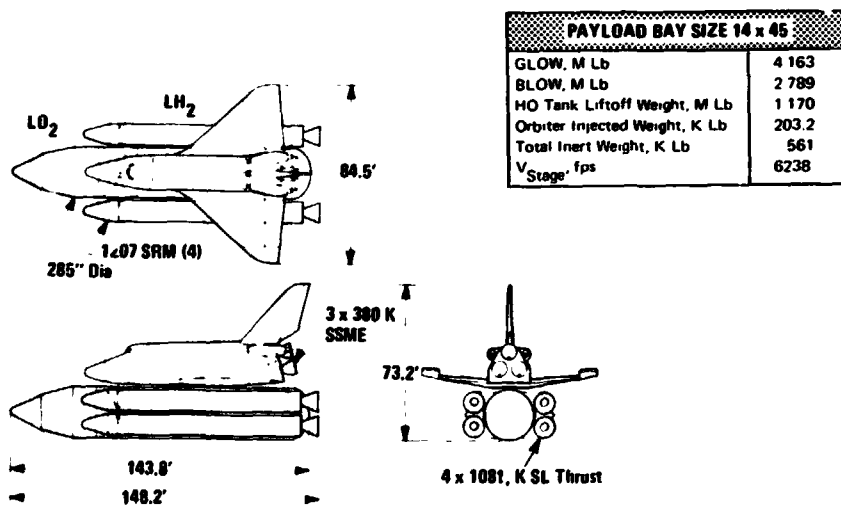


Figure 4-6 Parallel/1207 SRM 3 x 380K SSME Launch Configuration



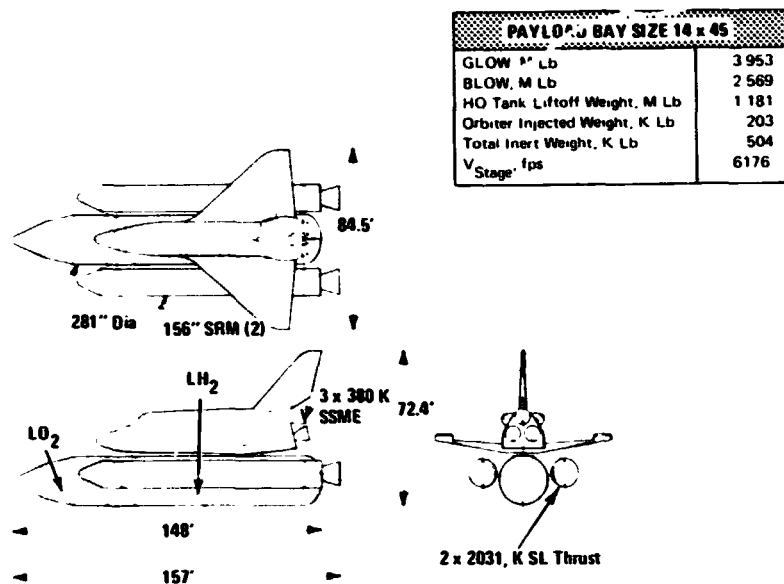


Figure 4-7 Parallel/156'' SRM 3 x 380K SSME Launch Configuration

As in the case of the 15x60 parallel/SRM configurations, the 14x45 stacks exhibit a significant reduction in total inert weight relative to the series/BRB baseline, the greatest reduction being exhibited by those configurations employing the fewest SRM's. However, a much larger percentage of the total inert weight (the spent boosters and the larger HO tank) is expended during each flight of the parallel burn/SRM stack.

Reducing the orbiter main engine thrust level lowers the orbiter dry weight, but the booster liftoff weight increases because of the lower performance of the orbiter. Note that the 472K version of the small payload bay orbiter can operate with four 1205 SRM's as a booster while the reduced thrust version requires four 1207 SRM's (refer to Table 4-2). This results in an increase in booster liftoff weight in excess of 750K lb. The overall effect is to increase the gross liftoff weight and the expended inert weight.

Table 4-2 summarizes the significant characteristics of the 14x45 payload bay stacks and includes the 15x60 series/BRB baseline for comparison.

#### 4.2 COSTS

A brief cost summary is presented in Figure 4-8 to complete the comparison of the small payload bay configurations. The Cost and Schedule Volume of this report presents a more detailed comparison of the cost data for all configurations.

Typically the DDT&E costs decrease with the use of solid boosters, (see Figure 2-54), and further decreases are available with the reduction in orbiter size and engine thrust as



Table 4-2 Vehicle Characteristics Summary Due East From ETR

Orb. Engines	3 x 472 K	3 x 472 K		3 x 380 K	
Launch Conf.	Series	Parallel			
Orbiter Type	15 x 60	14 x 45		14 x 45	
Booster Type	PR. F. BRB	1205 SRM	156" SRM	1207 SRM	156" SRM
GLOW, M Lb	6.386	3.738	3.705	4.163	3.953
V <sub>Stage</sub> , fps	4879	4045	5389	6238	6176
t <sub>Stage</sub> , Sec	139	124	141	149	151
a <sub>Stage</sub> , psf	70	141	79	48	46
T/W <sub>Stage</sub>	1.108	1.07	1.7 <sup>c</sup> 1	1.139	1.13
Alt <sub>Stage</sub> , K Ft	138	114	148	160	161
q <sub>Max</sub> , psf	631	643	638	665	638
W <sub>Stage</sub> , K Lb	1277	1321	1123	1001	1009
<b>Orbiter</b>					
Inert Weight, K Lb	243.8	210.7	210.7	203.2	203.2
Inert Weight, K Lb	150.5	141.2	141.2	132.6	132.6
Landed Weight, K Lb	184.2	159.9	159.9	152	152
Dry Weight, K Lb	139.4	130.3	130.3	122.4	122.4
<b>HD Tank</b>					
Total Weight, K Lb	1034	1495	1350	1170	1181
ΔV Prop. Weight, K Lb	969	1411	1274	1101	1112
Inert Weight, K Lb	64.9	84.2	76.6	69	69
Dry Weight, K Lb	54.0	68.3	61.7	53.4	53.9
<b>Booster</b>					
Number	1	4	2	4	2
Total Weight-Ea, K Lb	5119	508	1072	697	1284
ΔV Prop. Weight-Ea, K Lb	4176	436	943	607	1133
Inert Weight-Ea, K Lb	943	72	129	90	151
λ'	.815	.861	.88	.87	.882
No. Engines-Ea	7	1	1	1	1
FSL per Eng, K Lb	1136	895	1770	1081	2030
<b>Payloads</b>					
S. Polar - WTR, K Lb	42	23.5	23.7	24.2	23.9
55° - ETR, K Lb	39.8	22.6	23.5	24.3	24.4
Due East - ETR, K Lb	65	45	45	45	45
Total Inert Weight, K Lb	1158	513	476	561	504
Payload Margin, Lb	7500	11000	6900	8300	6600

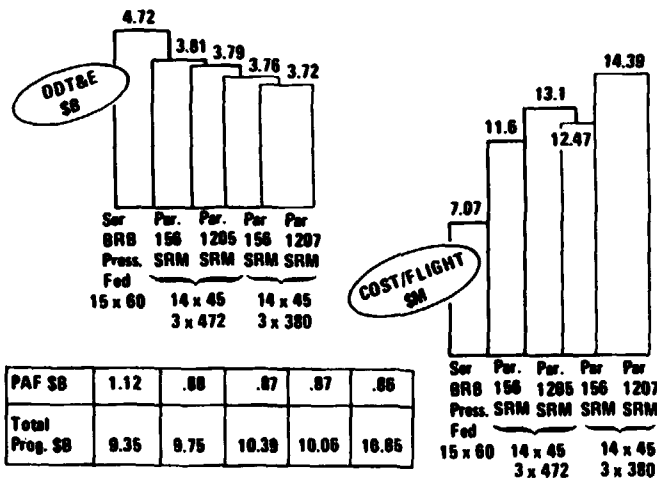


Figure 4-8 Series BRB 15 x 60 vs Parallel SRM 14 x 45



shown in Figure 4-8. However, this gain is offset by the increase in total program costs attributable to the higher cost of the expended tanks and to the fact that the solids are not recoverable.

#### 4.3 EFFECT OF PAYLOAD WEIGHT AND PAYLOAD BAY SIZE REDUCTION

In going from the standard 15x60 payload bay orbiter to nominally 14x45 payload orbiter systems, we changed not only the physical size of the orbiter but also, as per NASA direction, lowered the payload weight for the due east launch mission from 65K lb up and 40K lb down to 45K lb up and 25K lb down. It was of interest both to NASA and ourselves, to evaluate how much each of these changes in requirements contributes to the total orbiter weight and system cost reductions we have shown are attainable by going to the small orbiter configuration.

The orbiter dry weight decrease apportionment study was performed on the trending program input versions of the large and small orbiters, for which the dry weight differential was approximately 12K lb (as opposed to the 8K and 16K lb dry weight differentials indicated in Section 3, which apply to the aerodynamically optimized versions). The general conclusions are, however, pertinent to all configurations which are compared on the basis of equivalent aero performance.

To determine the effect of payload bay size reduction for equivalent payload capability, we developed two versions of a 14x45 orbiter. Each was sized for the large orbiter payload capability of 65K lb up/40K lb down in the small payload bay, but one was based on the same wing reference area as was used for the lower weight payload, while the other was based on equivalent wing loadings (larger wing area). The first approach assured a balanced configuration but with degraded performance (higher  $V_{Design}$ ), while the second approach maintained performance but reduced the longitudinal stability margin relative to the small payload bay, low payload weight design.

In practice, of course, an actual vehicle having the small bay but large payload would be like neither of the above versions but would be developed to meet the proper performance and stability requirements. However, the two versions we did configure represent the extremes of the weight deltas that would result and thus bracket the actual weight of such an intermediate orbiter.

The results of our study, shown in Figure 4-9, indicate that the payload bay size reduction is the predominant cause of the orbiter dry weight reduction, accounting for between 70% to 90% of the total. The main reasons for this result are briefly the following:

- The 20K lb decrease in up payload has only a minimal effect on dry weight since very little of the structure is designed by the end boost loads, which are primarily affected by the weight of the up payload
- The landed payload decrease reflects itself primarily in the allowable wing weight reduction for constant wing loading, and in somewhat lower landing gear weights. These wing and gear weight decreases are roughly in proportion to the percent decrease in landed weight, which, for the configuration studied, amounted to only about 12%
- The fuselage weight reduction due to decreased length and diameter is, however, approximately 550 lb per linear foot, which is relatively independent of payload weight, and thus represents a weight saving not associated with the payload weight reduction.

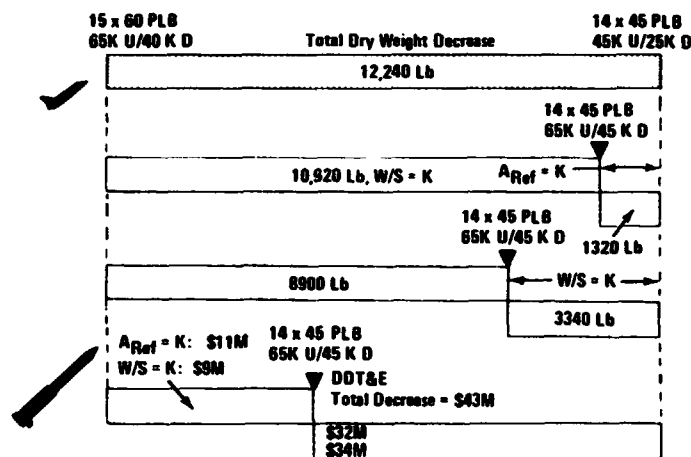


Figure 4-9 Bay Geometry & Payload Weight Effects on Orbiter

As far as overall system cost reductions are concerned the situation is quite different. Of the total development cost reduction of approximately \$43M accrued by going from a 15x60 bay orbiter/parallel/156" SRM system to the same configuration employing a 14x45 bay orbiter, only about 25% is due to bay size reduction and 75% due to payload weight reduction (see Figure 4-9). The main reason for this is that in the system cost picture, the effect of tank and booster dry weight decrease are also factored in, and it is here that the major effect of payload weight reduction manifests itself.

Thus, our overall conclusion is that, since cost is the most important factor, the weight of the payload is a more significant driver than the size of the bay. To save development cost, then, reduce the design payload weight but retain the 15x60 bay.



#### 4.4 SUMMARY

Typically, the parallel/SRM configurations show lower DDT&E costs reflecting the lower GLOW and total inert weight of these configurations relative to the series/BRB baseline. From a detail examination of the cost per flight of the parallel/SRM configurations it becomes clear that the most significant influence on the cost per flight is the number of boosters required, rather than the total booster liftoff weight. Thus, the 120" systems, although exhibiting a somewhat lower development cost, penalize the per flight cost since, generally, four of the 120" SRM's are required at the maximum payload specified, while two 156's can provide the same performance.

Reducing the orbiter size to the limiting capability of two 1207 SRM's would provide a low cost system but results in configurations with impractically small payload capabilities.

The reduction in payload weight and payload bay size produced, collectively, a 12K lb decrease in orbiter dry weight and a reduction of \$43M in total development cost. The reduction in payload weight accounts for about 75% of the total cost reduction available. Thus, the 15x60 payload bay size should be retained and any required cost reduction obtained by decreasing payload weight.

As compared to the baseline, the cost per flight is higher, with a lesser increase for the smaller bay orbiter. For the small payload bay orbiters studied, the reduced engine thrust version shows a higher cost per flight, since the weight of expendables is higher.

REPRODUCIBILITY OF THE ORIGINAL PAGE IS POOR.

## Section 5

### BOOSTER DESIGN AND ANALYSIS

The objectives of the booster study activity were to provide data to assist NASA in selecting (1) liquid vs. solid boosters, (2) parallel burn vs. series burn, configurations (3) motor sizes and numbers for the solid booster and (4) pressure-fed vs pump-fed liquid boosters. The various options for the study booster concepts are identified in Figure 5-1. The three cross-hatched booster configurations in Figure 5-1 indicate the areas of primary study activity. Key issues for the various booster concepts have been identified and addressed. Each major booster technology concept considered parallel and series burn combinations relative to the orbiter and in the case of the series burn, several major configuration arrangement alternatives were considered. Propulsion characteristics studies included options of 120" and 156" in. diameter solid rocket motors (SRM) for the solid boosters and pressure-fed and pump-fed alternatives for the liquid boosters. A total of nine major configurations were considered for use with an orbiter using a 15x60 payload bay. Several booster configurations were also developed for orbiters using 14x45 payload bay but these received less emphasis.

Subsequent subsections present a technical description of the solid and liquid boosters, including the rationale for selection of preferred solid and liquid boosters, followed by a summary comparison of these concepts and finally a recommendation for the best overall booster.

#### 5.1 SRM BOOSTERS

The configuration candidates considered for SRM boosters are shown in Figure 5-2. The configurations depicted illustrate the relative size of the various concepts when providing the same payload capability. In order to obtain the maximum amount of detail on the characteristics of SRM boosters, it was recognized that equal emphasis could not be given to all concepts. Therefore, following an early assessment that the parallel burn concept using 156" diameter SRM's offered the most potential, this concept was selected as the baseline and received the majority of the emphasis. Series burn concepts using 156" diameter SRM's were next in priority. The 120" diameter concepts received the least emphasis since early studies indicated the 156" diameter SRM concepts generally provided lower weight and cost and since many technical aspects associated with burn and arrangement combinations would be similar to those of the larger diameter concepts. Configuration, performance, and cost data were developed, however, for all of these concepts.



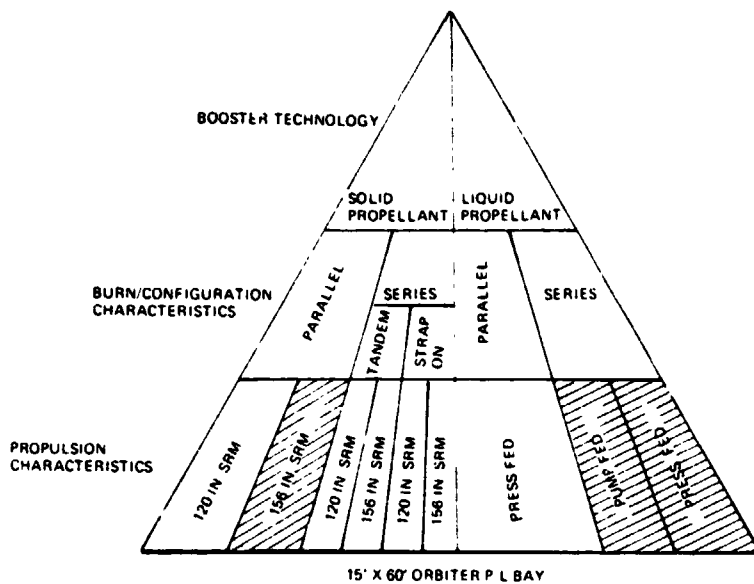


Figure 5-1 Booster Options

120 IN. DIA. SRM			156 IN. DIA. SRM		
PARALLEL BURN	SERIES BURN		PARALLEL BURN	SERIES BURN	
	TANDEM	STRAP-ON		TANDEM	STRAP-ON
979-166	979-163	979-182	979-164	979-177	979-182

Figure 5-2 SRM Booster Configurations Candidates

The key issues that have been identified relative to the overall SRM booster concepts include the following:

- SRM Diameter Selection
- Best Series Burn Concept
- Best SRM Booster Concept

In addition, the major issues considered significant in establishing the feasibility and credibility of the baseline parallel burn configuration included the following:

- Ascent Control Approach
- SRM Separation Approach
- Booster Reliability and Safety
- Stage Cost
- Reusability

The above issues will receive the major emphasis in subsequent paragraphs with supporting data also presented in the areas of propulsion, structures, avionics/power, performance, and operations.

### 5.1.1 Parallel Burn

#### 5.1.1.1 Configuration

The baseline parallel burn booster vehicle designated Model 979-164 is shown in Figure 5-3 and consists of two 156" diameter segmented SRM stages that are attached to the HO tank of the orbiter. Each SRM contains 1.2 million lb of propellant, ancillary equipment, a gimballed nozzle for assisting in vehicle thrust vector control and provides 2.28 million lb of thrust.

Note that the configuration characteristics shown on Figure 5-3 are somewhat different from the data presented earlier on Figure 2-11. Similar slight discrepancies will show up on later figures as well. The reason for these differences is that the requirement for freezing a booster size in order to be able to proceed with the detailed booster technical design occurred at a time when the tank and orbiter configuration characteristics were still in a state of flux. Thus, the stack drawings and data presented in earlier sections represent an updated version of the configurations, incorporating some design evolution of the individual elements comprising the stack.

Thrust termination ports are provided in each motor case for abort. Normal separation does not require thrust termination but relies on normal SRM burnout. Sufficient gimbal travel is provided to overcome asymmetric solid motor burn out.





The vehicle lifts off with all with all orbiter and booster engines operating. At 5400 fps relative velocity the booster propellants are expended. The empty motor cases are discarded and the orbiter proceeds to complete the mission.

The specific equipment that must be added to a basic SRM in order to operate as a stage is illustrated in Figure 5-4.

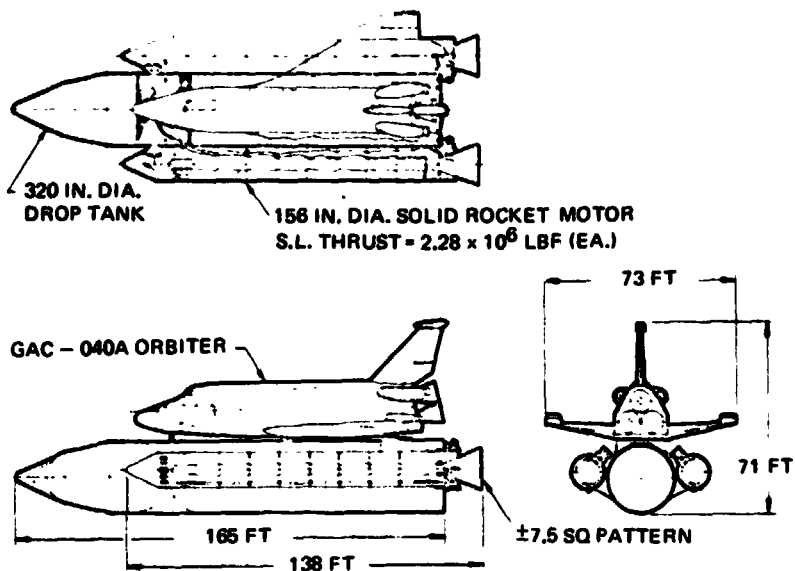
Forward and aft structural skirts are added to each SRM to provide housing for stage equipment, serve as the supporting surface for the attachment to the orbiter HO tank and separation rockets. Hold down posts are mounted on the aft skirt and provide means to support the weight of the vehicle while on the pad as well as to prevent lift off should one SRM propulsion system fail. The aft skirts also provides reaction points for the TVC system as well as storage location for TVC cold-gas-pressurized accumulators. An orbiter to booster communication path is provided by an interstage umbilical in the aft skirt region. A heat shield covers the aft face of the aft skirt to protect the stowed equipment from heating by orbiter and booster exhaust gases.

A raceway provides power and signal paths from nose cone and forward skirt to aft skirt. Avionics equipment including separation control unit and remote data acquisition units and battery power are mounted in the forward skirt. Thrust termination stacks pierce the forward skirt.

A malfunction detection system consisting of voted pressure sensors within the SRM provides abort q's. In the event of an emergency, thrust is first terminated to reduce the SRM pressure to about 200 psi. The separation motor are then ignited and attachments released to provide separation. After separation the range safety officer may elect to further reduce motor pressure by initiating the destruct system. The destruct system is provided at the mid section of one of the middle segments and consists of a structure cutter mounted radially.

#### 5.1.1.2 Weight

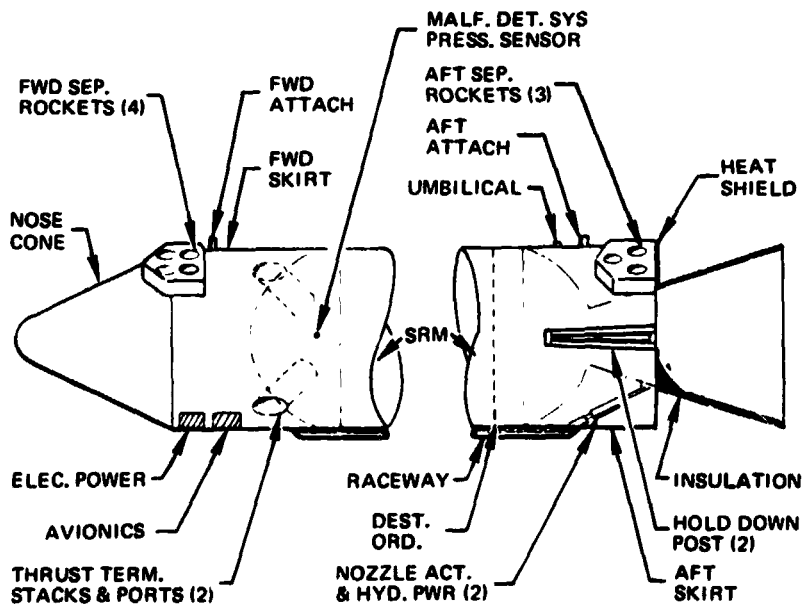
Major effort has been expended in the development of credible weight and other mass property analyses because of the sensitivity of system performance and cost to inert weight. The approach taken was one of maximizing the base for weight prediction on design layout; structural load prediction; stress analysis; wind tunnel, and other tests; flight control simulation; etc. Where possible, direct use was made of known weights of existing hardware. For those areas which were not subjected to this base, use of Boeing developed theoretical methodology and empirical correlation with similar existing subsystems was utilized. Supporting data for the weight estimates of the rocket engines were received from the



**DESIGN CHARACTERISTICS**

GLOW	=	4,574 K LBS	$\lambda'$	=	0.875
BLOW	=	2,767 K LBS	$W_p$	=	1,210 K LBS (EA.)
OLOW	=	1,807 K LBS	$P_c$	=	800 PSI (MAX.)
V <sub>STAGE</sub>	=	5,400 FT PER SEC.			

Figure 5-3 Parallel Burn SRM General Arrangement Model 976-164



NOTE: NO SCALE

Figure 5-4 SRM Stage Build-Up



major motor companies. Each booster concept evolved through the typical iterative preliminary design process of baseline definition, trade study and analysis, test, and update. Detail weight estimates and analyses were continually updated during this process. This evolution of weight data plus the mass property details for the resulting baselines are all documented in the Mass Properties Report, Volume III of the Final Report.

Table 5-1 shows the weight statement for the parallel-burn SRM booster configuration. The basic rocket motor assembly including TVC represents approximately 76% of the booster inert weight. Case weight is the dominant weight component of the basic motor. Internal insulation and nozzle, which includes the flexible bearing, are the next most significant weight contributors. The stage structure, separation system and other equipment represent 16% of the inert weight. The remaining 8% represents the specific allowance made for Weight Growth. This allowance reflects the general NASA-specified criteria of 10% of dry hardware weight. The resulting booster mass fraction is 0.875.

#### 5.1.1.3 Performance

The parallel burn booster trajectory for launching 40,000 lb into a South polar orbit is shown in Figure 5-5. The booster follows a gravity-turn trajectory (zero angle of attack) up to the staging point. The trajectory is shown subject to the constraints of liftoff ( $T/W$ ) = 1.25, maximum dynamic pressure < 650 psf, and maximum ascent acceleration = 3 g's. Trajectory constraints are met by appropriate tailoring of the SRM thrust trace with orbiter at 100% thrust. Flight conditions at points of interest (max q, 3 g point, and staging) are indicated. The trajectory shown beyond the staging point assumes no atmosphere.

Choice of a staging velocity (and hence vehicle size) is based on the criteria of providing approximately 5% growth allowance in the orbiter core weight without a change in the booster. Performance data indicate a BLOW of  $2.767 \times 10^6$  lb is required to provide the required payload. The major assumptions relating to this value include the following:

- $(T/W)_{LO} = 1.25$
- $I_B$  (Vac-booster) = 271.3 sec
- $T_B$  (S. L.) =  $2.2^{\circ} \times 10^6$  lbs. force (ea)
- $I_B$  (Vac-orbiter) = 454.5 sec
- $T_O$  (Vac-orbiter) = 3 x 469,100 psf

Table 5-1 Weight Statement - Model 979-164

<b>BASIC MOTOR</b>		<b>125,830</b>
CASE	83,840	
INSULATION	18,900	
LINER	3,050	
NOZZLE	16,600	
THRUST TERM. PORTS	1,100	
IGNITER	800	
TVC ACTUATION & POWER	1,340	
<b>STAGE STRUCTURE</b>		<b>17,570</b>
NOSE	530	
FWD SKIRT	1,720	
BASE SKIRT	4,170	
CLUSTER/ATTACH	6,650	
BASE HEAT	1,000	
RACEWAY	500	
<b>SEPARATION SYSTEM</b>		<b>9,300</b>
PROPELLANT	4,900	
CASE & NOZZLE (7)	2,100	
INSTALLATION	2,300	
<b>EQUIPMENT</b>		<b>500</b>
INSTRUMENTATION	10	
ENV. CONTROL	10	
WIRE & DISTRIBUTION	480	
<b>GROWTH (10% LESS PROPELLANTS)</b>		<b>14,800</b>
<b>UNUSABLE PROP.</b>		<b>5,700</b>
<b>MODULE INERTS (EACH)</b>		<b>17,500</b>
<b>USEFUL PROPELLANT</b>		<b>1,210,000</b>
<b>MODULE TOTAL (EACH)</b>		<b>1,383,500</b>
<b>TOTAL BLOW (2 MODULES)</b>		<b>2,767,000</b>
<b>BOOSTER λ</b>		<b>0.875</b>

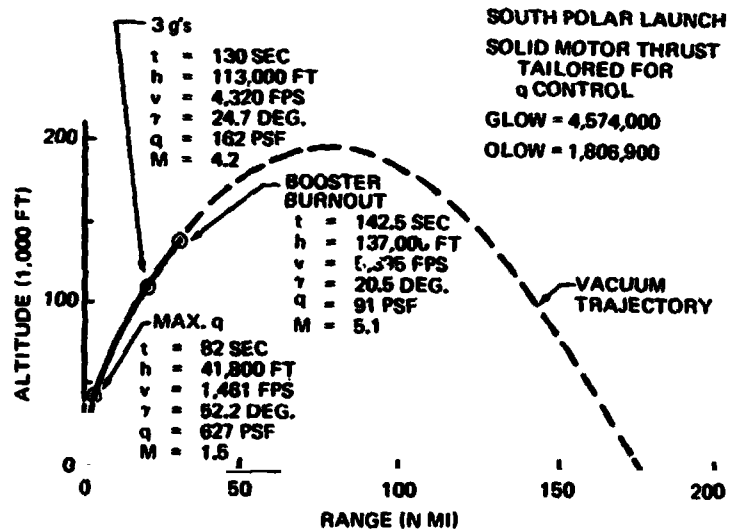


Figure 5-5 156" SRM Parallel-Burn Booster Trajectory - Model 979-164



#### 5.1.1.4 SRM Booster Trades

In the process of developing the baseline parallel burn configuration, several major trades were performed as indicated in Figure 5-6. Check marks (✓) indicate the selected design approach for each trade. The case material, SRM attachment and nozzle actuation trades will be discussed at this time and the remaining trades discussed in subsequent paragraphs.

The SRM case material selected was D6AC. This material has good production experience in the 120-in. diameter SRM used in Titanium IIC, results in the lowest weight, and provides adequate toughness and welding characteristics.

The SRM attachment concepts studied included twin load transfer attachments at both the fore and aft skirt locations and a single load transfer attachment with stabilizing rods at both the fore and aft skirts. The single attachment concept has been selected as it provides lower weight due to minimizing eccentric loads and provides a more straight-forward separation since heavy fittings do not require cutting.

A cold gas/hydraulic blowdown (single thread) configuration was selected to provide SRM nozzle actuation. This concept provides low cost, minimum complexity and technical risk, and acceptable weight. The simplicity of this system allows use of a single thread power source without significantly degrading overall TVC reliability.

#### 5.1.1.5 Structure Design & Analysis

5.1.1.5.1 Structural Design Concept - The major structural features of the SRM booster are shown in Figure 5-7. Thrust loads enter the orbiter HO drop tank from the forward attachment structure of the SRM's. The aft attachment is a shear fitting that permits relative elongation between the SRM's and the HO tank while restraining all other motion. Two forward and two aft compression struts complete the attachment. The SRM nose cone is an aluminum semimonocoque structure. The forward skirt is also an aluminum semimonocoque structure and contains two thrust termination ports (originating in the forward motor closure) and the main attachment thrust shear fittings. The nose cone and forward skirt are bolted together. Attachment of the forward skirt is to the forward motor closure Y-ring is by a clevis joint. A clevis fitting is also used to attach the semimonocoque aluminum aft skirt and the aft motor closure. SRM segments are also joined by clevis fittings.

5.1.1.5.2 Sizing Conditions - The conditions which size the major structural elements are summarized in Figure 5-8. The upper six segments of the SRM case are sized by the maximum

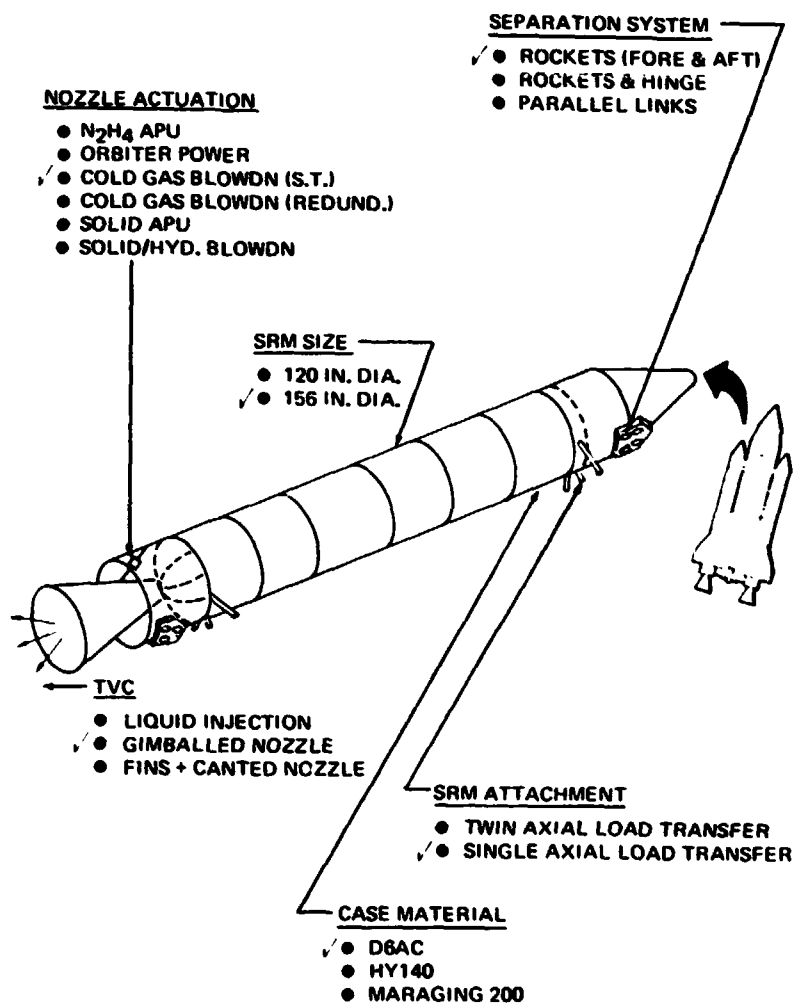


Figure 5-6 SRM Booster Trades



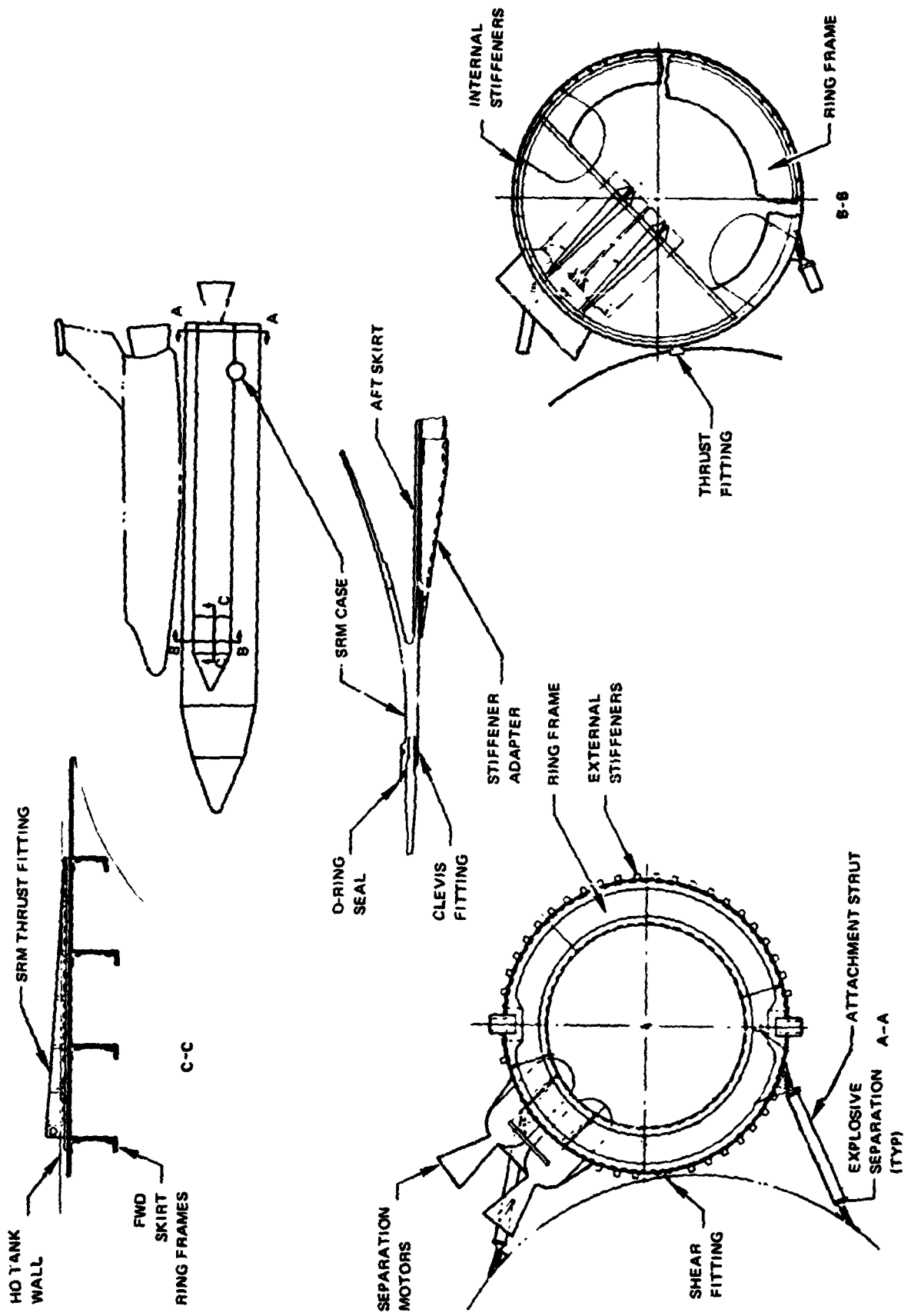


Figure 5-7 Structural Design Details

expected operating pressure (MEOP) of 960 psi. The lower two segments are sized by the moments induced by orbiter thrust build up plus ground wind (negative direction) and the dead weight axial loads (thrust buildup condition). The aft skirt and hold down structure are design by thrust buildup, maximum nozzle thrust vector deflection of  $\pm 7.5^\circ$  at boost  $q_\alpha$  maximum and one SRM out conditions. The forward attachment fittings and skirt are critical for the three g and maximum nozzle thrust vector deflection conditions. The aft attachment fittings are critical for the maximum nozzle vector thrust deflection conditions. Boost heating is critical for the nose cone.

5.1.1.5.3 Dynamics - Dynamic characteristics of an integrated vehicle were determined utilizing a finite element elastic model that included 35 nodes and a total of 115 degrees of freedom as depicted in Figure 5-9. Axial and bending stiffness of the HO tank, orbiter, and SRM's were considered as well as local stiffness in the vicinity of the attachments.

The fundamental mode is a symmetric mode consisting primarily of orbiter bending in the pitch plane. This mode could influence the pitch control system. The frequency of this mode is 1.17 cps which is well above the .85 cps minimum frequency required for control system design. A mode consisting primarily of yaw plane orbiter bending appears at 2.14 cps which also is significantly higher than the minimum required frequency of .85 cps for yaw control. An antisymmetric mode consisting of HO tank torsion and SRM pitching, which could couple with the roll control system, has a frequency of 3.008 which is only slightly above the minimum frequency of 3.0 cps. On the basis of these results, it is concluded that the stiffnesses of the vehicle components and attachment structure are adequate to prevent adverse effects on the pitch or yaw control systems but marginal in roll.

5.1.1.5.4 Heating - During the ascent trajectory, the booster is exposed to the thermal environments caused by aerodynamic heating and heating from the solid rocket and orbiter plumes. The aerodynamic heating does not result in any increase cone in structural thickness except at the tip of the aluminum nose where a .13 inch thickness is required to limit the maximum temperature to 350°F.

The aerodynamic heating is amplified due to flow field interference between the booster motor cases, HO tank, and orbiter. This is caused by the interaction of shock waves and the attendant increases in local pressure on the booster surfaces. The interference heating causes a temperature rise of approximately 85°F in the .42 inch steel motor case.

Plume heating will require thermal protection on the aluminum aft skirt. Protection is provided by a silicone ablative material .08 inch thick on the cylindrical surface and .35 inch thick on the aft heat shield facing surface will limit the aluminum structure to 350°F.





- ▶ 960 PSI MEOP, EXCEPT THRUST BUILD-UP (MINUS WIND) ON 2 AFT SEGMENTS
- ▶ 3 g BOOST
- ▶ MAX. SRM NOZZLE THRUST VECTOR AT MAX. q
- ▶ ORBITER THRUST BUILD-UP
- ▶ 1 BOOSTER OUT
- ▶ BOOST HEATING

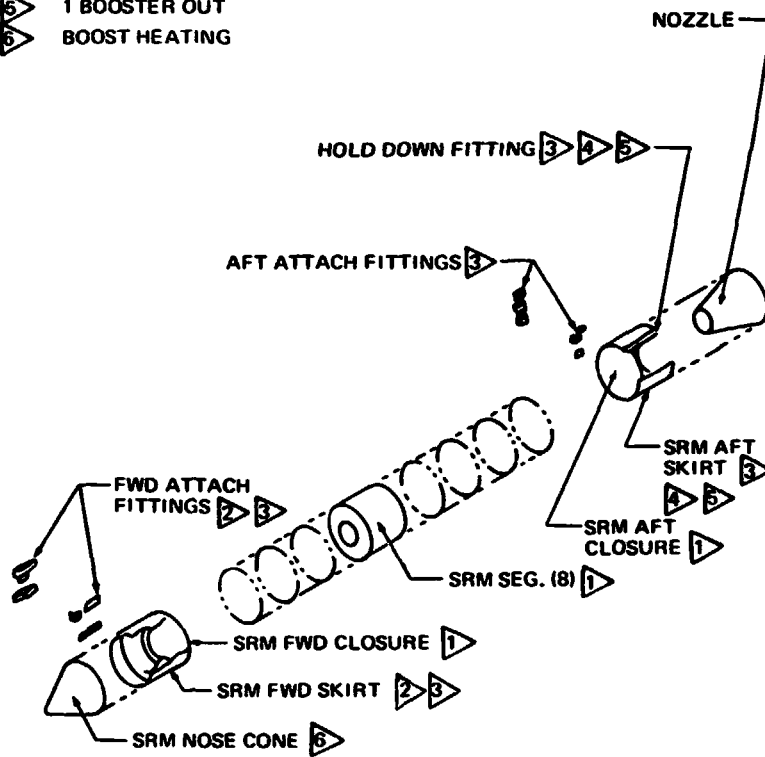


Figure 5-8 Structural Sizing Conditions

#### 5.1.1.6 Propulsion

**5.1.1.6.1 SRM Size Selection - Two SRM designs were evaluated for the parallel burn booster application: a modified 120" diameter seven-segmented Titan IIIM development motor, and a 156" diameter segmented motor design based on the SRM design technology demonstrated on the USAF 623 program. A 156" diameter design was selected for evaluation since it represents the maximum diameter segment that can be transported by rail from existing SRM manufacturing plants to either ETR or WTR.**

The comparison of the two candidate SRM's is presented in Table 5-2. The 120" diameter SRM is a more mature design than the 156" SRM, but offers no other advantages when integrated as a booster stage. The 120" SRM stage requires four motors per stage resulting in greater complexity in stage structure and ancillary systems than the 156". SRM stage which requires only two motors per stage to accomplish the mission. Thus the assessed reliability of the four-motor stage is substantially lower than the two-motor stage. The 156" diameter SRM stage shows only a slight penalty in DDT&E cost because considerable design work is also necessary for the new stage equipment for the 120" dia. SRM and the associated integration cost. The larger motor, however, has a decided program cost advantage reflecting a design choice for the parallel burn booster. Although this SRM selection process was done considering a parallel burn configuration the same basic reasons (i. e. more motors) would apply in series burn concepts.

**5.1.1.6.2 SRM Design - The baseline 156" diameter SRM design shown in Figure 5-10 is based on existing technology. The selected motor design consists of eight identical cylindrical segments and a fore and aft end closure. The HTPB propellant grains are designed to provide a thrust profile to limit the dynamic pressure below 650 psf and acceleration below 3 g's. Each motor operates at a chamber pressure of 800 psi and provides 2.28M lbs thrust. The maximum expected operating pressure (MEOP) due to pressure variations is 960 psi. The segmented cases are made of D6AC steel and manufactured by processes identical to those currently used for Titan IIIC cases. Thrust termination capability is incorporated for emergency abort situations and is achieved by venting the motor through exhaust ports in the forward dome. Thrust vector control is provided by hydraulically actuated flexible bearing, moveable nozzles.**

#### 5.1.1.7 Ascent Control

The baseline 979-164 configuration is aerodynamically unstable in both pitch and yaw. Control of the baseline vehicle using only orbiter TVC and aerosurfaces is marginal. (See section 2.) (A free roll possibility has been studied, and does allow orbiter - only control



ELASTIC MODE	CONTROL AFFECTED	ELASTIC FREQ.	MINIMUM FREQ. REQUIRED	ASSESSMENT
SYMMETRIC ORBITER PITCH PLANE BENDING	PITCH	1.17	0.85	ADEQUATE
ORBITER YAW PLANE BENDING	YAW	2.14	0.85	ADEQUATE
ANTISYMMETRIC HO TANK TORSION/SRM PITCH	ROLL	3.008	3.0	MARGINAL

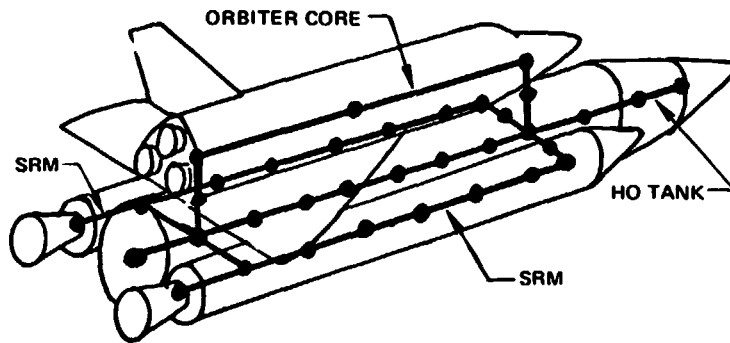
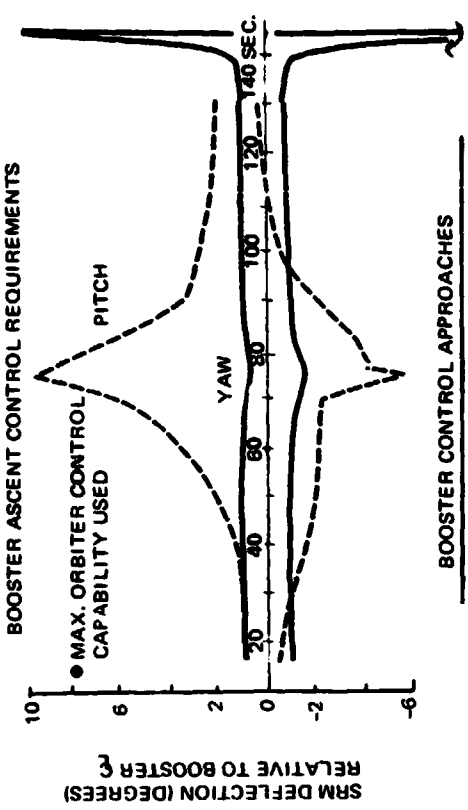


Figure 5-9 Results Parallel Burn Dynamic Analysis

Table 5-2 SRM Diameter Selection

979-165 120 IN. DIA.	DISCRIMINATORS	979-164 156 IN. DIA.
TITAN III C 10 DEVEL. 5 PFRT 18 FLIGHTS	EXPERIENCE	9 TEST FIRINGS THIokol & LOCKHEED
TITAN III M 4 DEVEL.	HANDLING AND TRANSPORT	RAIL O.K. - RESTRICTED ROUTES
EASIER . . . . UNRESTRICTED RAIL ROUTES GREATER	CONFIGURATION COMPLEXITY	-
0.98	RELIABILITY (BOOSTER)	0.99
1,780	MOTOR QUANTITY (PRODUCTION)	890
2.825 M LB.	BLOW COST, BOOSTER (\$10 <sup>6</sup> )	2.767 M LB.
340	DDT&E	369
3,949	PRODUCTION	3,419
488	OPERATIONS	394
4,777	TOTAL	4,182



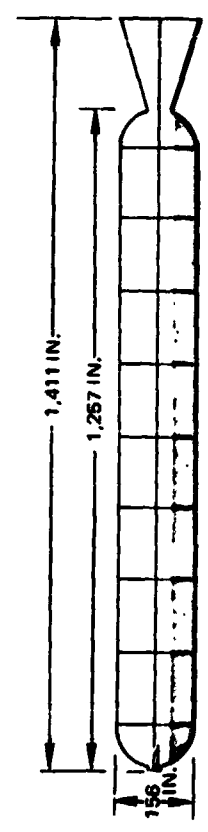
**BOOSTER ASCENT CONTROL REQUIREMENTS**

- MAX. ORBITER CONTROL CAPABILITY USED

**BOOSTER CONTROL APPROACHES**

- GIMBALLED NOZZLES -
  - GIMBAL  $\phi$  @  $\pm 2^\circ$  PITCH &  $5^\circ$  OUTBD YAW
  - $\pm 7.5^\circ$  SQUARE PATTERN
  - HYDRAULIC ACTUATION
- LIQUID INJECTION -
  - FIXED CANT @  $\pm 2^\circ$  PITCH &  $5^\circ$  OUTBD YAW
  - $\pm 7.5^\circ$  CIRCULAR PATTERN
  - $N_2O_4$  INJECTANT
- FINS AND CANTED NOZZLES
  - 1-600 SQ. FT. FIN ON HO TANK
  - $9^\circ$  FIXED OUTBOARD CANT

COMPARISON			
DISCRIMINATOR	GIMBALLED NOZZLES (BASELINE)	LIQUID INJECTION	FINS AND CANTED NOZZLES
WEIGHT (BLOW)	2,767,000 LBS	( $\Delta$ ) + 713,000 LBS	( $\Delta$ ) + 235,000 LBS
TECHNICAL RISK	LOW	LOW	HIGHEST
EXPERIENCE	3 PROD. STAGES	5 PROD. STAGES	SMALL ROCKETS
COST (PROG. \$10 <sup>6</sup> )	369	( $\Delta$ ) + 9.5	SAME AS GIMBALLED
DDT&E COST/FLT	8.2	( $\Delta$ ) + 1.7	( $\Delta$ ) + 0.19



**DESIGN CHARACTERISTICS**

- ACTION TIME, SEC. 139.4
- TOTAL IMPULSE (VAC), LBF-SEC 3.28 x 10<sup>8</sup>
- INITIAL THRUST (SL), LBF 2.28 x 10<sup>6</sup>
- THROAT AREA, SQ. IN. 1,942
- EXPANSION RATIO 10
- CHAMBER PRESSURE, PSIA 800
- MEOP, PSIA 960
- MASS FRACTION (MOTOR ONLY) 0.903
- CASE MATERIAL D6AC

**PROPELLANT**

- SPECIFIC IMPULSE (VAC), SEC. 271.3
- CHARACTERISTIC VELOCITY, FT/SEC. 5,244
- DENSITY, LMB/CU. IN. 0.086
- BINDER TYPE HP HTPB

**WEIGHTS**

- PROPELLANT 1,210,000
- CASE 84,000
- NOZZLE 17,000
- OTHER INERT 29,000
- TOTAL MOTOR 1,340,000

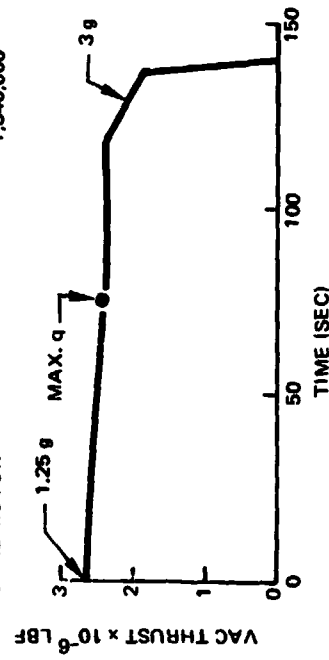


Figure 5-11 Parallel Burn - Ascent Control

Figure 5-10 156" Diameter SRM-Design



but it is considered operationally unattractive.) Thus the booster must provide some degree of control capability as shown in Figure 5-11.

The design approaches considered for booster control included gimballed nozzles, liquid injection, and fins plus canted SRM nozzles. Actuation of the  $\pm 7.5^\circ$  square pattern gimballed nozzle was provided by a cold gas/hydraulic blow down system. The actuators selected would have capability to position the gimbal centerline at an optimum location for lift-off and shutdown while providing sufficient TVC during ascent to maintain control during maximum crosswind conditions. Automatic centering of the actuator would occur upon failure.

The liquid injection system used  $N_2O_4$  as an injectant and had a  $\pm 7.5^\circ$  circular pattern capability. The third concept used a fin on the HO tank (jettisoned with SRM's) plus fixed outboard yaw cant on the SRM nozzles. However, the fin must be large to provide roll control and it must be positioned near the center of the hydrogen tank for the proper yaw control.

Based on weight and DDT&E and cost/flight the gimballed nozzle appears to be the best method of providing booster control. In addition to these factors, this concept provides greater flexibility in coping with vehicle design changes and abnormal conditions occurring during flight.

The cold gas/hydraulic system used with the gimballed nozzle is shown in schematic form in Figure 5-12. Each actuator is powered by MIL-H-83282 hydraulic fluid stored in a nitrogen charged accumulator. Hydraulic pressure is controlled by either the primary or secondary servo valve. A single umbilical provides GSE  $N_2$  and hydraulic oil for system charging and for ground operation. The accumulators are sized to provide hydraulic pressure from liftoff to separation. Following lift-off the actuator return fluid is vented overboard through the umbilical return port.

#### 5.1.1.8 Separation System

5.1.1.8.1 Concept Selection - Three design concepts shown in Figure 5-13 were considered for separating or staging the SRM's. One system is designed like the Titan with separation rocket motors fore and aft. Operating features include the ignition of four forward separation motors, and three aft motors, and breaking the compression links. Sufficient thrust is provided to overcome one separation motor out (either forward or aft). The rocket and hinge system retains three rockets at the forward end but uses a two degree of freedom hinge at the rear. The last system eliminates the need for separation rocket motors and

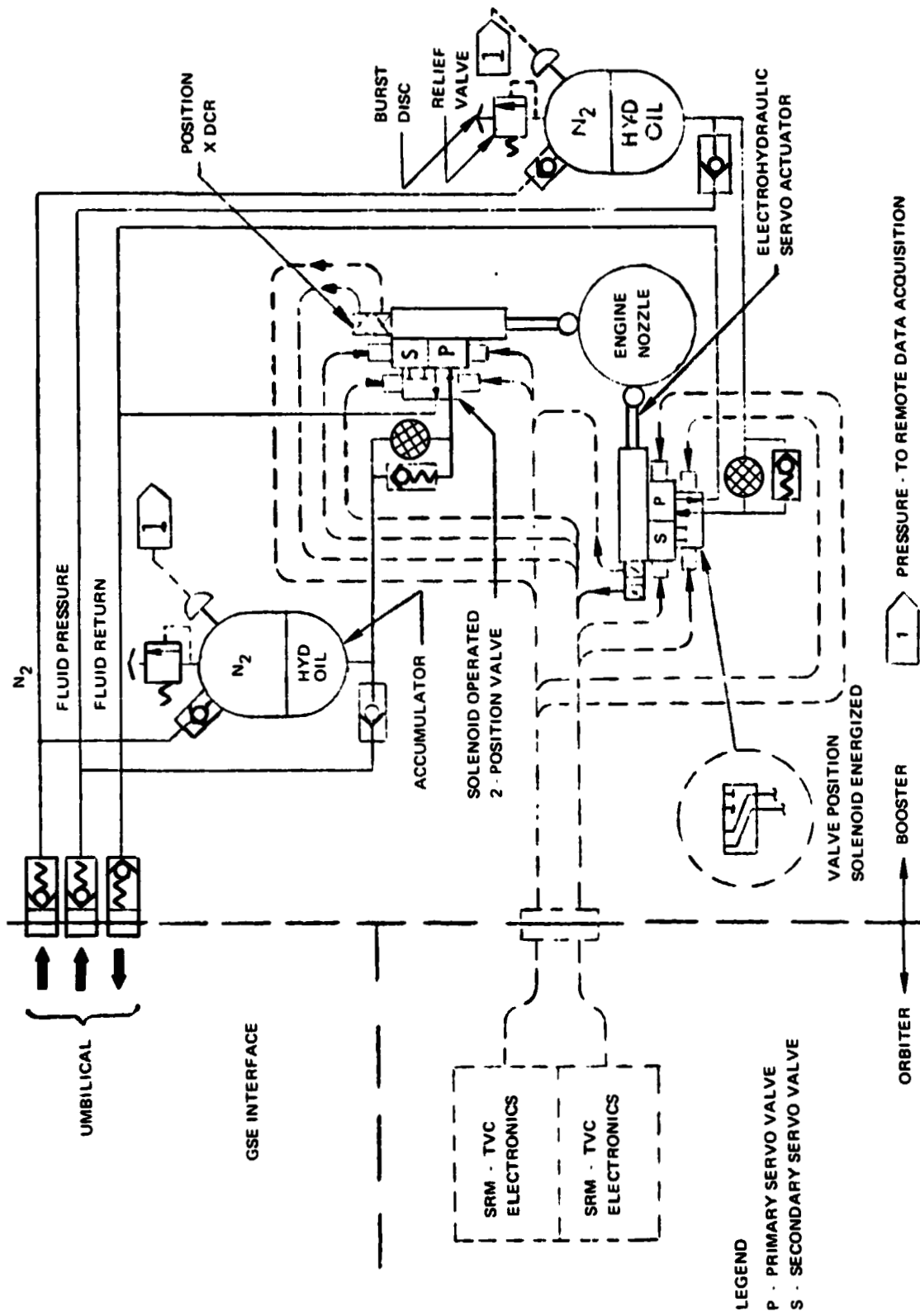


Figure 5-12 TVC Subsystem - Solid Rocket Motor (Typical)



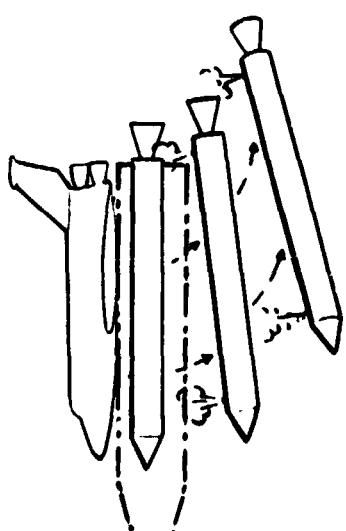
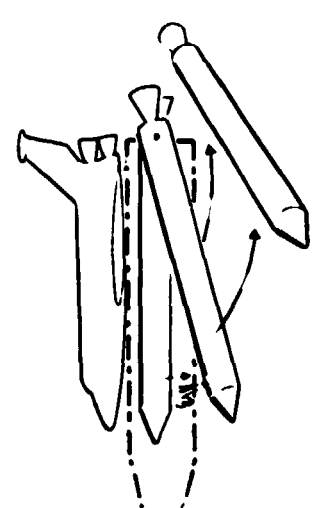
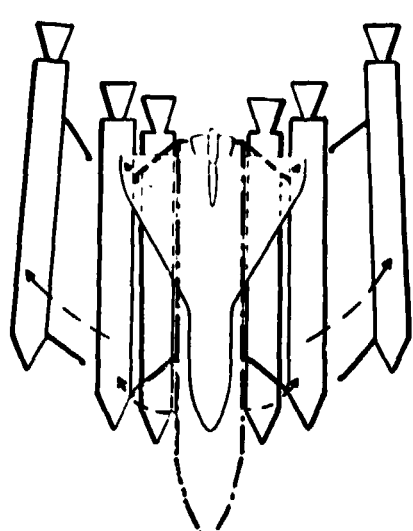
ROCKETS (FORE & AFT)	ROCKETS AND AFT HINGE	PARALLEL LINKAGE	
			
DISCRIMINATORS	ROCKETS (FORE & AFT)	ROCKETS & AFT HINGE	PARALLEL LINKAGE
ΔWEIGHT (LBS)			
BOOSTER	BASELINE	+8,180	-4,030
ORBITER	BASELINE	0	+5,770
PAYLOAD	BASE	- 600	-5,000
Δ SYSTEM COST - (\$10 <sup>6</sup> )			
DDTE	-	+ 4.2	+ 0.6
* COST/FLIGHT	-	+ 0.26	+ 0.12
PROGRAM	-	+ 119	+49.0
EXPERIENCE	TITAN III C	NONE	NONE
PLUME IMPINGMENT ON ORBITER	MODERATE	MODERATE	NONE
REACTION FORCES ON ORBITER	NEGLECTIBLE	MODERATE	MODERATE

Figure 5-13 Separation Approach

uses a parallelogram linkage to guide the SRM's away from the orbiter tank. Motive force is supplied by relative orbiter acceleration and aerodynamic drag.

The selected separation approach is rocket motors both fore and aft. This concept provides the least weight penalty, offers a significant advantage in cost, minimizes the reaction forces on the orbiter at separation, and has the least development risk since the basic concept is used successfully on the Titan IIIC.

5.1.8.8.2 Separation Motor Sizing - The separation motors are sized to separate the SRM's successfully from liftoff to burn out despite single motor failures. Even though successful termination and separation can be accomplished at liftoff with the system shown, it has been assumed that it will not be required until at least 20 seconds after liftoff. At that time with one aft separation motor out instantaneous center of rotation is aft of the insert SRM. Rotating about that center precludes the motor recontacting the orbiter. With one fore end separation motor out, the SRM will follow the trajectory indicated in Figure 5-14. Despite losing the rotational motion, the SRM translates down and away from the following orbiter. After three seconds, the SRM completely clears the orbiter. This analysis included the small influence of aerodynamic loads. The effect of aero loads increases at  $q_{max}$ , and  $q_{\alpha}$ ,  $q_{\beta}$  max but the reduction in motor weight compensates for increased air loads and the system works successfully.

The separation motor nozzles are slightly canted to direct thrust through the SRM long axis centerline and to avoid impinging on the orbiter engines. The forward motors will impinge on the orbiter tank and wing under abort conditions. Both surfaces are insulated and no problems are anticipated. Under normal separation conditions separation motor exhaust impinges on the orbiter tank for less than one second and hence should not present a problem.

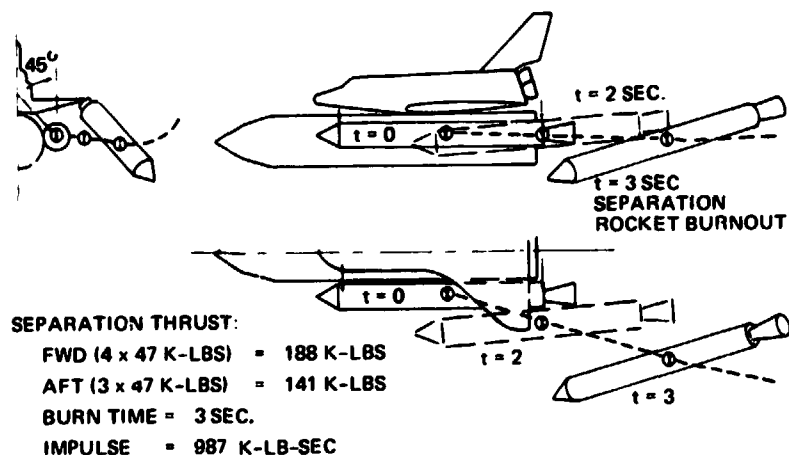


Figure 5-14 Separation Motor Sizing





#### **5.1.1.9 Avionics and Power**

The functional elements of the booster avionics and power systems together with the signal flow and interface relationships with the orbiter avionics are shown in Figure 5-15. A minimum of equipment is incorporated in the booster because the SRM's are not recovered following separation. The equipment indicated however is required in both SRMs.

The separation control unit has the function of initiating separation of the SRM's under normal and abort conditions. Under abort conditions it has the additional functions of initiating thrust termination prior to separation and if necessary, to initiate destruction for range safety reasons. A remote data acquisition unit processes instrumentation data from the booster systems and transfers this data to the orbiter to permit display of operational status and recording of selected parameters. A dual battery installation provides redundant sources of power. The guidance and control computations and the control interface electronics are provided in the orbiter.

#### **5.1.1.10 Reliability and Safety**

A reliability and safety assessment of the parallel burn SRM configuration is shown in Figure 5-16. Reliability and safety levels indicated are based on the predicted failures of two SRM's per vehicle and one million flights. It should also be noted that the values reflect improvements that have been incorporated such as design margins, redundancy, and safety provisions. Reliability values reflect the number of failures that will prevent mission completion. Safety failures reflect the number of failures that do not allow sufficient reaction time for the crew or equipment to complete a successful abort.

Motor case and closure failures are based on Titan IIIM data and primarily consist of liner and insulation failures resulting in case burn-through and also segment joint failures. Nozzle and gimbal actuation failures make up the bulk of the SRM failures. The indicated failure rates are based on most recent predictions for SRM stages. The major nozzle failure is in the seal while the hydraulics system constitutes the major failure in actuation. The most significant failures listed under "other" include the Separation Control Unit which controls the thrust termination and staging of the motors and the SRM attachment structure/mechanism.

As indicated, the resulting reliability prediction of 0.99 is comparable to that of liquid stages used on previous manned spacecraft programs. Safety predictions are comparable to SST type aircraft when considering relative exposure times.

A large number of SRM firings would be necessary to establish confidence in the stage reliability prediction. The current baseline test program includes 5 PFRT firings and, as

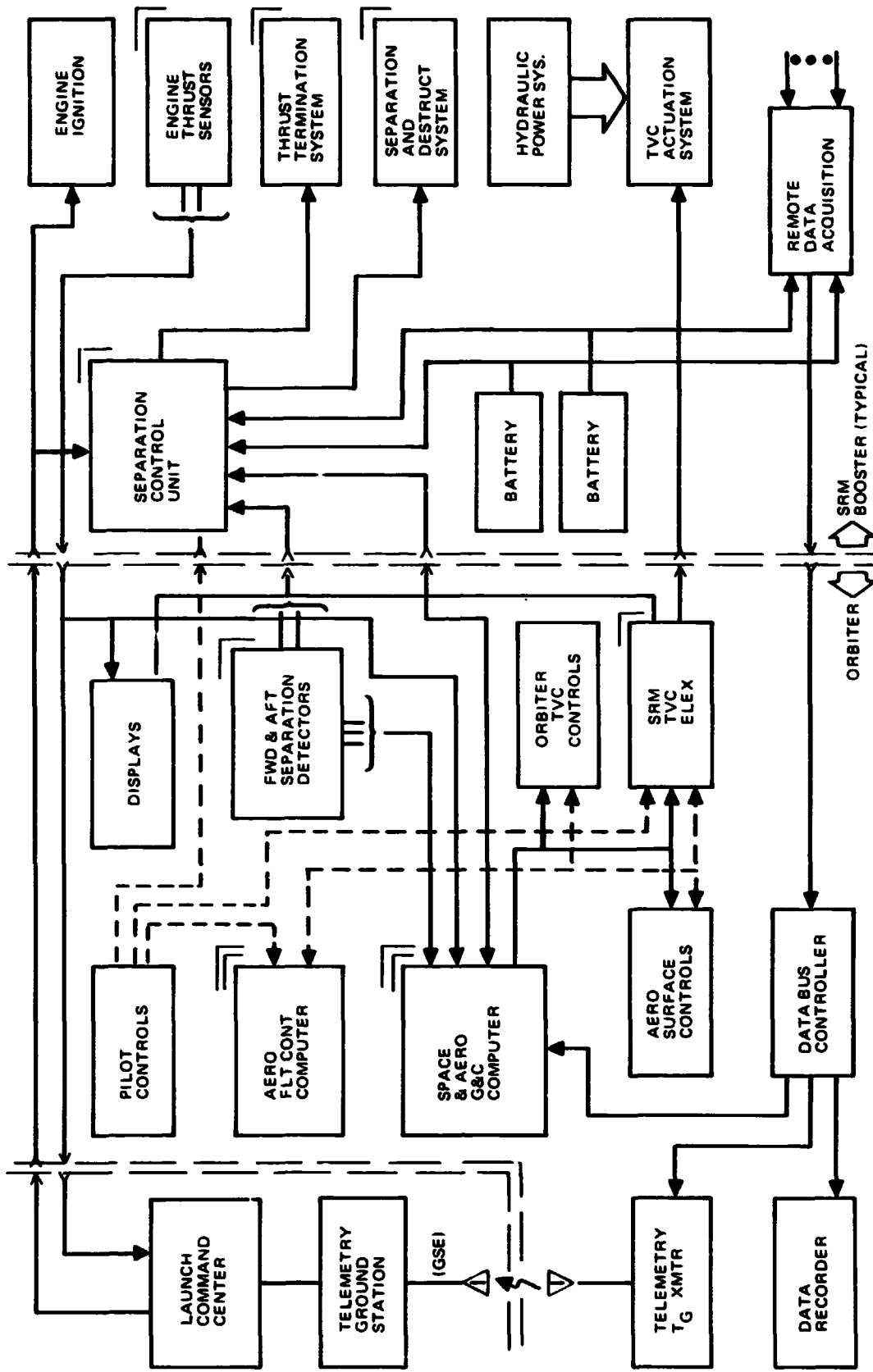


Figure 5-15 Booster Avionics Functional & Interface Diagram

- PARALLEL BURN, SRM
- SERIES BURN, SRM



● RELIABILITY AND SAFETY LEVELS ARE ACCEPTABLE

SRM BOOSTER MAJOR FAILURES	FAILURES/MILLION FLTS	
	RELIABILITY	SAFETY
MOTOR CASE & CLOSURE	680	340
NOZZLE (MOVABLE)	7,000	
GIMBAL ACTUATION SYS	2,060	
OTHER	~300	~ 60
	~ 10,000	~ 400
	R = 0.99	S = 0.9996

● SOLID BOOSTERS COMPARE FAVORABLE WITH LIQUID BOOSTERS

BOOSTER STAGE	RELIABILITY PREDICTION
S-1C	0.99
TITAN II 1ST STAGE 0.99	0.99

● ESTABLISHING CONFIDENCE REQUIRES  
SIGNIFICANT NUMBER OF FIRINGS

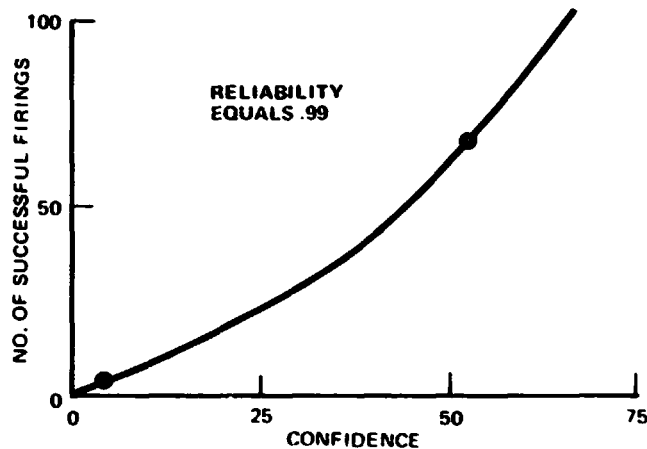


Figure 5-16 SRM Booster – Reliability & Safety

indicated from the curve, this would provide less than a 5% confidence that the stage has a reliability of 0.99. In order to achieve a 50% confidence, a total of 67 successful firings would be required and obviously be extremely expensive. So, although demonstration of reliability may be difficult, it is important to note that the Titan III, which uses large SRM similar in nature to the proposed booster, has proven to be reliable in all 17 flights.

5.1.1.11 Operations Concept

The operations concept for the parallel burn SRM booster is shown in Figure 5-17. The initial step has the booster SRM segments and shipped-loose hardware arriving at KSC by rail and being transferred to the Solid Rocket Motor Integration Building (SMIB) for inspection and storage. The Booster segments and systems will be assembled and

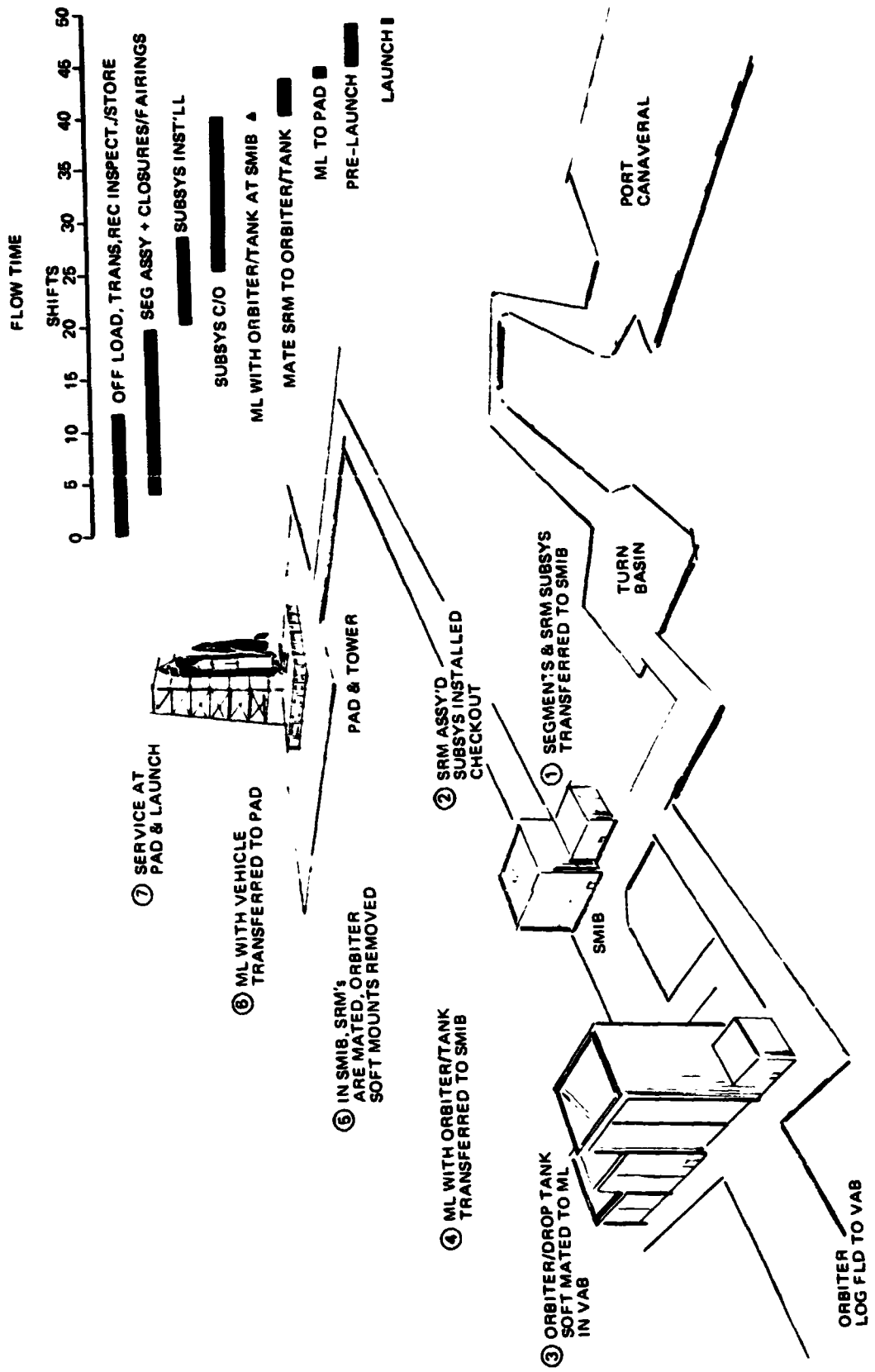


Figure 5-17 Operational Concept Parallel Burn SRM



tested prior to mating with the orbiter on the mobile launcher. The mobile launcher, on which an orbiter/HO tank has been soft mounted, will move to the SMIB mating bay, for mating with the SRM. The mobile launcher will then continue to the launch pad where it and the orbiter will be mated to the pad serving equipment including the umbilical tower. Final booster/orbiter/pad interfaces will be verified and the vehicle launched. The total flow time for these operations is estimated to be 50 shifts or 25 days.

The most significant modifications to the current Apollo equipment as a result of this booster design approach and the above operations concept include the following: The mobile launcher would consist of only the launcher base rather than launcher plus umbilical tower (tower is left at the pad) due to weight limitations on the crawler-transporter. Another change is the enlargement of the flame cutout in the launcher base in order to accommodate both orbiter and booster engine ignition. Structural beef-up of the launcher base is also required.

The most significant new facility required will be the solid Motor Integration Building (SMIB) used to assemble the SRM segments and mate the SRM with the orbiter.

An attractive alternate operations approach would use the existing KSC Vertical Assembly Building (VAB) for SRM buildup and checkout. In this case the completed booster would be transferred to the mobile launcher and the orbiter/drop tank would be mated with the booster. All subsequent operations would be as described above. The alternate approach is feasible if the type of solid propellant is inert enough to allow segment build-up and handling in a general work area such as the VAB. The cost savings associated with this alternative is estimated at approximately 26 million dollars.

The cost of the two approaches is as follows:

<u>VAB</u>		<u>SMIB</u>	
New 500T Cranes (2)	4.2M	New Structure	31.0M
Structural Mods	11.2M	Integration Bay (2)	20.0M
Other Associated Mods (Mech., elec., architectural)	9.6M		
Total VAB	25.0M	Total SMIB	51.0M

#### 5.1.1.12 Booster Program Schedule

The parallel burn-solid rocket motor booster master phasing schedule shown in Figure 5-18, reflects a June 1, 1972 authority to proceed with a first launch (unmanned) on October 1, 1977, 64 months after ATP. This unmanned launch requires the use of a powered orbiter. The first manned orbiter launch is scheduled for March 1, 1978 (69 months from ATP) using the second booster vehicle. The booster phasing assumes no recovery of the rocket motor boosters. The schedule allows individual breadboard testing and, subsequently, integrated testing of the booster subsystems prior to first launch.

Integration of the thrust termination and TVC subsystem tests with the rocket motor are programmed to occur at the motor manufacturer during motor test firings. Static load testing of one complete booster unit is programmed to occur before dynamic testing of the mated orbiter-booster vehicle which is scheduled to be completed prior to first launch.

#### 5.1.1.13 Stage Cost

The major cost elements for a parallel burn 156" SRM booster are shown in Table 5-3, for the DDT&E, production, and operations portion of a Shuttle program consisting of 445 flights. The SRM costs were developed from data supplied by the major solid rocket motor manufacturers. The inputs received from the solid motor manufacturers are also indicated. The remainder of the costs were developed from detailed manning, materials, and subcontract estimates. The structure costs include all structural elements and the TCV actuation. The propulsion estimate includes SRM integration and separation motors. The SE&I DDT&E estimate includes systems engineering (3.44M), systems integration (3.83M), vehicle design analysis (23.86M), vehicle design test analysis (2.03M), vehicle design analysis development shop (1.84M). The systems test cost estimate includes breadboards and major groundtest hardware. The system support cost is for ground support equipment and services for the DDT&E and production program. The largest cost element is flight test which consists of facilities, combined vehicle operations, ground operations, support the development flight operations. The DDT&E cost represents approximately 9 percent of the booster program cost. No cost has been included for an unmanned launch.

The production cost includes booster hardware for 444 operational flights plus system support and operations for the production phase of the program. The operations cost includes all booster operations plus one-half the operations common to both the booster and orbiter. The resulting booster cost/flight is \$8.2 million.



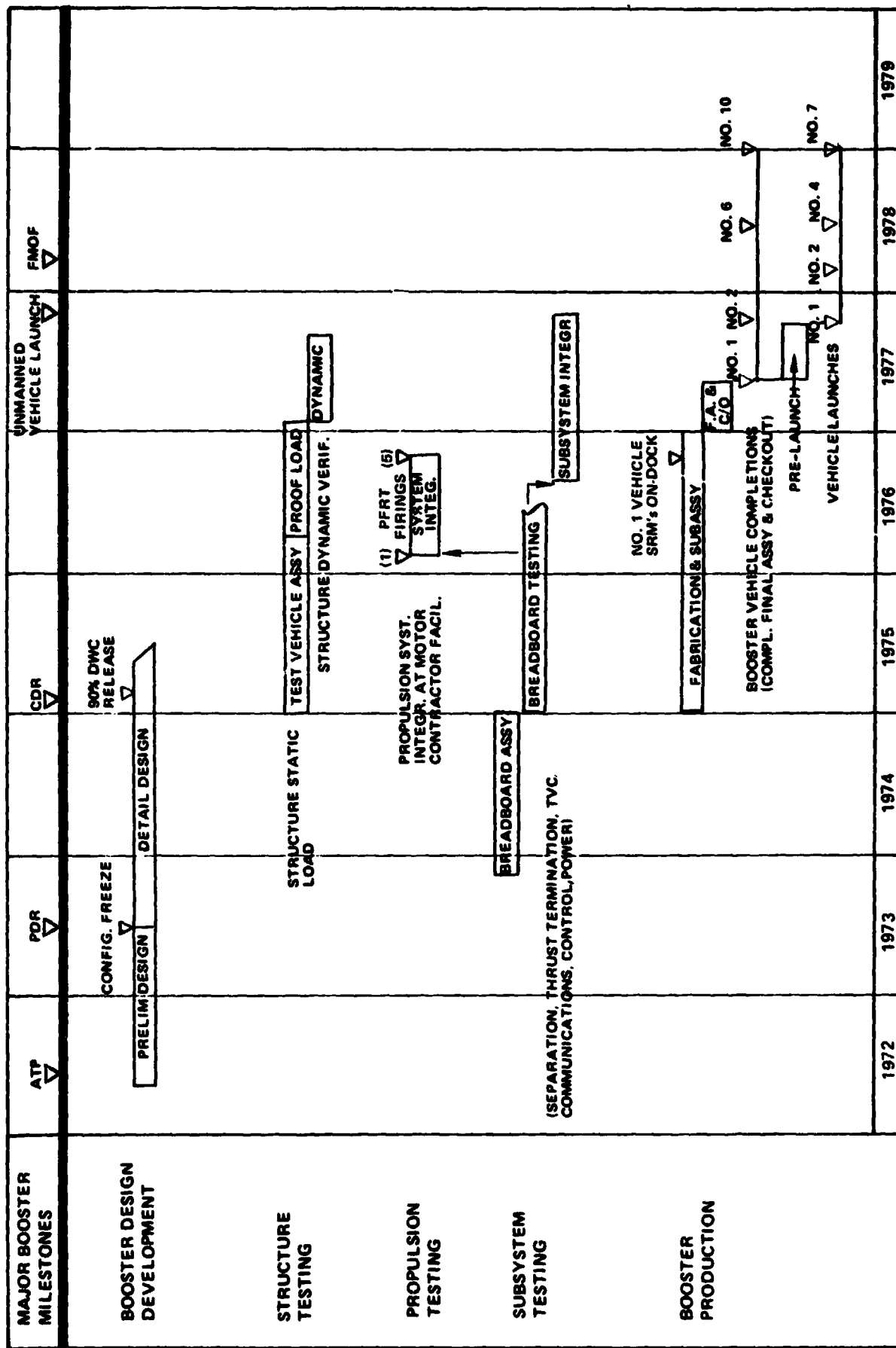


Figure 5-18 Parallel SRM Boosters (979-164)

**Table 5-3 Stage Cost – Parallel Burn – 156" SRM Booster**

BOOSTER COST (MILLIONS)			
ELEMENTS	DDT&E	PROD	OPS
SRM	75.0	2,373.0	
STAGE HARDWARE			
STRUCTURE	19.0	593.7	
PROPULSION	11.3	74.3	
AVIONICS	2.7	21.1	
POWER	3.9	55.8	
SE&I	35.0	16.5	
FACILITIES	10.3		
SYSTEMS TEST	24.5		
GROUND TEST	14.5		
HARDWARE			
FLIGHT TEST	15.2		
HARDWARE			
SYSTEM SUPPORT	21.4	110.0	
MANAGEMENT	11.5	42.8	
FLT TEST OPS	110.0		
OPERATIONS			379.0
<b>SUBTOTAL *</b>	<b>354.3</b>	<b>3,287.0</b>	<b>379.0</b>
<b>TOTAL BOOSTER PROGRAM *</b>		<b>4,020.3</b>	

\* DOES NOT INCLUDE SHUTTLE MANAGEMENT

SRM COST (MILLIONS)		
CONTRACTOR	DDT&E	PROD
A	87	2,426
B	53	2,092
C	80	1,800

### 5.1.2 Series Burn Concept

Strap-on and tandem configuration arrangements were considered for the series burn booster concept. The configurations and their comparison are shown in Figure 5-19.

The strap-on configuration designated Model 929-162 has two 156" diameter SRM's attached to the orbiter in the same manner as for the parallel burn concept. The tandem configuration designated Model 979-177 uses a cluster of three 156" diameter SRM's. Three SRM's have been used rather than two in order to avoid an extremely long stage. Clustering structure at the upper end of the SRM's attaches to a semimonocoque interstage that joins to the aft end of the HO tank.





The weight advantage in BLOW for the strap-on concept is due to a combination of having lighter attachment (clustering) structure, no interstage, and one less SRM meaning less stage structure and equipment. These weight savings plus the tandem configuration having a higher staging velocity constitutes the large BLOW difference.

Cost advantages for the strap-on are a direct result of less structure and stage equipment per flight.

A slight advantage in separation complexity is available with the tandem configuration since there is no possibility of SRM impact with the orbiter wing. Wind loads on the launch pad are worse for the tandem because of its length. However, flight loads into the SRM are greater for the strap-on because of the moment arm between the lower attachment structure and the thrust origin. Acoustic and heating characteristics relative to the orbiter are generally less severe for the tandem configuration due to being further away from SRM nozzle exit plane.

In summary, based on approximately a \$600 million savings in cost, lower inert weight and a technical assessment that does not reveal any major problems, the strap-on concept is selected as the preferred series burn approach.

### 5.1.3 Preferred SRM Booster

The comparison of the parallel burn and strap-on series burn configurations to allow a selection of the preferred SRM booster is shown in Figure 5-20.

Weight comparisons of these concepts indicate very little difference in GLOW but significant differences in BLOW and OLOW. The BLOW advantage for the parallel burn is related to having the orbiter burning during the booster portion of the flight and thereby increasing the average Isp. OLOW however favors the series burn concept since the HO tank propellant quantity is sized for orbiter engine firing only from the point of booster staging rather than during the entire powered flight. As witnessed by the comparatively close GLOW values these two factors just described tend to offset each other.

No significant DDTE cost difference exists between the two configurations since both are similar in design complexity. The parallel burn concept however does offer a significant advantage in cost/flight or program cost because of its lower inert weight.

Abort capability during booster burn favors the series from the point of view of higher T/W but the parallel system has the advantage of the orbiter engines already operating. Loads into the SRM are worse for the parallel burn due to large moment applied at orbiter ignition while on the pad. Flight loads are less severe however as a minimum moment arm exist between the aft attachment and thrust origin.

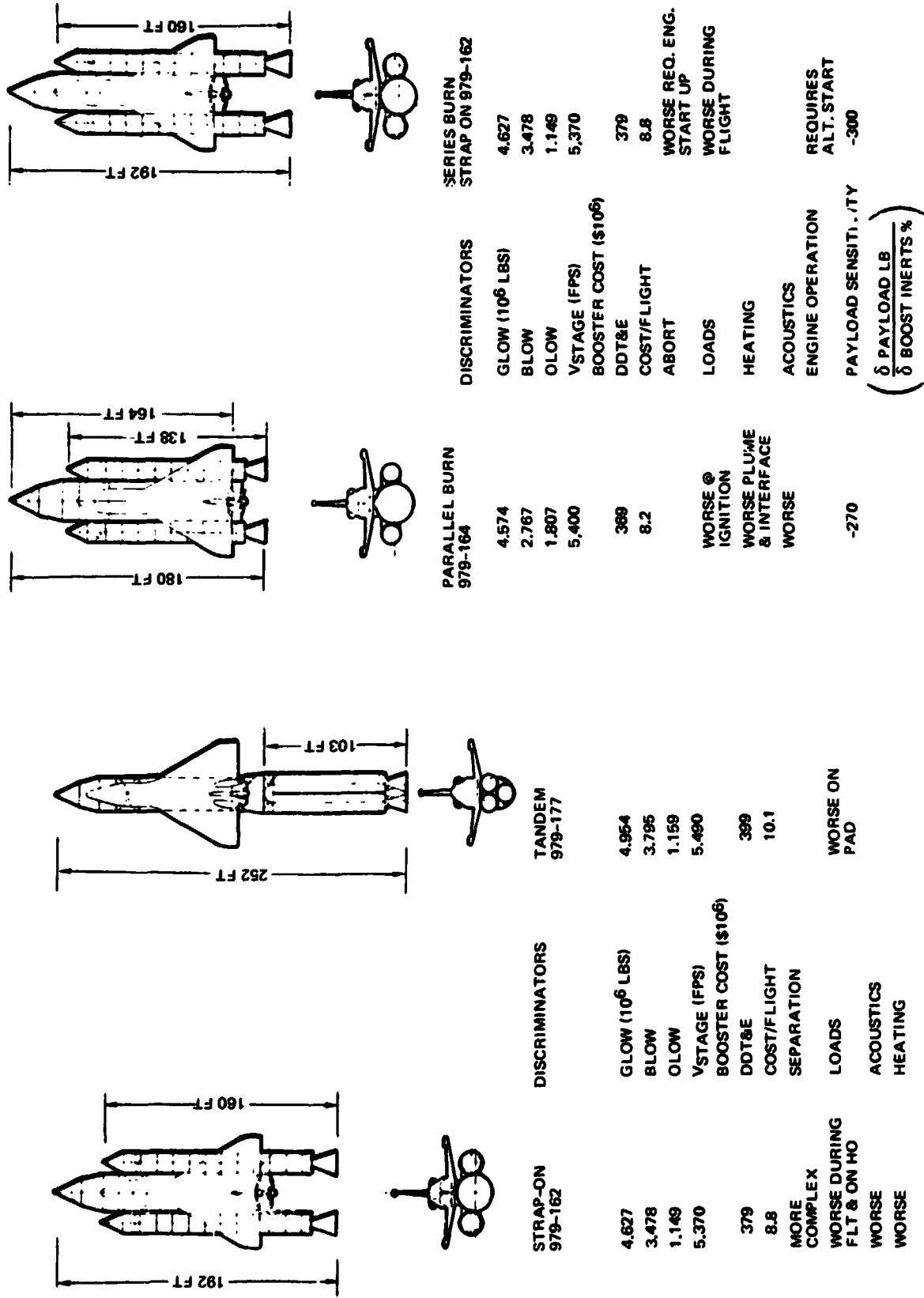


Figure 5-20 Selection SRM Booster

Figure 5-19 Series Burn SRM Boosters



Heating and acoustics impact on the orbiter favor the series burn due to the orbiter being a greater distance from the SRM nozzle. In the area of orbiter engine design, the parallel burn concepts shows an edge as the engine need only be designed for sea level start-up.

A final parameter of comparison between these concepts is the payload penalty that results per 1% increase in booster inerts. The difference is small again for the reason that the higher average Isp for the parallel burn concept during the booster burn phase is offset by the orbiter being less efficient during its own burn due to a larger HO tank.

In summary, as indicated in many of the parameters of comparison, the orbiter impact plays a major role. However, when considering only the booster, the parallel burn concept is the preferred SRM booster because of lower cost and weight and no technical problems that are considered high risk.

#### 5.1.4 SRM Booster Reuseability

A brief study has been conducted to assess the feasibility and weight and cost implications associated with recovery and reuseability of SRM boosters. The preferred parallel burn expendable solid booster was used as a starting point for this investigation. The approach used in this study was first to define the hardware changes necessary to allow recovery of each expendable SRM; and second, to resize the resulting configuration to recover the lost performance through the utilization of weight/performance trending data.

##### 5.1.4.1 Weight and Design Features

Drawing on the water recovery test and analysis work accomplished on the liquid propellant boosters, a judgement was made to use the same velocity reduction approach as for the pump fed configuration. In this approach, the SRM's enter the atmosphere at 0 deg. angle of attack and use a combination of drag brakes and parachutes to a velocity of 100 fps and solid propellant retros to reduce the velocity to 10 fps at water impact while in a horizontal attitude. These particular water entry conditions provided the least weight penalty and least component deflection by water pressure.

The accelerations, bending moment and impact pressures induced however did require the case thickness to increase for the two forward and two aft motor segments and vary from 0.70 at the top to 0.90 at the bottom of the cylinder cross-section. These gages represent an average 90 percent increase over the gage requirements for the expendable SRM. Through the four center segments, the gage requirement tapers from 0.50 to 0.65

from top to bottom. This is a 37 percent average increase over the ascent-only design condition. Similar analyses on other affected structure were conducted.

Having established the weight of a recoverable version of the expendable SRM, the next principal study step was the resizing which established the increase in propellant and necessary inerts to make up for the inerts required for recovery. The resulting configuration has been designated Model 979-164R.

Listed in Table 5-4 are the weight and certain other design implications related to SRM recovery. The first column lists the parameters of the recoverable 979-164R and the second column lists the differences when compared to the expendable 979-164. From this table may be noted:

- 1) The cylinder length of the rocket motor case increases 28%.
- 2) The number of cylindrical motor segments increases 25%.
- 3) The module inert weight increases 100% and with the additional propellant, the BLOW increases 37%.
- 4) The mass fraction decreases 5.9 points.

#### 5.1.4.2 Cost Implications

Cost associated with DDT&E, per flight, and total program for the recoverable booster concept are shown in Table 5-5. The \$196M increase in DDT&E for the recoverable concept reflects the heavier structure, the complete addition of the recovery system, and significant additions in avionics and power necessary to allow recovery. System test and SE&I increases also reflect the additional subsystems, analysis and test that are required to develop a reliable recovery system.

The major assumptions used in establishing cost/flight include 10 uses for the SRM case and 50 uses for other stage equipment. Values indicated for the recoverable portion relate to the percentage of unit cost that is recoverable. That equipment and/or material which is expendable in the SRM include propellant, liners, and insulation. Expendable stage equipment includes separation motors and attitude control propellant. The net effect of the savings and additions associated with the provisions required for recovery is a savings of \$1.7 million/flight resulting in a cost/flight of \$6.3 million (with amortization). To provide a direct comparison (without amortization--no production hardware cost) to liquid boosters, the recoverable SRM cost/flight is \$4.5 million.



Table 5-4 Weights & Other Parameter Implications of Recovery

	RECOVERABLE MODEL 979-164R	DIFFERENCES FROM 979-164
CASE CYLINDRICAL LENGTH	1,411 IN.	+ 310 IN.
NO. OF CYLINDRICAL SEGMENTS	10	+ 2
STAGING VELOCITY	5,100	- 300
<b>WEIGHT</b>		
BASIC MOTOR	213,500	+87,870
SEPARATION SYSTEM	12,900	+ 3,600
RECOVERY SYSTEM	44,500	+44,500
EQUIPMENT	3,000	+ 2,500
STAGE STRUCTURE	38,600	+21,030
GROWTH	30,500	+15,700
RESIDUALS	7,000	+ 1,300
MODULE INERT	350,000	+176,500
USEFUL PROPELLANT	1,550,000	+340,000
BLOW (MODULE)	1,900,000	+516,500
BLOW (TOTAL)	3,800,000	+1,033,000
MASS FRACTION	0.816	-0.059

Table 5-5 Booster Cost Impact of SRM Recovery

	DDT&E	
• EXPENDABLE	\$368M	
• CHANGES		
STRUCTURE RECOVERY	(+\$27M)	
OTHER SUBSYSTEMS	(+\$87M)	
SYSTEM TEST	(+\$24M)	
SE&B	(+\$15M)	
OTHER	(+\$25M)	
	(+\$17M)	
• RECOVERABLE	(\$196M)	
	\$564 ± \$50M	
<b>TOTAL BOOSTER PROGRAM</b>		
EXPENDABLE	\$4.2B	
RECOVERABLE	\$3.5B	
<b>ASSUMPTIONS</b>		
REUSE	SRM	STAGE
RECOVERABLE PORTION	10	50
	40%	96%
<b>COST/FLIGHT</b>		
• EXPENDABLE		\$8.16M
• CHANGES		
SAVINGS		
SRM PRODUCTION	-\$4.44M	
STAGE HARDWARE	-\$1.08M	
INCRD INCREASES		
SRM REFURBISHMENT	+\$2.95M	
STAGE REFURBISHMENT	+\$0.65M	
ADDITIONAL OPERATIONS	+\$0.07M	
• RECOVERABLE SRM (WITH AMORTIZATION)		\$6.31M
• RECOVERABLE SRM (WITHOUT AMORTIZATION)		\$4.5M ± \$0.5M

The total program cost of the recoverable SRM booster results in a 16% or \$700 million saving relative to an expendable SRM booster.

#### 5.1.5 SRM Booster Conclusions

The conclusions that have been reached relative to the key issues identified for the SRM boosters include the following:

- **SRM Diameter**

The 156" SRM's are preferred for all configurations due to a lower cost/flight and program cost, lower weight, and less configuration complexity because of fewer SRM's.

- **Best Series Burn Concept**

The series burn strap-on SRM arrangement is slightly favored over the tandem configuration primarily because of the lower cost/flight brought about by a lower BLOW.

- **Best SRM Booster Concept**

The parallel burn concept is preferred over the series burn strap-on when only considering the booster. Again, this conclusion is due to the lower cost/flight resulting from a lower BLOW.

- **Ascent Control Approach**

The gimballed nozzle design appears to offer advantages in both cost and weight and, in addition, is more flexible in coping with design changes in the vehicle or out of nominal conditions occurring during flight.

- **SRM Separation Approach**

Use of solid motor separation rockets both fore and aft on each SRM is preferred because of the lower cost and having operating procedures similar to those successfully employed by Titan IIIC.

- **Reliability and Safety**

A predicted reliability level of 0.99 for the parallel burn concept is comparable to liquid stages previously used for manned spacecraft. The predicted safety level of 0.9996 is also considered adequate when considering the goals associated with SST type aircraft and their relative exposure times.



- **Stage Cost**

Stage cost for the SRM booster appear reasonable relative to existing SRM booster stages when considering DDTE cost/pound and unit cost/pound.

- **Reusability**

Recovery and reusability of SRM's appear as feasible as for liquid stages. The cost/flight and booster program cost are significantly reduced relative to an expendable SRM booster, though the DDTE cost is increased by \$196 million or approximately 47%.

## **5.2 LIQUID PROPELLANT BOOSTERS**

This section describes the liquid booster systems, addresses key issues, and selects the best liquid system for comparison with the selected solid booster system in the following section. The significant issues include design and selection considerations as follows:

- **Pressure-fed booster design approach, as driven by:**
  - **Main Propulsion**
  - **Recovery**
- **Series Burn versus Parallel Burn, considering:**
  - **Cost**
  - **HO Tank Size**
- **Pressure Fed versus Pump Fed, considering:**
  - **Vehicle Efficiency (Weight)**
  - **New Development Requirements (Risk)**
  - **Cost**

These issues were resolved by performing in-depth preliminary design studies of pressure-fed and pump-fed series burn boosters, including extensive configuration trades. Parallel-burn pressure-fed booster configurations were developed by parametric scaling and weight trending. The presentation of this section describes the pressure-fed and pump-fed booster designs and analyses, followed by comparison and selection.

### 5.2.1 Pressure-Fed Series Burn Booster (Model 979-176B)

#### 5.2.1.1 Configuration-Pressure Fed Booster

This space shuttle concept is a two-stage integrated launch system combining a LOX/RP-1 series burn pressure-fed BRB first stage and a tandem-mounted LOX-LH<sub>2</sub> expendable drop tank/delta winged second stage orbiter. General arrangement, external dimensions and weights are shown in Figure 5-21. The selected booster airframe configuration is an integrated structure of separate oxidizer and fuel tanks connected with a cylindrical inter-tank shell. The propellant tanks are arranged with the LOX tank forward for stability to minimize the LITVC requirements during boost. The configuration features a shaped nose for minimizing the effects of water impact entry loads on booster inert weight. An integral liquid nitrogen pressurization supply tank is incorporated into the forward LOX tank. Inter-stage structure and stage separation structure attach to the LOX tank. The aft section behind the RP-1 tank includes the main engines, the engine thrust structure and engine water protection skirt. Weight characteristics are summarized in Table 5-6. The booster uses seven identical pressure-fed rocket engines each with a sea level thrust rating of 1,121,000 lb. Ascent guidance is provided from the orbiter and the booster provides ascent control by means of a liquid injection TVC system. Attached to the skirt are two fins sized to provide ascent stability during boost, and six deployable drag brakes sized to dissipate entry velocity. An altitude control system is employed to position the booster for a ballistic entry following its burnout and separation. Avionics installed on the booster provide redundant boost guidance and automatic subsystem checkout. During entry, the avionics subsystem provides altitude stabilizing command signals to the altitude control and event signals such as for parachute deployment.

#### 5.2.1.2 Performance Characteristics

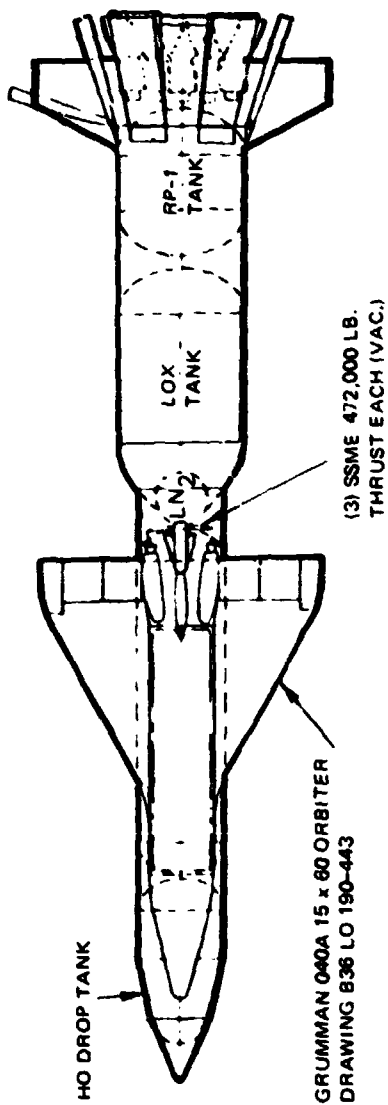
The pressure fed booster is sized for capability, in addition to boosting the baseline orbiter, to carry a growth orbiter with the HO tank enlarged sufficiently to carry the equivalent of a 5% increase in orbiter core interweight and retain the design payload. The equivalent inert weight increase was chosen for the design criterion because it is directly convertible to payload weight. Sizing the booster in this manner provides the capability to tolerate degradations in many parameters without requiring a change in booster design.

The booster trajectory as shown in Figure 5-22 has been designed to: 1) meet the ascent trajectory constraints, 2) have low ascent velocity losses, and 3) give consideration to the recovery subsystem requirements.









**DESIGN CHARACTERISTICS**

GLOW -	6,277,900 LB.
BLOW -	5,032,900 LB.
BLOW -	1,246,000 LB.
BOOSTER PROPELLANT WT.	
ASCENT -	3,999,300 LB.
LITVC FREON -	100,400 LB.
HYDRAZINE -	16,700 LB.
ENG. COOLANT (RP-1) -	30,000 LB.
EXPENDED N <sub>2</sub> -	4,700
$\lambda$ -	0.825
T/W @ 1 AUNCH -	1.25
MAX. "g" (BOOST) -	660 PSF
PAYLOAD -	40,000 LB (POLAR)
VSTAGE -	5,000 FT/SEC.

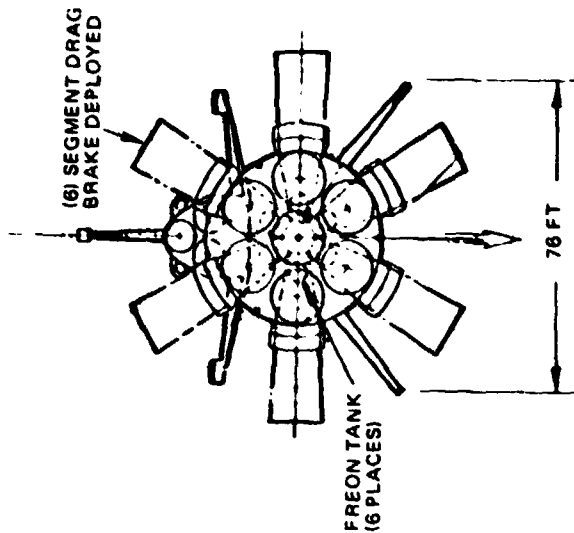
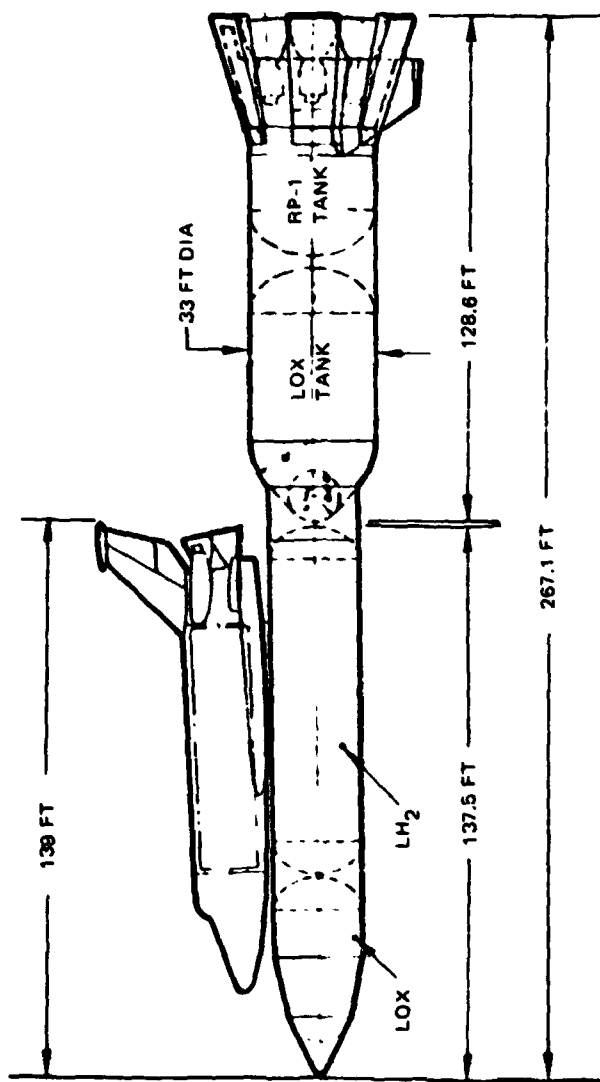


Figure 5-21 LOX/RP-1 Series Burn Pressure Fed BRB - Model 979-1766

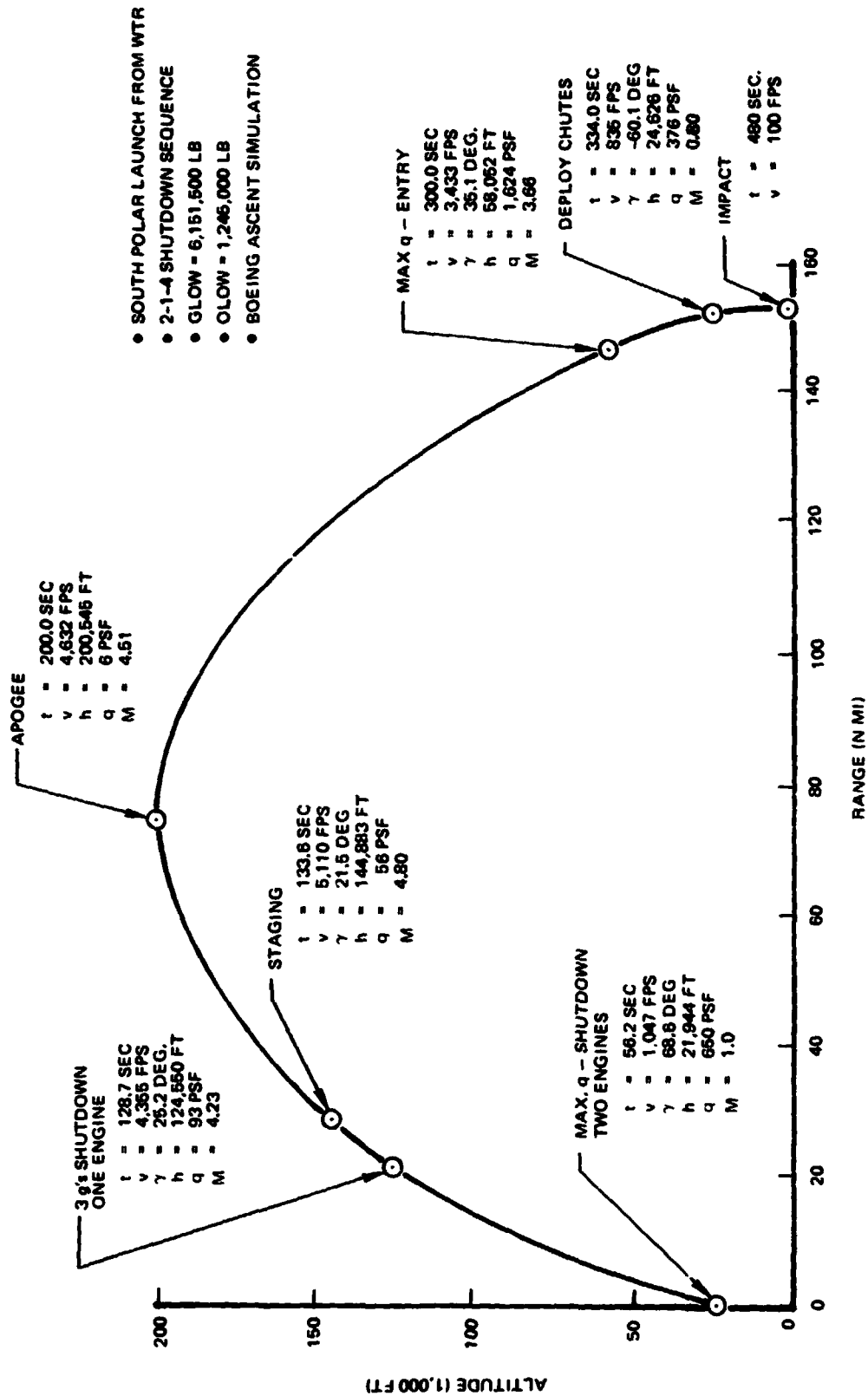


Figure 5-22 Pressura Fed Booster Trajectory - Model 979-176B

The maximum dynamic pressure constraint is met by shutting down two outboard engines when dynamic pressure reaches 650 psf. This reduction in acceleration keeps the dynamic pressure from increasing above 650 psf. The center engine is shutdown at an acceleration of 3 g's. The four remaining engines are shutdown at staging. This 2-1-4 sequence yields lower velocity losses than a 1-2-4 sequence, and has therefore been chosen as nominal. Engine throttling has been studied and has slightly lower velocity losses than the 2-1-4 sequence, but the sharply increased propulsion system complexity was considered too costly.

Following staging the booster flies a zero angle-of-attack trajectory to water impact. Near apogee, drag brakes are deployed to decelerate the booster during entry to a dynamic pressure of less than 400 psf, when parachute deployment is initiated.

#### 5.2.1.3 Structures Subsystem

The primary structural weight drivers on the pressure-fed vehicle are propellant tank pressure and water impact loads. Because of the relatively poor inherent efficiency of the pressure-fed system, i. e. , high inert weight and low engine performance, careful optimization of design conditions and structural arrangement was important.

The structure is designed to withstand all loading conditions and environments from launch to recovery for the vehicle's entire 50-mission life cycle. Where practical, low risk, state-of-the-art construction and materials are utilized to reduce cost and minimize the refurbishment steps required between missions. The primary structure shown in Figure 5-23 consists of an oxidizer tank including an integral liquid nitrogen bottle, a fuel tank, a thrust structure, an intertank, six drag brakes, two fins, a base heat shield and two raceways.

The critical load conditions and major design conditions for structural components are shown in Figure 5-23.

Boost ascent bending moment and axial flight loads were determined for the ground wind, maximum  $q_{\alpha}$ , and 3 g boost. Ground winds are computed for a one percent risk, one day exposure ten minute mean wind, with a gust factor of 3. Maximum launch wind shear assumed a  $q_{\alpha} = 4500$  psf deg. for computing loads, based on no load relief. The 3 g boost condition occurs after two engines have been shutdown to limit the dynamic pressure to 650 psf. No aerodynamic forces are considered for the 3 g case.

Water impact pressure distributions are shown in Figure 5-24 for conditions during impact on the nose and subsequent slap down of the aft skirt and engine bells. The nose



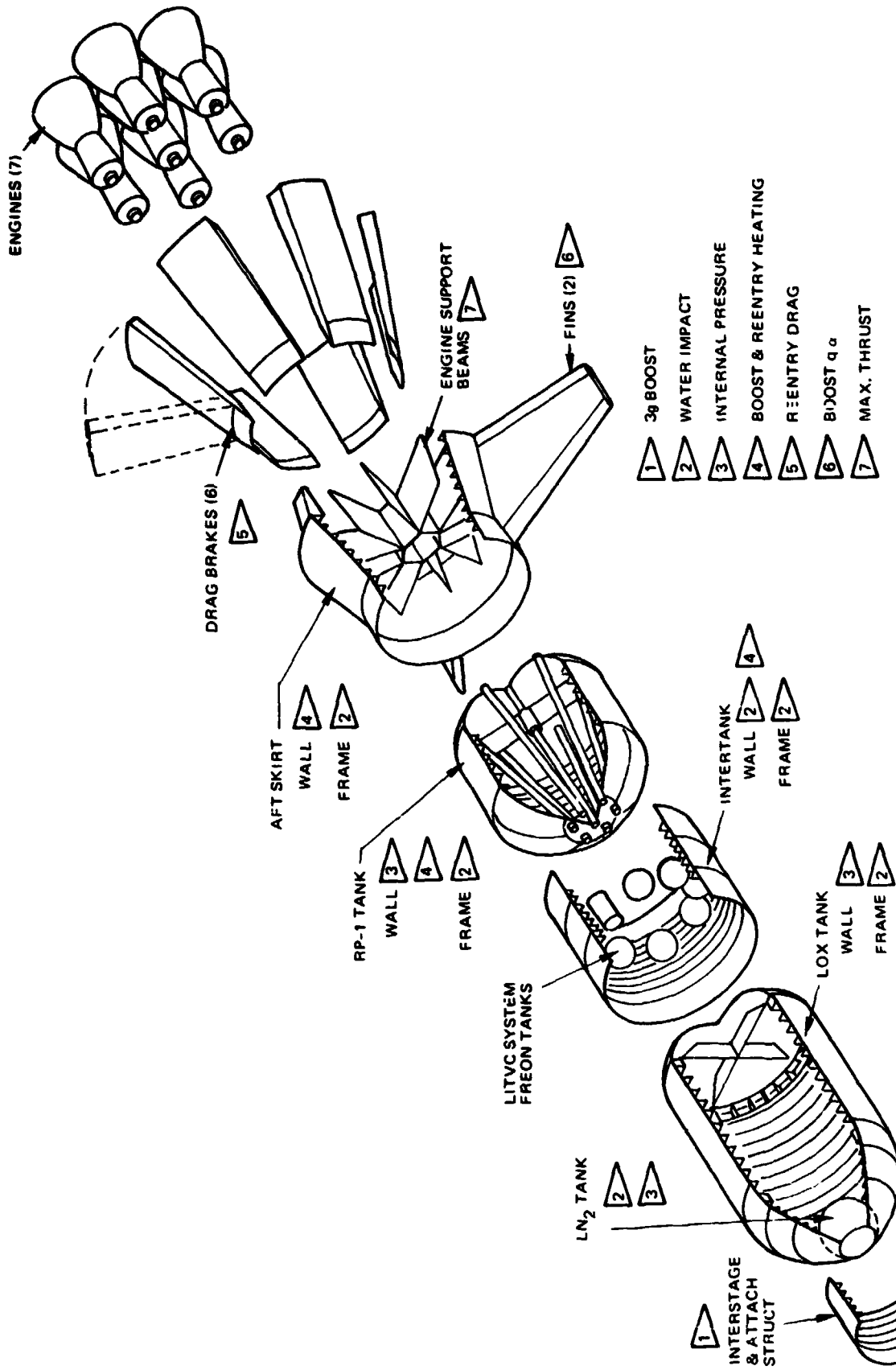


Figure 5-23 Pressure Fed Recoverable Booster Structural Arrangement and Major Structural Design Conditions

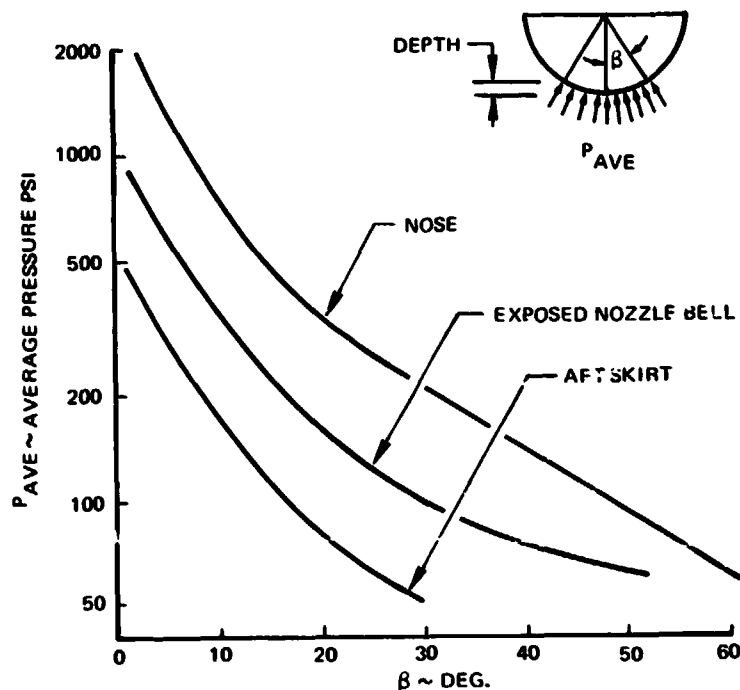


Figure 5-24 Water Impact Pressures  
 Pressure Fed Series Burn, BRB  
 Model 979-176  
 (Water Impact  $V_v = 100$  fps,  $\theta = 30^\circ$ )

pressure is computed for a spherical entry head using a virtual mass of water for computing the deceleration force. The aft skirt pressure distribution is determined from the peak lateral acceleration based on water impact model tests. The peak force for broadside impact occurs at an angle of  $\beta = 10^\circ$ . Pressure loads are shown for the engine bells as though they were exposed during slap down. (They are protected by the aft skirt.)

Water impact axial loads and moments are shown in Figure 5-25 for the booster during initial impact and subsequent slap down of the aft skirt. Initial conditions are 100 fps entry velocity and an angle of  $30^\circ$  from vertical, selected as a result of the weight trade for two water entry configurations shown in Figure 5-26. The primary system is one with no underwater drag device. Data for this trade were based on a total of over 200 water impact tests. Bounceout is prevented by entering at  $30^\circ$  from vertical. The weight has been minimized by entering at a vertical velocity of 100 fps as shown by the design point. The structural weight penalty associated with this point is 65,000 lb. The alternate entry configuration, which was rejected, is a vertical entry with an underwater drag device to prevent bounceout. Total structural weight penalty with the underwater drag device is 104,000 lb at an impact velocity of 100 fps.



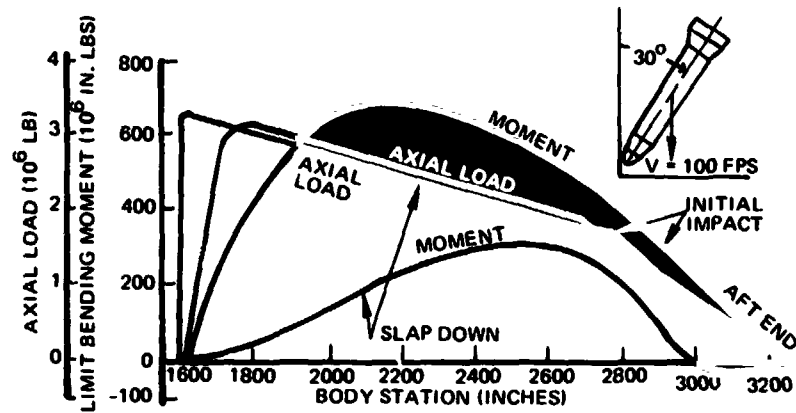


Figure 5-25 Water Impact Loads Pressure Fed, Series Burn, BRB Model 979-176

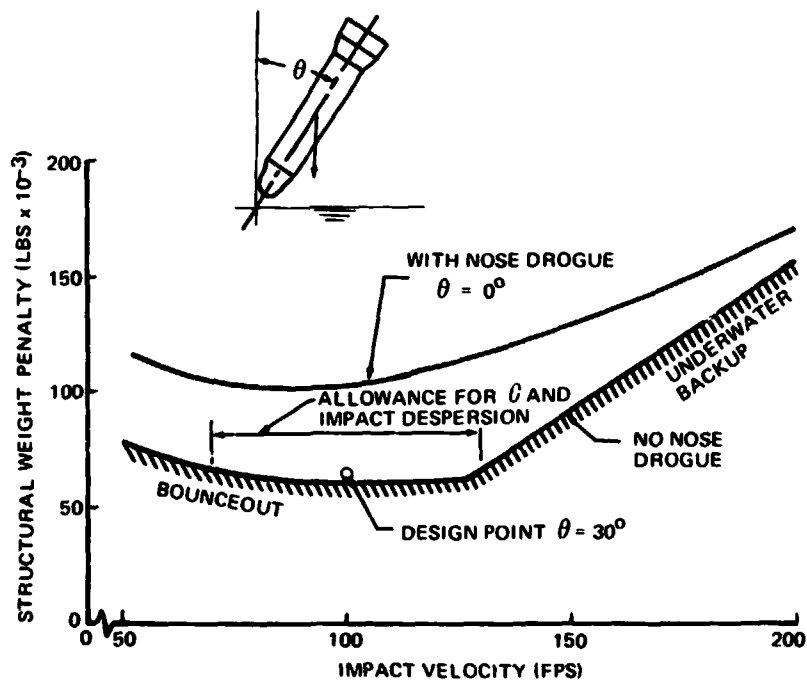


Figure 5-26 Water Impact Structural Weight Penalty

Major heating environments are plume heating in the base region, plume induced flow separation (PIFS) heating on the skirt and tanks, and internal heating from the pressurizing gases during ascent; and aerodynamic heating during reentry. Where the nose is integral with the LOX tank, there is no additional heat sink requirement, as is needed for the RP tank. The skirt and drag brakes are influenced primarily by the PIFS heating and reentry aerodynamic heating. A silicone ablator varying from .22 to .50 in. thick will be required to limit the aluminum temperature in these areas. Five principal trade studies were con-

ducted relating to structural design: a) separate tanks versus common bulkhead; b) tank and engine pressure; c) tank material selection; d) design life; and e) thrust structure.

Tank trades compared a common bulkhead design to the baseline. The baseline was not only lighter, but presented fewer technical difficulties and lower risk. Inconel 718 and aluminum overwrap were also traded against the all aluminum baseline and found to be less desirable if electron beam welding is incorporated on the baseline. Inconel was very expensive and difficult to machine and the overwrapped aluminum design had higher development cost and risk with little, if any, weight advantage.

A combined structural/propulsion trade optimized engine chamber pressure, resulting tank pressure, and engine mixture ratio and exit area ratio, considering the net effects of specific impulse and inert weight. The design life trade concluded that inert weight penalties for reserve were small. Therefore, the number of vehicles for the 445-flight program, twelve, was based on attrition estimates, turnaround time, and launch rate, and the required design life of fifty was a result.

Several thrust structure concepts were studied, including tank mounted engines, but all were found to be less attractive than the baseline because of weight, cost and/or technical risk.

The oxidizer tank is cylindrical, 33 feet in diameter, with a 45° elliptical dome at its aft end and a conical shaped forward end that tapers to a 160 inch diameter sphere containing the liquid nitrogen. Its outer shell is all welded from 2219 aluminum monocoque segments machined only to provide local reinforcement for penetrations, attach lugs, and weldments.

Slosh and vortex suppression baffles are provided. The slosh baffles are 30 inch deep frames that are also used to resist the high loading at impact. Baffles are built-up from 302 stainless steel sections to resist the high heating by the 900°F pressurization gases.

The fuel tank is identical, in material and type of construction, to the LOX tank except that it has a 45° elliptical dome at both ends and seven ring stiffened tunnels that span its length to provide passage for the LOX delivery lines. Stainless steel hoop reinforced bellows are provided at the upper end of the tunnels to allow for longitudinal expansion of the tank. Both tanks are proof tested to uniaxial yield with LN<sub>2</sub> to assure no catastrophic failure will occur over the life of the booster.

Propellant tanks are a major weight driver on the pressure fed booster as illustrated in Figure 5-27.





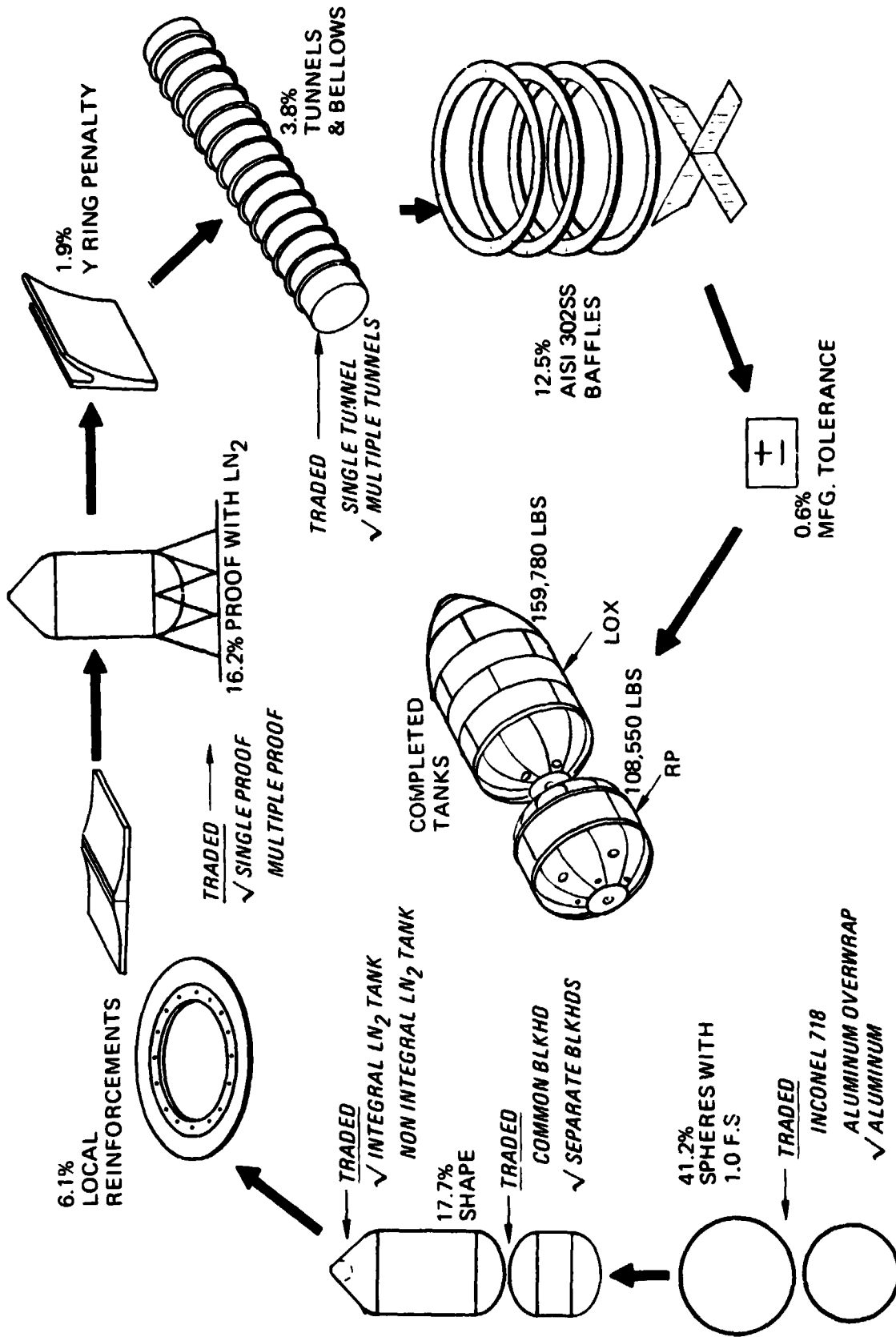


Figure 5-27 Tanks are a Major Weight Driver Because of Pressure

The intertank is a semimonocoque, ring stiffened structure 33 feet in diameter, sealed to prevent entry of sea water during impact and towback. The cylinder is all-welded from 2219 aluminum segments with integrally machined longitudinal T-stiffeners similar to the construction used in the S-1C propellant tanks. The ends are mechanically fastened to the adjacent tanks using a silicone sealant to achieve a watertight joint. The frames are built-up from 7075 aluminum sections.

The thrust structure is comprised of a conical outer ring stiffened shell and a network of 120-in. deep beams that support the seven main engines. The structure also supports the drag brakes, fins, parachute attachment and heat shield while providing for vehicle support holddown. The structure is totally sealed forward of the heat shield to prevent sea water entry as in the case of the intertank. The drag brakes and an extension of the outer shell protect the exposed portions of the engines at water impact.

The outer shell is an integrally stiffened skin of 7075-T73 aluminum that minimizes the faying surface requiring sealing. The main beams and ring frames are built-up from 7075 aluminum sheet and extruded sections. All thrust and holddown posts are machined from 7075 aluminum die forgings.

The base heat shield is a sealed bulkhead located at the throat of the engines. It is designed to withstand the plume heating of the engines and all loads associated with boost, entry, impact, and towback. Integrally machined 2024 aluminum panels with an ablative coating of silicone are mounted to a network of beams spanning between the main engine support beams.

The fixed fins are constructed using two spars, eleven ribs, and stiffened upper and lower skins. All elements are built-up of 2024 aluminum sheet and extruded sections. A silicone ablator is applied to the entire outer surface to protect the aluminum from heating (aerodynamic and plume effects) and to seal from sea water entry.

The six drag brakes are hinged at their forward edge and are free to pivot radially outboard. Each panel is actuated by two sets of folding linkages driven by hydraulic actuators. As in the case of the fins, the outer surfaces are coated with a silicone ablator for thermal protection and sea water sealing. The interstage is an aluminum semimonocoque, ring stiffened cylinder designed to be expended each flight. It is connected to the LOX tank and severed with a linear shaped charge around its circumference. This separation concept is similar to those used on the Saturn V.



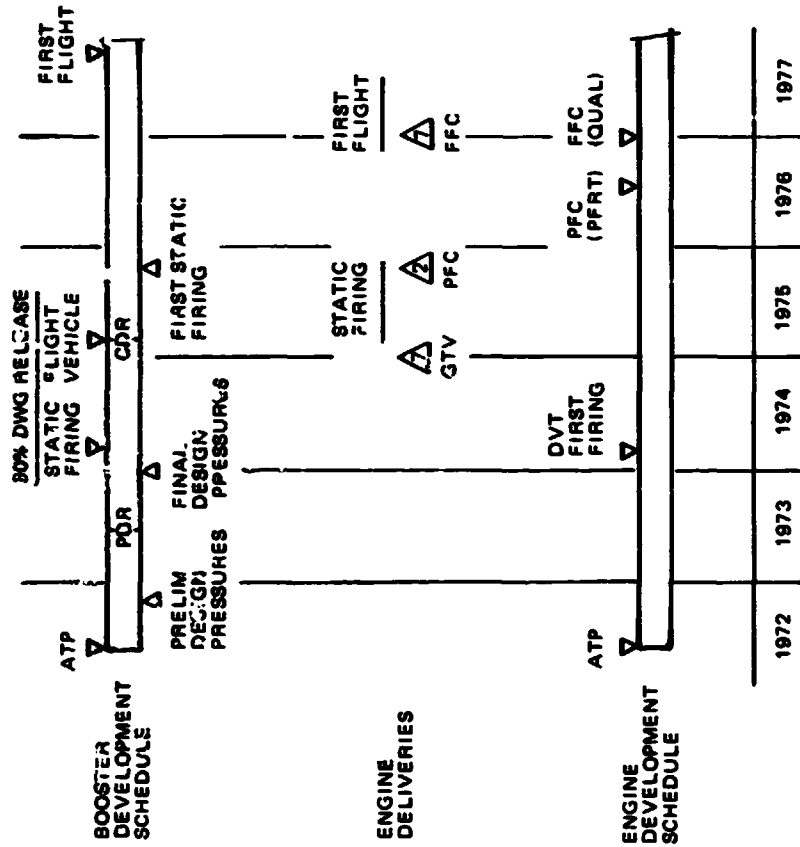
#### 5.2.1.4 Propulsion Subsystems - Pressured Fed Booster

The key issues within the propulsion systems of the pressure-fed booster are engine/vehicle integration, the pressurization system concept selection, and the development requirements which must be accomplished prior to detail system design. Thrust vector control is a key issue from the overall vehicle standpoint. LITVC was chosen over gimbaled engines based on structural consideration in the base region. The fixed engines with LITVC greatly simplify the base heat shield and sealed bulkhead. In addition, the base area and thus the aft fairing are also considerably smaller. The other propulsion subsystems, namely feed system, reaction control, and propellant utilization are straightforward. A passive PU system was chosen on the basis of simplicity. The weight trade between a passive and active system was indecisive since the weight penalty associated with the inlet pressure control band for the active system counteracted the advantage in residual weights.

Pressure fed booster pressure requirements so effect vehicle size and dynamic stability that engine/vehicle integration becomes a key development issue as illustrated in Figure 5-28. Chamber pressure in pressure fed engines is separated from feed system pressures primarily by injector pressure drop. This relationship requires integrated propulsion system testing at the earliest opportunity to refine and verify propulsion system design and to calibrate subsystem interactions. Since pressure fed engines of this size have not been developed, a tight engine development and delivery schedule is involved to provide flight configuration engines for integrated propulsion system testing. Close and continuous monitoring of engine and vehicle development will be necessary during this period. The main rocket engine installation is tested as an integrated system on the propulsion test vehicle (PTV). The first set of seven operable engines is provided nine months after engine DVT first firing, but prior to engine and vehicle CDR. Two of these engines will be replaced, after CDR, with PFC configuration engines for system calibration.

Analysis of candidate pressure fed booster designs has shown that engine-vehicle instabilities (POGO) can occur, similar to that encountered with S-1C and S-11 and Titan. The threshold of instability is actually lower because of the higher gain factors of pressure fed engines. Studies of passive and active POGO suppression techniques have shown that pressure fed vehicle POGO suppression is feasible using current technology. Passive gas filled accumulators can be used to suppress POGO modes in the 5-50 Hz frequency regime. Other suppression concepts are feasible but none approach the passive gas filled accumulators for ease of development, test, and demonstrated design capabilities.

ENGINE / P REQUIREMENTS DRIVE TASK DESIGN AND PRT SURVIVAL SYSTEM SIZING



ENGINE/VEHICLE COUPLED INSTABILITIES (POGO) DRIVE FEED SYSTEM CONFIGURATION

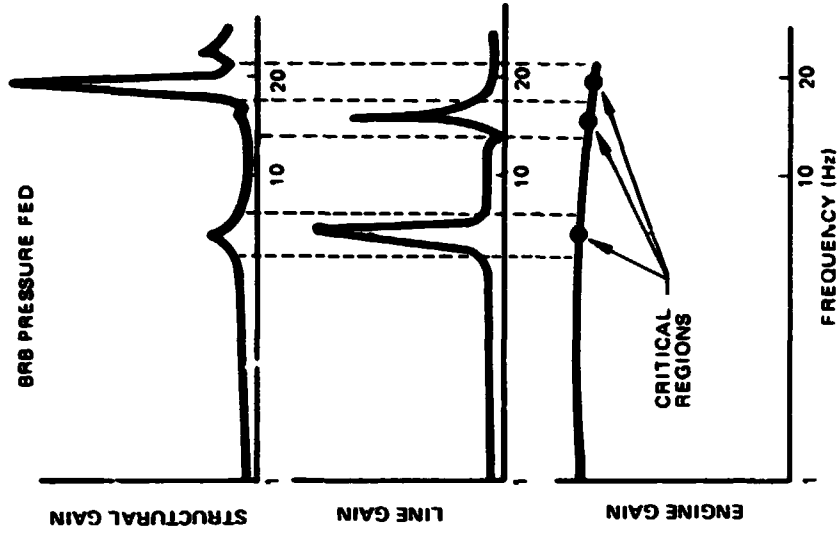


Figure 5-28 Engine/Vehicle Integration is a Key Booster Issue



The baseline pressurization system, shown as a single-thread schematic in Figure 5-29 pressurizes the main oxidizer (LO<sub>2</sub>) tank and the LITVC from tanks with heated nitrogen, and the main fuel (RP) tank with hydrazine decomposition product. The nitrogen is stored as a cryogenic liquid and is conditioned to 1260°R (800F) by a heat exchanger using a hydrazine gas generator heat source. A portion of this conditioner exhaust (hydrazine decomposition product) is used for RP tank pressurant. The LN<sub>2</sub> and hydrazine tanks are pressurized by ambient temperature helium. Isothermal helium blowdown is provided, with substantial weight savings. The nitrogen conditioner exhaust is routed through intank heat exchangers with bypass valving to maintain temperature. The exhaust is then propulsively vented overboard. Main tank ullage pressures are maintained by controlling pressurant gas flow using control valve modules that respond to tank pressure levels and rate of change. Hydrazine flow at the gas generator is controlled to maintain a constant conditioned nitrogen temperature.

The LO<sub>2</sub> and RP tank ullage pressures are maintained constant at 320 and 370 psia respectively during main engine burn. These pressures, when coupled with the effects of variations in vehicle acceleration and propellant level, provide an integrated effective engine inlet pressure matching the requirement of 375 psia. During the boost period, pressurant flow must vary to accommodate programmed engine shutdowns as well as control transients.

Six pressurization system concepts were studied in the process of concept selection. Of these, the selected concept represented a good compromise between cost, weight, complexity and developmental confidence.

Major development testing required for propulsion systems in the pressure fed booster concepts are outlined in Figure 5-30. A primary objective of the development test program to resolve uncertainties as early in the program as is feasible. Initial testing is directed at providing engineering and technology data for establishing requirements and verifying design approaches. These tests will involve components and scale and full size partial system breadboards. Later testing will provide design verification and will be conducted on full-scale breadboards. Full scale integrated qualification testing will use the propulsion test vehicle (PTV). This will include both cold-flow and hot firing tests.

Early breadboard tests will include:

- Providing large hydrazine gas generator design technology.
- Characterizing the pressurization subsystem nitrogen heat exchanger.
- Evaluating hot-gas flow control designs for LO<sub>2</sub> and RP tank pressure regulation.

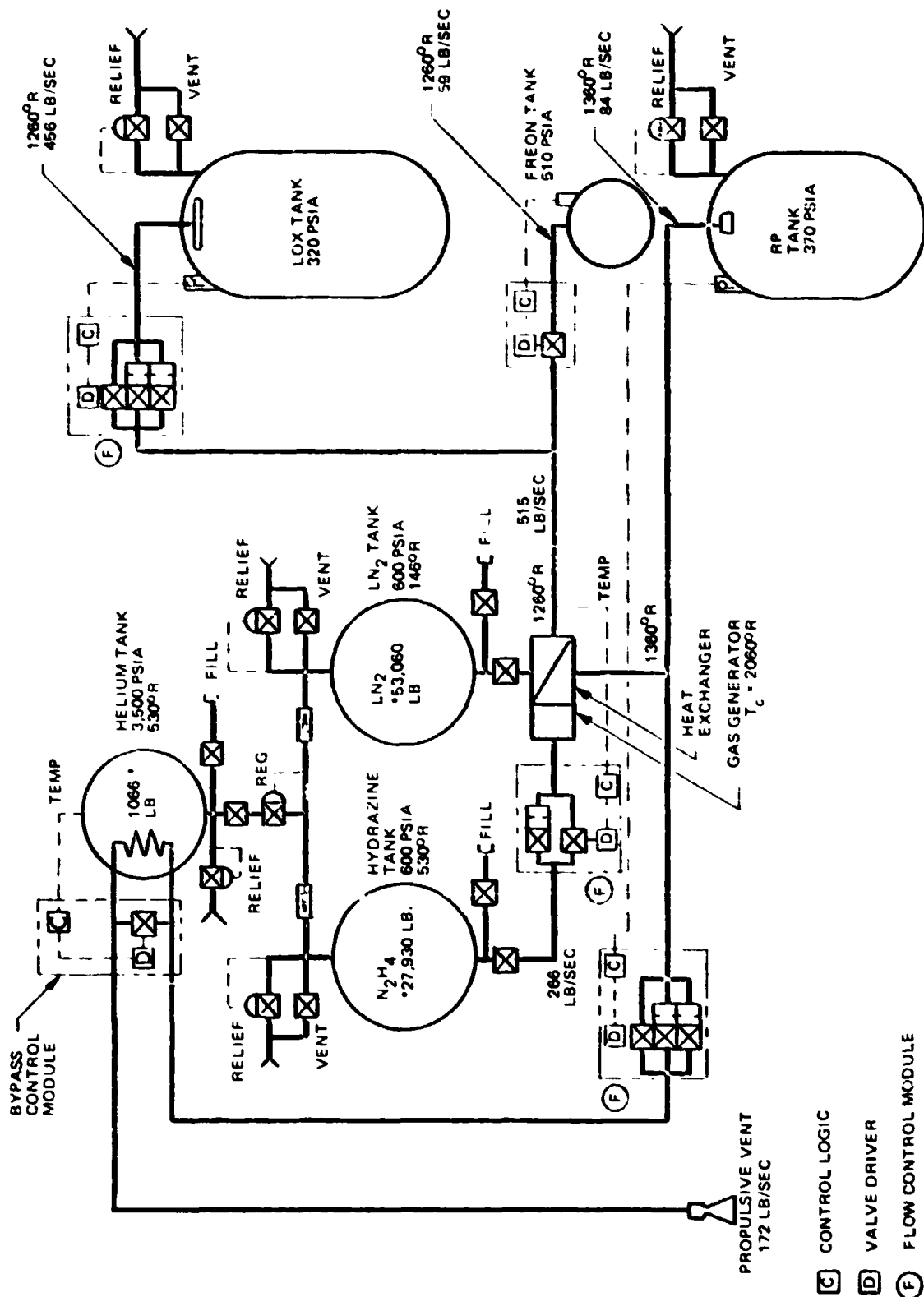


Figure 5-29 Pressurization Subsystem (Model 979-176B)  
Single Thread Schematic

- PRESSURIZATION SYSTEM HELIUM TANK HEATER DEVELOPMENT
- PRESSURIZATION FLOW CONTROL UNITS
- PRESSURIZATION SYSTEM GAS GENERATORS
- PRESSURIZATION SYSTEM HEAT EXCHANGERS
- VEHICLE BASE HEATING
- PROPELLANT FEED AND STRUCTURAL DYNAMICS
- LITVC VALVE HEAT SOAK BACK
- PROPULSION SUBSYSTEM SEA-WATER COMPATIBILITY
- PROPELLANT EXPULSION - FULL SCALE

*Figure 5-30 Development Testing Series & Parallel  
Burn Pressure Fed BRB's - Models  
979-176, -171*

- Obtaining intank thermodynamic data by scaled expulsion tests.
- Demonstrating the stability of the intank heat exchangers and bypass control of the pressurization system helium tanks.
- Verifying design approaches for controlling LITVC injectant valve heat soak back.
- Evaluating propellant feedline characteristics by single full size line flow tests.

A full scale pressurization subsystem integrated breadboard will be developed to verify system integrity and stability and to map performance characteristics.

PTA testing will demonstrate the compatibility of the pressurization system, propellant tanks, feed system and engines. These tests will also provide full-scale base heating data for sea level conditions.

#### 5.2.1.5 Aerodynamic Ascent and Descent - Pressure Fed Booster

The pressure fed configuration has two fins of 500 ft<sup>2</sup> each at 40° anhedral. The size and anhedral angle was chosen to provide the optimum balance between fin weight and LITVC fluid usage.

##### Ascent Characteristics

As shown in Figure 5-31 the ascent configuration is unstable in both pitch and yaw over most of the Mach number range. In the max q-range the aerodynamic centers both are about 200 inches ahead of the CG.

Due to the fins the roll stability is very low with subsequent low thrust vectoring requirements (Figure 5-32).

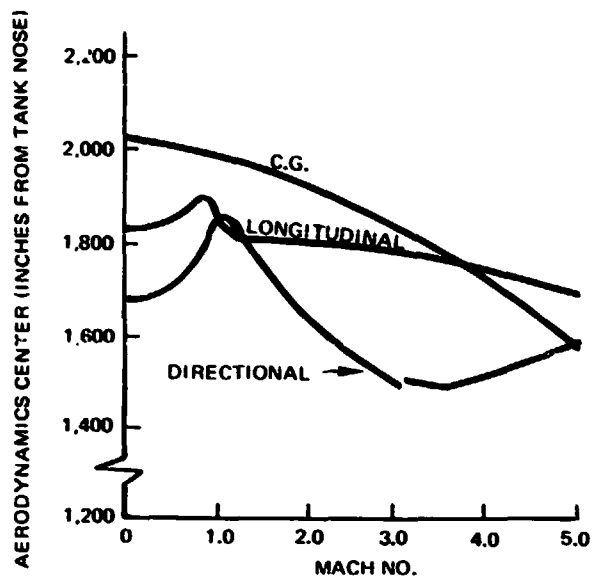


Figure 5-31 Ascent Stability - Pressure Fed

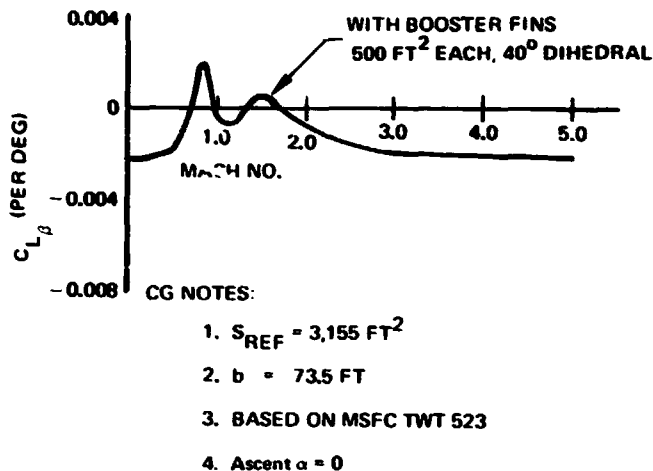


Figure 5-32 Ascent Roll Stability - Pressure Fed

### Entry Characteristics

Entering at high angle of attack has the advantage of providing adequate deceleration drag from the basic vehicle. The associated life also is beneficial because it gives a more shallow trajectory. However, it is not possible to configure a vehicle with fixed fins with a CG that allows both trim and sufficient stability margin. The alternatives were to use movable fins with a stability augmentation system or ballast the vehicle to a more forward CG. Both were found to be heavier than a configuration with drag petals to provide sufficient drag. The configuration with drag petals can be made to have substantial stability margin throughout the supersonic Mach number range.

Drag petals for the 979-176B configuration were sized to achieve a ballistic coefficient ( $W/C_{D0}$ ) less than 400 psf at speeds below Mach 1. This value of  $W/C_{D0}$  represents a design limit for satisfactory deployment of the parachutes. Drag petal design has not been changed to incorporate current weights, therefore, the designs have not been optimized. The ballistic coefficient is well below 400 psf at subsonic speeds providing a margin for variations in staging and atmospheric conditions, and weight growth (Figure 5-33).

A buildup of the zero-lift drag coefficient for the 979-176B design is shown in Figure 5-34. The six drag petals, deflected to 75°, contribute between 65 and 85 percent of the total  $C_{D0}$ .





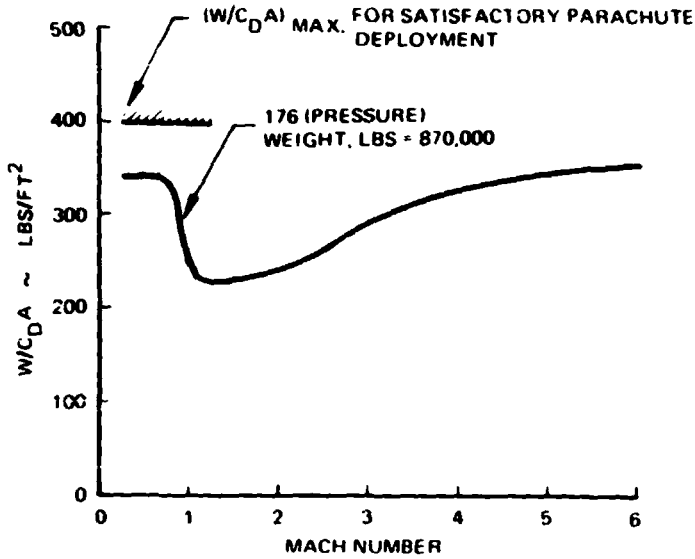


Figure 5-33 Reentry Ballistic Coefficients

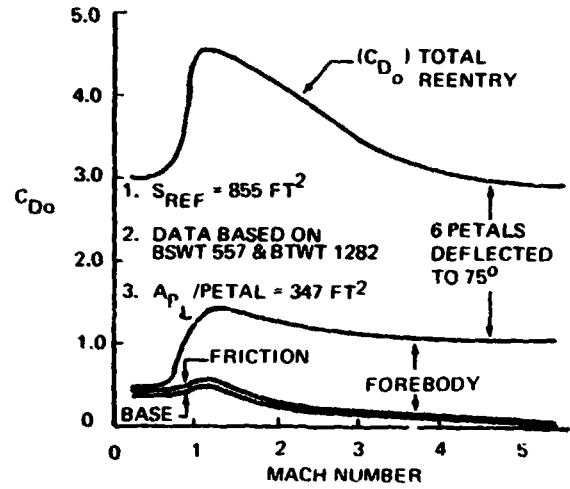


Figure 5-34 Zero Lift Drag Buildup - Pressure Fed

The drag petals on the 977-176B configuration are hinged at the forward end of the booster flare. This design has been tested recently in Boeing wind tunnel facilities, and has large positive static stability margins at all speeds above Mach 1. Below Mach 1, static stability is reduced to near neutral or slightly positive levels (Figure 5-35).

Aft-mounted drag petals have also been tested on the 979-176B body-flare combination. This arrangement has large static margins above Mach 1, with margins at subsonic speed much larger than those of the forward-mounted drag petal design. Forward-mounted petals were reflected on the basis of simpler actuation.

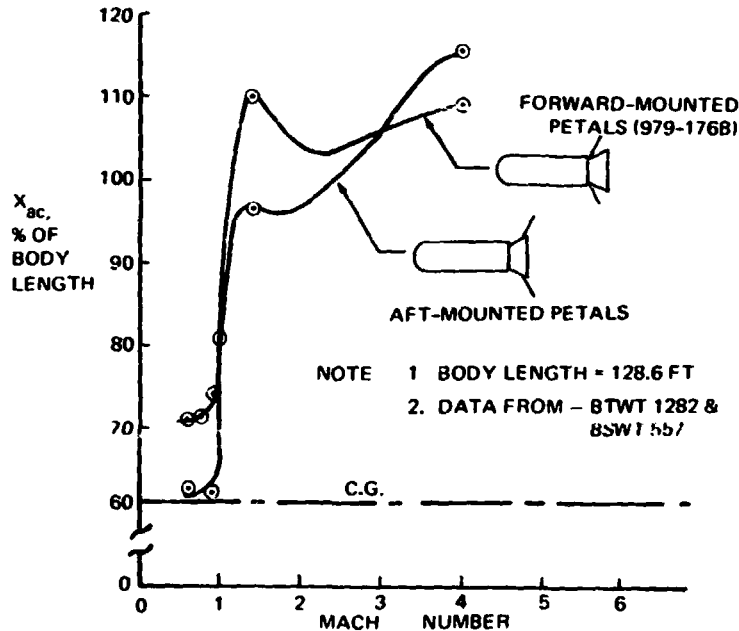


Figure 5-35 Static Stability - Pressure Fed

### 5.2.1.6 Flight Dynamics

#### Ascent

The maximum thrust deflection requirements result from a crosswind as does the maximum LITVC injectant integrated usage. Requirements include not only the wind requirement but also the C. G. uncertainty, slosh and bending and a transient for engine out. These combine to a total requirement of 2.9 degrees of thrust vectoring. Two engines are shut down when dynamic pressure reaches 650 fps, leaving only four engines for control. It is under this condition that the deflection requirements were generated. Should one engine fail during flight the opposite engine is shut down to regain symmetry and thus reduce injectant requirements. The orbiter ailerons and rudder were used for roll control to decrease injectant requirements. Figure 5-36 shows the thrust vector deflection requirement for the pressure fed BRB during ascent.

#### Separation

Simulations were performed for nominal separation conditions, as illustrated in Figure 5-37. A dual-plane concept was selected. The booster-interstage separation joint concept is also shown in Figure 5-37.

#### Attitude Control

A reaction control system is required for pitch, roll and yaw axes of the booster to arrest staging rates as shown on Figure 5-38 and provide pitch and yaw stability until the drag petals are deployed. This minimum energy system, while allowing very high angular excursions in both pitch and yaw, is sufficient to prevent booster tumbling after separation.

The drag petal deployment near apogee produces an aerodynamic center shift which provides a high degree of static stability in both pitch and yaw. After deployment, the pitch and yaw reaction controls primarily provide damping.

### 5.2.1.7 Deceleration and Recovery Subsystem - Pressure Fed Booster

Several concepts that would develop the necessary drag to decelerate the -176A booster from a Mach number of approximately 1.0 down to the impact velocity of 100 fps were studied. Primary concepts included an all parachute system; all retro-rocket system; and a hybrid parachute/retrorocket system. Other concepts such as rotors, parafoils, ballutes etc. were also considered but either were not technically feasible or not competitive with the primary concepts.

The selection criteria for the recovery system was low technical risk, minimum cost, light weight and minimal booster vehicle structural penalty. Figure 5-39 represents the



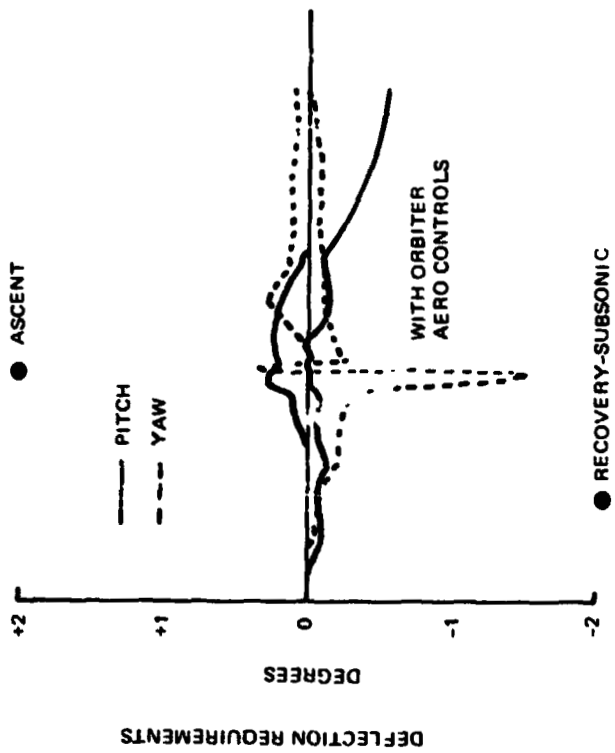


Figure 5-36 Pressure Fed Ascent and Recovery Characteristics

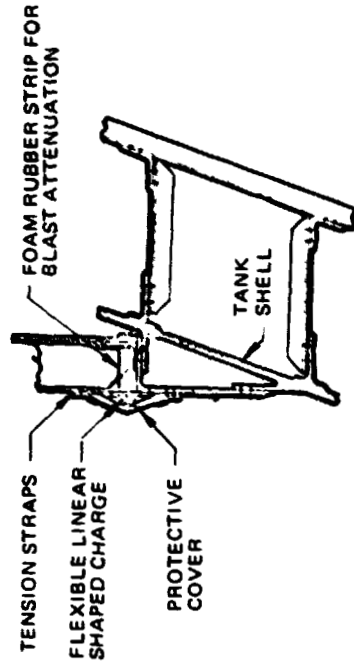
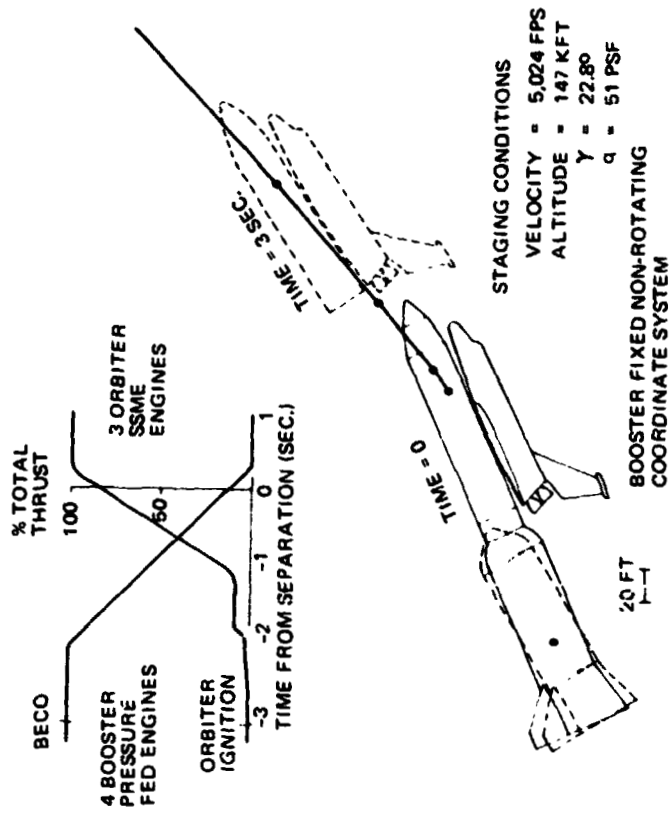


Figure 5-37 Series Burn Pressure Fed BRB (-176) Nominal Separation

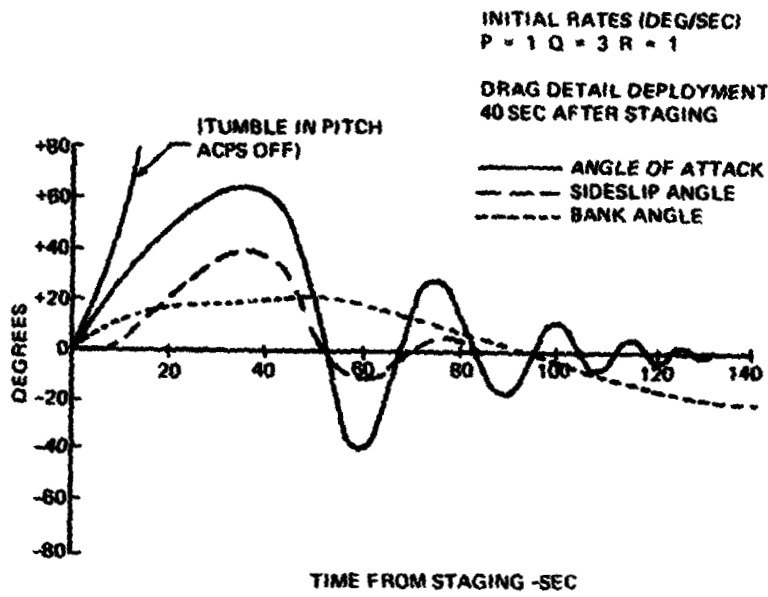


Figure 5-38 Series Burn, Pressure Fed, BRB Separation Dynamics

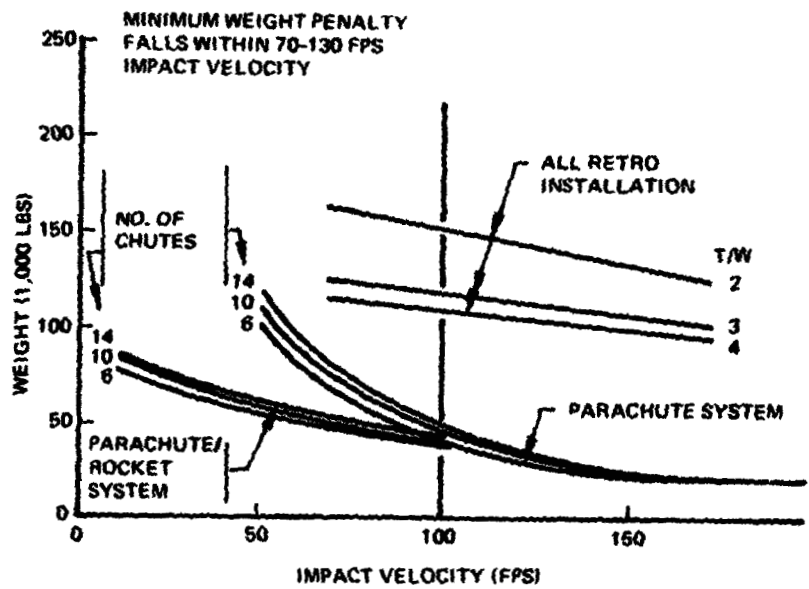


Figure 5-39 Recovery System Selection



results of a typical parametric study showing weight as a function of impact velocity for several recovery concepts, and as a function of the number of parachutes in a cluster. The impact velocity of concern ranged from approximately 20 to 200 fps.

For all impact velocities considered, the all retrorocket installation is much heavier than the all parachute system or the parachute/retro-rocket hybrid system. The all parachute system was selected at 100 fps impact velocity because it was close to being the lightest and it had the simplicity of a single system. The 100 fps impact velocity was selected as the best considering both the structural penalty from impact and the recovery system.

When comparing a parachute cluster of 14, 10 and 6 parachutes for a specific impact velocity, the cluster of six was the lightest. Other considerations when selecting the number of parachutes are parachute diameter and reliability in the case of a single parachute failure.

Six 165-ft diameter parachutes were selected based on technical risk, cost and weight. This system from technology standpoint is within the current state-of-the-art. The required process for parachute clustering and large parachutes for the baseline recovery system is straightforward.

#### Recovery Sequence (Pressure Fed)

The recovery sequence for the -176A pressure fed booster is shown on Figure 5-40. After orbiter/booster separation the booster is oriented at a 0 degree angle of attack reentry angle by the attitude control system. Six drag brakes with a total area of 2082 ft<sup>2</sup> are deployed to develop additional drag for deceleration and give the booster balance during the reentry phase. The maximum q attained during the reentry phase is 1630 fps.

At a Mach number of .9 and 27,700 ft altitude, three 9-ft diameter pilot parachutes are mortar deployed. Five seconds later at a Mach number of .8 and 24,300-ft altitude, three 70-ft diameter drogue parachutes are deployed. The drogue parachutes use a single stage of reefing. Then, 10.3 seconds later at a Mach number of .44 and 18,300-ft altitude, six 165-foot-diameter main parachutes are deployed. The main parachutes use two stages of reefing. The maximum g load felt by the main parachutes is 3.0 g's.

During the main parachute descent, the drag brakes are retracted. Prior to water impact the vehicle is oriented with the nose downwind and enters the water at an entry angle of 30 degrees from the vertical with an impact velocity of 100 fps. The selected orientation and entry angle minimizes the water impact loads and rebound load conditions. At water impact, the six main parachutes are disconnected and parachute flotation devices are inflated.

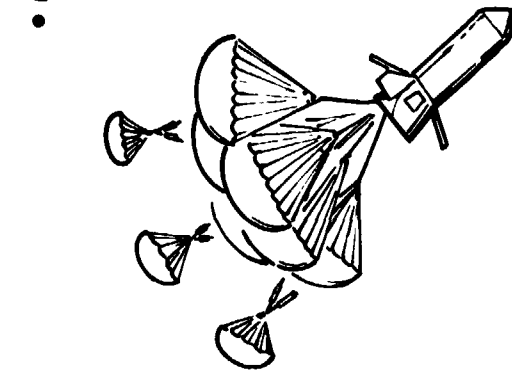
- ORIENTATION
- REENTRY
- DECELERATION



BOOSTER  
ORIENTED  
BY RCS  
REENTRY  
 $\alpha = 0$   
DRAG BRAKES  
DEPLOYED



DEPLOY 3-70 FT  
DROGUES



DEPLOY 6 - 165 FT  
MAINS  
2 STAGES OF REEFING  
DRAG BRAKES  
RETRACTED  
NOSE DOWNWIND  
ORIENTED BY RCS

- PARACHUTE DEPLOYMENT

RECOVERY SEQUENCE  
BOOSTER MODEL 979-176

- RETRIEVAL



$L_V = 30^\circ$   
 $V = 100\text{FPS}$



- IMPACT



Figure 5-40 Recovery Sequence - Booster Model 979-176

The parachute system is installed external to the thrust structure between the stabilization fins and the drag brakes. Three individual compartments, protected by thermally insulated fairings, will house a single pilot and drogue parachute and two main parachutes. Aft facing compartment covers will be pyrotechnically ejected prior to initiation of the parachute subsystem.

Each of three pilot parachute mortar assemblies consist of a 9-ft  $D_0$  parachute and integral riser, deployment bag, mortar tube, cover, breech, robot and pyrotechnic cartridge. Each assembly will be 18 in. in diameter, 24 in. long and weigh approximately 175 lb.

Each drogue parachute riser is attached to two main parachute deployment bags and will break the pack stowed restraints, extract the main parachutes from their stowed position and progressively deploy the main parachutes. The drogue parachute pack assembly consists of a 70-ft  $D_0$  conical ribbon parachute, with integral riser, deployment bag, pilot parachute to deployment bag bridle and mechanically initiated pyrotechnically reefing line cutter. Each pack assembly weighs approximately 4300 lb and requires a volume of 130 cu ft. The maximum load exerted on the vehicle by each of three drogue parachutes is 430,000 lb.

Two stage active reefing of the main cluster is selected to maintain balanced peak deceleration forces. In order to assure near synchronous disreefing of the main parachutes, subminiature radio receivers designed to initiate pyrotechnic reefing line cutter, will be installed in each parachute. Each main parachute will be provided with a self-inflating flotation system adequate to support the weight of the parachute and the previously disconnected attach fitting.

The main parachute pack assembly consists of a 165-ft  $D_0$  conical ribbon parachute with integral riser, deployment bag, drogue parachute to deployment bag bridle, pyrotechnic reefing line cutters and subminiature radio receivers. Each pack assembly weighs approximately 5,400 lb and requires a volume of 170 cu ft. The maximum load exerted on the vehicle by each of the six parachutes is 430,000 lb.

#### Retrieval System

The retrieval system must upright and stabilize the booster after impact as well as furnish the necessary equipment for locating the booster, minimizing wind drift, ship lights and provide a means for attaching a tow line.

Two righting bags attached to the skirt and located below each fin are selectively inflated to provide the required righting force.

Stabilizing bags located at the normal water line are both inflated as soon as the one that is submerged is in a position to exert the correct righting force.

An antenna for the radio locating beacon is situated on top of the booster in the intertank area.

The locating beacon transmits 1K pulse per sec (pps) to provide an RF signal suitable to locate the vehicle on the water.

#### 5.2.1.8 Subsystems - Pressure Fed Booster

This section summarizes the main subsystems besides propulsion, structure and recovery. Since subsystems contained herein are not key issues or configuration drivers they are only summarized.

5.2.1.8.1 Drag Brake Actuation - The power and actuation system is typical for each drag brake (Figure 5-41). Mechanical power is provided by MIL-H-83282 hydraulic fluid stored in nitrogen charged accumulators at 3000 psi nominal pressure. A two-position solenoid valve receiving commands from the avionics subsystem controls actuator extend and retract pressure. An integral mechanical lock retains the actuator piston in this position until released by energizing the solenoid valve and pressurizing the "Panel Deployed" cylinder. A two-position solenoid arming valve installed upstream of each actuator provides redundant protection against inadvertent deployment of brakes during ascent.

5.2.1.8.2 Environmental Control - Environmental control requirements and characteristics of the Model 979-176B are similar to those of the S-1C booster. Compartment purging and cooling of the avionic/electrical components located in the intertank and thrust structure compartments maintains safe hazardous gas levels, excludes sea water during water immersion, and provides suitable temperatures and pressures for equipment through launch preparations, and retrieval operations. GSE/ECS has control of temperatures and pressures of the thermal control and purge media, which are supplied to valves in the flight umbilicals.

5.2.1.8.3 Electrical Power Subsystems - An electrical power and distribution system will be provided to supply electrical power to booster loads from time of ground power transfer to completion of mission. During the manned portion of flight, safety-of-flight will be assured by supplying all flight critical loads from redundant battery sources.





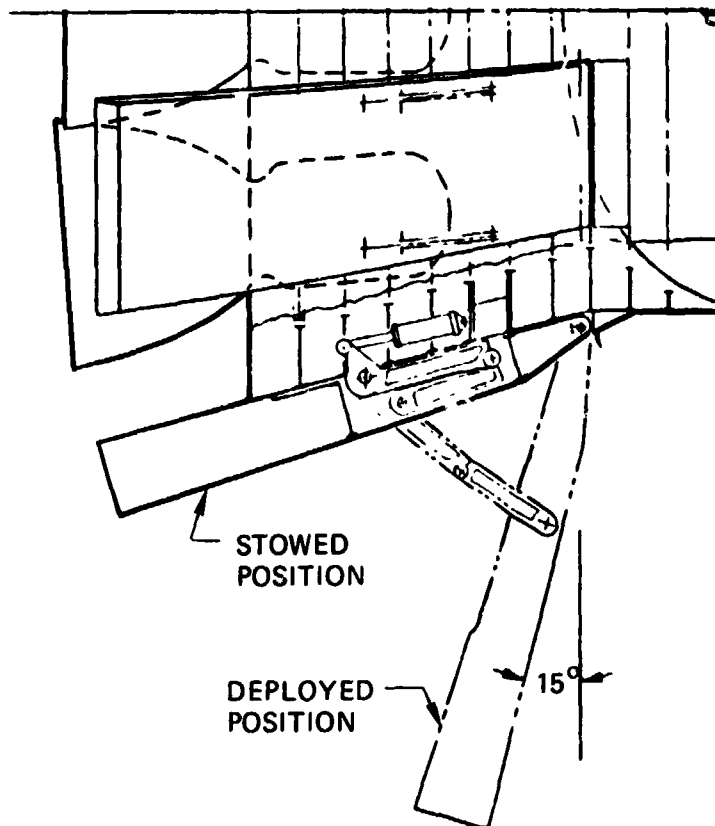


Figure 5-41 Drag Brake Concept

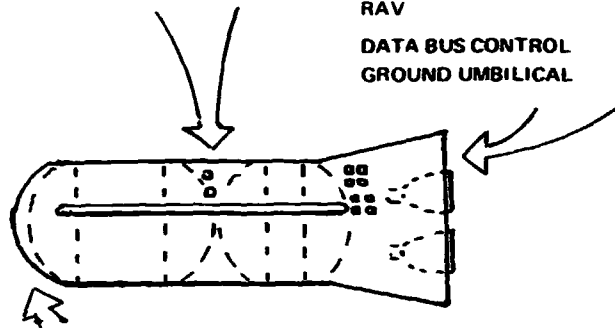
The major loads are: Guidance and Control, Engine Stow and Drag Brakes, Range Safety, Data Acquisition, Telemetry, Flight Recovery, and Retrieval.

5.2.1.8.4 E/E Equipment Installation and Wiring - The E/E equipment and wiring will be located in the booster as shown in Figure 5-42. The pump fed and pressure fed boosters will have similar installations except that radar altimeter equipment is used only on the pump fed. The installed equipment includes packaged avionic and electrical components (black boxes) installed on racks in the pressurized areas, and antenna and transducers installed outside the pressurized area.

5.2.1.9 Operations & Test - Pressure Fed Booster

5.2.1.9.1 Operations - New production boosters are received at KSC and installed in a refurbishment and checkout cell for pre-static firing operations. This effort is directed at installation of static firing instrumentation, range safety equipment, base heat shields, and secondary fire control deluge required after engine shut-down. After the flight readiness firing, the new boosters are refurbished and introduced into the operational flow when they are ready to support erection on the mobile-launcher and integration with an orbiter/drop-tank.

<u>INTERTANK AREA</u>	<u>PROD.</u>	<u>R/D</u>	<u>AFT THRUST STRUCT AREA</u>	<u>PROD.</u>	<u>R/D</u>
TRANSUCERS	50	204	INSTRUMENTATION		
RADAR ALTIMETER	1	1	TRANSUCERS	259	1064
RADAR ANTENNA	2	2	SIGNAL CONDITIONERS	98	406
RANGE SAFETY			DISTRIBUTION BOX	7	7
DIRECTION COUPLER	1	1	BATTERY 13 AH	6	6
HYBRID RING	1	1	BATTERY 100 AH	1	1
RECEIVER	2	2	GNC COMPUTER	1	1
DECODER	2	2	IMU	1	1
CONTROLLER	2	2	RECEIVER ELEX	1	1
TELEMETRY			ACPS ELEX	5	5
RF ASSY	2	4	ENG IGNITION ELEX	4	4
RF POWER DIVIDER	1	1	TVC ELECTRONICS	1	1
RF MULTICOUPLER	1	1	SYS SHUTDOWN ELEC.	1	1
TRACKING ANTENNA	1	1	RETRIEVAL SYS ELEX	1	1
TRANSPONDER	1	1	FIN CONTROL ELEC.	1	1
DECODER	1	1	CBW (21 CHANNEL)	1	2
RAU	1	2	CBW (36 CHANNEL)	0	1
			TAPE RECORDER	1	1
			RAV	2	5
			DATA BUS CONTROL	1	1
			GROUND UMBILICAL	1	1



<u>FWD AREA</u>	<u>PROD.</u>	<u>R/D</u>
TRANSUCERS	24	95
ORBITAL UMBILICAL	1	1
RANGE SAFETY ANT	2	2
TELEMETRY ANTENNA	2	2

Figure 5-42 E/E Equipment Location

During the integration operation the booster/orbiter/launcher mechanical, electrical, and fluid interfaces are verified, the range safety and separation ordnance is installed, and the flight vehicle is moved from the Vertical Assembly Building to the launch pad. At the launch pad, the ground interface is verified and pre-launch operations including propellant loading culminate with launch.

The booster flight control computer commands separation, reentry, and descent sequences during terminal flight. A recovery vessel receives and verified these events with a telemetry station configured to receive and record this data. Upon verification that all safing events were normal, the recovery vessel takes the expended booster in tow to Port Canaveral. The parachute recovery vessel retrieves the downed parachutes and assists



the booster tug with lateral and over-run control through the jetty and during docking. The booster is hoisted out of the water and placed in a ground transporter mounted on a barge. The barge is then towed to the KSC dock.

Upon receipt at the KSC dock, the booster is rolled off of the barge into a safing facility. The booster is washed, range safety equipment is removed, and the propellant and hydrazine containers are drained and purged.

The transporter is then towed to the VAB transfer aisle where the bridge cranes are used to transfer the booster into a refurbish cell. Here the major activity is centered around planned removals/replacement, engine flush and purge, detailed cleaning and inspection and painting.

The booster moves out of the refurbish cell into a checkout cell where all systems are verified and the booster is certified ready to support the next integrated flow.

The overall operations sequence is illustrated in Figure 5-43.

**5.2.1.9.2 Test -** Model testing will be accomplished to determine towing characteristics and water impact loads early in the program. Structural development testing will be accomplished on LOX and RP-1 tanks early in the program to determine structural reaction to bending loads and pressure cycles.

Subsystem development will be accomplished on breadboards for each subsystem. The breadboard will be constructed initially with prototype hardware and will be upgraded to flight configuration when qualified hardware is available. The avionics, electrical distribution and flight control breadboards will be integrated in the system integration lab to verify the subsystem interfaces.

Static structural and dynamic testing will be accomplished on one test article. Static proof tests will be accomplished on two sections, the sections will be assembled for the dynamics testing and then disassembled for the static ultimate tests.

Propulsion static firing will be accomplished on a vehicle which is essentially complete. The tanks and thrust structure may be heavy weight to withstand the full duration firing loads.

Retrieval testing will be accomplished on a boiler plate mass cg simulated booster. Parachute retrieval testing will be accomplished using parachutes from the drop tests.

The test program for the series and parallel burn boosters is the same. Overall test program costs will be less with the parallel burn configuration because the test articles are smaller and will therefore cost less.

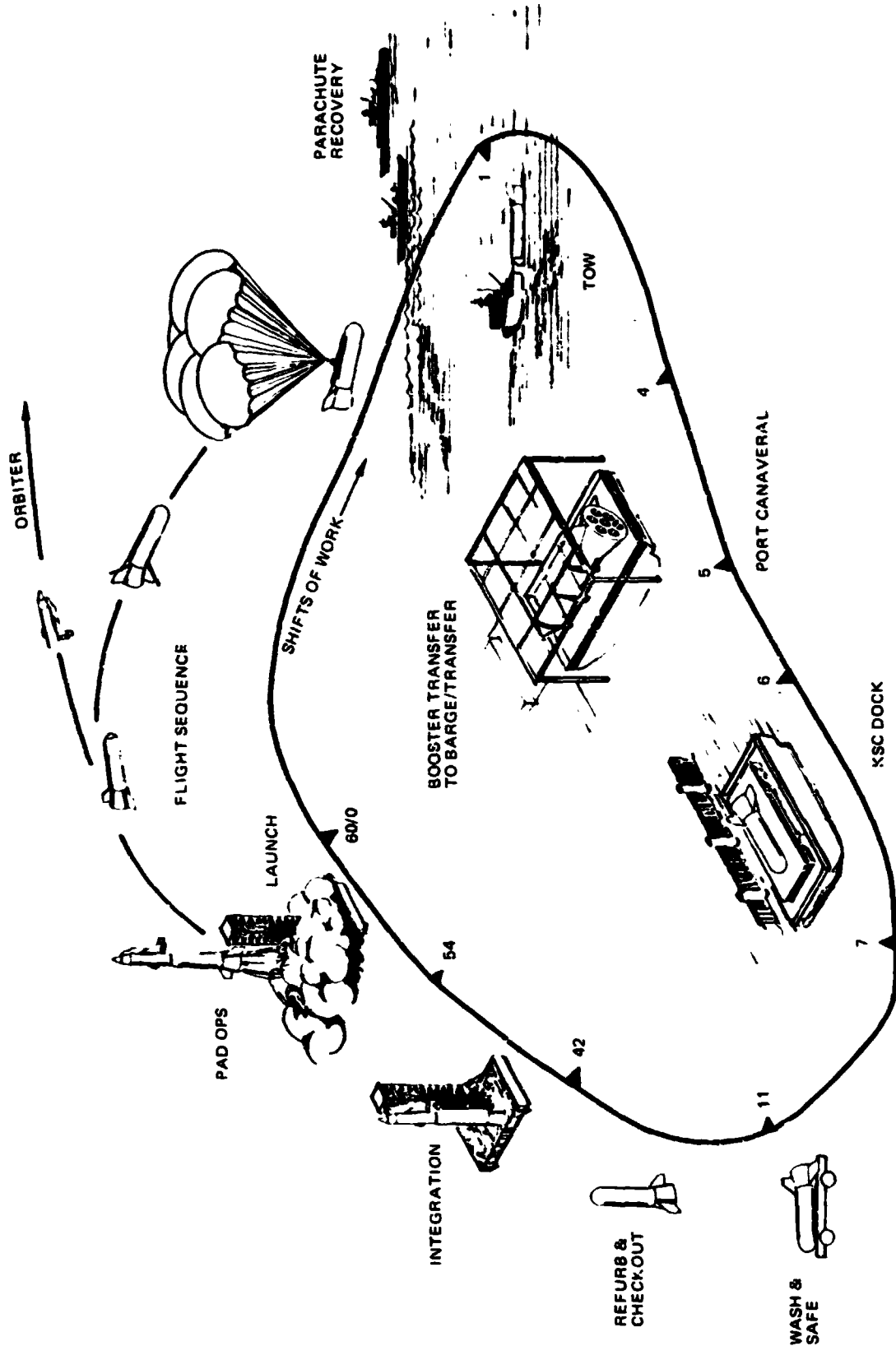


Figure 5-43 Operations and Refurbishment Cycle Complete in 60 Shifts (30 Days)



## Flight Test

The Pressure Fed Booster Flight Test Program consists of one unmanned launch and FMOF to demonstrate ascent performance. Recovery system development will require three launches based on impact damage uncertainties, current parachute technology, potential modification required on early flights, and recovery technique development. The major issue requiring the unmanned flight is POGO. The pressure fed system is particularly susceptible to POGO instabilities due to the extreme interaction and interdependence of the propellant pressurization, tankage, and feed system with the engines and structure.

The test program is summarized in Figure 5-44.

### 5.2.2 Pump Fed Series Burn Booster (Model 979-073A)

#### 5.2.2.1 Configuration

The pump-fed booster is sized for a 40K lb polar orbit payload capacity. The orbiter upper stage is identical to that used in the pressure fed vehicle (979-176B) and was sized to provide a basis for booster comparison. The vehicle separates at a staging velocity of 5300 fps. The general arrangement is shown in Figure 5-45.

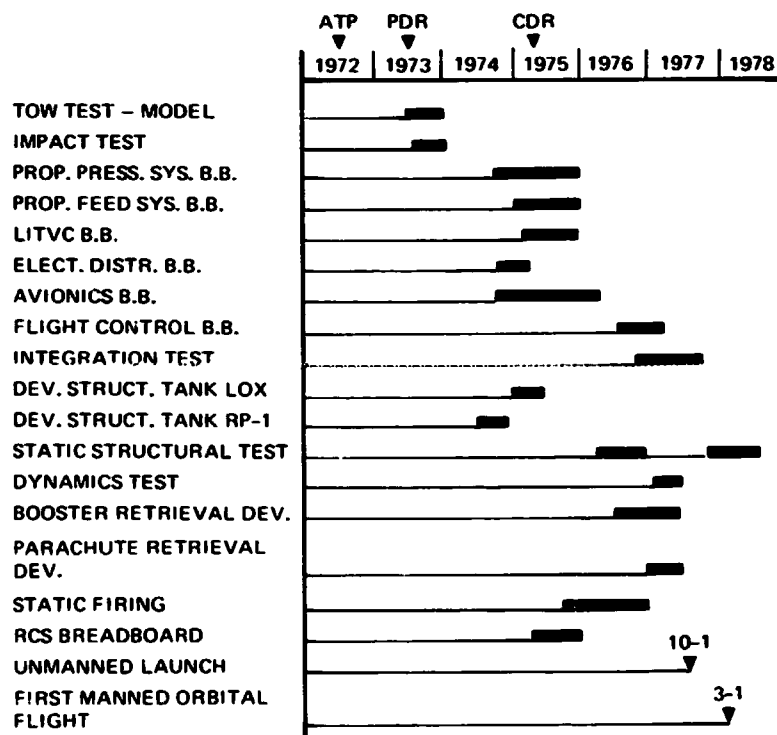
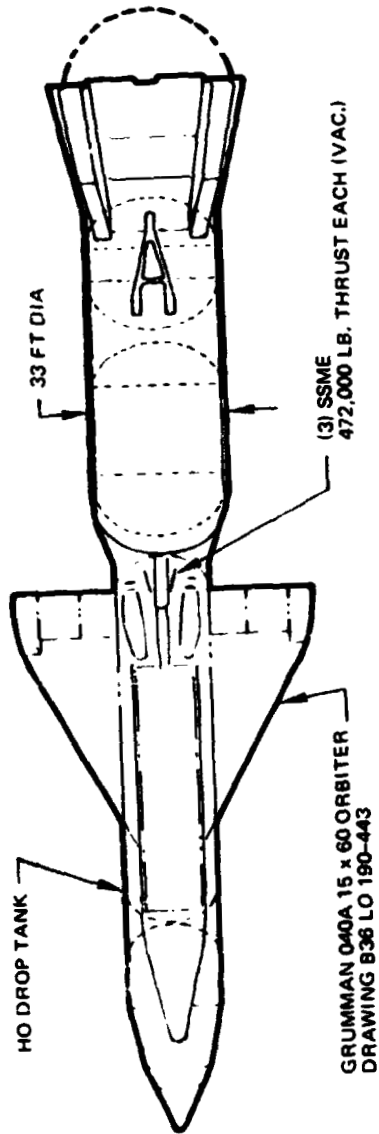


Figure 5-44 Test Program - Pressure Fed BRB



DESIGN CHARACTERISTICS:

- GLOW = 4,870,200 LBS
  - BLOW = 3,625,200 LBS
  - OLOW = 1,245,000 LBS
  - PAYLOAD (POLAR) = 40,000 LBS
  - VSTAGE = 5,300 FPS
  - BOOSTER ENGINES = (4) F-1 @ 1,522K LBS S.L. EA.
  - BOOSTER PROPELLANT = 3,100,000 LBS
  - ORBITER ENGINES (SSME) = 3 - 470K LB VAC.
  - RECOVERY SYSTEM = CHUTES & RETRO-ROCKETS
- T/W 1.25

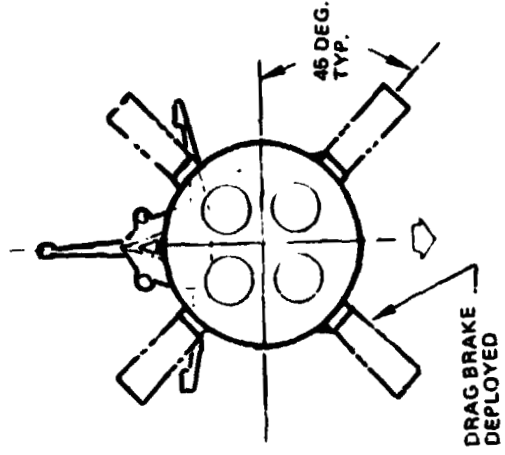
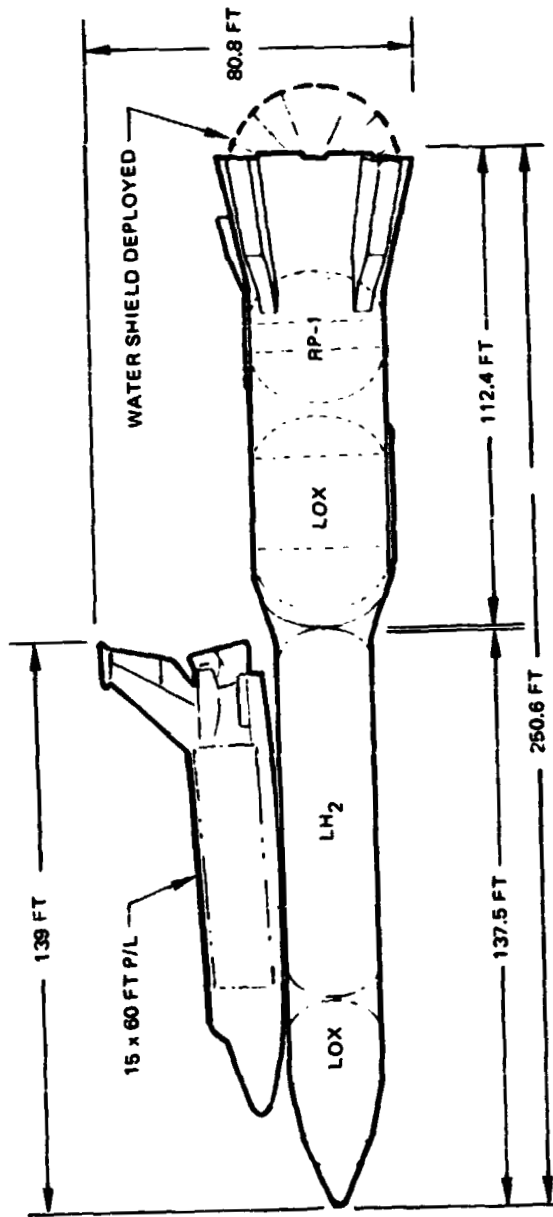


Figure 5-45 Pump Fed LOX/ RP-1 Series Burn BRB - Model 979-073A



Booster ascent propulsion is provided by four gimballed 1.522 million lb thrust (S. L.) F-1 engines. Ascent control is by 5.15-degree TVC augmented by orbiter aerodynamic controls. Primary ascent guidance is provided by the orbiter stage and backed up by redundant capability installed on the booster.

The booster is designed to enter at zero angle of attack with drag brakes deployed for additional drag. The attitude control subsystem is used to preposition the booster prior to entry. Attitude reference is provided by on-board avionics. Recovery is achieved by parachutes and retro rockets. Drogue chutes (2) deploy when the vehicle decelerates to  $M = 0.8$  (380-400 fps). As the vehicle continues to decelerate to 150 psf, 6 reefed main chutes deploy. Following a two-stage disreefing the vehicle reaches a terminal speed of 100 fps. At terminal recovery the impact velocity is reduced to approximately 10 fps by solid retro motors for a horizontal attitude contact with the water.

The weight statement for Booster Model 979-073A is presented in Table 5-7. The booster has an ascent propellant load of 3,100,000 lb, an inert weight of 525,200 lb and a mass fraction of 0.855.

#### 5.2.2.2 Performance - Pump Fed Booster

The pump-fed booster utilizes four standard F-1 rocket engines for the booster propulsion system. The trajectory is lofted to limit maximum dynamic pressure. This technique avoids the need for early shutdown of one engine with its more severe nozzle cooling problems. With the lofted trajectory, the first engine shutdown is at 112 sec after launch to prevent the longitudinal acceleration from exceeding 3 g's. The remaining three engines are shutdown at staging, 30 sec later. The mission profile for the booster given by Figure 5-46 shows maximum dynamic pressure occurring at an altitude of 39,000 ft, one engine shutdown at 110,000 ft, and staging at 200,000 ft. The booster coasts upward to an apogee of nearly 400,000 ft. Reentry follows with water landing about 200 n mi down range.

The booster is designed to deploy drag devices in a low dynamic pressure region to dissipate the system energy to the point where parachute recovery is possible.

The pump-fed booster configuration has the inherent capability to accommodate heavier orbiter landed weights because the F-1 engine can be uprated in thrust. Figure 5-47 shows a typical relationship between orbiter landed weight and the required F-1 thrust level. Also shown are the staging velocity and booster propellant loading.

Table 5-7 Weight Statement – Model 979-073A

<b>Airframe</b>		<b>262,200</b>
Interstage	4,800	
Oxidizer Tank	31,900	
Fuel Tank	23,200	
Intertank	23,800	
Aft Body	99,200	
Raceways And Fairings	7,250	
Drag Petals – Incl. Act.	28,800	
Base Heat Protection	10,800	
Separation System	150	
Range Safety System	300	
Forward Body	32,000	
<b>Propulsion</b>		<b>101,000</b>
Main Engine & Install.	75,000	
Oxidizer System	15,800	
Fuel System	10,200	
<b>Avionics And Power</b>		<b>5,200</b>
<b>Recovery</b>		<b>65,200</b>
Parachute System	24,000	
Attitude Control System	800	
Water Impact & Flotation	9,300	
Retrieval Provisions	1,100	
Retro Rockets – Incl. Prop.	30,000	
<b>Environmental Control</b>		<b>400</b>
<b>Control Actuation</b>		<b>4,100</b>
Thrust Vector Control	4,100	
<b>Growth</b>		<b>28,000</b>
Airframe	21,500	
Propulsion	1,000	
Avionics And Power	250	
Recovery	5,000	
Environmental Control	50	
Control Actuation	200	
<b>Dry Weight</b>		<b>466,100</b>
<b>Propellant And Gases – ACS System</b>		<b>1,900</b>
Usable Prop.	1,700	
Reserve Prop.	80	
Residual Prop. And Gases	120	
<b>Residuals – Rocket System</b>		<b>52,900</b>
Trapped Ascent Propellant	41,130	
Pressurants	5,750	
Bias Propellant	3,850	
Other	2,170	
<b>Thrust Decay</b>		<b>4,300</b>
<b>Inert Weight</b>		<b>525,200</b>
<b>Propellant</b>		<b>3,100,000</b>
<b>BLOW</b>		<b>3,625,200</b>
<b>Booster λ'</b>		<b>0.866</b>





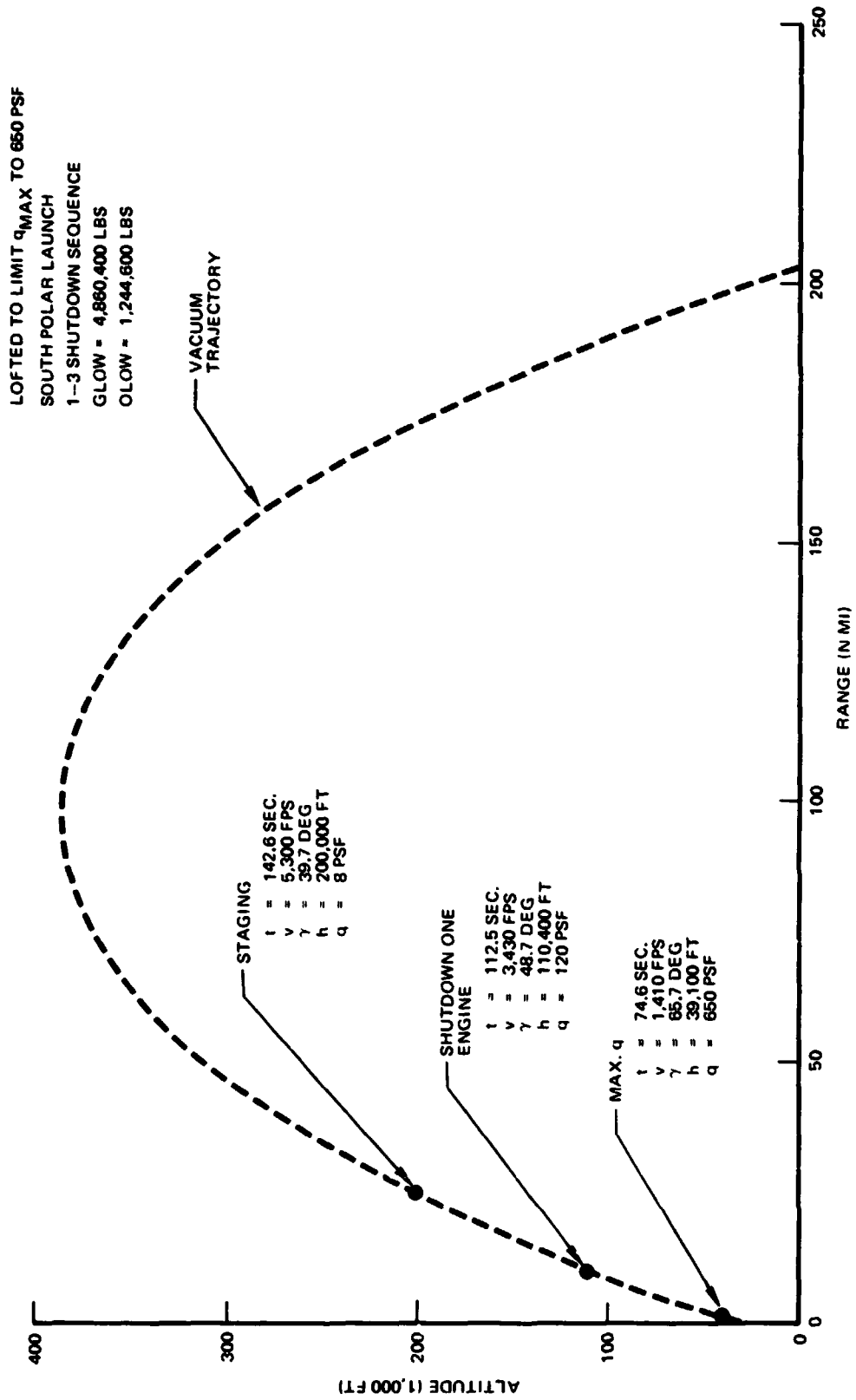


Figure 5-46 Pump-Fed Booster Trajectory - Model 979-0668

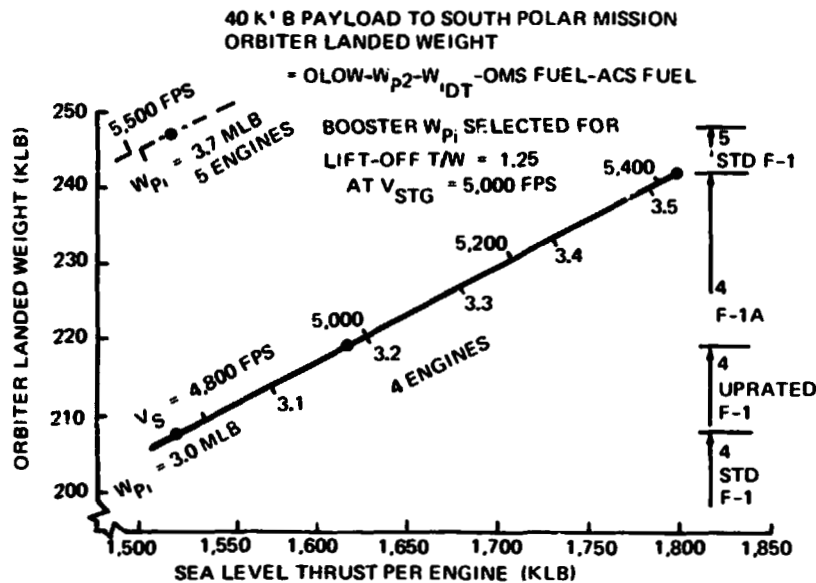


Figure 5-47 F-1 Pump Fed Booster Permits Heavier Orbiters

This booster data is based upon point designs for each of the F-1 engine combinations with the booster propellant weight selected so that the lift-off thrust-to-weight ratio is 1.25 at a staging velocity of 5000 fps. The lift-off T/W will be more than 1.25 for staging velocities above 5000 fps, and less than 1.25 for staging velocities below 5000 fps.

### 5.2.2.3 Structures - Pump Fed

In order to drive the development cost of the structure to a minimum, the design utilizes Saturn materials, technology, and tooling as much as practical. This approach provides not only the lowest technical risk but also a firm base for accurate cost estimation.

The primary structural arrangement shown in Figure 5-48 consists of an oxidizer tank, a forward entry dome, a fuel tank, a thrust structure, an intertank, four drag brakes, a base heat shield and two raceways.

Structural loads, design conditions and structural deflections under water impact loading were determined to provide design requirements. An envelope of bending moments for flight and water impact is shown in Figure 5-49. The bending moments on the booster when under tow in Sea State 6 are compared to the envelope of flight and water impact bending moments.

Water impact pressures were determined as a function of impact condition from a series of over 140 tests. The pressure, shown in Figure 5-50, includes the effect of Sea State 5 (12-ft waves) and velocity dispersions caused by one retrocket out or one streamed



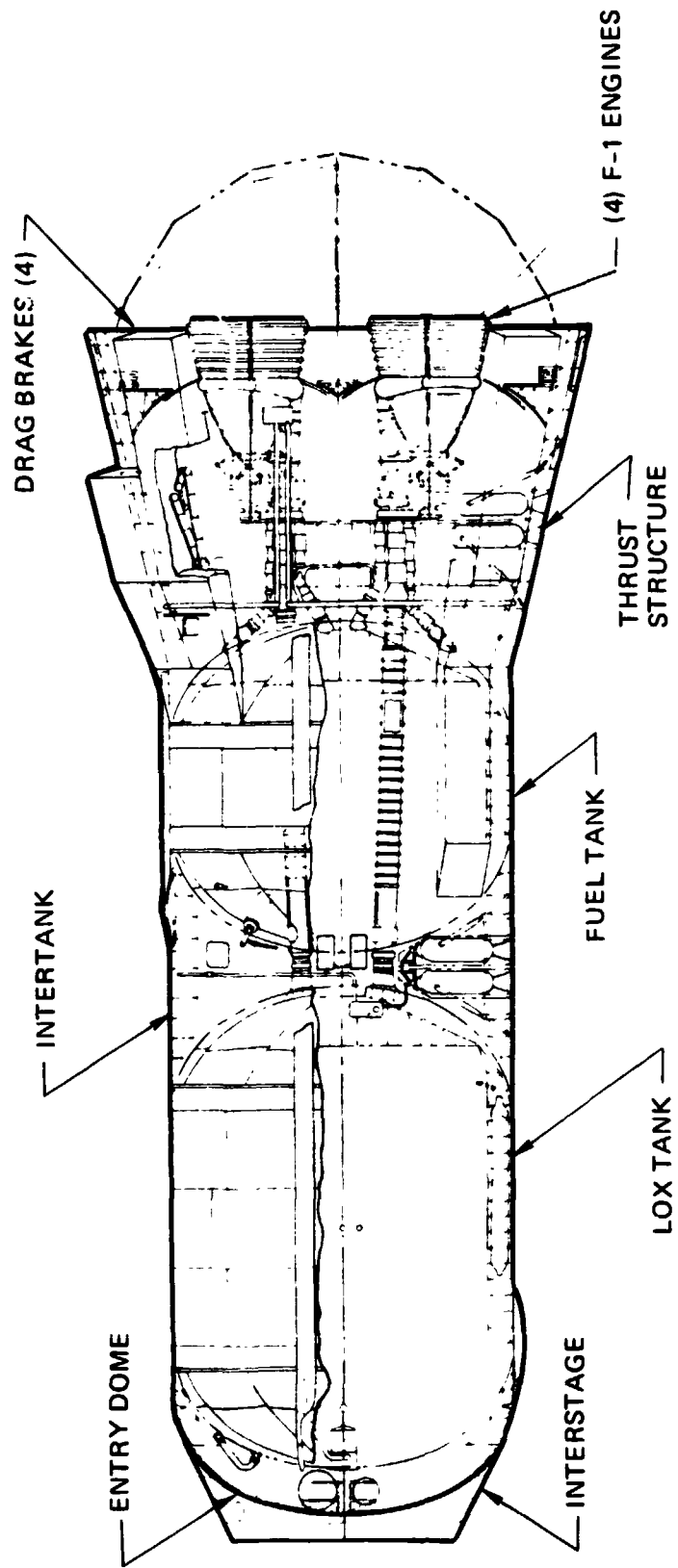


Figure 5-48 Pump Fed Recoverable Booster General Arrangement

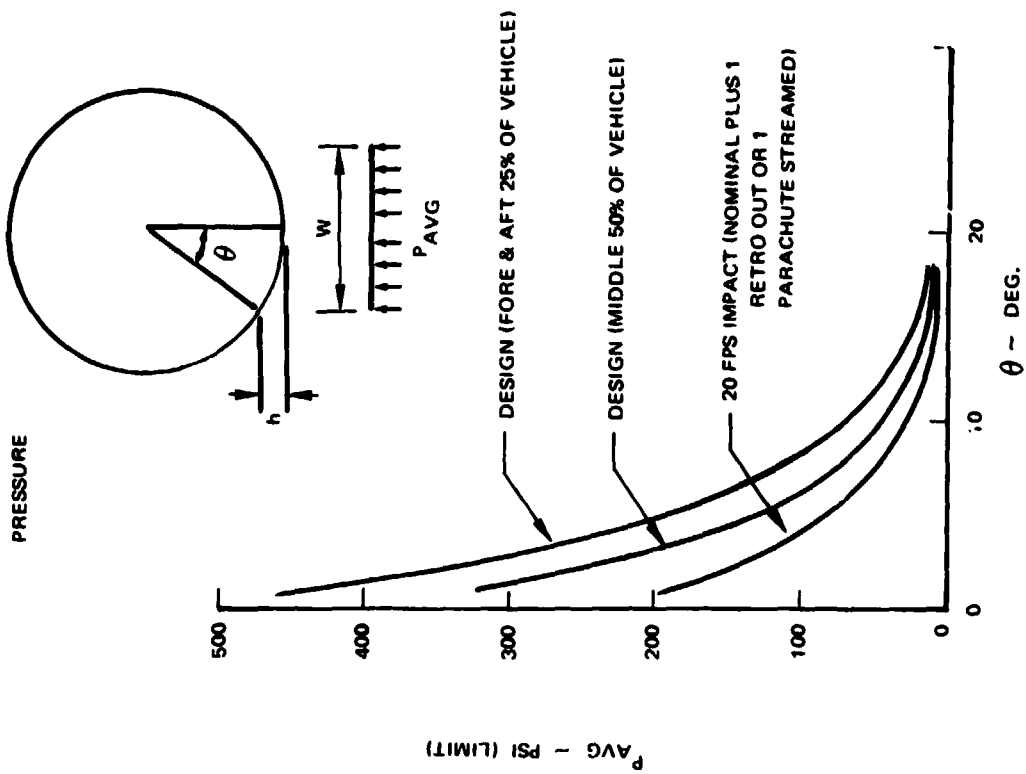


Figure 5-50 Water Impact Loads Pump Fed BRB 979-066, -073

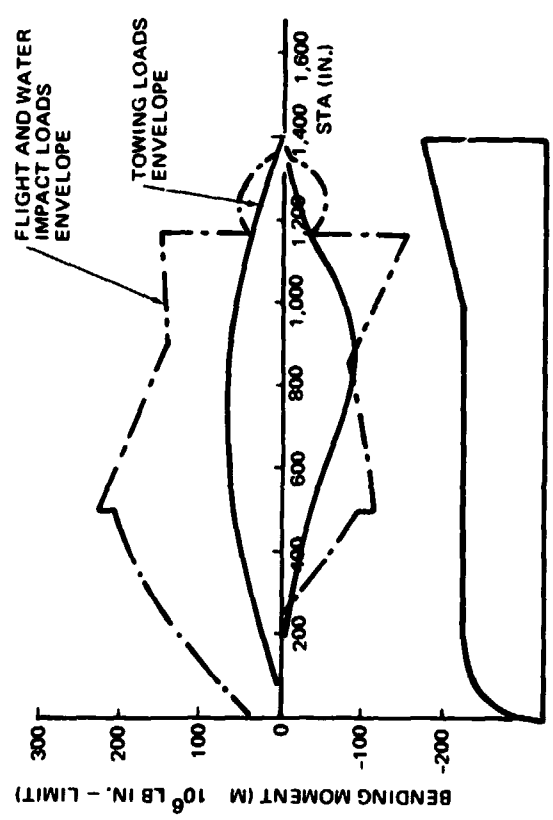


Figure 5-49 Bending Moments Pump Fed, Series BurnBooster Model 979-066, -073



parachute. The primary effect of sea state is to increase the local velocity at which the side of the booster impacts the water. In the middle 50% of the booster the increased velocity is caused by the vertical velocity of the wave (5 fps). On the fore and aft ends of the vehicle, the increased velocity occurs when one end hits on the top of a wave and the other end is slammed into the wave trough.

The lateral acceleration at the tail as measured in drop tests of the pump fed configuration is shown in Figure 5-51. The data show the effect of velocity and attitude on the tail acceleration. The design point without effects of sea state was horizontal entry with a velocity of 20 fps. The dispersion due to sea state was +5 fps vertical wave velocity and +8° average inclination of a maximum height wave. This then leads to the design lateral g level including sea state effects.

Major heating environments are plume heating in the base region and plume induced flow separation (PIFS) heating on the skirt and tanks during ascent; and aerodynamic heating during reentry. The nose and drag brakes are the only components which require significant

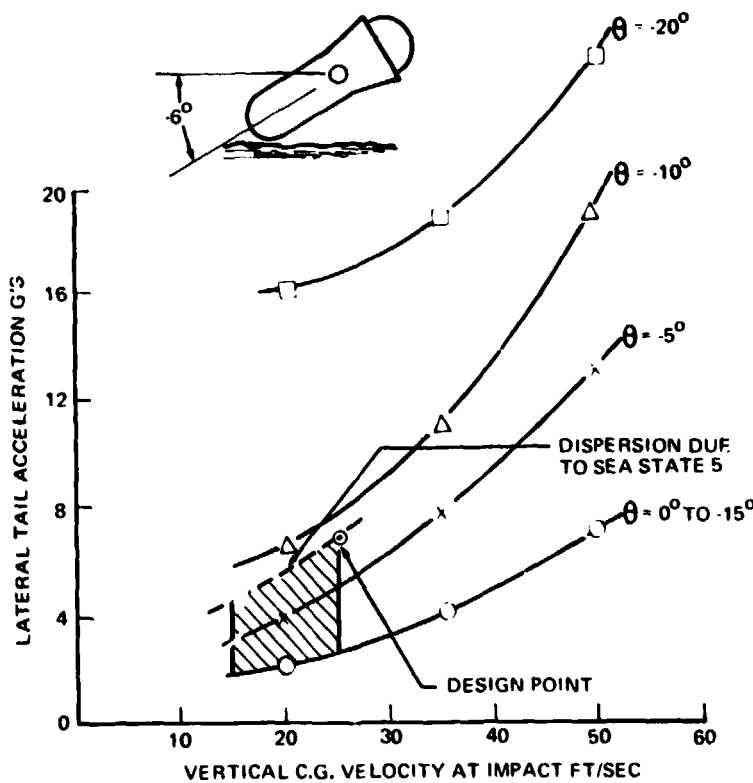


Figure 5-51 Water Impact Lateral Acceleration Pump Fed BRB 979-066, -073 (Drift Velocity - 50 Ft/Sec)

increases above the structural requirements. Thermal protection for the base heat shield requires from .20 to .34 in of silicone, depending on distance from the exit plane, to limit the aluminum structure to the allowable temperature.

Material selection considerations are summarized in Table 5-8.

*Table 5-8 Pump Fed Booster 979-073 Materials, Heat Sink Requirements, Design Conditions*

COMPONENT	MATERIAL	T <sub>MAX</sub>	H.T. SINK THICK	STRUCT. THICK.	DESIGN CONDITION
NOSE	2219-T87 Al.	350	0.45	.10 → .25	ENTRY/WATER IMPACT
LOX TANK	2219-T87 Al.	350	0.06	.16 → .20	INT. PRESSURE
INTERTANK	2219-T87 Al.	350	0.06	.15 → .20	BOOST & REENTRY HT'G
RP TANK	2219-T87 Al.	350	0.07	.16 → .18	INTERNAL PRESSURE
SKIRT FWD	2219-T87 Al.	350	0.20	.10 → .20	WATER IMPACT/BOOST & REENTRY HEATING
SKIRT AFT	6-2-4-2 Ti.	900	0.11	.10 → .32	GROUND WIND
DRAG BRAKE	6-2-4-2 Ti.	800	0.14	.05	REENTRY HEATING

The oxidizer tank is cylindrical, 33 ft in diameter with a 45° elliptical dome at each end. The cylinder is stiffened with integrally machined longitudinal T-shaped stringers and stabilized by ring frames that serve as slosh suppression baffles. Intermediate chordal frame sections are installed between each major frame over 54° of arc to provide structural capability. A comparison of this type construction and that of the S-1C is shown in Figure 5-52. A cruciform vortex baffle consisting of four stiffened webs intersecting 90° apart is suspended from the lowermost slosh baffle. All baffles are built-up from 2024 sheet and extruded sections while the primary pressure shell is all welded from 2219 aluminum segments.

The fuel tank is also cylindrical, 33 ft in diameter with 45° elliptical domes at either end but has four ring stiffened tunnels that span its length to provide passage for the LOX delivery lines. Each tunnel has a stainless steel bellows at its upper end to allow the tank expansion. Like the LOX tank, the fuel tank has vortex and slosh suppression baffles with intermediate chordal frame segments for water impact. The materials and type of construction are also the same.

Both tanks are proof tested to uniaxial yield with LN<sub>2</sub> to assure no catastrophic failure will occur over the life of the booster.



Except for their length, sizing, the baffle material, the intermediate frame segments and the number of tunnels, the tanks are essentially the same as the S-1C tanks and will utilize the same tooling.

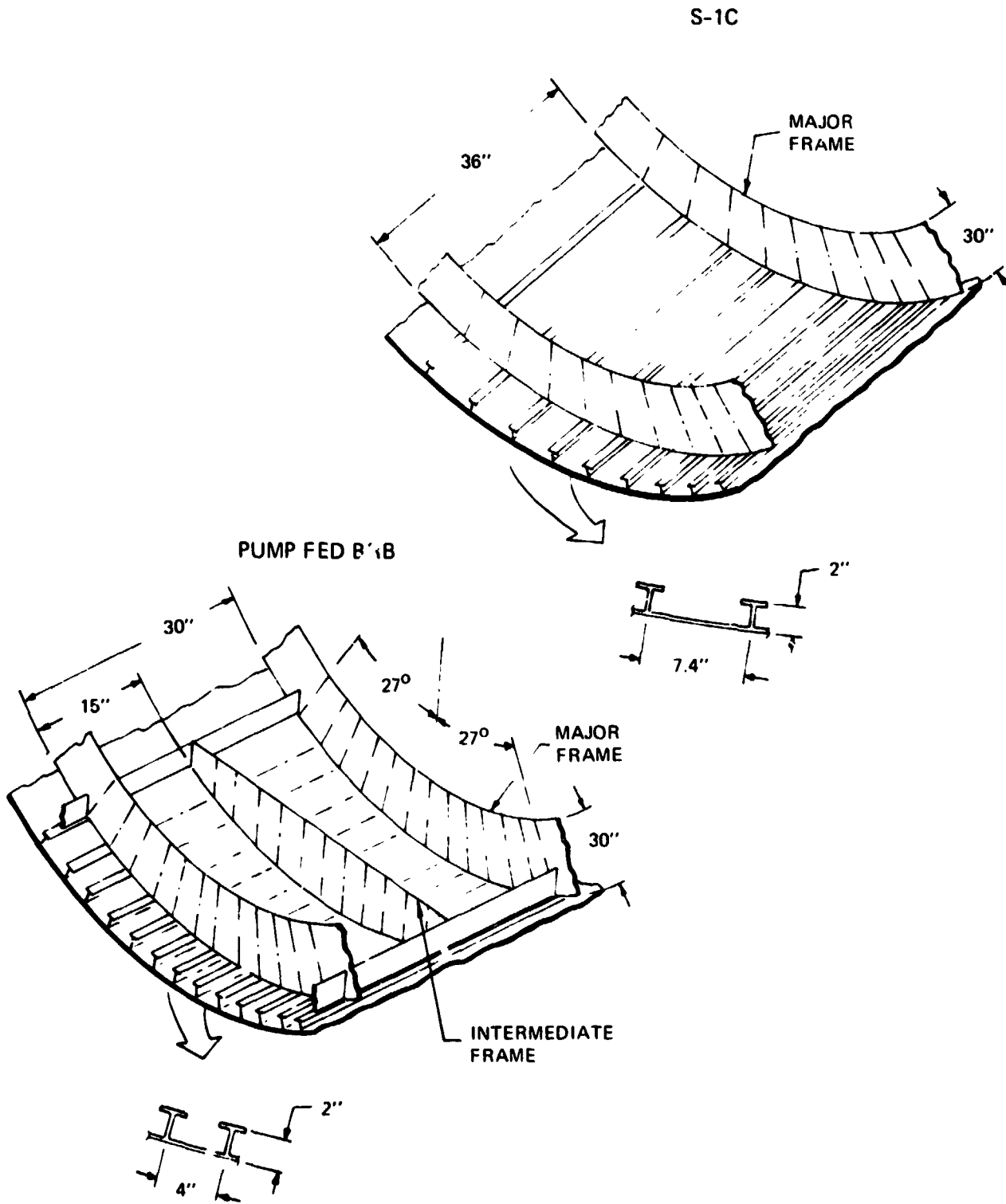


Figure 5-52 Pump 1BRB

The intertank is a semimonocoque, ring stiffened structure 33 feet in diameter, sealed to prevent entry of sea water during impact and towback. The cylinder is all welded from 2219 aluminum segments with integrally machined longitudinal T-stiffeners similar to the construction used in the propellant tanks. The ends are mechanically fastened to the adjacent tanks using a silicone sealant to achieve a watertight joint. The frames are built-up from 2024 aluminum sections.

The thrust structure consists of a conical outer ring stiffened shell and four 70 inch deep beams that support the four F-1 engines. The structure also provides support for the heat shield, the aft parachute attach, the retro rockets, and the drag brakes in addition to providing for vehicle support and holddown. The structure is sealed forward of the heat shield to prevent sea water entry during impact and towback. This seal is a back-up since a cover is deployed over the entire exit plane of the vehicle.

The outer shell is an integrally stiffened skin of 2024 aluminum that minimizes faying surfaces requiring sealing. The main beams and ring frames are built-up from 7075 aluminum sheet and extruded sections. All thrust and holddown posts are machined from 2024 aluminum die forgings.

The base heat shield is a sealed bulkhead located at the turbine exhaust manifold of the engines. It is designed to withstand the plume heating of the engines and all pressure loads associated with boost and entry. Integrally machined 2024 aluminum panels with an ablative coating of silicone are mounted to a network of beams supported from the main engine beams. A spherical heat shield segment mounted to the engine seals the base as the engine gimbals.

Four drag brakes are hinged at their forward edge and are free to pivot radially outboard. Each panel is actuated by folding linkages driven by hydraulic actuators. The design utilizes a spar/rib construction with upper and lower stiffened skins. All components are fabricated from 2024 aluminum sheet and extrusions. A silicone ablator is applied to the entire outer surface to protect the aluminum from heating (aerodynamic and plume effects) and to seal from sea water entry.

The forward entry dome is an all welded 2219 aluminum, 45° elliptical dome designed with enough heat sink capability to absorb the heat load during reentry. It is mechanically attached to a short skirt on the forward end of the LOX tank and sealed to prevent sea water entry.





A conical, ring stiffened, semi-monocoque aluminum interstage is connected to the forward entry dome. The joint is severed with a linear shaped charge around its circumference. This separation concept is similar to those used on Saturn V.

#### 5.2.2.4 Propulsion Subsystems - Pump Fed Booster

The pump-fed ballistic recoverable booster (Model 979-073A) uses existing main propulsion subsystem concepts and components. The fuel pressurization system is typical in the respect that all components of the system are used in the S-1C. The primary differences are in manifold configurations and line lengths dictated by fewer engines and smaller tanks than the S-1C. All valves, gimbals, bellows, helium tanks, etc. are already developed. The primary change required to this hardware will be requalification for reusability; however, there are two new requirements for propulsion subsystems; a reaction control subsystem, and letdown rockets. The latter are described as part of the Deceleration and Recovery system. The Reaction Control Subsystem provides 3-axis rotational accelerations during post-separation stabilization, preentry orientation and booster orientation prior to splash-down for proper positioning with respect to drift and wave direction. Six 1500-lb thrusters with a total system delivered impulse of 330,500 lb/sec. control the  $\pm$  pitch, yaw accelerations to  $0.36/\text{sec}^2$  and roll to  $0.28^\circ/\text{sec}^2$  under vacuum conditions,  $0.20^\circ/\text{sec}^2$  and  $0.20^\circ/\text{sec}^2$  respectively at sea level. The propellant is hydrazine ( $\text{N}_2\text{H}_4$ ) and 1810 lb is required. The propellant is pressurized from a 7.8 ft<sup>3</sup> helium tank containing 15.3 lb of helium at 3200 psia.

The baseline engine selected for the 979-073A pump-fed ballistic recoverable booster is a low cost version of the F-1 engine incorporating a 6 + 6 turbopump, 30-in. turbopump with a Hasteloy manifold, a 6,000-sec life thrust chamber, diagnostic instrumentation and certain configuration and material changes for salt water compatibility. The booster incorporates four of these engines and has a 1-1-2 engine shutdown sequence with a maximum burn duration of approximately 160 sec. Ocean impact occurs approximately 5 min after booster cutoff at a maximum velocity of 20 fps. Model water impact tests have resulted in engine installation design studies for impact loads up to 8 g's. The vehicle incorporates a base skirt to protect the engines from sea water impact and a base region closure to protect the engine from sea water immersion. The engines interface at the throat with a reusable base heat shield that protects the upper part of the engine from base region recirculation and radiation environments during boost. This heat shield serves as a secondary barrier to sea water intrusion.

Thrust vector control is accomplished by use of the actuation and fluid power system used on S-1C and the same 5'9" square gimbal pattern is used.

The engine is equipped with a heat exchanger which delivers heated helium for fuel tank pressurization and GOX for LOX pressurization through systems identical to those designed and used successfully on the S-1C.

Figure 5-53 highlights the key propulsion system development tests which would be conducted early in the first two years of the booster development program. The relatively minor nature of these tests reflect the already advanced state of propulsion system development.

- FEED LINES AND SUPPORT STRUCTURE DYNAMICS
- VEHICLE BASE HEATING
- PROPULSION SUBSYSTEM SEA-WATER COMPATIBILITY
- LET-DOWN ROCKET THRUST TIME TRACE
- RCS THRUSTER REUSABILITY

*Figure 5-53 Development Testing Pump Fed BRS - Model 979-073A Propulsion System Test Requirements*

#### 5.2.2.5 Aerodynamic Ascent and Descent, Pump-Fed Booster

##### Ascent Characteristics

As the pump-fed booster has gimballed engines, thrust vectoring capability is sufficient to allow a booster configuration without fins for ascent. As a consequence the ascent configuration is quite unstable through most of the Mach number range. Around the max-q condition the longitudinal AC is approximately 300 in ahead of the CG and the directional AC about 450 inches ahead of the cg (Figure 5-54).

Similarly due to the lack of booster fins and ascent configuration is quite roll stable (Figure 5-55).

##### Entry Characteristics

Due to its low density and aft CG location entry at  $\alpha = 0^\circ$  is a natural choice.

Drag petals for the 979-073A configuration were sized to achieve a ballistic coefficient ( $W/C_D A$ ) less than  $400 \text{ Lb/ft}^2$  at speeds below Mach 1. This value of  $W/C_D A$  represents a design limit for satisfactory deployment of the parachutes. The drag petal design cycle has not been iterated to incorporate revised weights, therefore, the designs have not been optimized. The ballistic coefficient is well below  $400 \text{ Lb/ft}^2$  at subsonic speeds to produce a margin for variation in staging and atmospheric conditions, and weight growth (Figure 5-56).



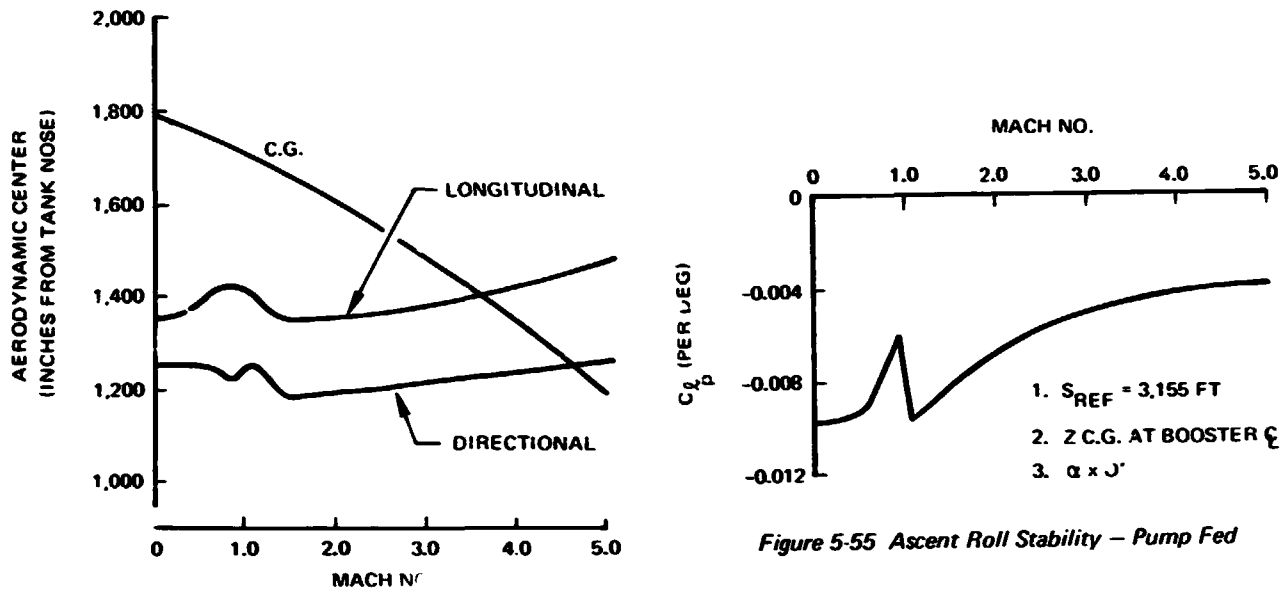


Figure 5-54 Ascent Stability – Pump Fed

The drag petals on the 979-073A configuration are located with their forward ends attached to the body at the forward end of the body flare. The zero-lift drag buildup is shown in Figure 5-57. Recent wind tunnel test data indicate that this reentry configuration is only slightly stable at speeds down to about  $M = 3.5$  (Figure 5-58). At lower speeds the booster becomes increasingly unstable. Results from the same tests show that hinging the petals at their aft end and moving the hinge point to the aft end of the flare provides a design that has positive stability during reentry down to  $M = 0.9$ . The effect on weight of the aft petal location is not known, but the test results shows a 15 percent increase in drag. This could

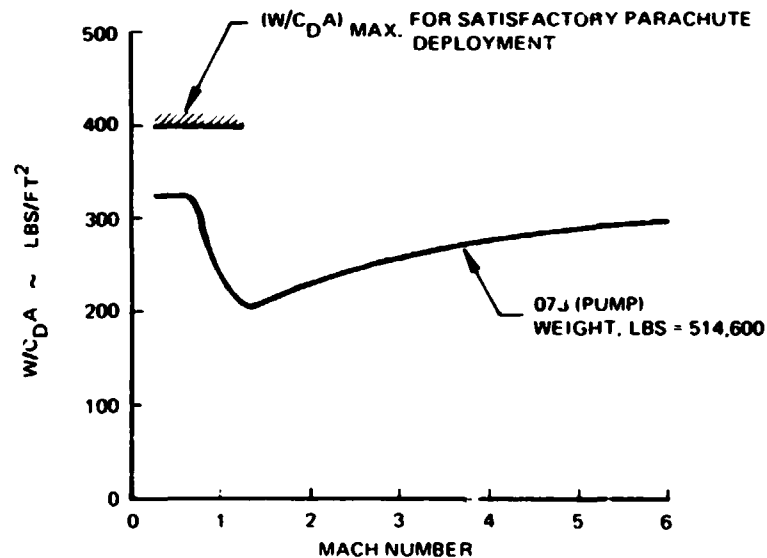


Figure 5-56 Reentry Ballistic Coefficients

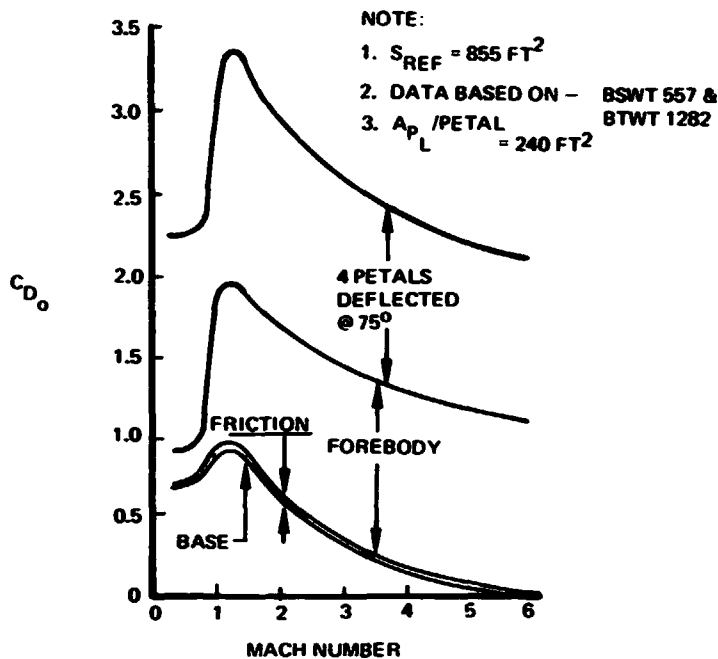


Figure 5-57 Zero Lift Drag – Pump Fed

result in smaller petals and a reduction in weight. Test results also indicate that increasing the number of panels has a favorable impact on stability even at constant total area.

#### 5.2.2.6 Flight Dynamics

##### Ascent

The maximum thrust vector deflection results from a cross wind with a gust at 10 kilometers. The maximum thrust deflection due to winds was 3.8 degrees. To this value an allowance must be added for slosh and bending and engine out. With one engine out and the design wind, the deflection requirement was 5.0 degrees. When in this case the yaw engines were canted outboard five degrees to minimize the transient due to engine out. Thus the thrust deflection requirement does not exceed the 5.15 degree gimbal capability of the F-1 engine. Orbiter aero surfaces were used for additional roll control torque during ascent. Figure 5-59 shows the thrust vector deflection requirements for control during ascent.

##### Attitude Control.

A reaction control system is required for pitch, roll and yaw axis of the booster to arrest staging rates and provide pitch and yaw stability. This minimum energy system,



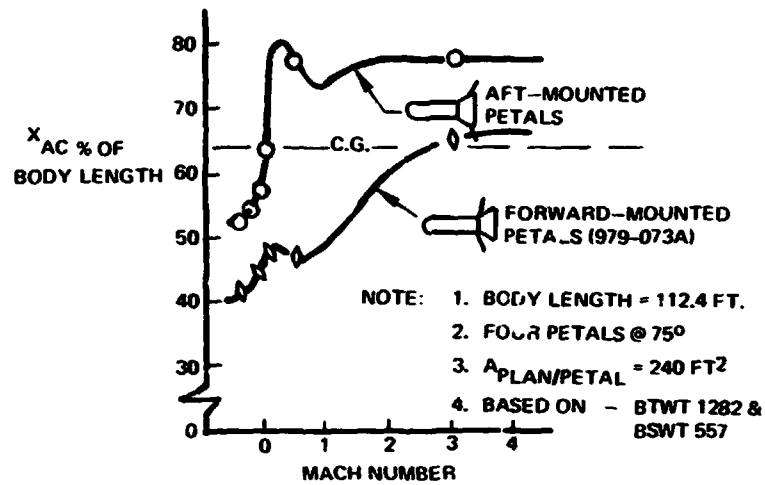


Figure 5-58 Static Stability – Pump Fed

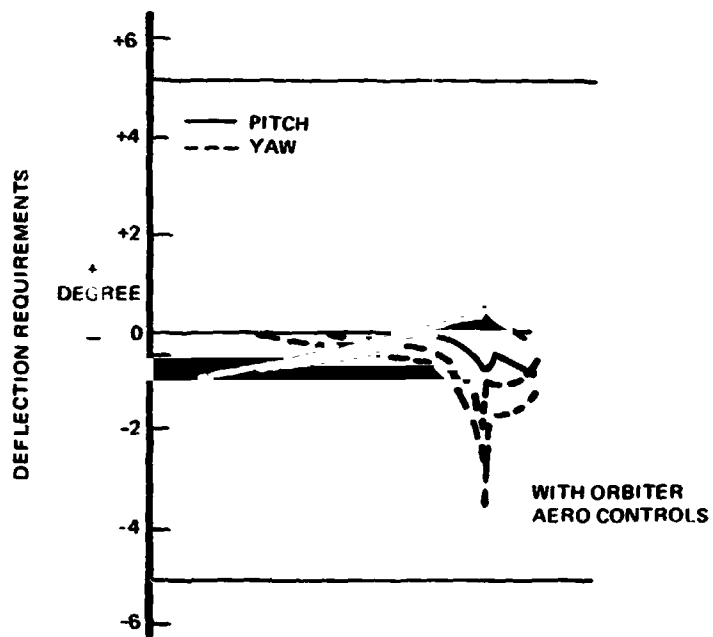


Figure 5-59 Pump Fed Ascent & Recovery Characteristics

while allowing very high angular excursions about trim, is sufficient to prevent tumbling or excessive roll rates prior to parachute deployment. The two fin configuration does have a stable bank angle; however, roll reaction controls are required to reduce the strong roll-yaw coupling. Analyses resulted in pitch attitude time histories between separation and parachute deployment which were similar to those shown for the pressure-fed vehicle.

#### 5.2.2.7 Other Subsystems - Pump Fed Booster

These subsystems for the pump fed booster are basically the same as for the pressure fed booster.

#### 5.2.2.8 Deceleration and Recovery Subsystem - Pump Fed Booster

##### Rationale for Selection

The trades and rationale for selecting the baseline recovery system for the pump fed booster is similar to the pressure fed with one exception. The lightweight pump fed booster structure is sensitive to impact velocity and therefore an ocean impact as benign as possible was required. Solid motor/parachute dispersion studies showed that an impact velocity of 10 fps (nominal), 20 fps (maximum) and 0 fps (minimum) was possible. To achieve the required impact conditions for the pump fed booster a hybrid solid motor/parachute system was selected for reasons as explained in the pressure fed recovery section.

Six 128 foot diameter parachutes and 12 solid motors (14,400 lb total propellant weight) were selected based on technical risk, cost and weight. This system from a technology standpoint is well within the current state-of-the-art.

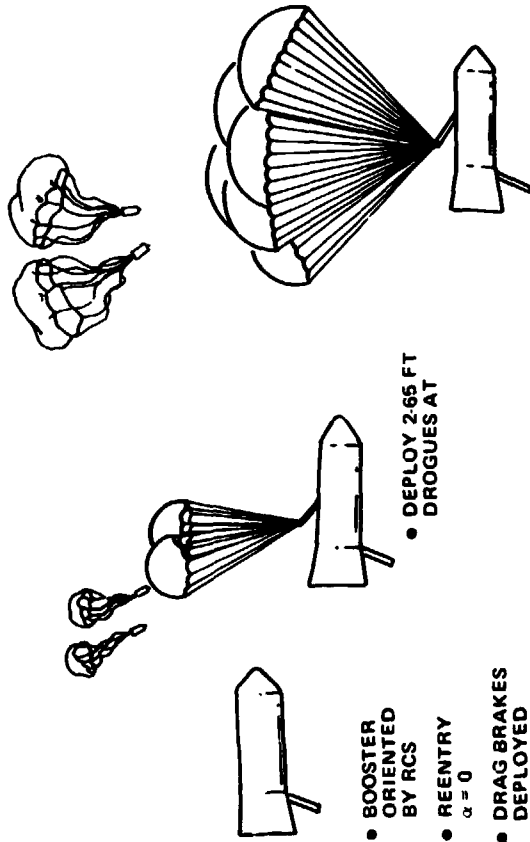
##### Recovery Sequence (Pump Fed)

The recovery sequence for the -073 pump fed booster is shown in Figure 5-60. After orbiter/booster separation the booster is oriented at a 0 degree angle of attack reentry angle by the attitude control system. Four drag brakes with a total area of 960 ft<sup>2</sup> are deployed to develop additional drag for deceleration to give the booster balance during the reentry phase. The maximum q attained during the reentry phase is 2095 psf.

At a Mach number of .89 and 27,400 ft altitude, two 9 ft. diameter pilot parachutes are mortar deployed. Four seconds later at a Mach number of .8 and 24,800 ft altitude two 65 foot diameter drogue parachutes are deployed. The drogue parachutes use a single stage of reefing. 10.4 seconds later at a Mach number of .444 and 18,200 ft altitude, six 128 foot diameter main parachutes are deployed. The main parachutes use two stages of reefing. The maximum g loads felt by the main parachutes is 2.9 g's.



**ORIENTATION  
REENTRY  
DECELERATION**



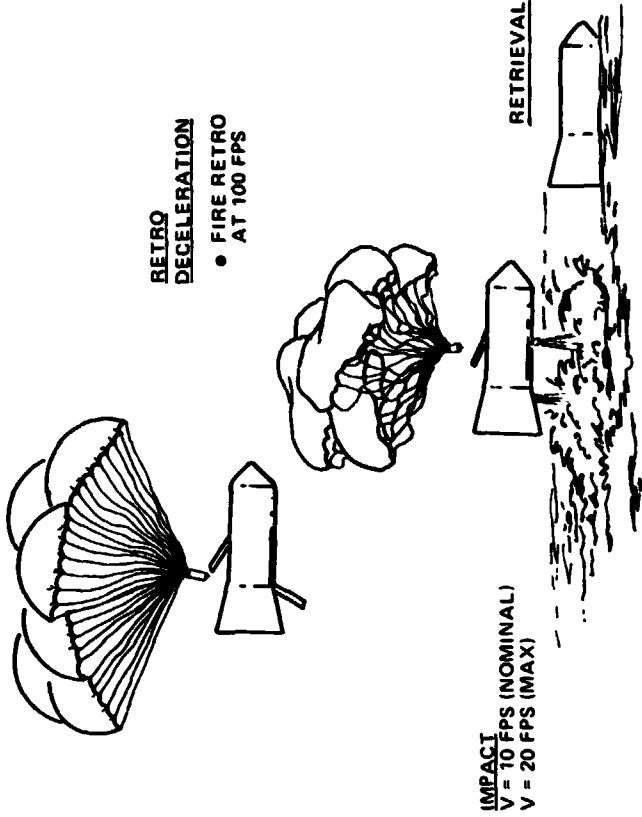
- BOOSTER ORIENTED BY RCS
- REENTRY  $\alpha = 0$
- DRAG BRAKES DEPLOYED

- DEPLOY 2-65 FT DROGUES AT

- DEPLOY 6 - 128 FT MAINS AT
- 2 STAGES OF KEEPING
- DETACH LOWER FIN
- NOSE DOWNWIND ORIENTED BY RCS

**RETRO  
DECELERATION**

- FIRE RETRO AT 100 FPS



**IMPACT**  
V = 10 FPS (NOMINAL)  
V = 20 FPS (MAX)

**RETRIEVAL**

Figure 5-60 Recovery Sequence -- Pump Fed Booster

Prior to water impact the vehicle enters the water in a horizontal position with a nominal impact velocity of 10 fps and a maximum impact velocity of 20 fps.

### Recovery System Description (Pump Fed)

#### Parachute System

The selected parachute system consists of two 9 foot diameter ( $D_0$ ) pilot parachutes, two 65-foot diameter ( $D_0$ ) drogue parachutes and six 128-foot diameter ( $D_0$ ) main parachutes.

The complete parachute system is installed in an enclosed area external to the thrust structure between the two upper drag brakes. This area will be covered by a thermally insulated fairing, on which aft facing compartment cover panels will be pyrotechnically ejected prior to initiation of the parachute subsystem. The physical support of the parachute packs within this area is such that the aft acting acceleration forces will be reacted against the compartment cover panels, which are later ejected to allow parachute deployment. The parachute deployment bags will be insulated to protect the parachutes against the thermal environment existing at time of cover ejection.

Because the vehicle C. G. is in the fuel tank, the main parachutes are attached to a tripod to avoid introducing the parachute loads directly into its sidewall. The forward two members are attached to a frame in the intertank and a frame in the thrust structure. The forward members form a rigid A-Frame. The third member is a cable, released from its storage position in the thrust structure under resistance, to control the vehicle rotation during chute deployment. After main chute release, the A-Frame falls to rest on the upper surface of the vehicle. A snubber on each leg of the A-Frame restrains its downward motion until it comes to rest on an energy absorption fitting located on the thrust structure. The A-Frame is locked down at this point to prevent movement during towback.

Analysis shows that failure of one rocket to fire will result in a maximum pitch change of  $9-1/2^\circ$  and an impact velocity of 24 feet per second maximum.

Rocket thrust loads are taken out through the forward skirt, through a bolted-on fitting and into the vehicle main structure. The nozzle end of the rocket is stabilized by links connecting the pin fittings on the rocket flange to vehicle structure.

#### Retro Rocket System

The let-down rocket installation slows the parachute suspended booster prior to water impact from approximately 100 fps at an altitude of 80 feet to a velocity of 0 to 20 fps at water impact. The rocket motors are identical and incorporate a shaped thrust time profile





to provide a maximum of 2 g upward force at ignition and a thrust tailoff at the end of their 4+ second burn time for controlled impact velocity. Total propellant weight is 14,400 lb.

Six of the retrorockets are located in the intertank area at Station 626 and four rockets are located in the thrust structure compartment at Station 105.

The number and location of the rockets is selected so that:

- Each group produces equal moment about the booster CG
- Individual rockets produce no roll moment about the longitudinal axis
- Maximum deceleration is 2 g upward.

#### Retrieval and Protection System

This system must furnish stabilization, flotation, protection from the elements as well as furnish the necessary equipment for locating the booster, minimizing wind drift, ship lights and provide a means for attaching a tow line. Most of this equipment is essentially the same as the pressure fed and the description won't be repeated here except for the engine protection system.

Protection for the F-1 engines is provided by a sealed hemispherical shape cover over the aft end of the booster (See Figure 5-61). This cover is deployed prior to splash-down. The cover is stowed and sealed to a semicircular container. The lower half of the cover is permanently sealed to the container and offers protection against the submerged salt water. The upper half which has an inflated seal is exposed only to abnormal wave action.

The cover is constructed of a double wall airmat that when deployed produces a hemispherical shape over the aft end of the booster. This cover requires approximately 4 psig to inflate and weighs approximately 2000 pounds.

The detailed description, sequencing, etc., of the parachute system is essentially the same for the pump fed as it was for the pressure fed system except for the sizing, and therefore will not be repeated in this section.

#### 5.2.2.9 Operations and Test

5.2.2.9.1 Operations - The operational sequence for the pump fed recoverable booster is basically the same as for the pressure fed recoverable booster.

5.2.2.9.2 Test -

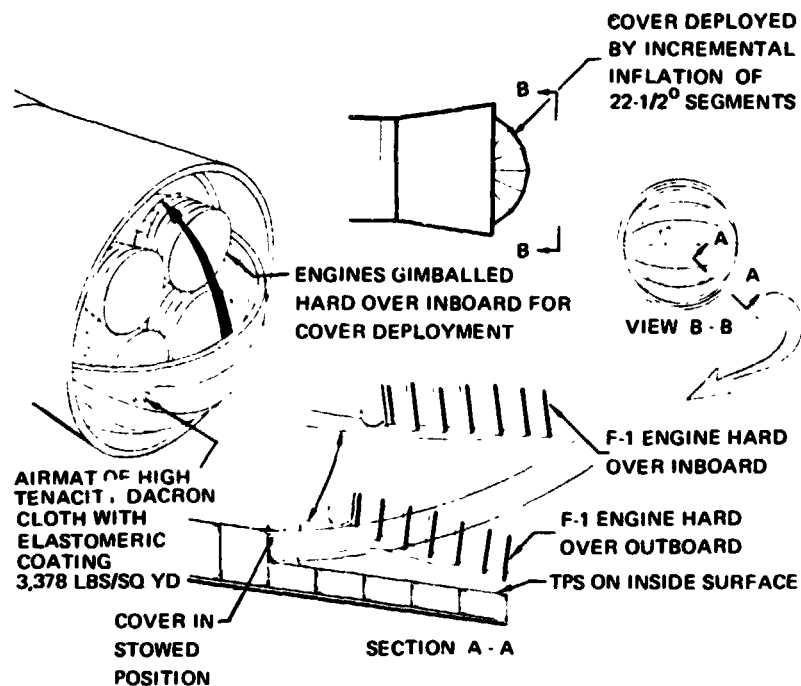


Figure 5-61 Engine Protection Model 979-066

**Test Program Pump Fed BRB**

Model testing will be accomplished to determine towing characteristics and water impact loads. Subsystem testing will be accomplished on avionics, electrical distribution and flight control breadboards. The breadboards will be integrated in the systems integration lab to verify the subsystem interfaces and verify total system operation under simulated flight conditions.

Structural testing will be accomplished on one test article. The static proof tests will be accomplished on two sections, LOX tank and interstage and RP-1 tank and thrust structure. The vehicle will be assembled for the dynamics test and disassembled for the static ultimate tests.

Retrieval tests will be accomplished on a boiler plate mass C. G. simulated booster. Parachute retrieval tests will be accomplished using parachutes from the air drop tests.

**Flight Test**

The Pump Fed Booster Flight Test Program consists of two launches to demonstrate ascent performance. Recovery system development will require three launches based on impact damage uncertainties, current parachute technology, potential modifications required on early flights, and recovery technique development.



An unmanned launch is not recommended for the Pump-Fed Booster because all booster systems have either been qualified and flown as part of the SIC/F-1 system, are not critical to manned flight, or will have sufficient ground tests prior to the first shuttle flight to provide the necessary assurance of crew safety and mission success.

The test program is summarized in Figure 5-62.

### 5.2.3 Parallel Burn Pressure-Fed BRB (Model 979-171 LOX/RP-1)

The Parallel Burn Launch system combines two LOX/RP-1 pressure-fed BRB's mounted in parallel with a LOX-LH<sub>2</sub> expendable drop tank/delta winged orbiter (Figure 5-63).

The Booster body is an integrated structure using the oxidizer and fuel tanks connected with a cylindrical intertank shell. LOX tanks are forward to minimize the LITVC requirements during boost. The configuration features a nose shaped for minimizing the effects of water impact entry loads on booster inert weight. The nose also contains the liquid nitrogen pressurization supply tank, interstage structure and stage separation structure. The aft section attached behind the RP-1 tank includes the main engines, the engine thrust structure and engine water protection skirt. Each Booster uses four identical pressure-fed rocket engines each with a sea level thrust rating of 790,000 lb. Ascent guidance is provided from the orbiter and the booster provides ascent control by means of a liquid injection TVC system. Attached to the skirt are four deployable drag brakes sized to dissipate entry velocity. An attitude control is employed to position the booster for a ballistic entry following its burnout and separation. Avionics installed on the booster provide redundant boost guidance and automatic subsystem checkout. During entry, the avionics subsystem provides altitude stabilizing command signals to the altitude control system and event singles such as for parachute deployment.

Trajectory characteristics include staging at 5500 fps at 154,000 ft altitude. Staging dynamic pressure is approximately 45 psf. Reentry characteristics features a zero degree angle-of-attack trajectory with a peak dynamic pressure of approximately 1600 psf at 55,000 ft altitude. Supplemental drag brakes are deployed to reduce the ballistic coefficient and after reaching  $M = 0.80$  and 24,500 ft altitude two 51-ft diameter drogue parachutes and six 98-ft diameter main parachute are deployed slowing the booster down until impacting the water 30° off vertical at 100 fps.

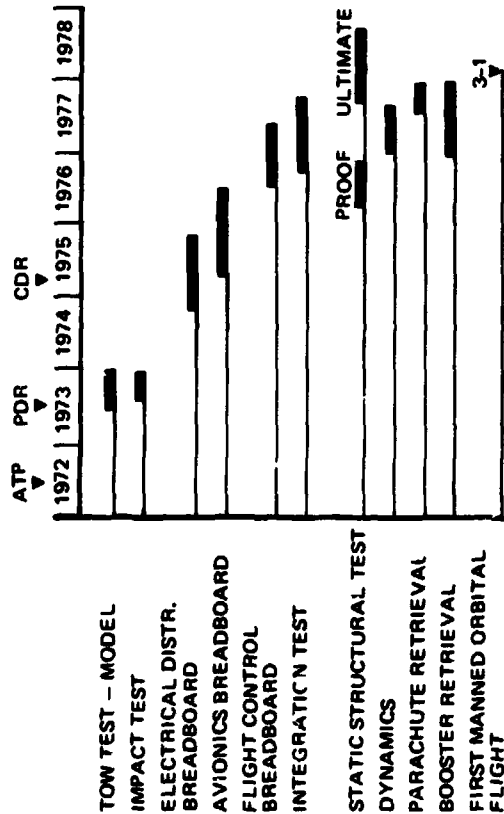


Figure 5-62 Test Program - Pump Fed BRB

**DESIGN CHARACTERISTICS**

PAYLOAD	40,000 LBS POLAR
GLOW	5,934,000 LBS
BLOW	2,102,000 LBS EACH
PROPELLANT	1,701,000 LBS EACH
OLOW	1,728,000 LBS
PROPELLANT	1,432,000 LBS
ORBITER INJ WT	208,400 LBS
V STAGE	5,521 fps
THRUST/WT (LIFTOFF)	1.25

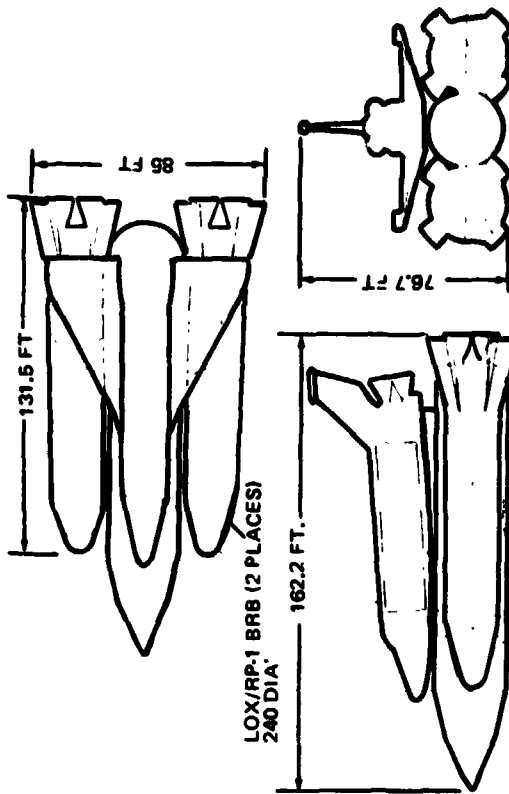


Figure 5-63 General Arrangement - LOX/RP-1 Parallel Burn Pressure Fed BRB - Model 979-171A



#### 5.2.4 Series Burn vs. Parallel Burn Pressure-Fed Boosters

The series burn booster liftoff weight is 18 percent higher than the parallel burn booster liftoff weight. The series burn booster DDT & E costs are 9 percent greater than the parallel burn booster costs. These advantages for the parallel burn system are compensated for by the 4 percent lower per flight cost of the series burn booster and the 24 percent lower weight and cost of the series burn HO drop tank. The comparison is illustrated in Figure 5-64.


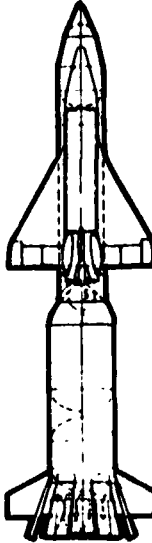
	<u>PARALLEL BURN</u>	<u>SERIES BURN</u>
		
● STAGING VELOCITY	5,500 FPS	5,000 FPS
● BOOSTER WT		
BLOW	4,276,200	5,032,900
INERT	773,400 (BOTH)	881,800
● BOOSTER COST (\$ IN MILLIONS)		
DDT&E	1,158	1,259
PER FLIGHT	2.6	2.5
● HO TANK		
INERT WT	85,300 LBS	64,900 LBS

Figure 5-64 Series Burn vs Parallel Burn Liquid Boosters

Due to the small trade differences between parallel and series burn, orbiter considerations should determine the selection.

#### 5.2.5 Pressure-Fed vs. Pump-Fed Liquid Boosters

The key issues in the pressure-fed/pump-fed comparison, identified in Figure 5-65, are engine/vehicle integration, thrust vector control, recovery and water impact, tank

fabrication, and booster cost. The pressure-fed requires a new engine development with unknowns that affect booster pressurization system design (an integral part of the main propulsion system), and result in late identification of potential POGO instabilities and a system highly dependent on engine performance. Thrust vector control system comparison of LITVC on pressure-fed and gimballed engines on the pump-fed favors gimballed engines due to the LITVC development, marginal capability and limited growth potential (inefficiency at higher deflection requirements). Both boosters represent a different water impact mode resulting from the inherent booster characteristics. The pressure-fed lower efficiency booster utilizes a direct nose-first impact from parachutes due to the ruggedness built into the high pressure tankage whereas the more efficient pump-fed booster favors incorporation of parachutes and retro motors to achieve impact velocities within the relative structural capability of the system. A disadvantage of the pressure-fed high pressure tankage is the resulting fabrication problems of thick walled shells as compared to the conventional S-1C type construction on the pump-fed.

ENGINE TYPE IS THE FORCING ISSUE BEHIND:	<u>PRESSURE FED</u>	<u>PUMP FED</u>
• ENGINE/VEHICLE INTEGRATION	NEW ENGINE DEPENDENT DEVELOPMENT	✓ EXISTING ENGINE INDEPENDENT DEVELOPMENT
• THRUST VECTOR CONTROL	NEW DEVELOPMENT LIMITED GROWTH	✓ GIMBALLED ENGINE
• RECOVERY & WATER IMPACT	✓ LOW $I_s$ AND LOW $\lambda$ REQUIRE HIGH PROPELLANT LOADS	✓ HIGH $I_s$ AND HIGH $\lambda$ RESULT IN SMALLER SIZE
• TANK FABRICATION	HIGH PRESSURES REQUIRED THICK WALLS	✓ NORMAL TANK WALL SIZES
• BOOSTER COST (\$ IN MILLIONS)		
RDT&E	\$1,259	✓ \$786
COST/FLT	\$2.5	✓ \$2.0

Figure 5-65 Pressure Fed vs Pump Fed Issue

Booster cost heavily favors the pump-fed because of the lower development cost and more efficient system. The pump-fed, in summary, is the most advantageous system since it has derivatives of developed hardware for the ascent portion of flight and both it and the pressure-fed have similar recovery considerations. Therefore, the pump-fed was selected to enter into the liquid versus solid comparisons.



### 5.3 SUMMARY AND CONCLUSIONS

Leading to the final comparison of liquid versus solid and selection of a preferred shuttle booster system, a summary of weights and costs of the alternative booster is presented.

#### 5.3.1 Weight Comparison

Candidate booster data presented previously included the estimated Booster liftoff Weights (BLOW's) and booster mass fractions. Figure 5-66 illustrates the booster inert weights by comparative bar charts. The figure shows the four primary study candidate boosters with the large P/L bay (15x60) and trending data on two solid motor boosters with the small P/L bay (14x45). The inert weights have been broken into the following categories: structure, recovery, propulsion, other, growth and residuals.

From the data may be noted the following:

- 1) The pressure-fed configuration, at 881,800 lb inert weight, is 68% heavier than the pump-fed configuration inert weight.
- 2) Structure comprises an interestingly similar percent of the total inert weight of these two liquid boosters (same is true of the solids). The total tank weight of the pressure-fed configuration, 86% of which is pressure critical, is shown to be approximately 57% of the structure group. This compares to only 22% for the pump-fed configuration. In pounds, the "other" structure groups are essentially the same. The additional nose structure on the pressure-fed tends to directly offset the lighter drag brakes, absence of fins and less water impact penalty on the pump-fed.
- 3) The lower water entry velocity of the pump-fed is seen to double the percentage of weight distributed to the recovery system.
- 4) All of the solid propellant vehicles are lighter in hardware weight and have better mass fractions than the liquids. Lack of recovery provisions on the solids contribute to this.
- 5) Utilization of the 156-in diameter SRM's rather than the 120-in diameter motors results in less inert weight and better mass fractions for both size orbiters considered.
- 6) Weight growth allowances are included in all vehicle weight estimates.

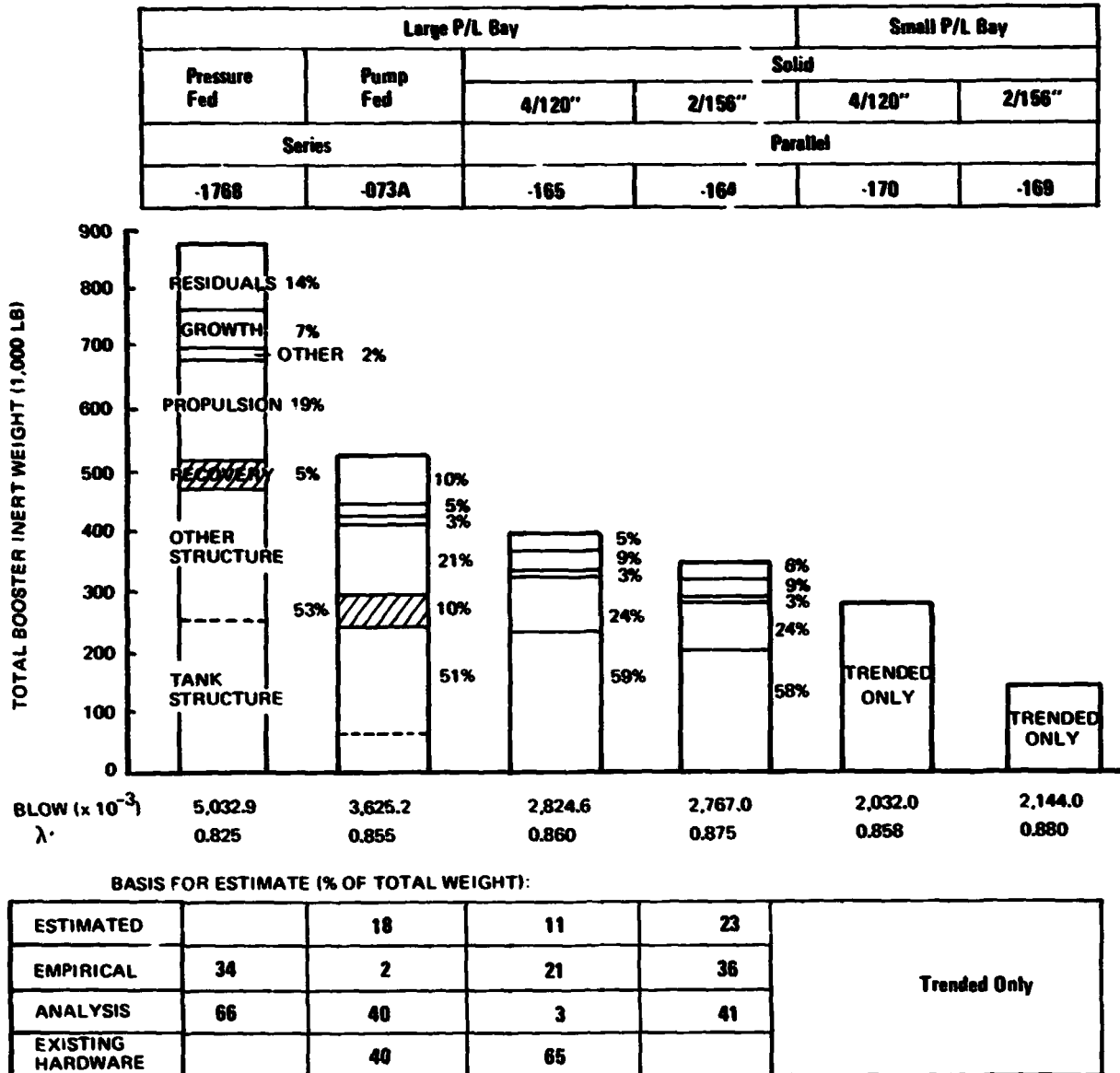


Figure 5-66 Booster Weight Comparison

Summarized at the bottom of Figure 5-66, as a relative indication of confidence levels, are the bases for the weight estimates for each of the six vehicles of prime NASA interest. Weight estimates for the four "Large Payload Bay" vehicles studied in detail all reflect high percentages of analysis or use of existing hardware weight. The two other boosters, though only trended in total inert weight estimates, have been delta from their counterparts.





### 5.3.2 Cost Comparison

Figure 5-67 illustrates the cost breakdown for all the booster configurations with the large P/L bay (15x60) orbiter that were studied. Costs have also been developed for the small P/L bay (14x45) orbiter, but are not shown in this section. These costs are presented in the cost and schedule volume of the final report. Figure 5-67 represents the total DDT&E, Production and Operations cost for each of the study booster configurations. The total number of booster stages in the program is 12 for the recoverable booster, and 445 for the expendable boosters. Flight test articles are considered recoverable where applicable; refurbished, and returned to the operational fleet.

DDT&E costs vary from a low of \$326M (Parallel-Burn, 120-in. SRMs) to a high of \$1211M for the series pressure-fed BRB with the pump fed at \$744M. The lower development cost of the SRM stage is anticipated as a result of the minimum development cost of the motor (\$50M - \$90M) and the booster element being expendable. The solid rocket motors have program production costs ranging from four to eight times greater than the recoverable liquids resulting in a cost/flight range of \$8.2M - \$13.4M versus \$1.7M - \$2.4M, respectively. Figure 5-68 illustrates the number of flight; crossover occurs at approximately 65 flights between the lowest cost SRM (2-156-in. parallel burn) and the lowest cost liquid (pump-fed series burn). The change in slope of the various solid motor configurations results from the greater number of SRM units required to make a stage, with the steepest slope occurring with the configuration of the most motors.

The key booster issues are summarized in Figure 5-69 highlighting the comparison of the solid and liquid boosters. The low development cost favors the solid rocket motor with the pump-fed and pressure-fed liquids having a distinct advantage in cost/flight as summarized earlier.

Primary considerations in the development risks include the propulsion, recovery, system flexibility and orbiter interface complexity. Both the SRMs and pump-fed boosters utilize developed propulsion systems whereas the pressure-fed is a totally new development. Recovery, not applicable to the SRM's, favors the pump-fed due to the lower recovered inert weight resulting from a more efficient ascent booster. The pump-fed also is the most flexible system due to the propulsion system efficiency and as a result can more easily accept potential system weight growth. Series mounting offers a less complex orbiter interfere due to the distributed loads introduced into the HO propellant tank and simpler booster separation as compared to parallel mounting. Environmental considerations favor the liquid LOX/RP boosters over the solids since the exhaust product effects are not as potentially hazardous as those from the SRM's.

445 FLIGHT PROGRAM	12 RECOVERABLE 445 EXPENDABLE	979-162 SERIES 156"	979-163 SERIES 120"	979-164 PARALLEL 156"	979-166 PARALLEL 120"	979-177 SERIES 156"	979-176 B SERIES PRESSURE FED	979-171 PARALLEL PRESSURE FED	979-073 A SERIES PUMP FED						
										DDT&E	PRODUCTION	OPERATIONS	SHUTTLE MGMT	TOTAL PROGRAM	COST/FLIGHT
		384	372	354	<u>326</u>	384	1,211	1,114	744	3,563	5,521	488	255	6,636	13.4
		<u>379</u>	488	<u>379</u>	468	431	1,036	1,110	776	3,379	4,888	468	255	6,636	13.4
		172	255	161	184	196	120	118	90	4,478	5,098	3,126	3,073	2,361	1.7
		8.8	10.1	8.2	9.5	10.1	2.2	2.4	1.7	8.8	10.1	2.2	2.4	1.7	1.7

Figure 5-67 Shuttle Booster Cost Comparison (Dollars in Millions)



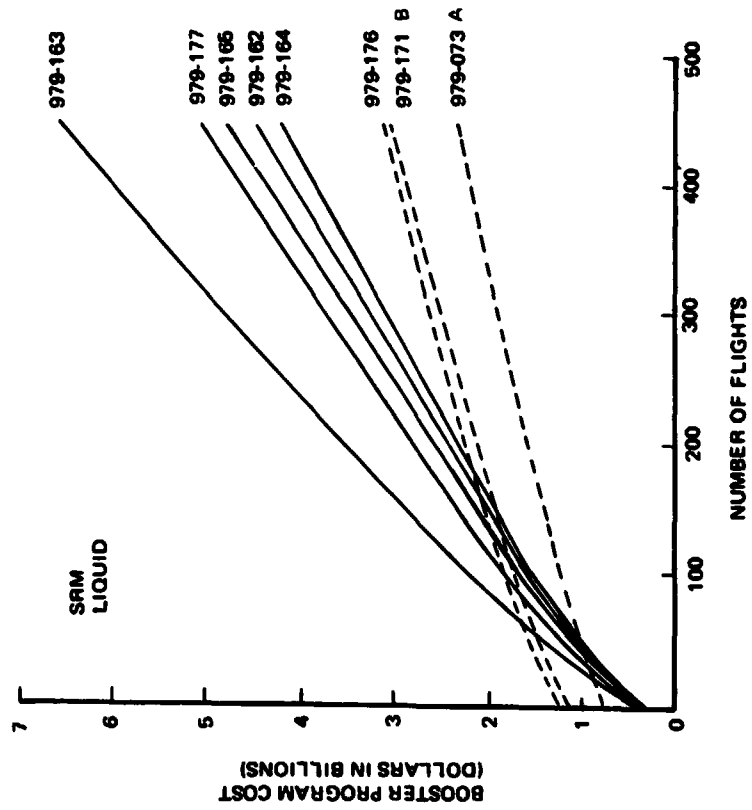


Figure 5-68 Alternative Booster Costs March 2, 1972

	PARALLEL SRM 979-164	BRB SERIES PRESSURE FED 979-176	BRB SERIES PUMP FED 979-073
BOOSTER DEV. COST	0.35 B ✓	1.21 B	0.74 B
POTENTIAL LOW COST/ FLIGHT		✓	✓
DEV. RISK			
PROPULSION	✓		✓
RECOVERY	✓		
SYSTEM FLEXIBILITY			✓
ORB/BOOSTER INTERFACE COMPLEXITIES		✓	✓
ENVIRONMENTAL ISSUES		✓	✓

Figure 5-69 The Issues

**The pump-fed booster is recommended because it provides the best balance between DDT&E cost and cost/flight with the most flexible system to accommodate weight growth with minimum development risk.**



PAD ABORT

REPRODUCIBILITY OF THE ORIGINAL PAGE IS POOR.

## Section 6

### PAD ABORT

#### 6.1 INTRODUCTION

The present baseline system (series BRB) does not include pad abort capability and as a result, does not provide a means of escape from time-critical failures on the pad prior to launch. A feasibility study was undertaken to identify the pad abort requirements, to develop design approaches to the implementation of these requirements, and to determine the impact to the system in providing such capability. The time frame considered for pad abort was from booster engine ignition to launch vehicle tower clearance (Figure 6-1). The most critical pad failure was considered to be an incipient launch vehicle (booster plus HO tank) explosion. To escape such a catastrophic environment, the flyaway orbiter must be equipped with a dedicated abort propulsion system or it must be modified to utilize its own engines for this function. The ground rules and assumptions used for the pad abort feasibility study were as follows:

- Three engine orbiter -  $T_{vac} = 472 \text{ K lb/eng}$
- Only single failures were considered
- Pad aborts to consider orbiter flyaway only (HO tank remains with booster)
- No airbreather engine operations to be utilized.

The series BRB configuration at a total propellant weight of approximately 5.0 M lb was used as the study baseline for determination of technical modifications, requirements, weight impact and cost.

#### 6.2 FAILURE MODES AND CRITERIA

An evaluation was performed to determine those failure modes that could result in a catastrophic situation requiring immediate abort. Of those failure modes identified, the booster/HO tank fire/explosion potential in the feed or propulsion system is the most time-critical (see Figure 6-2). Hence, the environment that the orbiter would be exposed to in the event of an explosion is a hemispherical blast wave propagating through the atmosphere at sonic speed. The overpressure level and time of arrival of the blast wave resulting from a pad explosion at a given altitude is shown in Figure 6-3 for a 10, 20 and 100% TNT equivalency of the exploding propellants. The explosion effectiveness, or yield,



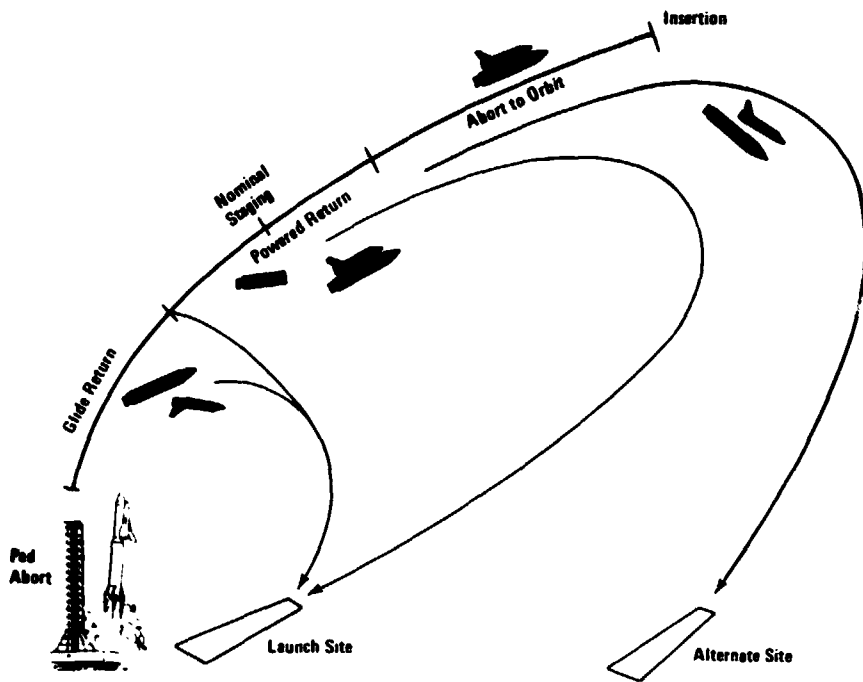
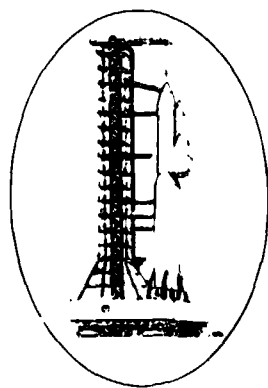


Figure 6-1 Abort Regimes



	Prior to Liftoff	Post Liftoff
BRB/HO Feed Sys/Eng. Fire/Explosion	Most Critical	Most Critical
Rupture of Propellant Lines	?	Rapid Escape
Overpressure of Booster or HO Tank	Non-Time Critical	Not Time Critical
Inadvertent Release of Restraint System	Time Critical at Engine Ignition	Time Critical at Engine Ignition
Loss of an Outboard Engine		Time Critical
Guidance and Control		Time Critical
Solid Booster Fails to Start	Non-Time Critical	
Solid Booster Burn Through	Time Critical	Time Critical
Solid Booster Nozzle Failure		Time Critical
TVC Failure (Solid)		Time Critical

Figure 6-2 Failure Criticalities

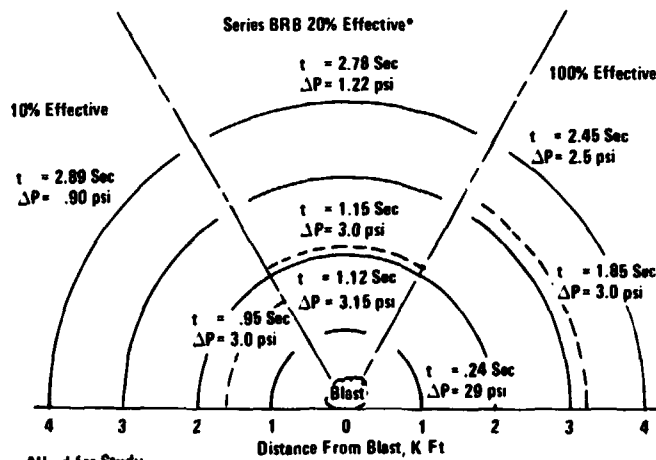


Figure 6-3 Blast Wave Characteristics

is the ratio of an equivalent TNT weight to the weight of exploding propellant that would create the same environment. For the purpose of this study, a 20% effective explosion was assumed. The prerequisite for orbiter survivability is a combination of sufficient warning time and acceleration away from the blast source such that the orbiter can reach an altitude for which the overpressure conditions are tolerable. Warning time is defined as the minimum detection time of incipient liquid propellant explosion plus the time elapsed for the shock wave to propagate to the survival altitude.

#### 6.3 VEHICLE DESIGN CONSTRAINTS

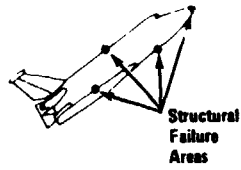
To escape an impending launch vehicle explosion, the flyaway orbiter must be capable of accelerating to a safe altitude within a short period of time. In addition to the time constraint, the flyaway orbiter structural integrity and flying qualities must be maintained. A structural analysis was performed to determine the limiting design constraints of the vehicle. The analysis included the effects of shockwave overpressure, longitudinal acceleration and SRM start-up transient. It was found that the 3 psi shockwave overpressure shown in Figure 6-4 is the limiting overpressure that the orbiter fuselage can sustain without increasing the strength of the pressure frames, cargo door support frames and cargo doors. This overpressure will occur at an altitude of approximately 2000 feet at about 1.1 seconds after the explosion of a 20% effective blast (Figure 6-3). The maximum longitudinal acceleration of 4.2g shown in Figure 6-4 is based on the 3g operational design limit and has a 1.4 safety factor. A dynamic magnification factor of 1.3 was also included in the analysis to account for the steep slope experienced with SRM ignition. The vehicle design constraints shown in Figure 6-4 satisfy the structural integrity requirement but the vehicle may experience some permanent deformation. This deformation would not, however, degrade the flying qualities of the vehicle.

#### 6.4 FLIGHT REQUIREMENTS

In addition to the identified environmental and vehicle design constraints, the location and heading of the proposed airfield is of significance to the propellant sizing requirement. For the proposed KSC airfield location and heading shown in Figure 6-5, an orbiter flyaway pad abort requirement was generated. The flight profile, Figure 6-6, which corresponds to the proposed airfield coordinates shows a specific energy requirement of approximately 17,000 ft (10,000 ft altitude and 600 ft/sec velocity) that must be attained to satisfy orbiter flying qualities. The specific energy (the sum of potential and kinetic energies per unit weight) must be provided by the pad abort propulsion system. The pad abort burnout conditions that satisfy the initial conditions for the orbiter glide return profile were obtained from Figure 6-7. A set of generalized energy level curves were generated and plotted as







- Dynamic Pressure (q)
- Vehicle Longitudinal Acc.
- Vehicle Normal Acc.
- Shockwave Pressure Differential Limit
- Maximum Landing Velocity
- Orbiter Engine Emergency Start-Up Time
- Orbiter Post-Abort Landing
- Range of Orbiter Landing Weights

Constraint	Basis
1000 psf	TPS Struct Failure
4.2 g	Primary Struct.
+3.0 g	Primary Struct.
-1.0 g	Primary Struct.
3.0 psi	Primary Struct.
240 Kt	Tire Blowout
2.0 Sec	Present NASA Plans
New Strip at KSC	Present NASA Plans
85 K	0 to Max P.L.

Figure 6-4 Pad Abort Design Constraints

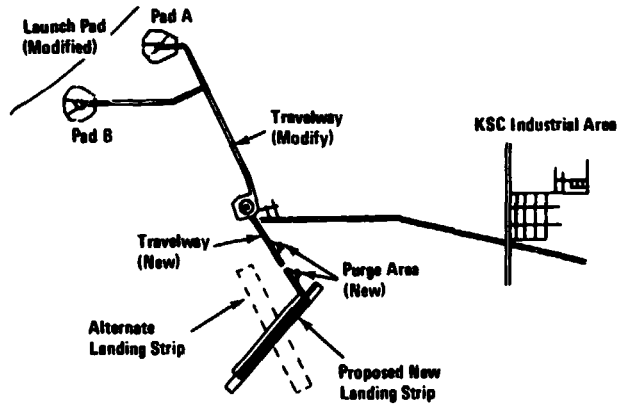


Figure 6-5 KSC Landing Strip Location

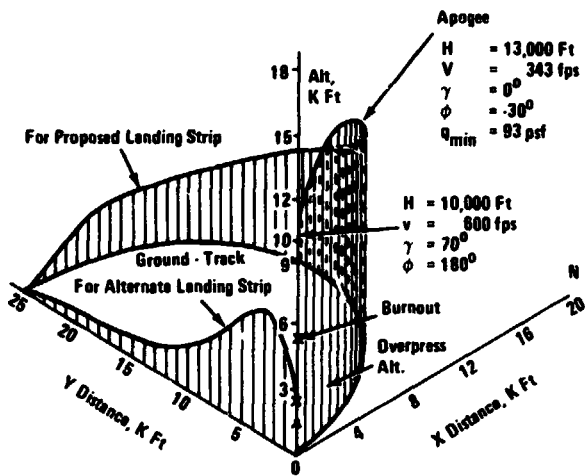


Figure 6-6 Pad Abort Flight Profile

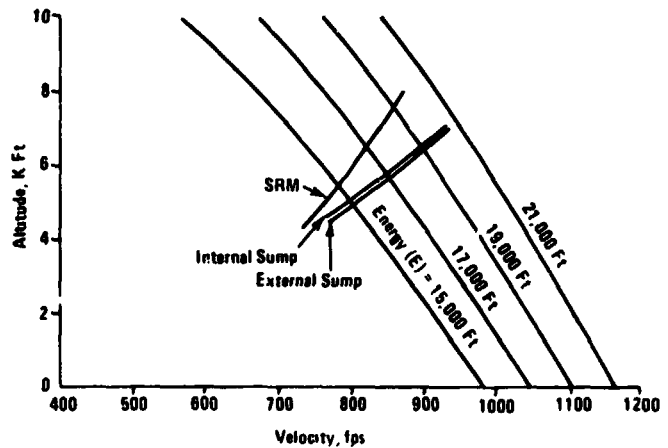


Figure 6-7 Burnout Conditions As A Function of Energy Level

a function of altitude and velocity. These curves indicate the velocity required for a given altitude which satisfies the given energy level. Superimposed on the generalized energy level curve the burnout altitude and velocity attainable with various propellant quantities have been plotted. The intersection of these curves with the energy level plots yield the abort system burnout requirements for any given energy level.

## 6.5 CONFIGURATIONS CONSIDERED

### 6.5.1 SSME Configuration

The pad abort study considered both the feasibility of utilizing the existing orbiter propulsion system (SSME) as well as the addition of dedicated abort rockets (SRM's) to satisfy the previously discussed requirements and constraints. The configurations considered for pad aborts are shown in Figures 6-8a and 6-8b. The configurations shown in Figure 6-8a are variations to the SRM installation approach on a conventional engine orbiter shown at the top of Figure 6-8a. Table 6-1 shows the propellant required for the respective burnout condition to size the SRM or sumps. Sumps are propellant ( $LO_2$  and  $LH_2$ ) storage containers integrated with orbiter fuselage structure, and can be either internal or external to the fuselage as shown in Figure 6-8a. The added configuration approaches shown in Figure 6-8b were eliminated early in the study for various reasons, such as structural complexities, plume impingement, and aero control surface interference. The concept of utilizing the existing orbiter propulsion system for pad aborts was also eliminated for the following generic reasons:

- A configuration study indicated that even with maximum gimbaling angles of all three engines the net thrust direction of the engines would still be toward the stack. As a consequence, only two engines can be utilized to assume that the orbiter path is away from the stack, which yields a thrust-to-weight ratio of 2.72
- In order for the engines to fire through the orbiter-alone cg the gimbaling envelope must be expanded from the present  $\pm 10$  to  $\pm 15.5$  degrees
- The present SSME cannot be started at sea level at an angle of greater than  $3^\circ$  to the gimbaling null line because of high side loads created during the ignition sequence.
- At emergency start-up of the SSME the time to reach full thrust is two seconds, which increases the warning time required to escape the blast wave by that amount.
- The inert weight penalties for the three sump configurations shown in Figure 6-8a are:



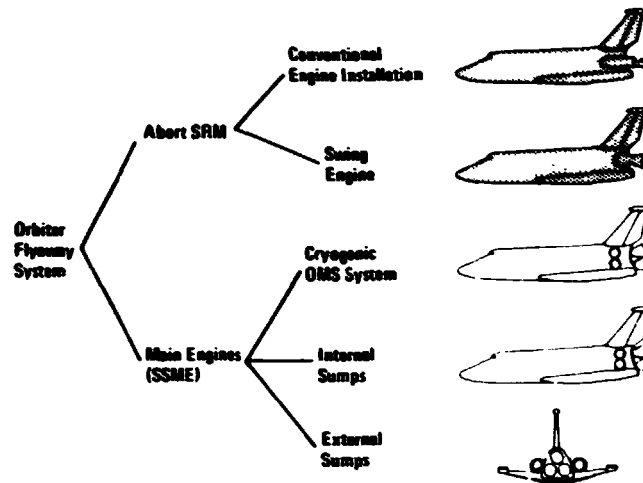


Figure 8a Configurations Considered for Pad Aborts

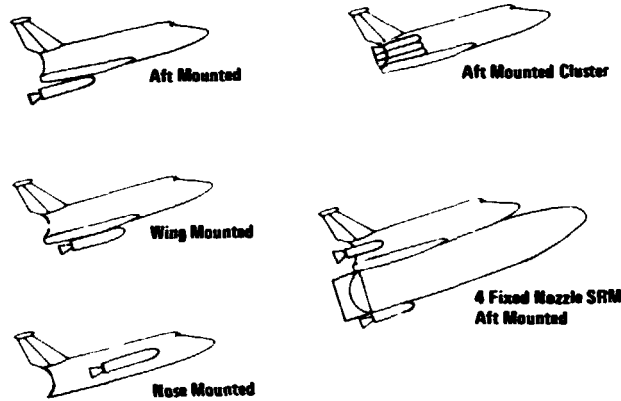


Figure 6-8B Additional Configuration Approaches Considered

Table 6-1 Propellant Required

Internal Sump:	Burnout Velocity = 845 fps Burnout Altitude = 5900 Ft Propellant (LH <sub>2</sub> + LO <sub>2</sub> ) = 31,800 Lb
External Sump:	Burnout Velocity = 855 fps Burnout Altitude = 5700 Ft Propellant (LH <sub>2</sub> + LO <sub>2</sub> ) = 30,200 Lb
SRM:	Burnout Velocity = 820 fps Burnout Altitude = 6600 Ft Propellant = 50,738 Lb

Energy Level/Unit Weight = 17,000 Ft

- Internal sumps approximate inert weight increase = 14,000 lb
- Cryogenic OMS (internal sumps) approximate inert weight increase = 17,000 lb
- External sumps approximate inert weight increase = 4,000 lb.

These penalties are effective through the entire mission and have a greater overall effect than a heavier abort rocket which is only carried to booster staging.

The prime configuration selected for study, Figure 6-9, is the baseline orbiter with two abort rockets attached to the existing fuselage structure. This configuration was selected for study because of its minimum impact on vehicle thrust structure, minimum plume impingement and because the SRM casing can be retained until landing under abort conditions. The SRM's are located above the wing with the nozzle exit plane located in the plane of the main propulsion system.

The other configuration selected for study is the swing engine concept, employing a single solid abort rocket. The SSME's are mounted on the HO tank aft section during normal ascent burn phases and are then transferred into the orbiter prior to HO tank separation. An attractive feature of the swing engine concept is the lack of propellant line interfaces between tank and orbiter which minimizes the abort separation complexity. The abort rockets shown in Figure 6-10 and 6-11 have been sized to satisfy the requirements and constraints shown in Figures 6-3, 6-4 and 6-7 respectively. Since the swing engine approach has profound orbiter, tank and abort rocket design implications, the next section will be devoted to a detailed discussion of that configuration.

#### 6.5.2 Swing Engine Configuration

In the swing engine concept the orbiter engines are mounted on the propellant tanks as on a conventional launch vehicle stage, but at the completion of firing, the engine package is transferred to and stowed within the orbiter instead of jettisoning it with the tank. (Figure 6-12).

The potential advantages of the concept are:

- Reduction in tank weight because the  $LO_2$  tank can be located aft of the hydrogen tank.
- Reduction in orbiter inert weight because main engine thrust loads are no longer carried through the orbiter structure.
- Reduced POGO susceptibility
- A good pad abort potential

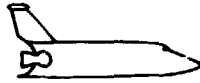


● SRM Strap-On

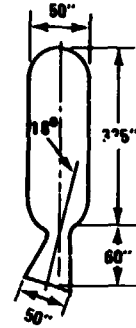


- SRM Attached to Existing Thrust Structure
- No TVC Required for Abort Operations
- Can Be Retained Till Landing for Aborts
- Minimizes Plume Impingement
- Could Be Fired During Normal Flights
- Minimum Number of Strap-Ons

● Swing Engine



- Convenient SRM Location
- No Propellant Line Interfaces Between Tank and Orbiter
- Single SRM Required
- Minimizes c.g. Shift for Abort
- SRM Can Be Retained Till Landing for Aborts

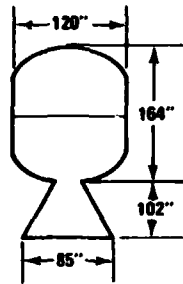


2 Motors Required

- Thrust Start (S.L.) = 500 K Lb
- Thrust Burnout (S.L.) = 380 K Lb
- $I_{sp}$  S.L. = 242 Sec
- Burn Time = 14.6 sec
- Chamber Press. (Avg) 1400 psia
- Total Impulse C.L. =  $645 \times 10^6$  Lb · Sec
- Inert Weight = 6 K Lb
- Propellant Weight = 26,700 Lb.
- Total Weight = 32,700 Lb.
- Mass Fraction = 0.82

Figure 6-10 Abort SRM Characteristics

Figure 6-9 Configurations Selected for Study



- Thrust Start (S.L.) = 900 K Lb
- Thrust Burnout (S.L.) = 680 K Lb
- $I_{sp}$  S.L. = 242 Sec
- Burn Time = 15 Sec
- Chamber Press (Avg) = 900 psia
- Total Impulse =  $11.7 \times 10^6$  Lb·Sec
- Inert Weight = 10,721 Lb
- Propellant Weight = 48,838 Lb
- Total Weight = 59,559 Lb
- Mass Fraction = 0.82

Figure 6-11 Abort SRM Characteristics – Swing Engine Configuration

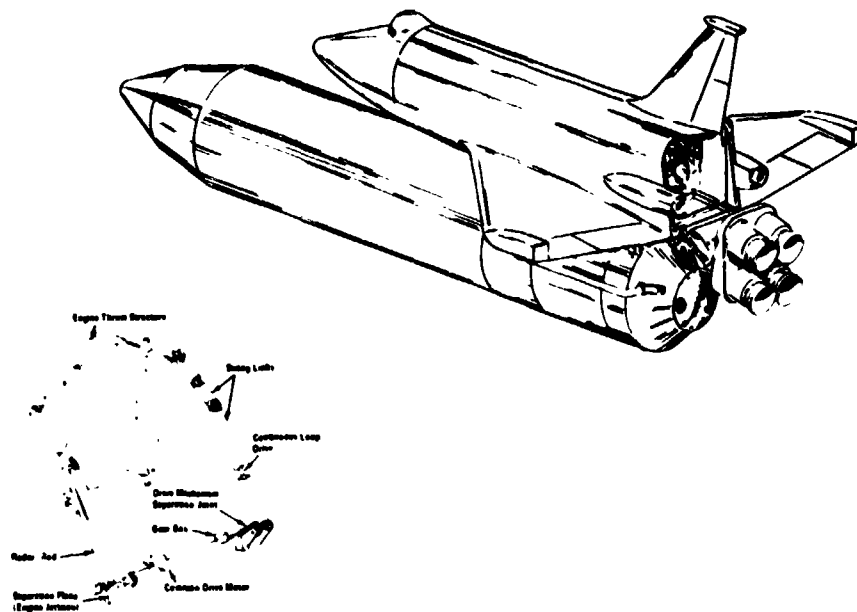


Figure 6-12 Swing Engine Installation

- The propulsion development program is decoupled from the Orbiter
- The tankage/engine package can be used as a launch vehicle stage for large alternate payloads.

A study was initiated in October 1971 to evaluate the swing engine concept. Up to the 15 December mid-term report, the studies centered around the four J-2S version of the orbiter and evaluated its merits as a configuration alternate. The feasibility of the propulsion installation and the swing mechanism were established. Engine stowage aft of the payload bay was determined to be the best location and orbiter/tank weight savings of approximately 9,000 lb were calculated. These preliminary evaluations were reported in B35-43RP-30, Volume III Orbiter Data submitted under the Contract Study NAS 9-11160.

For the second half of the current Phase B extension study, the emphasis of the study was shifted to the pad abort application of the swing engine approach. The configuration that evolved and which forms the basis of the updated weights, is shown in Figure 6-13 and 6-14.

The orbiter is the basic 040 configuration with the SSME thrust structure replaced by a truss-frame thrust structure for the pad abort rocket.

The swing mechanism consists of fixed radius swing links with engine motion controlled by an internal torque driver. Low horsepower electric motors located at a mechanism pivot, power the mechanism.

Table 6-2 is a summary of the major weight changes of the swing engine orbiter relative to the conventional series burn, tandem-mounted orbiter, with both orbiters being designed for pad abort capability.

The major advantage of the swing engine approach is that it allows the installation of the  $LO_2$  in the HO tank aft end, thereby precluding the cg location/engine gimbaling problem of the conventional orbiter. This tank design approach leads to a significant decrease in tank structural fraction. The swing engine orbiter tank Figure 6-15 is composed of seven major subassemblies, the nose cone, retro-motor thrust structure,  $LH_2$  tanks, intertank skirt,  $LO_2$  tank, engine support cone, and interstage skirt.

The nose cone and retro-motor support structures are the same as the series burn HO tank.

The  $LH_2$  tank is a welded aluminum alloy shell, stabilized in flight by pressurant gas forward of the forward orbiter attachment, and by a machined grid of stringers and frame supports, augmented by mechanically fastened ring frames, aft of the forward orbiter attachment.



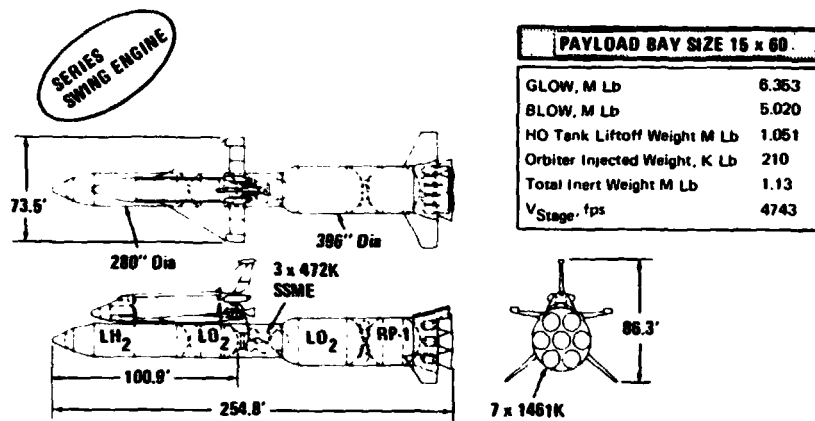


Figure 6-13 Launch Configuration

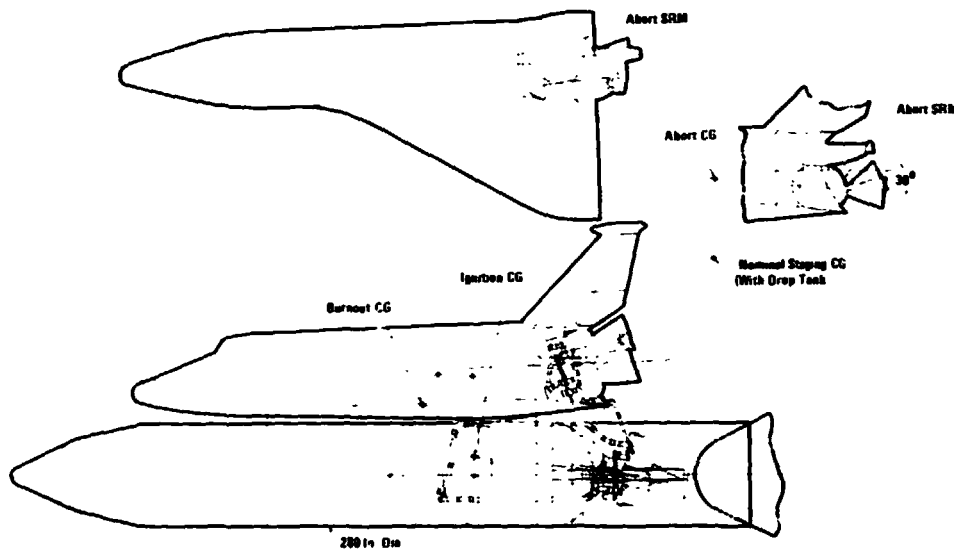


Figure 6-14 Swing Engine Orbiter Design

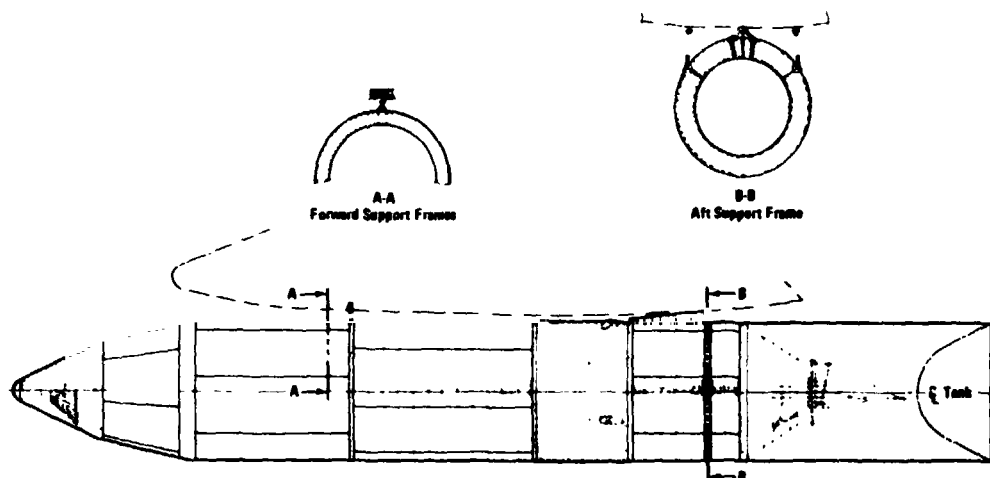


Figure 6-15 Structural Arrangement Swing Engine Design Ho Tank

Table 6-2 Orbiter Weight Changes

Major Item	Swing Engine - ΔLb	Weight Derivation
Structure		
SSME Thrust	-3314	Calculated From Loads and Vehicle Layouts
Fuselage	- 678	
Abort Rocket Thrust (Swing Engine)	+1424	
Abort Rocket Thrust (Conventional)	- 849	
Swing Mechanism	+1966	Estimated From Layouts
Base Heat Shield	+ 464	Estimated From Layouts
Engine Package	+ 616	Calculated - Includes 420 Lb/Engine for Self-Contained Hydraulics
Miscellaneous - RCS + Iteration	+ 98	
Total Dry Weight Change	- 264 Lb	

The intertank skirt acts as a spacer between the LH<sub>2</sub> and LO<sub>2</sub> tank domes; construction is internally stiffened aluminum alloy sheet.

The LO<sub>2</sub> tank incorporates the orbiter aft attachment struts and drag fitting together with the required redistribution structure, and provides interfaces for the engine support cone and interstage skirt. Construction is of welded grid stiffened aluminum alloy plates with mechanically fastened stabilizing frames. The orbiter aft attachment frame is butt welded into the pressure vessel.

The engine support cone adapts the LO<sub>2</sub> tank aft end to the engine support and disconnect structure, and provides guide tracks for the intertank skirt jettison system. Constructed of semi-monocoque aluminum sheet, it redistributes engine thrust loads into the LO<sub>2</sub> tank ring aft. Cutouts are provided for fuel line routing.

The interstage skirt, much longer than for the series burn HO tank, is also of semi-monocoque aluminum alloy sheet construction. Slots in the orbiter side of the skirt provide clearance for the swing engine stowage struts. Rollers on each side of the skirt engage in tracks on the engine aft support structure, acting as guides to assure engine clearance when the skirt is jettisoned.

The propellant lines to the engine are separated from the tank by explosive clamp disconnects. The disconnects provide for the tank and engine line shutoff. Hydraulic power for valve and gimbal actuation is self-contained on each engine. The only propulsion interface to the orbiter is the electrical harnesses.

Table 6-3 is a summary weight statement of the LO<sub>2</sub> aft tank used in the swing engine configuration compared to the conventional series burn tandem mounted orbiter. These weights derive from loads analysis and tank layouts.





**Table 6-3 Tank Weight Comparison – No Pad Abort**

Item	Series/ORB 15 x 60	Parallel/SRM 15 x 60	Swing Engines LO <sub>2</sub> AFT
Propellant Weight	968,794	1,468,886	980,835
LN <sub>2</sub> Tank	23,628	29,457	8,743
Miscellaneous	630	886	680
Integral/Tank Support	4185	5,591	2,621
LO <sub>2</sub> Tank	10,134	12,134	12,865
Aft Skirt	885	-	2534
TPS/Insulation	4067	7574	6658
Nose Cone	722	1384	882
Separation/De-Orbit	3800	4816	3907
Propulsion	2180	2228	2175
Electronics	350	483	450
Contingency	1012	1281	681
Thrust Structure	-	-	2488
Total Dry Weight	51,593	65,844	44,895
Propellant Fraction	.9372	.9439	.9347
Dry Weight	.0525	.0445	.04488
Loaded Propellant			

The weight advantage is due to three factors:

- The hydrogen tank does not carry the load of the LO<sub>2</sub>
- The bending moments are lower
- The oxygen tank pressure is lower because of the short line runs.

There is one adverse aspect of the swing engine configuration that merits discussion. Failure of the engine package to retract and lock creates an abort situation unique to the swing engine concept. Figure 6-16 illustrates this problem.

The nominal orbiter entry cg positions are between 65.7% and 67.7% of the body length, with and without payload. If the swing mechanism fails, the engine package must be jettisoned. Continuation of the mission would result in a final cg position at 60.6%. This is clearly beyond the aerodynamic control capability of the vehicle; if the mission is terminated, sufficient OMS and RCS propellant can be retained to perform a safe low  $\alpha$  entry with the cg at the 64% position.

## 6.6 RESULTS

### 6.6.1 Warning Time

Refer to Figure 6-3 shows that if the maximum allowable overpressure of 3.0 psi is not to be exceeded in the case of a pad explosion, the orbiter must reach a 2000 ft altitude within 1.15 seconds of the blast. Clearly this capability is not attainable with any propulsive thrust that does not exceed orbiter acceleration tolerance. Consequently safe abort for this critical case is only possible if there is some period prior to the explosion

at which a warning of the incipient catastrophic event is received. The evaluation of warning time requirement and the design approach towards minimizing the warning time were key items in the pad abort study.

The required warning time is shown on Figure 6-17 as a function of T/W of the abort propulsion system and of tolerable overpressure levels. It can be seen from Figure 6-17 that the configurations that utilize the main propulsion system require 10 seconds of warning time, whereas the configurations utilizing the dedicated abort system (SRM's) require only 6.75 seconds of warning time. The 3.25 seconds higher warning time required for the main propulsion system concept is due to the lower vehicle acceleration during abort thrusting and also because of the 2-second start up time required for the main propulsion system to achieve full thrust. The 6.75 seconds warning time for the dedicated abort system concept shown in Figure 6-17 applies to the case of maximum payload (65,000 lb) accelerating at 3.25 g's, which corresponds to the same vehicle with zero payload acceleration at the maximum allowable level of 4.2g.

From Figure 6-17 it can be seen that increasing the overpressure from 3 to 4 psi reduces the warning time from 5.5 to 4.8 seconds, respectively. This reduction in warning time imposes a structural weight increase of approximately 150 lb.

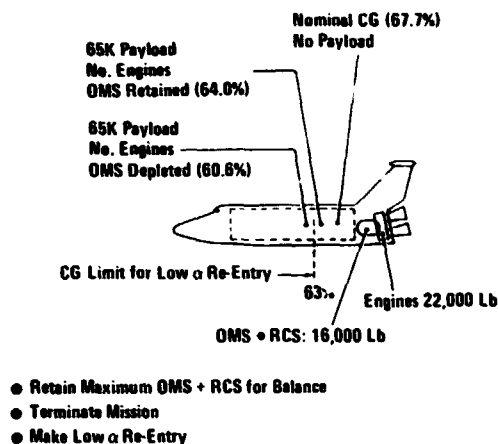


Figure 6-16 Effect of Swing Mechanism Failure

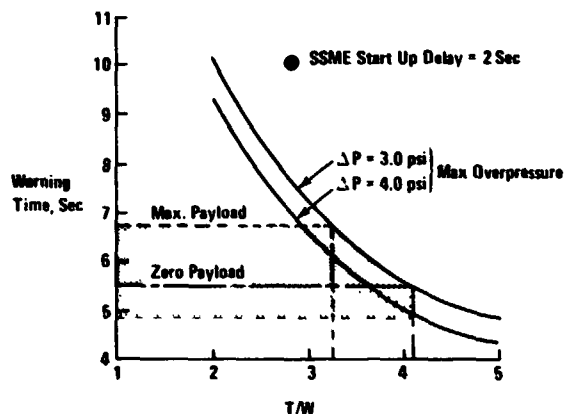


Figure 6-17 Warning Time Requirements

### 6.6.2 Fall-Back Zone

The installation of abort rockets on the vehicle will eliminate the fall-back zone, i. e., the region within which, if separation were to occur, the orbiter would impact ground level. This condition exists because without an abort rocket, the thrust-to-weight ratio (T/W) of the orbiter plus HO tank is less than unity. However, in lieu of the fall-back zone,



there exists a minimum safe abort altitude after lift off (Figure 6-18) below which the impact of the tank/booster on the pad generates a higher TNT equivalent blast wave than an explosion on the pad itself. An abort below altitude (170 ft) would result in the this orbiter experiencing a shockwave pressure differential of greater than 3 psi.

### 6.6.3 Gantry Clearance

The launch pad stack configuration shows that the orbiter is sandwiched between the gantry and the launch vehicle. From Figure 6-19 it can be seen that the gantry structure is placed at approximately  $45^{\circ}$  angle to the orbiter minus Z axis and 264 in. from the closest wing tip. In addition, swing arm motion and velocity provide further potential of orbiter interference. Figure 6-17 shows the flight path of the flyaway orbiter and clearance relative to the gantry during a pad abort. It was found that the orbiter's wing tip clears the top of the gantry by approximately 40 in. without consideration given to wind load effects. It was also found that the crew compartment arm must be capable of being retracted approximately 20 ft in two seconds.

During the first few seconds of flight the vehicle (orbiter) is on a ballistic path with no means of control. Thus, 40 in. does not appear to be adequate clearance and further study is required on techniques to increase the clearance. Changing the orbiter placement on the pad relative to the gantry on tailoring the initial lift-off trajectory are two approaches under consideration.

### 6.6.4 Performance and Cost

The impact of providing pad abort capability to the baseline system is summarized in Figure 6-20. It must be noted that the penalties shown were based on jettisoning the SRM's at nominal staging without firing them. The cost of providing SRM jettison capability is shown in Figure 6-21. The performance penalties shown in Figure 6-20 can be reduced if the abort rockets are utilized during the nominal mission, but the cost penalty will be essentially the same.

## 6.7 CONCLUSION

In summary, an incipient launch vehicle explosion potential imposes the most severe environment and time critical condition that the orbiter (flyaway) must be capable of escaping from. The explosion environment that was considered a criterion in establishing the need of pad abort capability was derived from failure mode analysis. The analysis identified those failures that could lead to a catastrophic situation requiring immediate abort. The explosion potential criterion dictated the thrust profile and magnitude of the

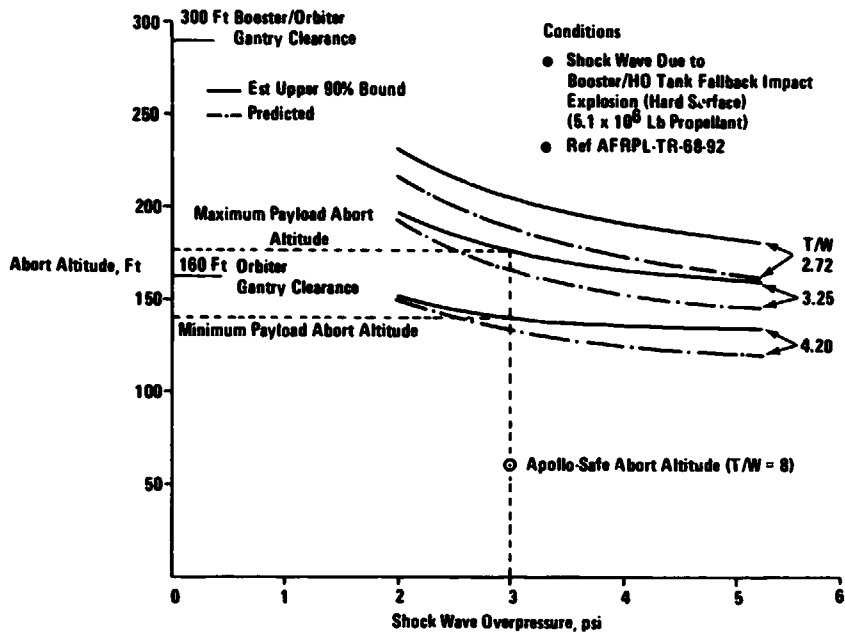


Figure 6-18 Pad Abort - Minimum Safe Altitude

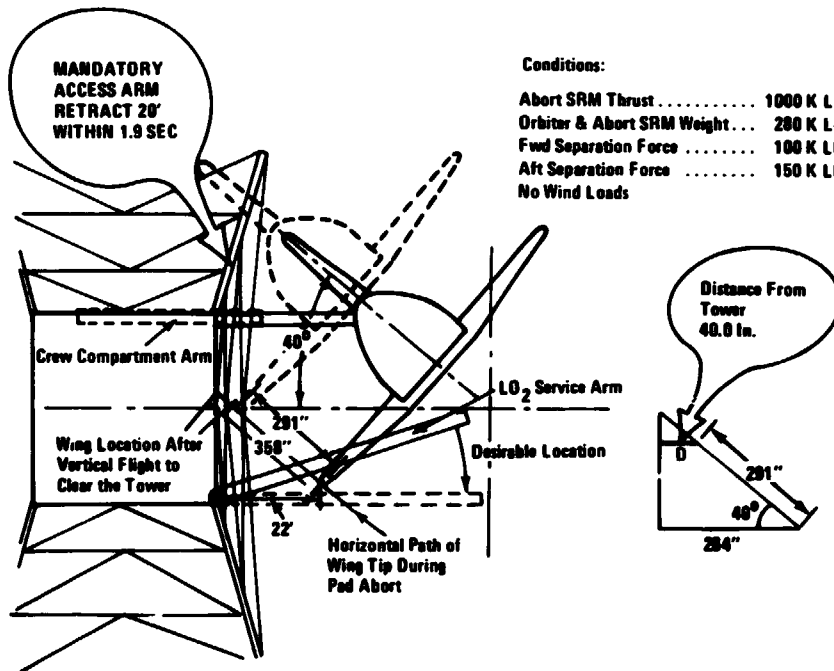


Figure 6-19 Pad Abort Tower Clearance



GLOW for Pad Abort 6.60 4.82 6.35  
 GLOW for No Pad Abort 6.36 4.62 6.16

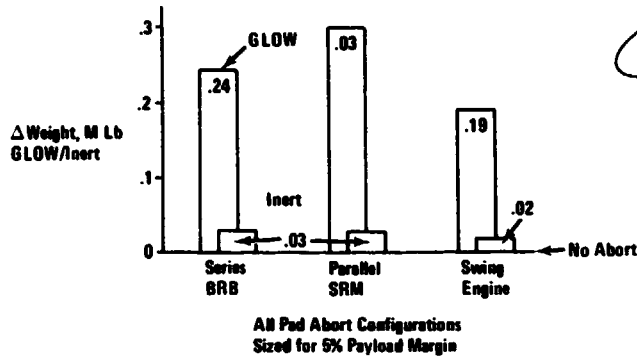


Figure 6-20 Δ Weight Glow/Inert For Pad Abort

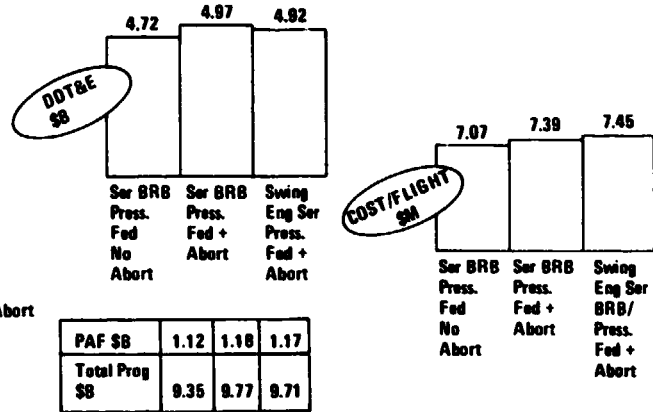


Figure 6-21 Pad Abort Cost Comparisons

propulsion system, whereas the proposed KSC airfield location and heading dictated the quantity of pad abort propellant required. In addition, vehicle design constraints limited the acceleration capability of the system. As a result, warning time is required to abort safely.

Because of the large warning time requirements associated with the main propulsion system (SSME), they were considered to be incapable of providing the required pad abort capability. A dedicated pad abort propulsion system minimizes system complexities and requires least warning time. The installation of two solid rocket motors to the side of the fuselage has least design and cost impact. For the swing engine concept, the installation of the single abort rocket in the main engine cavity satisfies the pad abort requirement with minimum scar weight to the orbiter.

Providing pad abort capability for the orbiter will increase GLOW and inert weight of the series BRB by 0.24 M lb and 0.03 M lb respectively. A comparison of the Δ GLOW/ inert weight shows that the pad abort capability has less impact on the swing engine than the series BRB concept. The performance penalty to the launch vehicle as a result of including pad abort capability can be eliminated if the rockets are utilized during the nominal mission. This would require a two position nozzle on the rocket, whereas for this analysis a fixed nozzle firing through the orbiter cg was assumed. Thus, the cost impact on the system would be about the same.

A fallout of providing pad abort capability with solid rocket motors is the reduction in the safe abort zone, which classically, is established by fall-back of the orbiter because of less than unity T/W.

REPRODUCIBILITY OF THE ORIGINAL PAGE IS POOR.

## Section 7

### ENVIRONMENTAL IMPACT

#### 7.1 INTRODUCTION

President Nixon's first official act in 1970 was to sign into law the National Environmental Policy Act of 1969 (NEPA). With his signature, the President established a powerful tool for safeguarding the environment whose consequences for Federal programs and actions have yet to be fully assessed.

The NEPA requires all federal agencies to include environmental considerations in every activity likely to affect the environment, and to take all practical means to protect it. Section 102 (2) (C) of NEPA requires a detailed statement (sometimes called a "102 statement") to be submitted for every proposal for federal legislation or other action with a significant environmental effect. The statement must include:

- The environmental impact of the proposed action,
- Any adverse environmental effects which cannot be avoided should the proposal be implemented,
- Alternatives to the proposed action,
- The relationship between local short-term uses of man's environment and the maintenance and enhancement of long-term productivity, and
- Any irreversible and irretrievable commitments of resources which would be involved in the proposed action should it be implemented.

NEPA also established the Council on Environmental Quality (CEQ) to review 102 statements and to advise the President on environmental matters. Guidelines set by CEQ require public disclosure of draft statements with adequate time for all affected agencies and groups to comment before a final statement is submitted.

The adequacy of some 102 statements, especially with regard to consideration of alternatives to proposed actions, has been successfully challenged in court, e.g. Calvert Cliffs nuclear power plant and offshore Louisiana oil and gas lease sale.

The Environmental Protection Agency (EPA) has the responsibility to comment on virtually all 102 statements. The EPA has provided a checklist of types of environmental impacts for consideration in 102 statements. The applicability of this list to the space shuttle is shown in Figure 7-1.



	<u>Shuttle?</u>
Project Description	✓
Water Quality and Pollution Control	✓
Air Quality and Pollution Control	✓
Water Supply and Hygiene	✓
Solid Waste Management	✓
Radiation Problems	✓
Pesticide Use and Control	-
Noise	✓
Toxic Materials	✓
Herbicides	✓
Land Use and Management	✓
Electric Power Generation	✓
Urban Development	✓
Industrial Development	-
Transportation and Handling Hazardous Materials	✓
Aesthetics, Aquatic and Terrestrial Ecosystems	✓

Figure 7-1 EIS Considerations

Three areas of particular concern noted by shading are air quality and pollution control, solid waste management, and noise as shown in Figure 7-2.

## 7.2 AIR QUALITY AND POLLUTION CONTROL

NEPA requires that both primary and secondary environmental consequences of particular actions be considered. For the shuttle, an important primary impact may result from booster exhaust products at launch, while a secondary impact aspect of booster selection may be the pollution created from propellant manufacture.

- Air Quality and Pollution Control
  - Booster Exhaust
  - Fuel Manufacture Pollutant Generation
- Noise
  - Orbiter Re-Entry Noise
- Solid Waste Management
  - HO Tank Disposal
  - Skirt Jettison
  - Booster Disposal

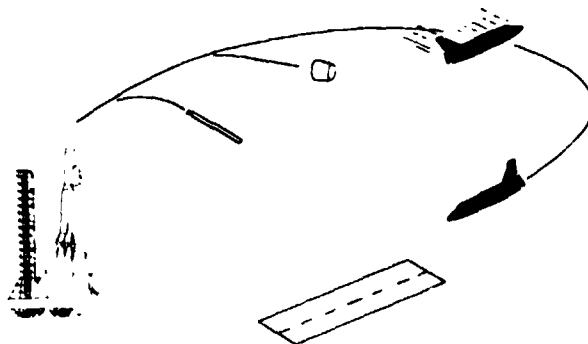


Figure 7-2 Potential Shuttle Impact Items



The total contaminant products for solid and liquid booster configurations based on 60 shuttle flights per year, are compared with 1971 ETR launch emissions and annual estimated emissions of CO from New York City automobiles and Kennedy Airport operations in Figure 7-3.

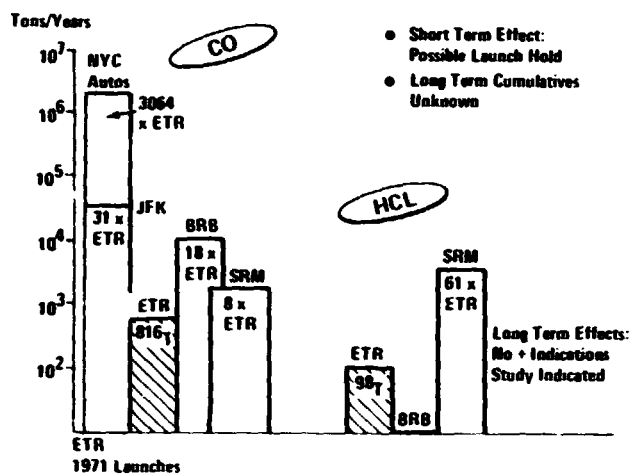


Figure 7-3 Total Contaminant Products

Although, in an absolute sense, any new addition of contaminants to the atmosphere is undesirable, those added by space shuttle operations must be viewed in proper perspective (note the log scale in Figure 7-3). New York City automobiles alone annually inject 170 times the projected BRB CO emission at maximum flight rate (320 times the SRM emission).

Total U.S. emissions of HCl from all sources were estimated to be 907,600 tons in 1969, or nearly 150 times the total SRM emission at the maximum flight rate. Although the long term cumulative effects of shuttle booster emissions are not known with certainty, it appears that they will be trivial compared to other sources already existing.

Solid rocket emissions of HCl could present a short-term local hazard, however, depending on weather stagnation and wind direction at launch. Time histories of HCl concentrations at a point 20 km downwind of launch, at various combinations of cloud buoyancy and weather stability, are shown in Figure 7-4. The example assumed the first 5000 ft of a vertical rocket plume were divided into five segments of equal time interval. Each segment was treated as a point source of pollution, and the ground concentration from each was calculated using a Gaussian puff model and diffusion parameters described in "Meteorology and Atomic Energy" 1958, U.S. Atomic Energy



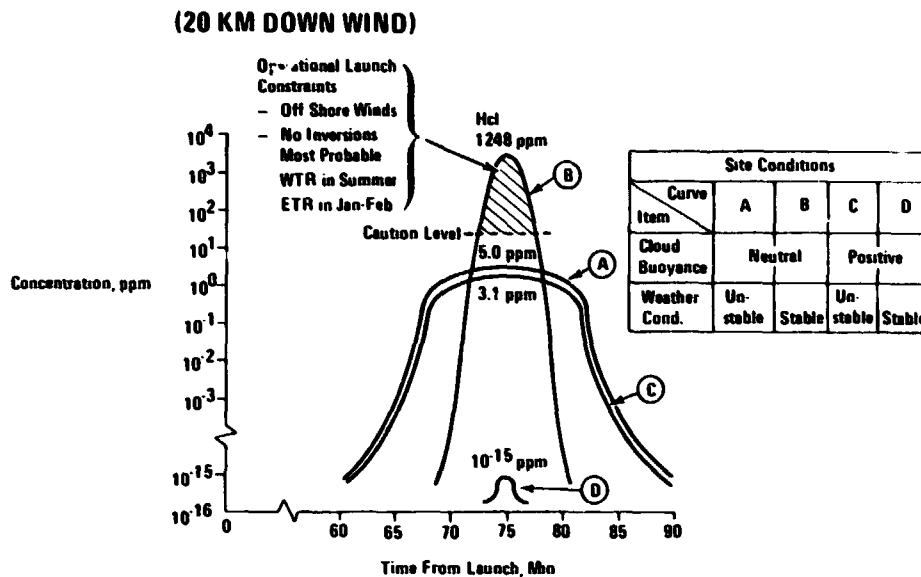


Figure 7-4 Representative Exposure to Peak HCL Concentrations

Commission, 1968, David H. Dade, Editor. The altitude of each point source was assumed to be at the actual emission point for neutral cloud buoyancy, and was assumed to be 1640 ft higher for positive cloud buoyancy. A constant wind of 10 mph and an unlimited mixing height were also assumed.

Figure 7-4 shows that caution level concentrations of HCl may be exceeded during periods of neutral cloud buoyancy combined with stable weather, and launch hold to avoid such periods may be necessary. Further study is needed to assess the buoyancy of the rocket plume under various weather conditions to determine whether caution is in fact justified.

Although the exhaust emission caused by the firings of the propellants may not constitute an environmental hazard, the by-products of propellant manufacture may be of concern. While quantitative values have not been estimated for the environmental effects of propellant manufacture, Table 7-1 presents some qualitative aspects. Solid fuels have presented particular difficulty in disposal of scrap by combustion; an alternate method of disposal could eliminate or at least reduce this objection. Nevertheless, solid rocket motors could create the greater environmental problems during both manufacture and operational firing.

SECONDARY ENVIRONMENTAL EFFECTS

	LN <sub>2</sub>	LO <sub>2</sub>	PBAN	RP
Environmental Impacts	<ul style="list-style-type: none"> <li>• CO<sub>2</sub></li> <li>• Oil Residue</li> <li>• Heat</li> </ul>	<ul style="list-style-type: none"> <li>• Heat</li> </ul>	<ul style="list-style-type: none"> <li>• HCl</li> <li>• Al<sub>2</sub>O<sub>3</sub></li> <li>• CO</li> </ul>	<ul style="list-style-type: none"> <li>• NOX</li> <li>• SO<sub>2</sub></li> <li>• Particulates</li> <li>• Hydrocarbons</li> <li>• H<sub>2</sub>S</li> </ul>
Source	<ul style="list-style-type: none"> <li>• Methane Combustion</li> <li>• Cooling Tower</li> </ul>	<ul style="list-style-type: none"> <li>• Cooling Towers</li> </ul>	<ul style="list-style-type: none"> <li>• Scrap Propellant Combustion</li> </ul>	<ul style="list-style-type: none"> <li>• Heaters</li> <li>• Leaks</li> <li>• Overflows</li> </ul>
Estimated Impact	<ul style="list-style-type: none"> <li>• Small</li> <li>- CO<sub>2</sub> Partially Bottled</li> <li>- Residue Buried Company Property</li> </ul>	<ul style="list-style-type: none"> <li>• Small</li> <li>- Alternative Process Under Evaluation</li> </ul>	<ul style="list-style-type: none"> <li>• Need Alternate Disposal Method</li> </ul>	<ul style="list-style-type: none"> <li>• Industry Satisfying State, Local Fed Regs</li> <li>• Sulphur Remains Problem</li> </ul>
Natural Resources Used	<ul style="list-style-type: none"> <li>• Natural Gas</li> </ul>	<ul style="list-style-type: none"> <li>• Air or</li> <li>• Water</li> </ul>	<ul style="list-style-type: none"> <li>• Aluminum</li> <li>• Air</li> <li>• Water</li> <li>• Rubber</li> <li>• Sodium Chloride</li> </ul>	<ul style="list-style-type: none"> <li>• Crude Oil</li> <li>• Water</li> <li>• Hydrogen</li> </ul>

Table 7-1 Propellant Manufacture

### 7.3 SOLID WASTES

During the course of the shuttle program, a certain amount of solid debris will be added to the ocean. A tank skirt and HO tank will be ejected on every flight, and, for parallel/SRM systems, two booster cases will be similarly expended. The total annual tonnage of solid waste at the maximum launch rate is compared with 1969 maritime losses in Figure 7-5. If these losses are representative of what may be expected in the time period of shuttle operations, the additional ocean pollution caused by shuttle debris constitutes a trivial increment.

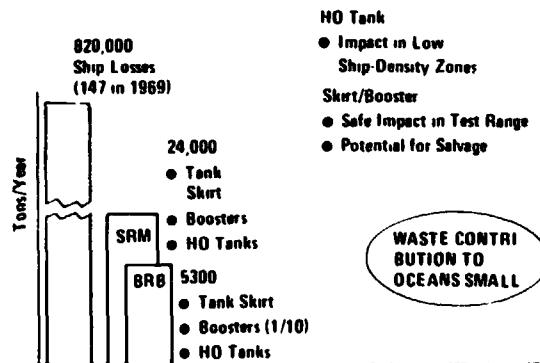


Figure 7-5 Solid Wastes



The debris from the shuttle should be quite inert, especially compared to typical ship constituents (e.g., bunker fuel, crude oil and other hazardous cargo, etc.). The possibility of local contamination by residual fuel after a launch abort should be no greater than for present Titan or Saturn operations.

#### 7.4 ORBITER REENTRY NOISE

Recent detailed analysis of sonic boom ground overpressure contours has indicated that objectionable levels are possible during supersonic transition, and a caustic, the ground laws of reinforcing shockwaves, can form near the low end of the trajectory. The overpressures vary greatly with the trajectory flown and so the sonic boom levels can probably be made acceptable through careful trajectory shaping.

NASA studies have shown the sonic boom to be insensitive to the vehicle configuration shape, while sensitive to trajectory parameters. Overpressure levels are most sensitive to altitude at a given Mach number, indicating the desirability of maximizing altitude over populated areas in the post-blackout phase. This, however, does impact the configuration, as it places a requirement on the trimmed angle of attack boundary at low supersonic speeds. Reasonable end constraints in the transonic regime must also be observed and the impact on the subsonic footprint must be assessed.

The overpressure levels are also somewhat sensitive to other parameters. Further reductions are possible, for example, through modulation of vehicle roll angle, and it might be possible to avoid the formation of a caustic by appropriate selection of the flight path angle rate. Post-blackout trajectory constraints may have to be reviewed and relaxed where feasible.

It would be highly desirable if all boom overpressures occurred over the ocean, reducing environmental concern and also minimizing constraints and demands upon the transition trajectory. Orbit and reentry trajectory studies may reveal a possibility for overwater transition in approaching KSC. It appears possible also to simply overfly the landing site, placing any objectionable overpressures east of KSC, and then to perform a 180° subsonic turn for a westbound landing approach. This requires proper balancing of the transition trajectory end point with an acceptable subsonic footprint, subject to G&N position errors. Should all else fail, selection of a west coast landing site, such as Mac Dill Air Force Base, would place the entire approach over water, and eliminate many constraints and requirements (see Figure 7-6).

- SOLUTIONS**
- Trajectory Designed to Minimize Boom (Some Leeway)
  - Overshoot KSC With Subsonic Return
  - Select Landing Site (Mac Dill AFB) or Others

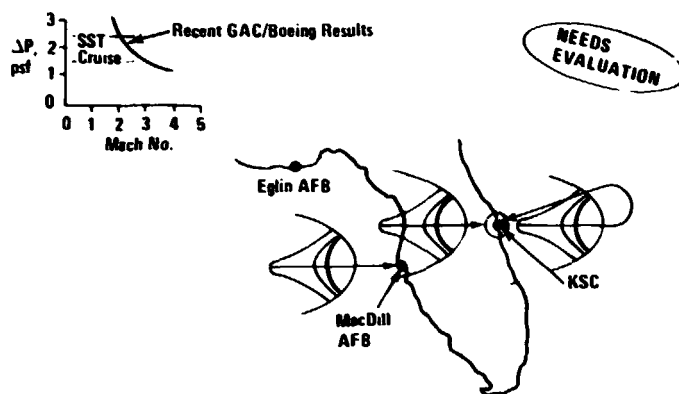


Figure 7-6 Orbiter Re-Entry Noise

## 7.5 SUMMARY

- Shuttle launches appear to offer no long-term air pollution problems, but to prevent local concentrations of HCl from SRM exhaust during stagnant weather conditions, launch holds may be required
- Solid waste jettisoned into the ocean during the shuttle program will be trivial compared to current annual shipping losses
- Orbiter reentry overpressures vary greatly with the trajectory flown. The levels can be minimized and perhaps maintained at acceptable levels through careful selection of the trajectory.

Other environmental problems may arise during shuttle development and operation, and should be evaluated for their significance and means of mitigation. Nevertheless, the space shuttle program at this point is not expected to create any objectionable environmental impact that cannot be avoided through judicious design selection and mission profile tailoring.

REPRODUCIBILITY OF THE ORIGINAL PAGE IS POOR.

## Section 8

### TEST, OPERATIONS, AND FACILITIES

#### 8.1 TEST

##### 8.1.1 Summary

The emphasis in the test analysis area during the Phase B follow-on study has been concentrated on updating the information provided in the Phase B Integrated Test Plan<sup>(1)</sup> to the current program schedule, and incorporation of three booster alternates in the program. The following specific tasks were completed:

- Updating ground test and horizontal flight test programs
- Definitions of test programs for pressure- and pump-fed liquid propellant recoverable and SRM expendable boosters
- Feasibility study of an unmanned orbiter flight
- Continuation of the air tow and suborbital studies for high-speed orbiter flights.

The results of these tasks are summarized in the following paragraphs and indicate the following basic conclusions:

- The pressure-fed BRB presents the longest development program
- An unmanned launch is desirable to qualify the pressure fed BRB and SRM configurations
- The orbiter horizontal flight test program can be initiated early by utilizing only those vehicle systems required to perform the horizontal test program. The total test program consists of 157 flights/361 hrs
- The orbiter is compatible with the air-tow/rocket engine envelope expansion program
- An unmanned orbiter flight is feasible, without excessive vehicle modifications but results in a 6-month FMOF slip.

-----

(1) GAC Report 552-43 RP-3 Integrated Test Plan, Space Shuttle Program Preliminary C/D Report, 6 July 1971



## 8.1.2 Ground Development Testing

### 8.1.2.1 Booster

The pressure-fed Liquid Propellant Recoverable Booster development test program is the most complex and longest in terms of total test months required. This is due primarily to the development requirements associated with the propellant feed system, thrust vector control and new tank design. The three development test programs are compared in Table 8-1.

Table 8-1 Booster Development Tests

Development Test Program	Press. Fed Recov Test Mo	Pump Fed Recov Test Mo	SRM Test Mo
1. Tow Test Model	6	7	
2. Impact Test	5	6	
3. Prop. Press. Sys Breadboard	15		
4. Prop. Feed Sys Breadboard	12		
5. LI TVC Breadboard	10		
6. Elect. Dist Breadboard	7	12	9
7. Avionics Breadboard	18	15	15
8. Flt Control Breadboard	8	10	
9. Integration Test	12	13	12
10. Development Struct Tank - LO <sub>2</sub>	6		
11. Development Struct Tank - RP 1	6		
12. Static Struct Test	18	18	9
13. Dynamics Test	6	7	6
14. Booster Retrieval Development	12	12	
15. Parachute Retrieval Development	6	6	
16. Static Firing	15		
17. RCS Breadboard	9		
18. Thrust Termination Breadboard			6
19. Separation System Breadboard			6
20. TVC Breadboard			10
21. Unmanned Launch Desirable	(X)		(X)
<b>Totals</b>	<b>171 Test Mo (+1 Launch)</b>	<b>106 Test Mo</b>	<b>64 Test Mo (+1 Launch)</b>

Model testing is required for the two recoverable configurations to determine towing characteristics and water impact loads early in the program. This type of testing is not required for the SRM configuration.

8.1.2.1.1 Subsystem Test - Subsystem development for all three boosters is accomplished on a "breadboard" basis for each subsystem. The breadboards will be constructed initially with prototype hardware, and will be upgraded to flight configuration when qualified hardware becomes available. The avionics, electrical distribution, and flight control systems will be integrated in the systems integration lab to verify all interfaces. For the SRM configuration additional breadboard and systems integration testing is required to verify TVC, separations and thrust termination subsystems.



**8.1.2.1.2 Structural Test - For the two recoverable configurations, static structural and dynamic testing will be accomplished on one major test article. Static proof tests will be accomplished on two sections: LOX tank/interstage and RP-1 tank, and thrust structure. The sections will be assembled for the dynamic testing, and then disassembled for static ultimate load tests.**

For the SRM configuration, static structural testing will be accomplished on one motor unit, and analytically applied to the total vehicle. Dynamic testing will be performed on an assembled booster loaded with inert propellants.

**8.1.2.1.3 Propulsion - Engine/propellant feed systems will be verified on the pressure-fed booster by use at a propulsion test article. The vehicle will be an essentially complete booster, with heavyweight tanks and thrust structure to withstand full duration static firing. The pump-fed booster does not require this test because critical booster systems have been flown as part of the qualification program and do not require further verification.**

**8.1.2.1.4 Retrieval Tests - For the recoverable boosters, retrieval tests will be performed on a boiler plate unit with mass and cg simulation. Parachutes from the booster air-drop tests will be used for the parachute retrieval testing.**

**8.1.2.1.5 Parallel Burn Configurations - The ground development test program for the series and parallel burn boosters are the same. Overall program costs will be less with the parallel burn configurations because of the smaller size and simplification of the vehicles, and in the case of the SRM's, fewer units will be needed for dynamic testing.**

#### **8.1.2.2 Orbiter**

The major orbiter ground tests consist of: a full airframe structural test program preceded by element tests to verify design and analysis assumptions in high-risk areas; a full-scale orbiter vertical vibration mode survey; and a heavy-weight tank propulsion test article. A mated booster and orbiter test will not be performed if a satisfactory modal coupling analysis technique can be verified by the reduced scale model tests.

The HO tank ground test program will consist of development tests for design data and fracture control characteristics of materials and components, acceptance tests to verify adequacy of each HO tank system prior to flight, and qualification tests for certification of design performed on component and major assemblies.

The orbiter development schedule is shown in Figure 8-1, and is similar to the previous schedule (Ref. 1) with the exception of the added dynamic tests to the structural test article flow.



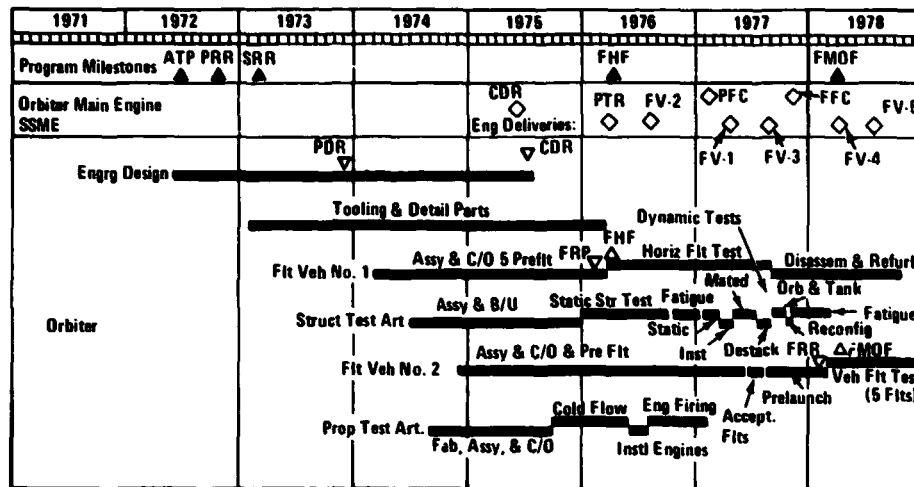


Figure 8-1 HO Orbiter Development Test Program

### 8.1.3 Horizontal Flight Test

The orbiter is common to all 3 booster test programs. The orbiter flight testing consists of 361 horizontal flight hours allocated as shown in Table 8-2.

Table 8-2 Flight Hour Summary

Test Category	Orbiter No. 1 Hr		Orbiter No. 2 Hr		Total
	Initial	Final	Initial	Final	
Performance	25	26	5		56
Stability/Control	26	60	0		86
ABPS	15	36	0		51
Structural	16	25	0		41
Electro Mechanical	4	6	2		12
Fit Controls	40	0	5		45
Avionics	18	7	20	25	70
<b>Total</b>	<b>144</b>	<b>160</b>	<b>32</b>	<b>25</b>	<b>361</b>

As indicated in Figure 8-2, the horizontal flight test program is not an FMOF constraint. This has been accomplished by going to an FHF concept in which the orbiter used for horizontal flight contains only those systems required for that test program. The airframe will, however, be in its final configuration allowing us to clear the approach and landing envelope for FMOF. Ferry configuration testing is delayed until all FMOF constraint tests are completed; however, the early FHF allows completion of all horizontal flight testing well in advance of FMOF.

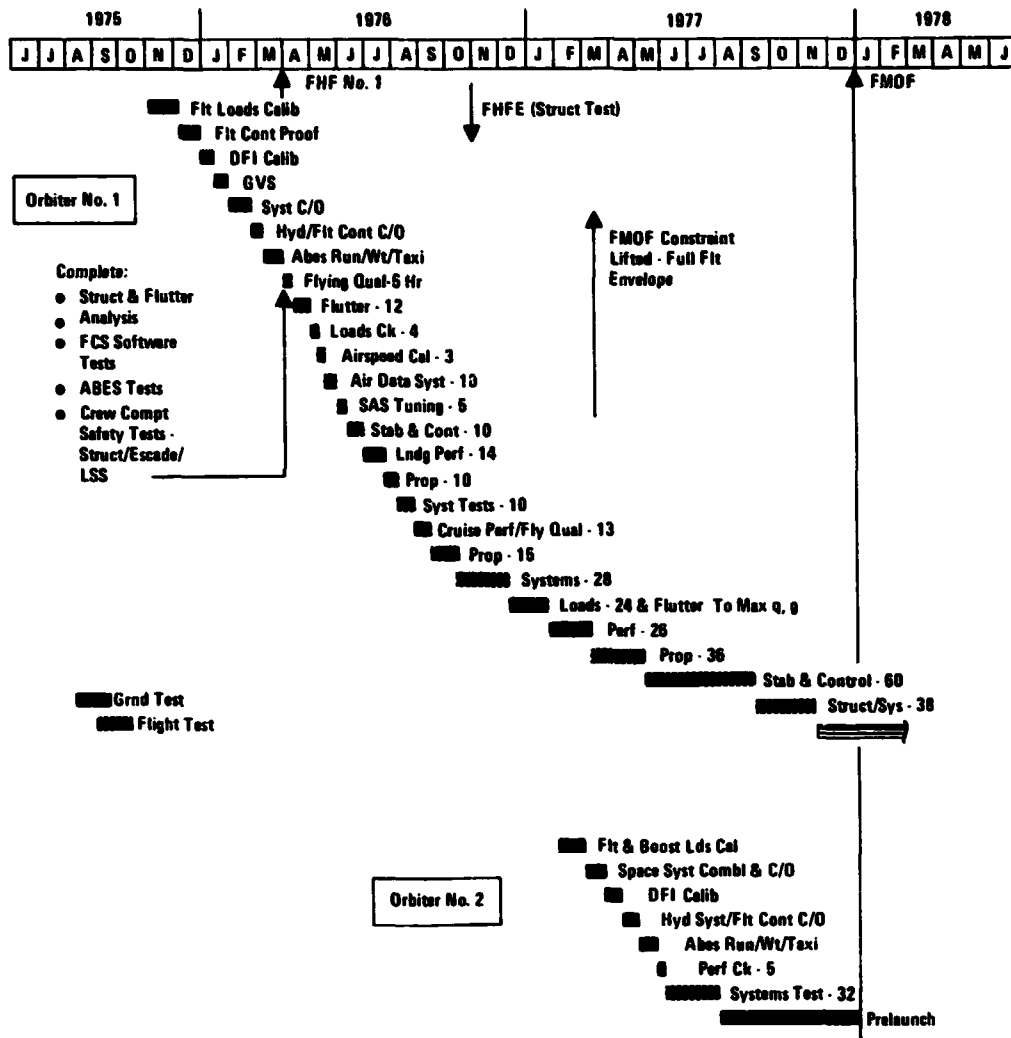


Figure 8-2 Orbiter Horizontal Flight Test

### 8.1.4 Vertical Flight Test

The baseline vertical flight test program consists of five manned launches during the first year following FMOF. These flights are intended to build up in capability to full mission operations at the end of the year. The pressure-fed recoverable vehicle also includes an unmanned booster flight rating test five months prior to FMOF.

For the SRM booster, an unmanned flight is desirable for the parallel burn solid configuration, the major issue being the flight control and separation demonstration. The option for the unmanned launch should be retained until the design has matured enough and sufficient experience has been obtained from the ground development program to make a proper evaluation. If an unmanned launch is ultimately required for this configuration, the required orbiter will be a full operational vehicle.



The pressure-fed booster flight test program will require two launches to demonstrate ascent performance. Recovery system development will require three launches based on impact damage uncertainties, current parachute technology, potential modification required on early flights, and recovery technique development. At the present time an unmanned launch is highly desirable for the pressure-fed booster, the major issue being POGO. The pressure fed system is particularly susceptible to POGO instabilities due to the interdependence of the propellant pressurization, tankage, and feed system with the engines and structure.

The option for an unmanned launch should be retained for this configuration with the final decision being made after the design margins have been established and sufficient experience has been obtained in the ground development program to evaluate properly this potential problem. If an unmanned launch is ultimately required for this configuration the minimum orbiter requirements, from a booster point of view, are a mass-simulated orbiter and a HO tank.

The pump-fed booster flight test program also consists of two launches to demonstrate ascent performance. Recovery systems development will require three launches based on impact damage uncertainties, current parachute technology, potential modifications required on early flights, and recovery technique development.

An unmanned launch is not recommended for the pump-fed booster because all booster systems have either been qualified and flown as part of the S-IC/F-1 system, are not critical to manned flight, or will have sufficient ground tests prior to the first shuttle flight to provide the necessary assurance of crew safety and mission success.

#### 8.1.5 Tradeoff Studies

##### 8.1.5.1 Implications of an Unmanned Orbiter Flight

Unmanned flight for the orbiter is feasible without excessive vehicle scarring. Normal mission modes of the orbiter use fully automatic guidance and sequencing with manual initiation supervision and override available to the pilot. On an unmanned vehicle, this manual control could be accomplished by a pilot located in a remote control station, whether it be on the ground or in a chase aircraft (the latter being more difficult to implement and use). Certain physical sensations such as vividness of motion, vibration, visual and sound cues would be lacking but would not impose a serious handicap. Extensive training would be required. Flight modes essentially remain the same as in the manned orbiter. The auto-landing system, using the microwave scan beam system (MSBS), remains essentially unchanged except that for unmanned flight the MSBS must be verified during horizontal flight

tests as operational under zero-zero visibility conditions even though visual backup for the landing will be provided through an onboard, forward-looking, vidicon ITV camera mounted to the back of the pilot's seat. Remote control override is effected through the addition of a program coupler system, similar to that used on unmanned LM's, tee connected to the orbiter via a junction box. These program couplers (there are three required per system) are essentially relay matrices that enable electronic activation of switches and throttles. The program couplers receive their direction from a remote control station issuing commands which are uplinked via S Band and/or UHF communication systems. Full-up remote control stations are required at both the launch and prime landing site (this latter is to serve as a system backup). Chase planes would be located, (1) each at the launch site, prime landing site, over West Central Africa and Darwin, Australia. These aircraft essentially provide for landing assist at all projected prime and abort landing sites. Chase planes carry remote control capability for aerodynamic functions only. Additionally, one tracking ship/plane must be provided to enable real-time coverage for HO tank separation. Optimized flight safety oriented toward man-rating the vehicle, as was the case studied, will have real-time telemetry coverage for less than 30% of the mission with the longest "blind" interval lasting 42 minutes. A comsat data system would alleviate this problem.

Although feasible, the implementation of a recoverable unmanned orbiter flight would result in a slip in FMOF by approximately six months, resulting in a program cost increase of approximately \$250M. In view of this and the fact that the chances of a successful return of the vehicle are greatly enhanced by the presence of a crew-on-board, every effort must be made to obtain the required confidence through the ground development and flight test program.

#### 8.1.5.2 High Speed Envelope Expansion

Two methods have been studied to achieve an incremental expansion of the critical high-speed portion of the orbiter flight envelope. These methods are (1) orbiter thrust augmentation by use of the vehicle main propulsion engines, and (2) the use of suborbital launches of the orbiter alone to achieve flight regime unobtainable with airbreathing engines only.

Thrust augmentation using the main propulsion system increases the performance of the orbiter to enable testing in the critical entry high-speed stability areas, reaching altitudes of 100K ft and speeds of Mach 3. In this regime entry longitudinal trim, static lateral stability, and longitudinal stability boundaries can be established. Studies with the H configuration indicated an airtow was required to enable the vehicle to reach an altitude high enough to start the MPS engine. When towed to 30K ft by use of its nominal



ABES and a B-52, a peak envelope of Mach 3.4 at 120K feet was obtained. Initial studies of the HO configuration indicate it will also be required to be towed to a high altitude, but being lighter, the B-52 will be able to tow it higher. This will enable the test vehicle to achieve the Mach 3 speed range as well. Modifications to the orbiter include the use of one MPS engine, addition of LO<sub>2</sub> and LH<sub>2</sub> tanks and propellant to the cargo bay, and modifications to engine feed lines. Table 8-3 and Figure 8-3 indicate the type of test program that could be accomplished with this method.

Table 8-3 Test Point Identification – Envelope Expansion MPS

Test Point	Mach No.	Alt Ft	q, psf	$\alpha$ , Deg	Test	Rationale
0	.5	27,000	120	12	Tow System Checkout	Verify Tow Technique, Cable Release System & ABES Stowage, Deployment & Airstart
1	1.0	70,000	500	0-5	Rocket Propulsion System Verification, Flutter Check, Stability Base Data Point, Static Loads	Verify Rocket Propulsion Operations, Gather Basic Stability & Control Data & Verify Static Loads & Flutter Margins at Max q Point
2	1.25	50,000	280	0-8	Stability & Control Flutter Check, & Loads Data at 3g	Verify Powered Flight Trajectory Control & Loadings During Max g Pullup
3	2.0	83,000	150	0-7	Stability & Control, Flutter Check, Loads During Transition	Begin Buildup to Stability & Control Boundaries & Transition to Nominal Entry $\alpha$
4	2.5	100,000	95	0-10	Same	Same
5	3.0	108,000	55	0-15	Same	Same
6	3.5	118,000	50	0-20	Same	Same
7	3.5	110,000	110	0-27	Same - Done at Point on Nominal Entry Trajectory	Verify Stability & Trim Margins

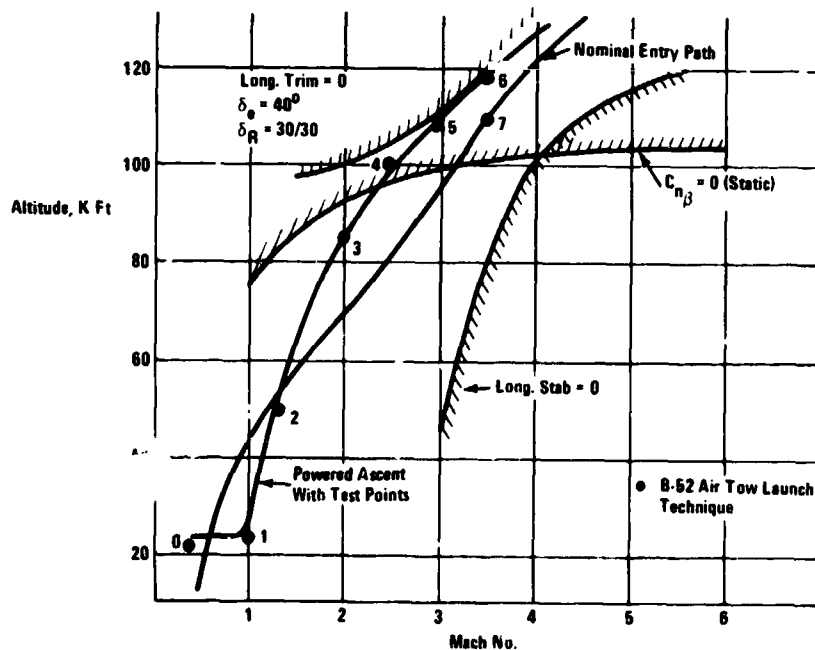


Figure 8-3 ABPS/MPS Envelope Expansion Profile

Suborbital launches of the orbiter alone will also achieve flight regimes in the critical high-speed entry and transition area. With the Mk I system with J-2S or SSME engines, careful trajectory shaping will enable the vehicle to obtain the Mach 6 speed range. The trajectory must be planned to stage the HO tank within the staging "q" limits of 15 psf and higher than a "q" of 5 psf to keep the entry deceleration less than 3.0 g. Modifications to the vehicle include addition of a launch pad hold-down structure of approximately 75K lb to enable vertical launch of the orbiter alone. This structure will be attached to the HO tank and will be jettisoned with it. Also the orbiter/tank separation maneuver may require the addition of a deceleration device on the tank to avoid recontact with the orbiter during entry.

Figure 8-4 shows the minimum and maximum capability of the considered suborbital launch system. This data shows that the critical stability region could be attained, but a buildup in test conditions is not possible, thus negating this method as a practical test procedure.

Envelope expansion remains a recognized problem, and the Air-Tow/MPS method remains under study as the baseline configuration evolves.

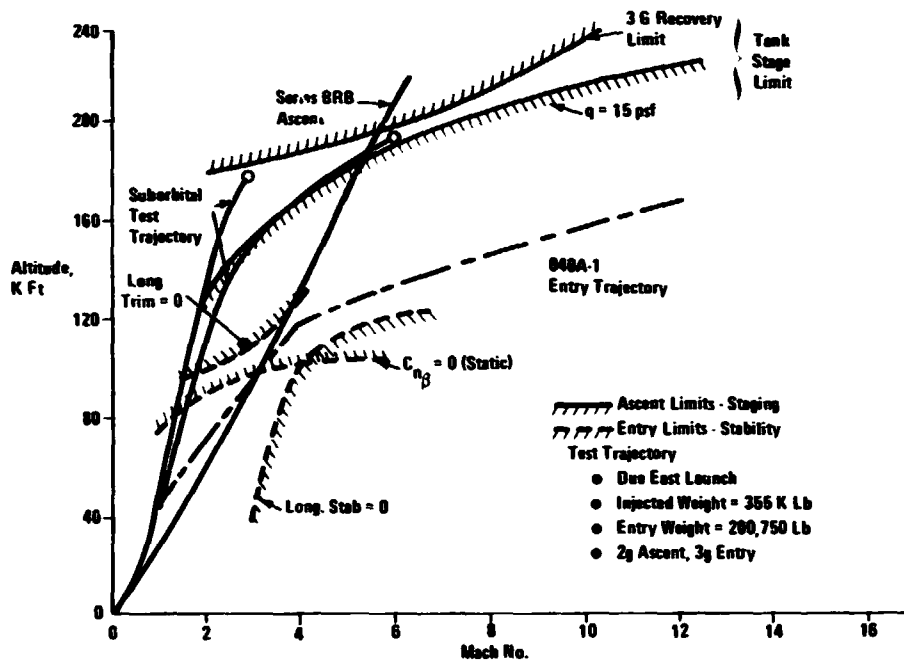


Figure 8-4 HO-Orbiter Suborbital Launch Study



## 8.2 OPERATIONAL FLOW

### 8.2.1 Overall Flow

#### 8.2.1.1 General

The operational flow for a series burn BRB/HO/orbiter is presented in Figure 8-5. The total flow time for an orbiter from landing to liftoff is 200 hours. The booster flow time from recovery through preparation for orbiter mate is 16 days, and the external HO tank processing from receipt at KSC through orbiter mate is 60 hours. The pad and LUT refurbish time after each launch is 48 hours. These times are considered to be operational times and would be factored up with an appropriate learning curve for earlier missions.

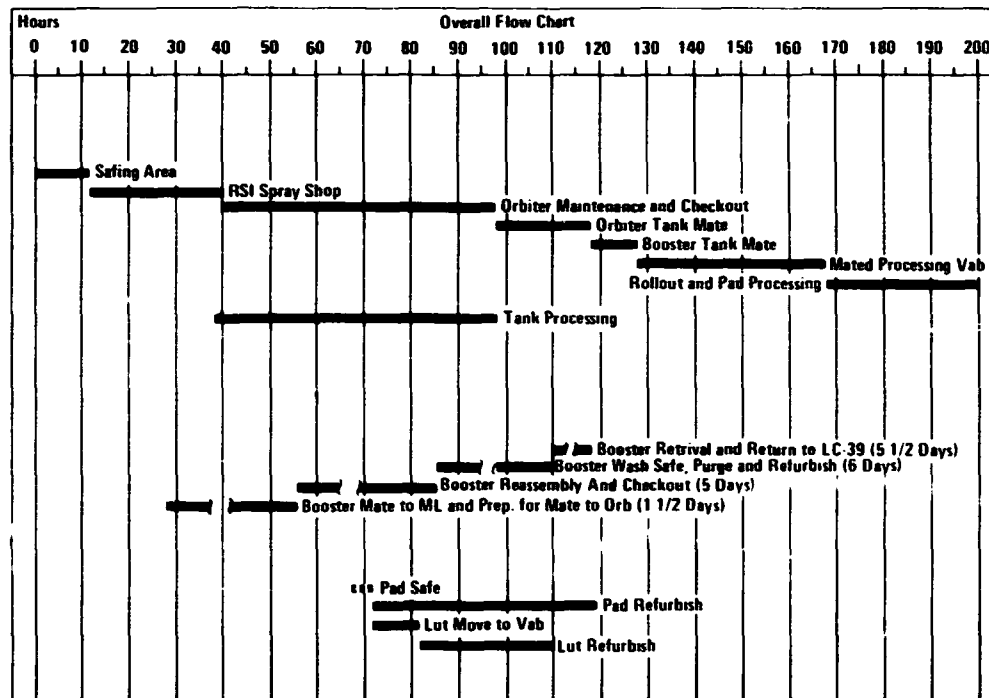


Figure 8-5 BRB/HO/Orbiter Operational Flow

#### 8.2.1.2 Flow Description

The details of the activities in each of the functional areas are contained in the subsequent paragraphs.

#### 8.2.2 Safing Area

The operations in the safing area will be limited to those necessary to secure, safe, and prepare the orbiter for move to the RSI spray shop.



After landing, the orbiter will taxi or be towed to a safing area located adjacent to the landing strip. In the safing area, the vehicle's systems will be secured, safed, and prepared for move to the RSI spray shop. Safing operations will include purging the APU reactor turbines and feed lines, draining the fuel cell supply of liquid oxygen and liquid hydrogen, purging the main propulsion system feed lines and engine, removing APU pods, OMS pods, and RCS pods. The ABES JP-4 fuel will be topped off or drained, as required, to support the next flight. The total time in the safing area is 22 hours.

### 8.2.3 RSI Spray Shop

The RSI Spray Shop will be located adjacent to the VAB. Because of the toxic and flammable nature of the RSI coating, this shop will be used exclusively for RSI spray operations.

After the orbiter is positioned in the spray shop, a complete inspection of the RSI will be performed and damaged tiles removed. All openings and critical surfaces will be masked for protection from the RSI spray coating. The spraying will be accomplished by several crews wearing protective clothing and auxiliary breathing equipment. Access to the vehicle will be by portable workstands. After the spray operation is complete, the masking will be removed, and the orbiter moved immediately to the maintenance and checkout area of the VAB. Total time in the RSI spray shop is 28 hours.

### 8.2.4 Orbiter Maintenance and Checkout

Maintenance and checkout contain the tasks necessary to establish and maintain the integrity of the orbiter in preparation for preflight and launch operations. Included in these tasks is the changeout of Lowest Replaceable Units (LRU) requiring periodic maintenance or calibration and the investigation and resolution of anomalies from the previous flight.

The ground cooling and ground power systems will be connected to the vehicle and configured for support mode. The instrumentation and data management system will be turned on and verified, and the electrical power system interface verification performed. The caution and warning electronic assembly trip levels will be verified, and displays/telemetry correlation performed. All exterior and internal lighting will be verified.

The communications system and ECLSS maintenance and checkout items will be accomplished. The flight control system will be checked out, and all interfaces with the RCS, ABES, OMS, MPS, and control surfaces will be verified. In parallel with the systems checkout, a functional and leak check of the MPS will be performed.

The payload will be installed in the cargo bay, and all interfaces, including electrical power, instrumentation, environmental control and deployment systems required to support the payload during launch processing, transport into orbit, and orbit deployment will be verified. The total flow time in the maintenance and checkout area is 58 hours. The flow for this area is presented in Figure 8-6.

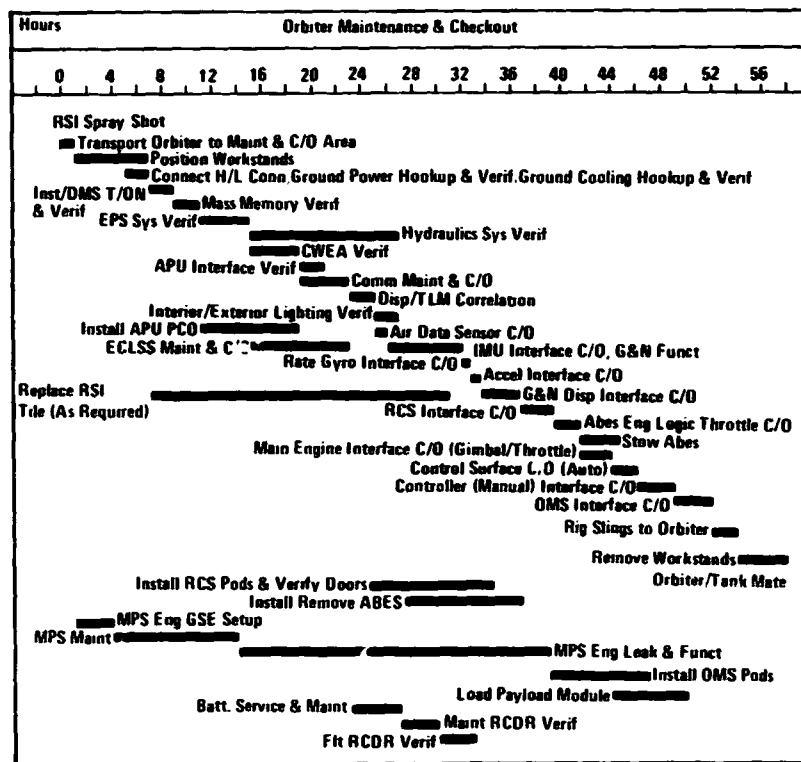


Figure 8-6 BRB/HO Orbiter Operational Flow

### 8.2.5 Tank Processing

The HO tank will be received as a complete assembly less the de-orbit SRM and nose fairing. Each tank will have completed a fluid leak check and electrical verification prior to shipment to KSC. The inspections and testing at KSC will check for shipping damage and establish the integrity of each tank prior to mate with the orbiter.

Each HO tank will be received on its shipping transporter. The tank will be inspected for possible defects caused by factory handling, shipment, and unloading. The presence of proper pad pressure will be verified, and the data package reviewed. A leak check involving mechanical connections, manhole covers, and electrical feed-throughs will be performed immediately after receiving inspection. The HO tank electrical and fluid interface verification will be accomplished after the HO Orbiter is mated to the booster. After inspection and leak checks, the HO tank will be transferred on its transporter to either a re-

pair station or outside storage area. Each tank in storage will remain in an on-demand condition for transfer to the orbiter mate area. During the storage period, pad pressure on each tank section will be monitored. Gross pressure decay curve will be developed and reviewed to further certify tank integrity. The total time for tank processing from receipt through orbiter tank mate is 60 hours.

#### 8.2.6 Orbiter/HO Tank Mate

Mating of the orbiter to the HO tank will be accomplished in the horizontal attitude. This will permit the necessary access to the mating interfaces and provide the best control of alignment and loads. The orbiter/HO tank interface checks will be performed after mate to the booster. This will eliminate the requirement for checkout equipment in the mating area and allow for verification of the LUT interfaces as a concurrent operation.

The HO tank will be towed to the high bay transfer aisle in the VAB for orbiter mate. After the tank transporter is in position in the mating location, it will be transit-leveled and secured in place.

The orbiter will be horizontally hoisted to retract landing gear and moved from the checkout area to the transfer aisle for mate to the tank and transporter. The hoisted orbiter will be positioned and soft-mated to the tank. After alignments are verified, the orbiter load will be gradually released to accomplish a hard mate. The tanks must be pressurized to 5 psi to support a full horizontal orbiter load transfer. The total time to mate the orbiter to the HO tank is 20 hours.

#### 8.2.7 Booster/Orbiter Mate

The orbiter/HO tank will be mated to the booster after the booster has been mated to the LUT. The mating will consist of mechanically joining the HO tank to the booster and mating the electrical connectors.

The orbiter/HO tank will be raised and rotated to the vertical position using the transfer aisle crane and a high bay crane. Once in the vertical position, the high bay crane will be used to position the HO tank over the booster, and the interstage mated. The HO tank de-orbit SRM and nose fairing will then be mated to the tank assembly. The VAB work platforms will be closed and the swing arms positioned and umbilicals connected. The total time for booster mate to orbiter/HO tank is 10 hours.

#### 8.2.8 Mated Processing VAB

The test performed in the VAB after mating will serve to establish the integrity of interfaces between the HO/orbiter and the LUT and between the HO/orbiter and the booster. This test and the installation of batteries and ordnance will minimize the pad flow.



After the swing arms are positioned and umbilicals connected, the orbiter will be powered up and all electrical interfaces with the booster and HO tank will be verified. The HO tank LOX section will be pressurized with GN<sub>2</sub>, and the LH<sub>2</sub> section with GHe to verify tank sensors and leak check the umbilical and orbiter interstage connections.

The HO tank separation and de-orbit systems will be verified and the flight batteries installed.

The space shuttle overall systems test will demonstrate the compatibility of all systems in a flight mission profile, including backup and abort modes.

All space shuttle ordnance will be installed and connected under controlled conditions prior to rollout. The total time for mated operations in the VAB is 20 hours.

#### 8.2.9 Rollout and Pad Processing

Pad processing will be limited to those activities necessary to mate the mobile launcher to the pad, final systems power-up, initiation of the launch sequence, propellant loading and crew ingress. Propellant loading and crew ingress will be accomplished in the final two hours of countdown and the capability shall exist to hold and re-cycle to a standby condition for two hours at T-2 hours.

Move to pad includes the tasks of preparing the VAB work platforms and LUT swing arms for move, positioning the crawler/transporter, disconnecting checkout equipment interfaces and transferring facility power. At the pad, the ML will be secured to the hard mounts, facility power transferred, and the firex system connected. The ECS air will be sampled and connected, and the swing arm tips extended and connected. The pad propellant, GN<sub>2</sub>, and He systems will be connected to the LUT and sampled.

The electrical power system and data management systems will be turned on and configured for launch. The communication links will be verified, IMU parameters will be determined and gyro torqueing will start. Final flight control interface checks will be performed and the propellant gauging system verified. The MPS engine thrust chamber jacket, turbo pump and LO<sub>2</sub> injector manifold will be purged and the booster RP-1 fuel will be loaded.

At T-2 hours, the crew will ingress and orbiter and booster cryogenic propellant loading will be accomplished as a parallel operation. The HO tanks LO<sub>2</sub> servicing will consist of system cooldown, slow fill to 5% at 500 gpm, fast fill to 98% at 4500 gpm, slow fill to 100% at 1,000 gpm, replenish will continue to launch.

Booster LO<sub>2</sub> servicing will consist of system cooldown, slow fill to 6-1/2% at 1100 to 1200 gpm, fast fill to 98% at 10,000 gpm. LOX replenish will continue through launch. HO tank liquid hydrogen servicing will consist of system cooldown, slow fill to 5% at 1,000 gpm, fast fill to 98% at 10,000 gpm, slow fill to 100% at 1,000 gpm. Replenish will continue through launch. The orbiter fuel cells LO<sub>2</sub> and hydrogen will be serviced and lines disconnected. The total time for rollout and pad processing is 32 hours.

#### 8.2.10 Pad and LUT Refurbish

The pad propellant transfer system will be placed in a safe condition and the firex system secured. The launch damage inspection will start and the LUT prepared for move to the VAB for refurbish.

Refurbishment will consist of local area sand-blasting, painting and replacement of fluid lines, electrical cables, and structural items damaged during launch. Replacement of the items with readily available spares will be facilitated by providing termination points immediately beyond the blast protectors.

To reduce the amount of blast damage and thus the refurbishment required, special care will be given to routing of the lines and cables and effective use of the water spray system and blast shields to provide maximum protection.

The time required for refurbishing the pad is 48 hours and for the LUT, 32 hours.

#### 8.2.11 Booster Processing

The sequence of operations for processing the pressure-fed booster at KSC is shown in Figures 8-7 through 8-10. The first flow of each booster as shown identifies the major sequence of events for receiving, final assembly, short duration flight readiness firing, and post firing checkout. The concept is for the booster and orbiter checkout to be in separate areas, vertical mating on a modified mobile launcher transport to the pad via crawler/transporter and launches from an LC-39 pad.

The booster will impact the water approximately 200 miles down range, where it will be recovered and towed to Port Canaveral. At the port, it will be loaded on a barge/transporter and towed to LC-39 turn basin. The booster will then be off-loaded from the barge on its transporter and moved to a wash, safe, and purge facility.

From the wash, safe, and purge facility, the booster will be transported to the VAB, rotated to the vertical, and placed on a vertical workstand for refurbishment, maintenance, and checkout. Boosters not suitable for follow-on flight will be returned by barge to the manufacturing site for disposition.



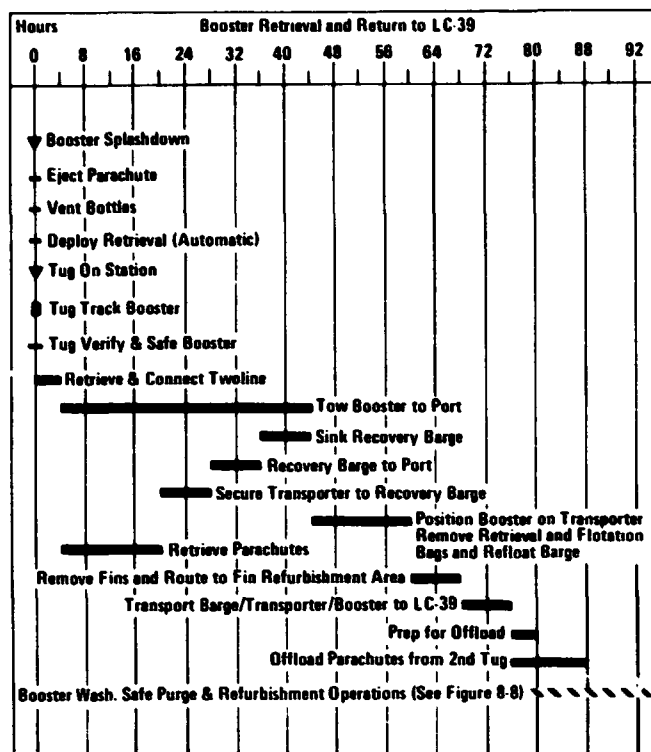


Figure 8-7 BRB/HO/Orbiter Operational Flow

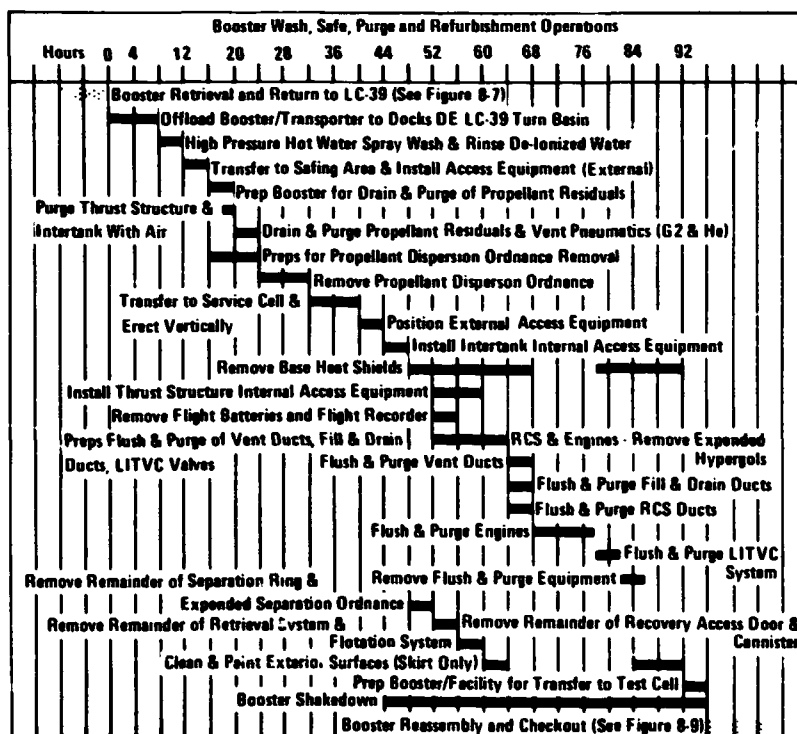


Figure 8-8 BRB/HO/Orbiter Operational Flow

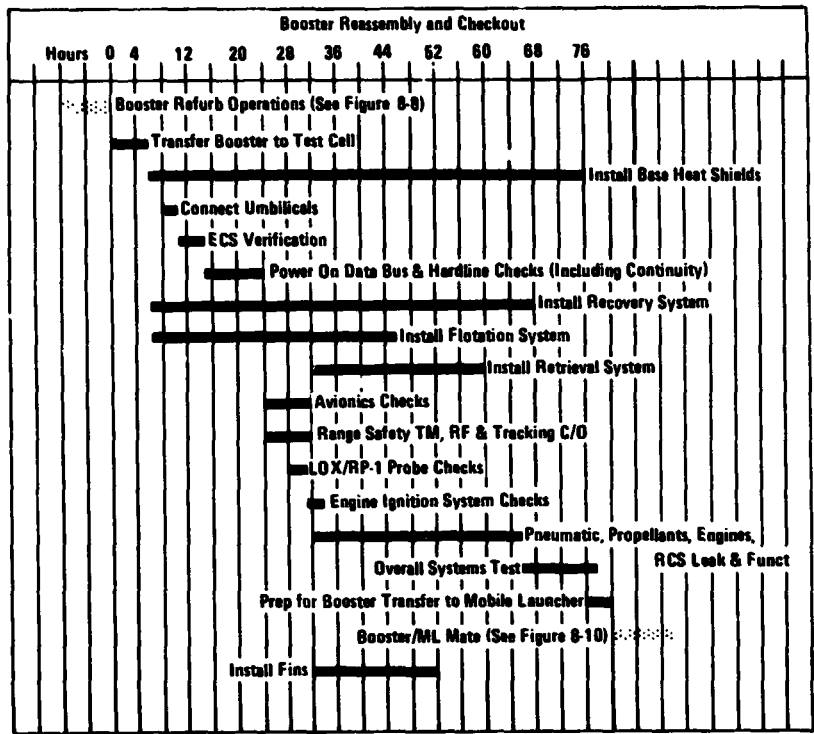


Figure 8-9 BRB-HO/Orbiter Operational Flow

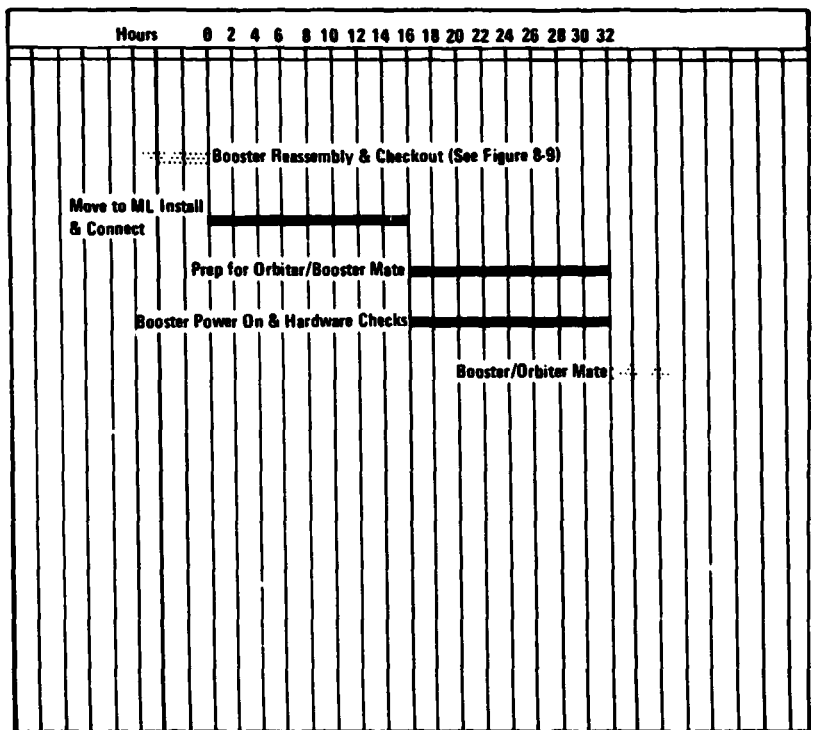


Figure 8-10 BRB/HO/Orbiter Flow



To minimize the quantity of mobile launchers required, orbiter and booster testing will be accomplished prior to mating on the mobile launcher. The checkout concept requires extensive use of automated test methods. A central computer facility, using data bus techniques, will be used for control and monitor of the vehicle and GSE. Ground systems will be designed with automatic fault-isolation capability and redundancy on critical circuits to meet turnaround and launch on-time criteria without jeopardizing vehicle integrity.

#### 8.2.12 SRM/HO/Orbiter Operational Concepts

The Orbiter and HO Tank Flow are the same as described for the BRB/Series configuration up through Orbiter/Tank mate.

#### 8.2.13. Booster/Orbiter Mate

The SRM's will be mated to the orbiter/tank after the orbiter/tank has been mated to the Mobile Launcher. The mating will consist of mechanically joining the SRM segments and end closures and mating with the HO Tank.

The mated orbiter/HO tank is erected and translated into the VAB high bay containing the modified mobile launcher using the transfer aisle crane and the high bay crane. The Orbiter/Tank is soft mated to the ML (See Memo B35-400MO-233 for soft mount description). The tail service masts are then connected.

The SRM segments and end closures will then be assembled using the High Bay crane. The hold-down arms will be connected and the Booster will be hard-mated to the HO tank. The total time for boosters mate to orbiter is 30 hours.

#### 8.2.14 Mated Processing VAB

The tests performed in the VAB after mating will serve to establish the integrity of the Orbiter/Tank/Boosters. This test and the installation of batteries and ordnance will minimize the pad flow time.

After the mating is complete, the orbiter will be powered up and all electrical interfaces with the boosters and HO tank will be verified. The HO Tank LO<sub>2</sub> section will be pressurized with GN<sub>2</sub>, and the LH<sub>2</sub> section with GHe to verify tank sensors and leak check the umbilical and orbiter interstage connections.

The HO tank separation and deorbit systems will be verified and the flight batteries installed.



All space shuttle ordance will be installed and connected under controlled conditions prior to rollout. The total time for mated operations is 20 hours.

#### 8.2.15 Rollout and Pad Processing

Pad processing will be limited to those activities necessary to mate the mobile launcher to the pad, final systems power up, initiation of the launch sequence, propellant loading and crew ingress. Propellant loading and crew ingress will be accomplished in the final two hours of countdown and the capability shall exist to hold and re-cycle to a standby condition for two hours at T-2 hours.

Move to pad includes the tasks of removing the VAB work platforms positioning the crawler/transporter, disconnecting checkout equipment interfaces and transferring facility power. At the pad, the MI. will be secured to the hard mounts. The swingarms connected and verified, facility power transferred, and the firex system connected. The ECS air will be sampled and connected, and the swing arm tips extended and connected. The pad propellant, GN<sub>2</sub>, and He systems will be connected to the LUT and sampled.

The electrical power system and data management systems will be turned on and configured for launch. The communication links will be verified, IMU parameters will be determined and gyro torqueing will start. Final flight control interface checks will be performed and the propellant gauging system verified. The MPS engine thrust chamber jacket, turbo pump and LOX injector manifold will be purged.

At T-2 hours, the crew will ingress and orbiter cryogenic propellant loading will be accomplished as a parallel operation. The HO tanks LO<sub>2</sub> servicing will consist of system cooldown, slow fill to 5% at 500 gpm, fast fill to 98% at 4500 gpm, slow fill to 100% at 1,000 gpm, replenish will continue to launch.

The orbiter fuel cells LO<sub>2</sub> and hydrogen will be serviced and lines disconnected. The total time for rollout and pad processing is 32 hours.

#### 8.2.16 Conclusions

The orbiter vehicle turnaround operations are insensitive to the type of booster used and the method of launch; i. e., parallel or series burn.

- The time to process either configuration is approximately 215 hours
- The manpower required to process the BRB is 2.2 times greater than the manpower required to process the SRM over the life of the program.
- The Facility Costs for either method are approximately equal.



### 8.3 FACILITIES

The major facilities required for the BRB 15x60 Orbiter Shuttle are identified in Table 8-4. They are identified as to existing modified existing and new.

The major facilities required for the 156" SRM 15x60 Orbiter Shuttle are identified in the same manner in Table 8-5.

*Table 8-4 15 x 60 Orbiter/BRB – Facilities*

<u>Existing</u>	<u>Modify Existing</u>	<u>New</u>
LCC	VAB	RSI Removal/Spray
LC 39 Pad A	ML	
Crawler	Travel Ways	Airfield
Parachute Shop		Purge and Safe Graving Dock
Hypergolic Facility		
Labs and Shops		

*Table 8-5 15 x 60 Orbiter/SRM – Facilities*

<u>Existing</u>	<u>Modify Existing</u>	<u>New</u>
LCC	VAB	RSI Removal/Spray
LC 39 Pad A	ML	Airfield
Crawler	Travel Ways	Purge and Safe
Hypergolic Facility		SRM Receiving
Labs and Shops		Storage

REPRODUCIBILITY OF THE ORIGINAL PAGE IS POOR.

## Section 9

### SUMMARY AND CONCLUSIONS

#### 9.1 SERIES/ BRB VERSUS PARALLEL/SRM

##### 9.1.1 What Are the Physical Configuration Characteristics ?

In selecting the specific design points for all configurations studied, we used the approach of choosing that booster staging velocity which yielded 5% potential margin on orbiter inert weight. We define potential margin (or payload margin) as that amount of inert weight increase in the orbiter (or payload) which can be accommodated by simply expanding the HO tank while leaving all other elements of the system unchanged. This margin is over and above the 10%-2%-10% growth allowance built into the orbiter/tank/booster design. Note that design point selection based on potential margin is only applicable if the booster can be "rubberized", i. e., sized for any given orbiter/tank weight. In the case of 120 in. solids, the maximum total impulse is a fixed quantity and we are forced to accept whatever tank size falls out when we tailor the SRM thrust profile to meet max q and max g constraints. When we cite a potential payload margin for a 120" SRM configuration, it must be realized that the accommodation of such an increase in inert weight involves not only resizing the tank but also retalloring the SRM thrust profile.

Figure 9-1 shows the result of applying this 5% potential payload margin concept to the selection of the design point for both the baseline series/BRB as well as the parallel/156 in. SRM configurations. The payload margin is zero at or near the GLOW bucket and increases as we move towards the higher staging velocities. At the 7.5K lb margin point (5% of the approximately 150K orbiter inert weight), we pay about 300K lb and 200k lb GLOW penalty

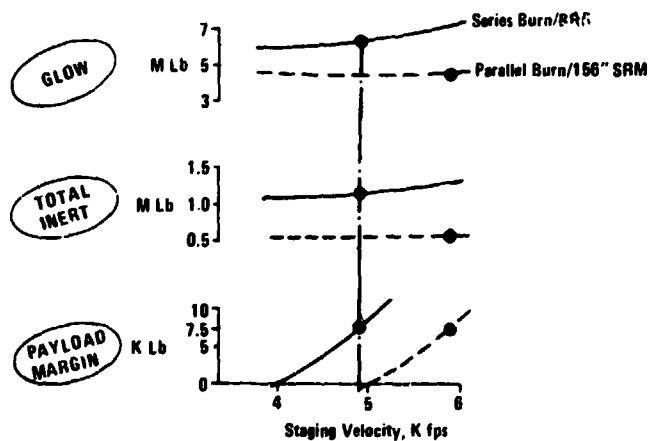


Figure 9-1 Launch Configuration Performance



respectively for the series/SRB and parallel/SRM cases. The cost penalty for this departure from the optimum is small so that this is a relatively cheap method of providing insurance against unexpected weight growth. We have made an extensive study of the cost implications of providing an inherent allowance for growth versus margin for a potential growth which may or may not realize, but a discussion of these results is not possible within the limitations of this summary. Our general conclusion is that a judicious mix of growth allowance and margin is the best method of achieving payload assurance, and that the extent of total contingency provided and the percentages thereof to be allocated to allowance and margin are a function of the level which we wish to impose.

A comparison of the major characteristics of the point design configurations is presented on Figure 9-2. Typically, the greater structural efficiency of the solid propellant boosters results in the parallel/SRM configuration exhibiting a decrease in GLOW of about 2.0M lb relative to the series/BRB case. Of greater interest, as being a stronger cost

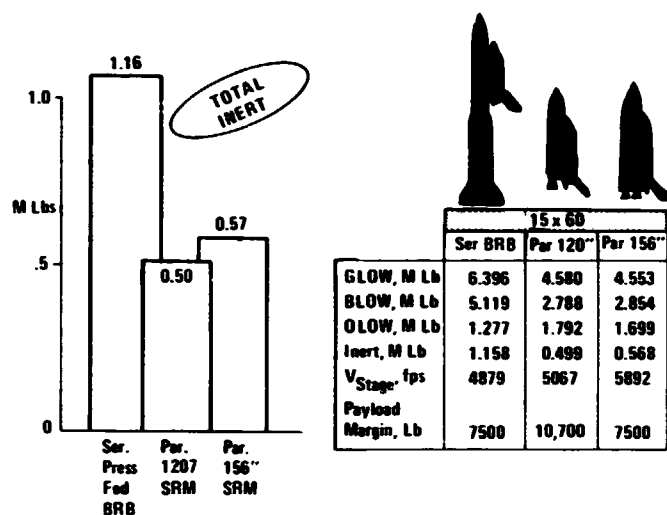


Figure 9-2 Launch Configurations Characteristic Comparison

driver, is the fact that the total inert weight of the former is less than half that of the baseline. The more efficient SRM also tends to drive the staging velocity of the parallel/156 in. SRM stack to near 6000 fps, which is typically about 1000 ft higher than that of the series system. This does tend to penalize the parallel configuration in cost per flight, since generally the minimum in the launch cost trends occur between 4000 fps and 4500 fps staging velocity.

### 9.1.2 What Is The Difference Between Series and Parallel HO Tanks ?

One of the major reasons for the GLOW difference between parallel and series configuration is the greater structural efficiency of the parallel HO tank. This efficiency is most

readily quantified in terms of pounds of dry tank weight per pound of loaded propellant. We designate this ratio the structural fraction" (SF) of the tank, with a lower SF indicating a more efficient structure. The parallel tanks generally exhibit a lower SF (or a higher propellant fraction, PF, which is the number of pounds of propellant per pound of total loaded tank weight) than series tanks. The reason for the higher efficiency of the parallel tanks becomes apparent if the tank design criteria and loading conditions for the series and parallel stack are compared. In order to clearly demonstrate the weight differences resulting from these loading conditions, we have taken a series tank at the design point propellant loading of one of our study configurations (14x45 payload bay orbiter/BRB) and compared its weight to a parallel tank designed for the same propellant weight.

Comparable elements of these tanks are, of course, designed by the same loading conditions, but the actual loads are quite different in the two cases. The series tank experiences significantly higher axial loads over most of the length of LH<sub>2</sub> tank and higher bending moments at the aft section of that tank than does the parallel one. The higher axial loads result from the difference in the manner in which booster thrust loads are applied to the HO tank. For the series stack, booster thrust is transmitted to the tank via the aft tank skirt, thus applying axial compression loads over the entire length of LH<sub>2</sub> tank and over part of the LO<sub>2</sub> tank up to the forward tank frame where the major load carrying orbiter attachment structure is located. By contrast, the parallel booster thrust loads are carried into the tank at the forward intertank area, so that the only axial loads seen by the parallel LH<sub>2</sub> tank are the orbiter thrust loads transmitted by the aft orbiter/tank attachment structure. Similarly, bending moments experienced by the series tank are higher in the aft section, since it is a cantilevered, end supported structure, while the parallel tank is supported forward and aft via the attachment structure to the booster. The LO<sub>2</sub> weight decrease of the parallel tank comes from the lower pressure head seen by that tank at the high g levels (near booster burnout) and the decrease in tank wall thickness that it allows. The reason for the pressure head being lower is, that, in a parallel burn configuration, the HO tank is being depleted during booster burn so that at staging the tanks are only about 70% full and the static pressure head due to liquid column height is commensurately lower.

Comparing the actual tanks for the configurations of specific interest in this section, we find that the series/BRB tank dry weight is 52K lb and that of the parallel/SRM (120 in) tank 66K lb. Although the parallel tank is significantly heavier, its SF is .0445 as compared to .0525 for the series tank. This is typically the case whenever we compare parallel to series configurations. Since the parallel burn orbiter engines fire during the entire ascent-



to-orbiter flight, the HO tank must carry more propellant and thus becomes heavier than for a comparable series configuration - but, although heavier, it is more efficient.

### 9.1.3 What is the SSME EPL for No Abort Gap ?

We considered the abort capability of the parallel series configurations relative to in-flight abort regimes. Of major concern is the ability of the configuration to avoid having to use an alternate site when aborting during ascent flight. This alternate site landing requirement arises from the inability to either abort back to the launch site or abort to orbit as a result of a failure, primarily that of an orbiter/engine, occurring during the ascent thrust phase. The time period during ascent flight in which a failure of the orbiter engine requires landing at a site other than the original launch site is designated as the "abort gap". It is important to minimize or eliminate this abort gap since alternate landing sites are either not available or, if there are possibilities for landing at such alternate sites, the problem of ferrying the orbiter back to the launch site may become exceedingly complex. Since the failure of an orbiter engine can be partially compensated for by increasing the thrust level of the remaining orbiter engines, (going, in other words, to the so-called "emergency power level", EPL), the extent to which such EPL capability is available on the SSME's, or the extent to which it is required to eliminate the abort gap is of considerable interest. Our studies have concentrated on determining the abort gap as a function of the EPL level of the SSME's. The 9% EPL, which is the one to which the SSME's are presently being designed, was found to be inadequate to eliminate this abort gap for all missions in both series and parallel configuration. In general, the parallel configuration has somewhat larger gaps than the series. Within the 9% present design level, the series configuration can close the abort gap on the south polar mission but not for a due east launch mission. The parallel configuration still has an abort gap for both missions at 9% EPL and requires about 17% to close the abort gap for all missions considered. Although, in general, the parallel configuration suffers by comparison to the series with respect to abort capability, later studies have shown that it is possible to close this abort gap for both configurations and all missions by applying various techniques such as increasing the flight performance reserves (FPR), or increasing the thrust level of the OMS engines. This latter approach has the dual benefit of increasing the rate at which OMS propellants are being depleted, as well as increasing the thrust level itself both of which increase the orbiter thrust to weight and improve start performance. Studies to date have shown that at some relatively minor weight penalty, a zero abort gap at zero or very small main engine EPL can probably be obtained.

#### 9.1.4 - Do Launch Acoustics and Interference Heating Penalize Parallel SRM?

Some of the features characteristic to parallel burn configurations - namely the simultaneous firing at all engines at lift off and the close conjunction of these engines to the base of the HO tank - tend to induce thermal and acoustic environments on that configuration which are more severe than those experienced on a series burn stack. In general, the parallel burn configuration experiences eight to nine db higher liftoff acoustic levels at the aft end of the configuration than does the series stack. This results from the simultaneous firing of booster and orbiter engines and the amplification of the ground reflection wave of the pad at or near liftoff. During transonic flight, there are localized areas on both configurations which experience higher vibration or acoustic levels than would be normally expected. The weight penalties imposed on the parallel burn configuration by these higher acoustic levels is approximately 1500 lb which goes towards increasing the gage of the payload bay door skins, fuselage side skins, and part of the vertical fin. There is no weight penalty attached to the tank structure per se for these higher acoustic levels since the tank wall thickness is designed by pressure considerations and is adequate to withstand the predicted acoustic levels. Additional weight penalties may result for the parallel system as a result of the increased vibration environments seen by orbiter equipments, particularly those in the aft sections. This will require the imposition of higher vibration qualification levels or a stronger structural design for those equipments at a cost and weight penalty that it is not possible to assess at this point.

The other area of more severe induced environment on a parallel burn configuration is caused by the booster plume impingement on the bottom of the HO tank. Radiation from the metallic particles contained in the SRM exhaust plume impose a high heat flux on the bottom of the HO tank which requires additional thermal protection in order to keep the temperatures within design limits. The additional heat flux generated by the SRM plume requires ablative protection on the tank, with a total weight penalty on the order of 1000 lb. We have also examined other potential sources of thermal environment penalties on the parallel configurations, such as interference heating between the tank and booster and plume induced recirculation heating near the aft section of the orbiter. We have found however, that neither of those phenomena have a severe enough effect to cause any additional weight penalty on the orbiter or tank.

#### 9.1.5 - Can TVC and Thrust Termination be Eliminated on Parallel SRM?

One of the original attractions of a parallel burn configuration was the possibility that thrust vector control might be eliminated on the booster and thus the cost and weight of the





booster could be significantly reduced. During the first half of the second extension study period, considerable preliminary control studies were performed to determine whether such an approach was feasible. Our conclusions at the mid-term briefing were that there was sufficient uncertainty about the ability to control the configuration with orbiter engines and orbiter control surfaces alone to warrant the recommendation that booster thrust vector control be included in all further studies of booster size and cost. During the final half of the study period, we continued and extended these control studies by using a six-degree-of-freedom digital simulation to cover all possible avenues of approach to the control of the combined configuration. Our control studies included examination of control authority requirements due to orbiter/booster roll-yaw coupling and aero disturbances generated by worst case wind shear conditions at various altitudes in the trajectory. We then studied several possible methods of providing the control authority required by looking first at the possibility of using orbiter engines alone and, then coupling the engine control capability with those of the orbiter aerosurfaces and finally looking at the combination of orbiter and booster engine control capability to provide the control authority. The results of these studies show that the torque available from orbiter engines alone even when all engines are firing, is insufficient to provide the requisite control authority. The combination of orbiter engines and orbiter aerosurface controls comes close to meeting control requirements. For the case of one orbiter engine out, however, this situation becomes sufficiently marginal for the pitch and yaw axes to still retain the mid-term conclusion that booster TVC is required. The data shown for aerosurface control is based on  $20^{\circ}$  deflection angle and  $25^{\circ}$  degree per second rate capability of the orbiter elevons which exceeds the normal requirements for reentry and supersonic aerodynamic control requirements. Thus a design and weight penalty must be paid even for the somewhat marginal control capability provided. A better control margin can be provided by the use of fins on the underside of the tank. Approximately 410 sq ft of fin area is required to provide a 20% excess of control torque available over that required. The use of such a fin would impose a weight penalty of approximately 2500 lb on the tanks. Additional fin surface could be added to reduce the aerosurface articulation requirements closer to present design capability. This, however, would increase the weight penalty on the tanks. If booster thrust vector control capability is provided, the combination of booster and orbiter engine control authority is more than sufficient to provide the control torque requirements. Booster thrust vector control capability with approximately plus or minus  $12^{\circ}$  gimbaling range would be sufficient to eliminate the necessity for the use of orbiter aerosurfaces.

In summary, then the question of "can booster TVC be eliminated?" can be answered as follows: Yes it can, by the proper combination of orbiter engine gimbaling, use of orbiter elevon and rudder deflection capability and by providing a relatively large fixed fin under the tank.

The question of whether SRM thrust termination can be eliminated, however, must be answered in the negative. For the situation of a mission abort contingency arising during the early phase of the ascent boost flight, the orbiter must be capable of separating from the booster which can only be accomplished if booster thrust is terminated or neutralized. Thus, the requirement for thrust termination of the SRM cannot be waived unless the probability of early mission abort is considered to be too small to design for.

### 9.1.6 How Do These Configurations Compare on Costs?

The comparative DDT&E cost per flight, and peak annual funding data for the three configurations considered in this section are presented in Figure 9-3. Note that, typically, the development cost of the SRM configurations is about \$900M less than that of a BRB series

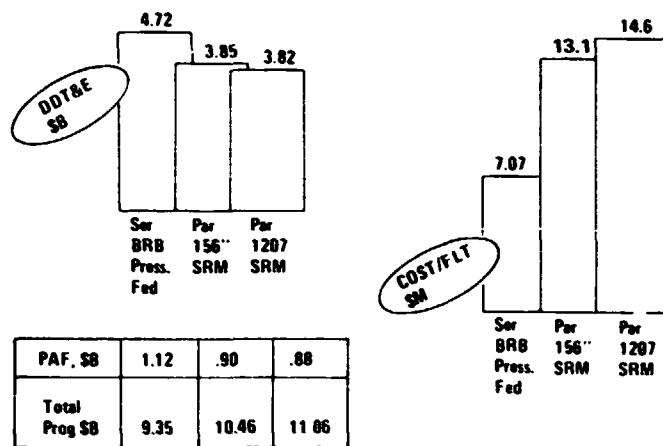


Figure 9-3 Series BRB Vs Parallel SRM  
15 X 60 Orbiter

burn system, but that the cost per flight of the expendable SRM configuration is nearly double that of the recoverable liquid propellant booster system. Peak annual funding for the liquid propellant booster system is on the order of \$100M to \$200M higher than that of the SRM configurations, but total program cost, of course, is significantly higher for the solids since, for a 445 flight standard traffic model, 900 solid boosters must be manufactured as opposed to only 12 of the liquid propellant recoverable boosters for the series burn system.



## 9.2 ORBITER STATUS

Before discussing the effect of payload weight and payload size reduction on the overall configuration performance and cost, it is necessary to digress somewhat into the problems of developing an orbiter configuration having acceptable aerodynamic characteristics in both the standard payload bay and small payload bay configurations. Since the payload size and weight effect on the overall system cannot be ascertained until its effect on the orbiter itself is determined, the discussion of these effects is deferred to the next section.

### 9.2.1 How Has the 15 x 60 Bay Orbiter Changed Since December 1971?

The recent orbiter weight history is depicted graphically on Figure 9-4. Of particular interest is the weight growth shown between the 161,000 lb landed weight of the December '71 version and the 190,000 lb target weight presently used in our weight reporting.

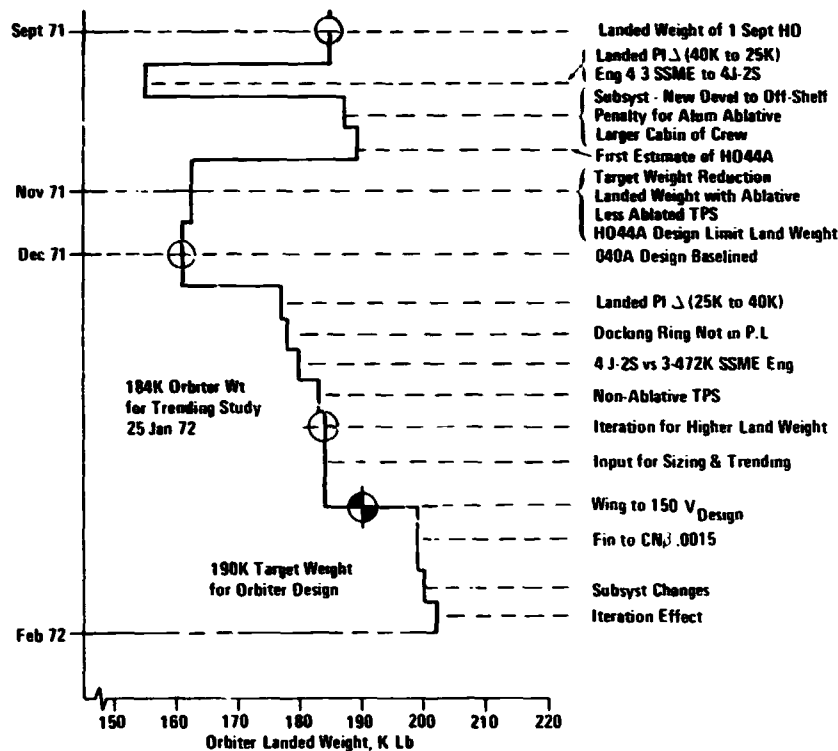


Figure 9-4 15 X 60 Orbiter Landed Weight History

This weight increase has resulted primarily from the changing requirements and ground-rules imposed on this study by the NASA. Up to Dec. 71, all orbiter design and performance requirements have been based on the Mark I version of the phased system. For the second half of the study, instead of the four J-2S engines previously required for the Mark I version of the orbiter, three 472K SSME's were now specified. Instead of the 25K up payload

for the south polar mission, 40K lb up payload was now specified and similarly the requirement for down payload went from 25K lb to 40K lb, thus increasing the orbiter landed weight to 184,000K lb. The most significant performance requirement change was the reduction in the design speed from 156 knots to 150 knots and it was this particular performance specification which had the greatest impact on the orbiter configuration and weight. Considerable aerodynamic studies were performed to examine all the configuration options in terms of wing area, wing cross section, wing sweep angle, fin area, etc., which would allow us to meet the design speed condition at the minimum weight penalty. The lowest weight solution, which still, however, imposed about 6,000 lb orbiter landed weight penalty, involved a change in the wing reference area from 3150 ft<sup>2</sup> to 3440 ft<sup>2</sup>, a change in the leading edge sweep from 60° to 49° and in trailing edge sweep from 0 to -5°, a change in the wing cross section from symmetrical to twisted cambered and a change in the tail area from 354 ft<sup>2</sup> to 550 ft<sup>2</sup>. The 15 x 60 payload bay orbiter configuration which corresponds to the present target weight of 190,000 lb, also incorporates such recent baseline changes as nose docking rather than hood docking and the change from LM ascent engines to LM descent engines in the OMS. All sizing and trending data, however, is based on the 184,000 lb. landed weight orbiter which was the version in existence on January 25 at the time when we had to finalize our input to the trending programs.

#### 9.2.2 Is the 14x45 Payload Bay Orbiter Feasible?

The major problem encountered in arriving at an aerodynamically acceptable configuration for 14 x 45 payload bay orbiter was the fact that the fuselage was reduced in length and diameter, but the engine weight remained the same, thus causing the cg to shift too far aft for acceptable aerodynamic performance. Two options were open to us. In one option the payload bay was extended from 45 to 50 ft in length, and in the other option the total thrust of the engine system was reduced from the 1.4M lb of three 472K engines to 1.1M lb, corresponding to two 380K engines. In both cases, the RCS pod on the fin had to be moved to the forward section of the fuselage and the APU's from the aft section to the mid-body in order to obtain acceptable cg locations. We developed an orbiter configuration meeting all aerodynamic design requirements for each of these two options and their characteristics are presented in Figure 9-5 where they are compared to each other as well as to the corresponding characteristics of the 15 x 60 payload bay orbiter. Note that the 14 x 45 orbiter version with the smaller engine sizes results in lower dry weight for the orbiter itself, but as will be seen later it increases the overall configuration weight because of the lower thrust to weight resulting from the lower engine thrust.



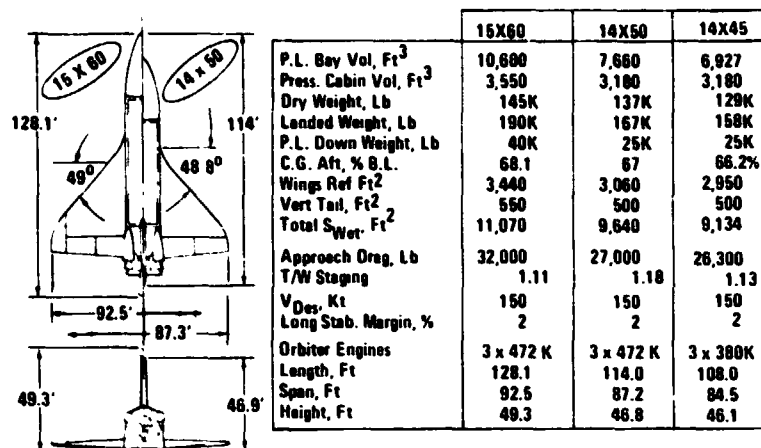


Figure 9-5 Orbiter Comparison

### 9.3 15 X 60/SERIES/BRB VERSUS 14 X 45/PARALLEL/SRM

#### 9.3.1 What are the Physical Characteristics of a 14 x 45/Parallel/SRM Configuration?

A comparison of major configuration characteristics of the 14x45 payload bay orbiter/SRM stacks using either four 120" or two 156" SRM's is presented in Figure 9-6 in which the baseline system characteristics are also included for reference. Again we see that the SRM configurations show a significant reduction in total inert as well as overall liftoff weight relative to the liquid propellant baseline. It should be noted that the use of low thrust engines, which as shown in the previous section, resulted in the lower dry weight in the orbiter, did however increase the stack weight by anywhere from 200K lb to 400K lb because of the lower performance capability at the low thrust engine.

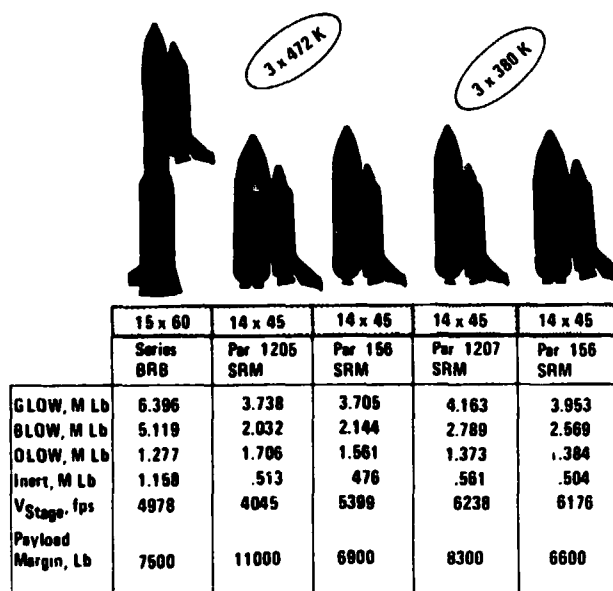


Figure 9-6 Launch Configuration Characteristics Comparison

### 9.3.2 How do Payload and Bay Size Weight Reductions Affect Cost?

The comparative costs of the small payload bay orbiter configurations relative to the baseline series liquid propellant booster system are shown on Figure 9-7. The general cost relationships shown on that figure follow the same trends previously evidenced whenever a liquid propellant and solid propellant booster configurations were compared. That is,

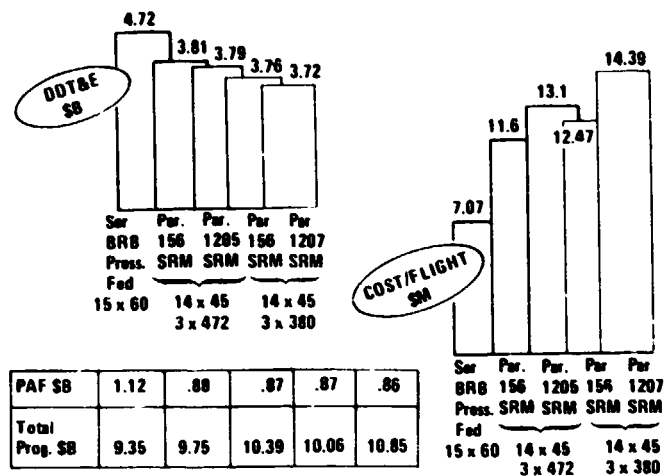


Figure 9-7 Series BRB 15 X 60 Parallel SRM 14 x 45

the development cost of the solid system is lower, but cost per flight and total program cost of the solid system is considerably higher than that of the liquid propellant booster configuration. In comparing the configuration options for the small payload bay orbiter, it may be noted that the low thrust version shows some reduction in development costs relative to the standard size engine version, but, as might be expected, the cost per flight increases since the increase in stack and tank weight more than compensates for the lower refurbishment costs of the orbiter itself. Relative to the standard payload bay size version of the of the parallel/SRM configuration, the small orbiter results in an approximately \$40M savings in development cost, nearly \$37M of which is the result of development cost savings in the orbiter itself. We found that 70% of the savings in development costs and accrual from the reduction in payload weight rather than in the size of the payload bay.

## 9.4 BOOSTER DESIGN

### 9.4.1 Solid Propellant Boosters

The solid propellant booster configurations considered in this study period are shown on Figure 9-8.



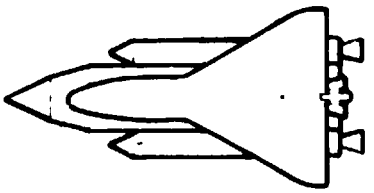
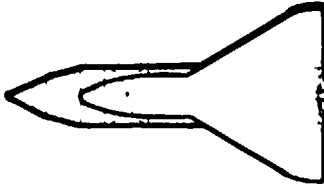
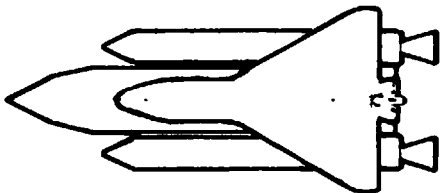
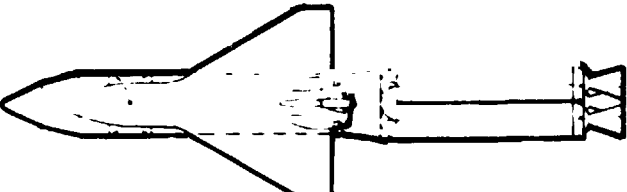
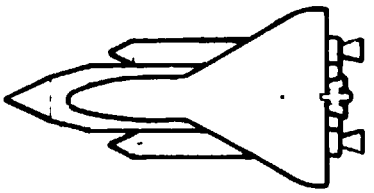
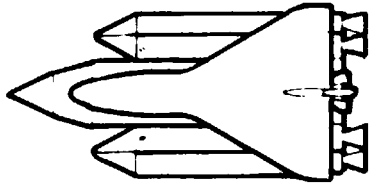
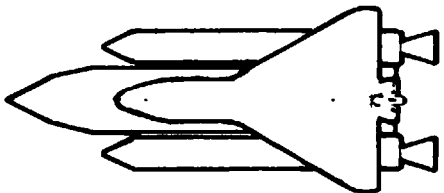
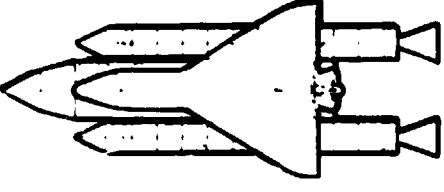
120 IN. DIA. SRM		156 IN. DIA SRM	
PARALLEL BURN	SERIES BURN	PARALLEL BURN	SERIES BURN
	TANDEM		TANDEM
	STRAP-ON		STRAP-ON
			
			

Figure 9-8 SRM Booster Configurations Candidates

Our study of solid propellant boosters concentrated on the resolution of these key issues:

- The best method of providing booster thrust vector control capability
- The booster separation technique for a parallel burn system
- The choice between 120 in. and 156 in. diameter SRM's
- The choice between parallel and series configurations and finally
- The detailed evaluation of solid booster cost buildup from the motor to the complete stages.

On the subject of ascent control, we had concluded that booster thrust vector control should be baselined for all configurations. We then performed a trade study to determine if liquid injection or mechanical nozzle gimbaling should be employed as the SRM TVC method. We compared a gimballed nozzle with  $\pm 7.5^\circ$  thrust vectoring capability to a liquid injection system capable of  $\pm 5^\circ$  thrust deflection. Our study showed that the liquid injection approach was heavier (by over 100 lb) and more costly (by about \$8M DDT&E and \$800K per flight) than the gimballed nozzle. Although the study was done specifically for a parallel system, the general results are equally applicable to a series configuration. We thus baselined the gimbaling nozzle as the thrust vectoring mechanism for all solid boosters.

For booster separation, we considered separation rockets only, mechanical linkages only and combination separation-rocket-forward/links-aft system. Although a pure rocket separation system turned out to be heavier (by about 11,600 lb as compared to linkages) and more costly (by about \$4M compared to a linkage system) than either of the other approaches considered, we decided that the lower development risk provided by previous Titan experience and the negligible load interaction with the orbiter warranted our baselining the rockets-only system as the booster separation approach.

We examined the factors relating to the choice of SRM diameter in some detail. Again, our studies were specifically oriented towards a parallel configuration, but the conclusions would apply equally well to a series system. Clearly, the experience factor favors the 120 in., since they have been used in operational Titan flights, whereas the 156 in. solids have only been test fired. This operational background reflects itself in a somewhat lower DDT&E cost, but the shuttle application requires sufficient additional motor and stage development on the 120's to make the development cost advantage about \$30M relative to the 156 in. insignificant. On the other hand, the fact that the 120 in. SRM configurations require generally twice as many motors than do 156 in. systems, increases the cost/flight



considerably (by about \$1.5M for the case of a parallel configuration), thus adding approximately \$600M to the total program cost at the standard traffic model. The relatively significant decrease in cost/flight coupled with the somewhat greater reliability because of the fewer components and lower stage complexity makes 156 in. the preferred solid booster diameter.

Having explored the major technical and cost factors relating to SRM's, we compared series and parallel configurations employing these solids (specifically 156 in. SRM's) as booster stages. We prefer the parallel system primarily because the lower GLOW and weight of total inerts of the parallel configuration (by about 300K lb in GLOW, and 100K lb in total inerts) and the reduction in number of SRM's required from three for series to two for parallel results in a \$2M saving in cost per flight without penalizing the development cost. From the booster point of view, the technical problems of integrating three SRM's into a tandem stage for a series configuration overshadow the attachment and separation problems of parallel mounted boosters, thus further adding to our preference for the parallel version of the SRM booster.

Considerable effort was devoted to estimating the cost of developing and producing a solid booster. Figure 9-9 summarizes the buildup of costs from the basic bottle (SRM) to a fully integrated and tested stage for the case of a parallel burn 156 in. solid. We concluded that the motor itself represents a relatively small fraction of the total development cost (about 20%), which accounts for the minor difference in development costs between 120 in. and 156 in. solids, but constitutes the major proportion of production costs, which makes it imperative to minimize the number of solids required for the program.

#### 9.4.2 Liquid Propellant Boosters

The liquid propellant booster systems considered are shown on Figure 9-10

The study of liquid propellant boosters aimed primarily at:

- Refining the pressure fed booster design with particular emphasis on ascent control, entry and recovery as being the major configuration drivers
- Evaluating the comparative advantages of series vs. parallel configurations employing liquid propellant recoverable boosters and
- Providing the data required to make a selection between pressure fed and pump fed boosters.

BOOSTER COST (MILLIONS)			
ELEMENTS	DOT&E	PROD	OPS
SRM	75.0	2,373.0	
STAGE HARDWARE			
STRUCTURE	19.0	593.7	
PROPULSION	11.3	74.3	
AVIONICS	2.7	21.1	
POWER	3.9	55.8	
SE&I	35.0	16.5	
FACILITIES	10.3		
SYSTEMS TEST	24.5		
GROUND TEST HARDWARE	14.5		
FLIGHT TEST HARDWARE	15.2		
SYSTEM SUPPORT	21.4	110.0	
MANAGEMENT	11.5	42.8	
FLT TEST OPS	110.0		
OPERATIONS			379.0
SUBTOTAL	354.3	3,287.0	379.0
TOTAL BOOSTER PROGRAM		4,020.3	

DOES NOT INCLUDE SHUTTLE MANAGEMENT

SRM COST (MILLIONS)		
CONTRACTOR	DOT&E	PROD
A	87	2,426
B	53	2,092
C		
D		

Figure 9-9 Stage Cost (Parallel Burn - 156 In SRM Booster)

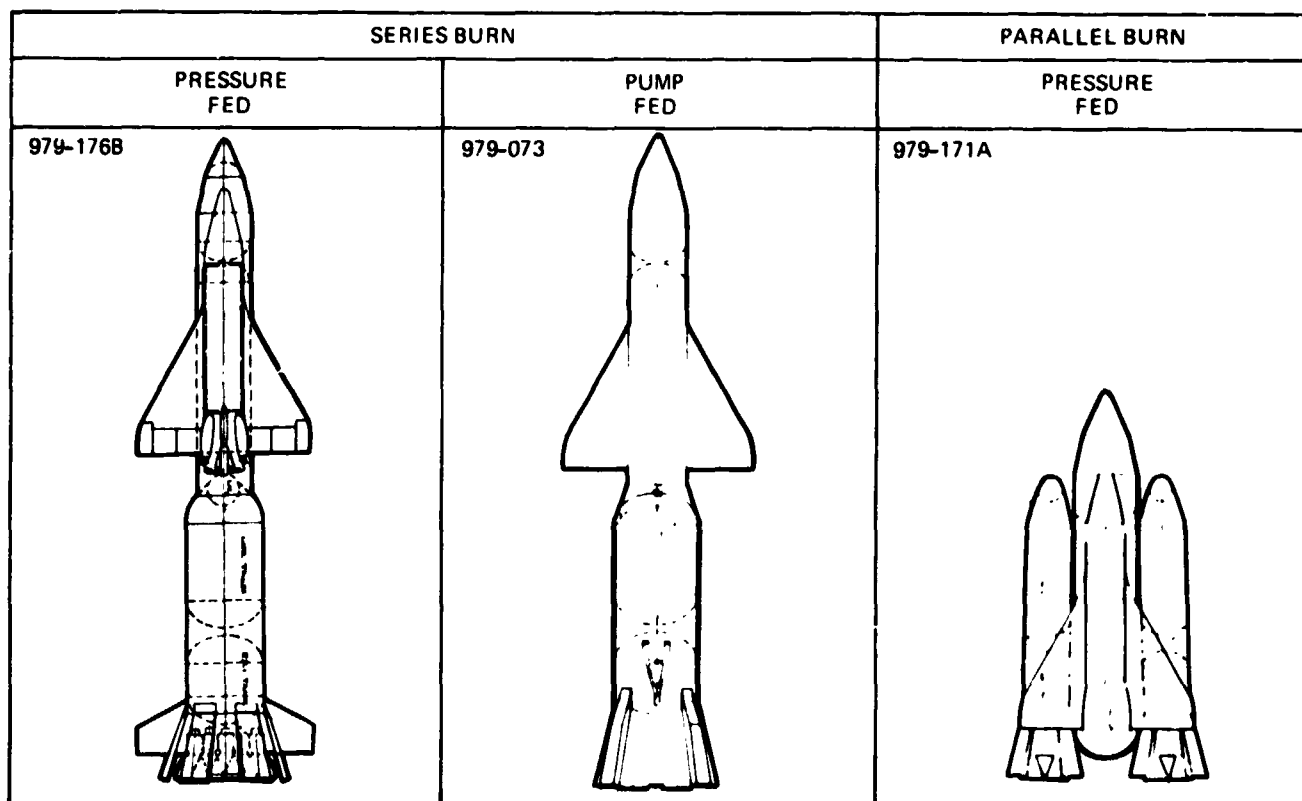


Figure 9-10 Liquid Booster Configuration



Unlike the conclusions we reached for the solids, the optimum method of providing booster thrust vector control for liquid propellant boosters turned out to be liquid injection rather than mechanical gimbaling. The major considerations for the case of the liquids were the additional weight and complexity that mechanical gimbals would add to the base structure which would tend to compromise the capability for water impact survival and intact recovery. The control study also showed that a combination of orbiter control surface and booster engine control authority would minimize the deflection requirements and system weight.

For entry we concluded that zero rather than high angle of attack was the preferred mode. This type of entry assures aerodynamic stability without moveable fins and active control systems. The recovery system selected is one consisting of parachutes only. The all parachute system is weight competitive with a combined retro-rocket/parachute system at the selected impact velocity of 100 fps, but is simpler and lower in cost than a combined system.

The comparison between series and parallel liquid propellant showed that, from the booster point of view, the situation is very nearly a standoff in both development and per-flight costs. When the overall system is considered, however, the reduction in HO tank weight and production cost results in a lower cost/flight of the series configuration relative to the parallel burn by about \$300K on the average. This cost advantage, coupled with the greater technical difficulties of integrating two parallel mounted boosters rather than a single tandem booster makes us prefer the series configuration in the case of liquid booster system.

We investigated in some detail the design and cost aspects of a pump fed booster for a series system for comparison with a pressure fed stage. Compared to the pressure fed device, its inert weight is over 350K lb lower and its gross liftoff weight about 1.4M lb lower. One of the major advantages of the pump fed booster is the decoupling between the engine and stage development, since the turbopumps make the engine performance relatively independent of tank pressures. Furthermore, since we propose the existing F-1 engine for the pump-fed stage, and engine development program is not required and the development cost and risk is accordingly reduced.

We concluded that because of the lower development risk and cost (by about \$500M) and the lower cost/flight (by about \$500K), we prefer the pump-fed to the pressure fed liquid propellant booster.

## 9.5 PAD ABORT

One of the major concerns of this final study period was the evaluation of the implications of providing pad abort capability. We consider the subject sufficiently important to devote a separate section to a discussion of what we did, why we did it and what we found out about pad abort.

### 9.5.1 What Requirements Are We Trying to Meet?

In order to determine the system requirements for pad abort capability, we systematically postulated all the failures which could require pad abort. We then evaluated the criticality of each of the failure conditions to establish which ones would impose the most severe requirements on the pad abort system. We found that the most time-critical failure would be an explosion of either the booster or HO tank caused by uncontrollable over-pressurization or by fire. This occurrence would generate a blast wave having the characteristics shown on Figure 9-11 which depicts the overpressure ( $\Delta P$  over atmospheric) conditions

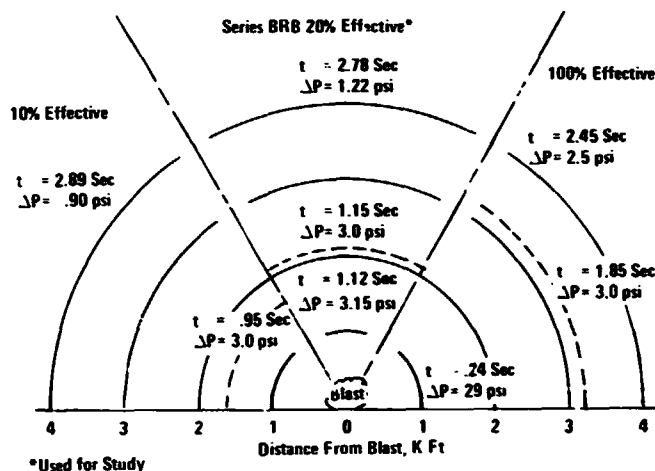


Figure 9-11 Blast Wave Characteristics

at the altitudes and times indicated. For the purpose of our pad abort studies, we assumed a 20% TNT equivalence of the baseline series/BRB combination of propellants. The  $\Delta P = 3.0$  psi dashed line represents the maximum over-pressure the orbiter is considered capable of withstanding without sustaining damage that would prevent a successful glide return to the landing strip. (Later studies showed that this value might be increased to 4 psi with a small structural penalty).

Since abort capability improves as the ability to accelerate away from the source of the blastwave increases, we looked into the maximum g loading the orbiter could tolerate if designed in accordance with nominal requirements plus safety factors. This turned out



to be between 4 and 4.5 g acceleration (3 g design limit and 1.4 to 1.5 safety factor for purely axial loading). The constraint of maximum allowable vehicle acceleration established that we could not escape the wave front without experiencing catastrophic overpressure, unless there was some warning of the incipience of an explosion. The warning time required is between five and seven seconds if a pad abort capability is to exist.

### 9.5.2 Configuration Approaches

The approaches considered for providing pad abort capability are shown on Figure 9-12. The configurations employing the main orbiter engines to provide abort thrust were eliminated after a brief study because:

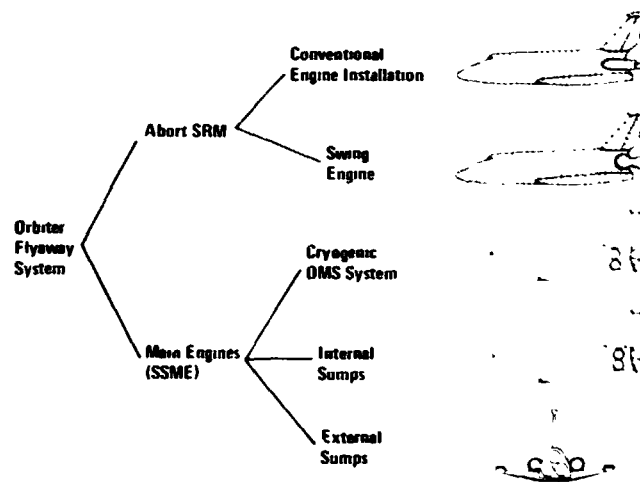


Figure 9-12 Configurations Considered For Pad Aborts

- Since only two of the three engines are usable for abort (three engines do not allow thrust vectoring away from the tank) the T/W is too low ( $T/W = 2.56$ ) for effective abort
- The inert weight penalties imposed by the requirement for propellant storage on the orbiter are effective for the entire mission as opposed to the abort rocket system, in which the unused inert weight can be jettisoned at or before booster staging.

We selected for further studies a series/ERB stack with two orbiter versions - one a conventional orbiter with two abort rockets strapped to the aft end of the fuselage above the wings - the other a swing engine orbiter with a single abort rocket mounted in the cavity in which the engines are stowed after orbit insertion. The abort rockets for these orbiters were sized to provide the maximum allowable T/W for a zero payload launch and to provide the impulse to impart sufficient energy to the orbiter for a glideback to the proposed new landing strip at KSC (825 fps at a burnout altitude of 6600 ft).

We concluded from our configuration studies that both approaches to providing pad abort capability were feasible, but that the swing engine configuration has a number of attractive advantages relative to a conventional orbiter. It permits the use of a single rocket and provides a convenient mounting location for it and it eliminates the concern about propellant line disconnect clearance for abort separation of the orbiter from the tank. Furthermore, since it allows a more efficient HO tank design (with the LO<sub>2</sub> tank aft) it results in a lower GLOW configuration. Although the swing engine orbiter is somewhat heavier than the baseline, the improvement in tank efficiency more than overbalances the orbiter weight penalty to the extent where, even with pad abort capability, the swing engine system is lighter than the no-pad-abort baseline.

### 9.5.3 What is the Impact of Providing Pad Abort Capability?

The weight penalties for implementing pad abort capability, are on the order of 200-300K lb in GLOW and 20-30K lb in total inerts.

Based on Apollo experience in designing and qualifying the launch escape system, we estimate a \$250M development cost penalty for providing pad abort capability. The cost per flight increase is relatively small, about \$300K, the major portion of which is the cost of the abort rockets.

## 9.6 SYSTEMS EVALUATION AND CONCLUSIONS

Our overall system evaluation and comparison was generally confined to those configurations which survived the pre-screening applied in each of the study areas discussed previously. For the case of series/BRB baseline, we did, however, consider both pressure-fed and pump-fed boosters, and for the representative 14x45 orbiter configuration we used the 120 in. rather than the 156 in. booster stack as having the lowest development cost of all options studies. The factors used for evaluation were the usual cost elements - development, per flight and total program - technical factors related to design complexity - in-flight abort capability, severity of induced environment and control of the combined configuration - and the impact on the environment.

The results of our evaluation are summarized on Figure 9-13. We have checkmarked the configurations which we consider the best performers relative to each of the evaluation factors used.

The lowest total program cost system turned out to be the series/pump-fed BRB configuration. This is the consequence of the lowest cost/flight combined with relatively low development cost of a system using that type of booster. If only DDT&E costs are considered,





	Ser/6 SRB 15 x 6 Orbiter		Par/SRM 15 x 63 Orb.	Par, SRM 14 x 45 Orb.
	Press. Fed	Pump Fed	156"	1205"
				
Lowest Total Program Cost, \$B	9.35	8.66	10.46	10.39
Lowest DDT&E, \$B	4.72	4.23	3.85	3.79
Lowest Cost/Flight, \$M	7.07	6.62	13.1	13.1
Least Complex Design				
• Least Acoustic Impact	<input checked="" type="checkbox"/>	<input checked="" type="checkbox"/>	<input type="checkbox"/>	<input type="checkbox"/>
• Easiest Ascent Control	<input checked="" type="checkbox"/>	<input checked="" type="checkbox"/>	<input type="checkbox"/>	<input type="checkbox"/>
Least Environmental Impact	<input checked="" type="checkbox"/>	<input checked="" type="checkbox"/>	HCL	

Figure 9-13 Configuration Comparison Summary

the parallel/SRM configurations are the best performers, with the small payload bay orbiter showing only relatively minor reduction in development cost, however, as compared to the standard orbiter/parallel/SRM system. Cost per flight favors the series systems, since the recoverability of the liquid propellant boosters significantly reduces the out-of-pocket costs for each launch. The pump-fed booster system exhibits a somewhat lower launch cost than the pressure-fed. This is attributed to the fact that the pump-fed booster, employing only four high thrust engines, has a smaller base cross-sectional area than the seven engine pressure-fed booster thus allowing use of a deployable shield for engine protection at water impact and a commensurate reduction in refurbishment cost. In the technical areas affecting design complexity, the series systems are generally superior. The control problem is simpler, since the roll moments, which pose the most stringent control authority requirements, are lower. The acoustic and thermal induced environments are more benign, since the orbiter engines are not fired during ascent boost. The series system abort capability is somewhat better because the orbiter T/W at equivalent energy-levels is higher. The difference in abort gap does, however, disappear when the use of two LM descent engines (at 9700 lb thrust each) is assumed for the OMS rather than two LM ascent engines (at 3500 lb thrust each), for which the data shown was initially developed.

The parallel solid systems do exhibit an adverse environmental impact characteristic in that they generate HCl as a combustion product, but the total amount of the pollutant is very small compared to that produced throughout the world by industrial operations.

Based on the above evaluation, our conclusions and recommendations can be summarized as follows:

#### **SRM's**

- All SRM's have lower DDT&E but significantly higher cost per flight than liquid boosters
- All SRM's applications make program vulnerable to environmental criticism (HCl)
- On the basis of high cost/flight and environmental vulnerability - SRM's appear less attractive than liquids over the long haul. For lower cost, during development SRM's are preferred, but then the program becomes more vulnerable on the environmental issue

#### **LIQUIDS**

- We prefer the Series Liquid Booster for shuttle development - cost per flight is vital in the future
- Pump-fed liquid has right combination of cost/risk/performance

#### **PAYLOAD**

- Most cost reduction benefit is derived from payload weight reduction of 20K rather than inert weight of orbiter
- Balance of orbiter is difficult; bay needs 50 ft length with 3 x 472 SSME or lower thrust engines (380K) must be provided
- If we must minimize DDT&E, reduce payload requirement first - but hold on to 60 ft bay

#### **PAD ABORT**

- Can be achieved, but as on previous programs will compound the design effort
- Will increase cost per flight by 300K
- Let's make sure we understand all implications before we proceed with requirements
- Swing engine is preferred arrangement for pad abort - minimizes cost to system.

